Characterisation of human mtRF1 and C12orf65: What are their roles in mitochondrial protein synthesis?

Aleksandra Pajak M.Res

Thesis submitted to Newcastle University in candidature for the degree of Doctor of Philosophy

Newcastle University
Faculty of Medical Sciences
Institute for Ageing and Health
Mitochondrial Research Group
January 2013

Abstract

Mitochondria have their own protein synthesis machinery that synthesises the oxidative phosphorylation components encoded by their mtDNA. This translation process consists of four main phases: initiation, elongation, termination and ribosome recycling. Termination and its control have been the least investigated. Recently, however, the termination factor, mtRF1a, has been characterised as sufficient to release all the nascent proteins from the mitoribosome. Furthermore, bioinformatics has identified three additional members of this mitochondrial release factor family namely, mtRF1, C12orf65 and ICT1. The latter is now known to be incorporated into the mitoribosome but its exact function remains unclear.

My project has therefore focussed on characterising the remaining two factors; mtRF1 and C12orf65, and investigating their possible involvement in mitochondrial protein synthesis.

It has been demonstrated that protein synthesis is not perfect and bacterial ribosomes not infrequently stall during translation. This can result from limiting amounts of charged tRNAs, stable secondary structures, or truncated/degraded transcripts. Ribosome stalling has been shown to cause growth arrest. In order to prevent that and maintain high efficiency of mitochondrial protein synthesis such stalled complexes need to be rapidly recycled. Bacteria have developed at least three distinct mechanisms by which ribosomes can be rescued. Contrastingly, despite the presence of truncated mRNAs in mitochondria, no such quality control mechanisms have been identified in these organelles. This study investigates the potential role of mtRF1 and C12orf65 in quality control of protein synthesis in mitochondria. Both mtRF1 and C12orf65 demonstrate conservative motifs which would suggest their potential role in ribosome rescue. My findings indicate that the conserved motifs in mtRF1 are crucial to maintain normal cell metabolism and that its mutated forms negatively affect cell growth. Since these motifs are required for ribosome dependent peptidyl-tRNA hydrolysis, the data presented strongly imply that mtRF1 plays a crucial role in intra-organellar protein synthesis.

Acknowledgments

I would like to express my sincere gratitude to my supervisors, Prof. Zofia Chrzanowska-Lightowlers and Prof. Robert Lightowlers for providing me with the opportunity to study mitochondrial protein synthesis as a member of their group. They have been a steady influence throughout my Ph.D. studies, their scientific expertise, advice, but also many anecdotes have been invaluable to me and their hard work have set an example for many years. I would also like to thank them for their kindness, patience and all the encouragement I needed during difficult times. This work would not have been possible without their constant support and motivation; it has been a real pleasure to curry out my research in this laboratory.

Additionally, I have been privileged to meet and collaborate with many fantastic people, who also become good friends over last 4 years. I would like to thank Ricarda Richter for all the time spent with me on the bench, teaching and helping me. Also I thank Sven Dennerlein, who introduced me to the Northern Blotting techniques. All the people, who I worked with everyday and who have been my 'secodn', extended family, thank you Agata, Francesco, Alina, Tran, Marysia, Casey, Kyle, Martin and Abdulraheem for the sharing of knowledge (not only scientific) many discussions, maintaining a good atmosphere in the lab and a good laugh at times. Thanks to all the members of the Mitochondrial Research Group (MRG).

I thank the Biotechnology and Biological Sciences Research Council (BBSRC), Centre for Brain Ageing and Vitality (CBAV) and Newcastle University for funding and providing excellent working facilities.

I owe special thanks to Karolina Rygiel, Agata Rozanska and Justyna Colliander. Thank you for being patient listeners to my worries, for many stimulating conversations and for being there for me always. Without your everyday moral support and all the help, when I needed it, I would not been able to make it this far and complete this thesis.

Finally, I would like to thank my parents and the rest of my family for their understanding, the support from the distance and love.

Statement of originality

I declare that the data presented in this thesis is based solely work carried out by the author, unless stated otherwise. Moreover, this thesis has not been submitted before for any other degree or award. The contributions by others were acknowledged, where appropriate,

Aleksandra Pajak

Table of contents

Table of Figures:

List of Tables:

Abbreviations

aa - amino acid(s)

aa - tRNA - aminoacyl-tRNA

ADP - adenosine diphosphate

Amp - ampicillin

APS - ammonium-persulphate

ArfA - an alternative ribosome factor A

ArfB - alternative ribosome factor B

A-site - aminoacyl-tRNA site within the ribosome

ATP - adenosine triphosphate

BAE - beads after elution

BBE - beads before elution

BN - Blue Native

bp - base pair(s)

BSA - bovine serum albumin

c - cytochrome *c*

CBB - Coomassie Brilliant Blue

CL - cell lysate

CLIP - Crosslinking immunoprecipitation

COX - Cytochrome *c* oxidase

CoQ - Coenzyme Q

cpm - counts per minute

C-terminus - carboxyl-terminus

CTDs - C-terminal domains

cyt - cytochrome

DC - decoding centre

DEPC - diethyl pyrocarbonate

dH_2O - distilled water

D-loop - displacement loop

DMEM - Dulbecco's modified Eagle's medium

DMSO - dimethyl-sulphoxide

DNA - deoxyribonucleic acid

dNTP - deoxynucleotide triphosphate

dsDNA - double stranded DNA

DTT - dithiothreitol

E. coli - Escherichia coli

EDTA - ethylene diamine tetra-acetic acid

EF(-G/-Ts/-Tu) - elongation factor (-G/-Ts/-Tu)

EGTA - ethylene glycol tetra-acetic acid

EJC - exon junction complexes

EM - electron microscopic

EMEM - Earle's Minimal Essential Medium

EMPAI - experimental modified Protein Abundance

ER - endoplasmic reticulum

E-site - exit site within the ribosome

EtOH - ethanol

FAD - flavin-adenine dinucleotide

FADH2 - reduced flavin-adenine dinucleotide

FBS - foetal bovine serum

FCS - folding competent state

FCCP - trifluorocarbonylcyanide phenylhydrazone

Fe-S iron-sulfur

fmet - formyl-methionine

FRT - Flp-recombination-target

GDP - guanine diphosphate

Glc - glucose

GST - Glutathione-S-transferase

GTP - guanine triphosphate

h - hour(s)

H. sapiens - Homo sapiens

H - strand heavy strand

HEK293T - human embryonic kidney cells

HeLa - human cervical cancer carcinoma cells from Henrietta La

hmtPAP - human mitochondrial poly(A) polymerase

IAA - isoamylalcohol

IF - initiation factor

IgG - immunoglobulin type G

I_{H1} and I_{H2} - heavy strand initiation promoters

I_L - light strand initiation promoter

IMM - inner mitochondrial membrane

IMS - intermembrane space

IP - immunoprecipitation

IPTG - Isopropyl β-D-1-thiogalactopyranoside

kDa - kilo-Dalton

kb - kilo-base(pairs)

KCl - potassium chloride

KOD - DNA polymerase from *Thermococcus kodakaraensis*

L-strand light strand

LB - Luria-Bertani

LC MS/MS - liquid chromatography - tandem mass spectrometry

LRPPRC - leucine-rich pentatricopeptide-repeat containing protein

LSU - large subunit

M - mitochondria

MEFs - mouse embryonic fibroblasts cells

min - minute(s)

MOPS - morpholinopropanesulfonic acid

MPP - mitochondrial processing peptidase

mRNA - messenger RNA

MRP(L/S) - mitochondrial ribosomal protein (of the LSU/ SSU)

mt - mitochondrial

mtDNA - mitochondrial genome

N - terminus amino-terminus

NAD - nicotinamide-adenine dinucleotide

NADH+H+ - reduced nicotinamide-adenine dinucleotide

NGD - No-go decay

ND - NADH dehydrogenase

nDNA - nuclear DNA

NMD - Nonsense-mediated mRNA decay

NOA1 - nitric oxide-associated-1

NP-40 - Nonidet P-40, octyl phenoxy-polyethoxy-ethanol

NSD - Nonstop mRNA decay

nt - nucleotide(s)

NTDs - N-terminal domains

OD - optical density

o/e - overexpressed, overexpressor

OMM - outer mitochondrial membrane

ORF - open reading frame

OXPHOS - oxidative phosphorylation

p - p-value

PAGE polyacrylamide gel electrophoresis

PAS - polypeptide accessible site

PBS - phosphate buffered saline

PCR - polymerase chain reaction

Pfu DNA - polymerase from *Pyrococcus furiosus,*

PI-Mix - protease inhibitor cocktail (Roche)

PKs - pseudoknots

PMSF - phenylmethylsulphonyl fluoride

POLRMT - mitochondrial RNA polymerase

PPR - putative pentatricopeptide repeat

P-site - peptidyl-tRNA site within the ribosome

PTC - peptidyl-transferase centre

PTH - peptidyl-tRNA hydrolase

PVDF - polyvinyliden fluoride

QH_2 - ubiquinone

RBP - RNA binding protein

RF - release factor

RNA - ribonucleic acid

ROS - reactive oxygen species

rpm - rounds per minute

RRF - ribosome recycling factor

rRNA - ribosomal RNA

sec. - seconds

SDH - Succinate-dehydrogenase

SDS - sodium-dodecyl-sulphate

siRNA - silencing RNA, small interfering RNA

SLIRP - stem-loop interacting RNA binding protein

SN - supernatant

S. pombe - Schizosaccharomyces pombe

ssDNA - single stranded DNA

SSPE - saline sodium phosphate EDTA buffer

SSU - small subunit

SU - subunit

Su9 - ATPase subunit 9

TAE - tris-acetate EDTA

Taq - DNA polymerase from *Thermus aquaticus*

TBS - tris buffered saline

TBS-T tris buffered saline, containing Tween-20

Tc - tetracycline

TEMED - N, N, N', N'-tetramethylethylene-diamine

TFAM - transcription factor A

TFB1M and TFB2M - mitochondrial transcription factor B

TIM - translocase of the inner mitochondrial membrane

tmRNA - transfer-messenger RNA

TOM - translocase of the outer mitochondrial membrane

tRNA - transfer RNA

Tris - 2-Amino-2-hydroxymethyl-propane-1,3-diol

Triton X-100 - polyethylene glycol p-(1,1,3,3-tetramethylbutyl)-phenyl ether

T. thermophilus - *Thermus thermophilus*

Tween-20 - polyoxyethylene sorbitanmonolaurate

U - unit (enzyme activity; 1U = 1µmol/ min)

UPF - upstream frameshifting

UTR - untranslated region

UV - ultra-violet

vol - volume

v/v - volume/ volume

WT - wildtype

w/v - weight/ volume

xg - relative centrifugal force

Chapter 1

Introduction

Chapter 1. Introduction

1.1. Mitochondria- the importance and uniqueness

1.1.1. Evolution of Mitochondria

Early in the life on earth mitochondria, most probably as proteobacteria, became a part of an anaerobic archaeobacteria based on a symbiotic relationship. This theory has been widely accepted and more recently proven by comparison to the genome of Rickettsia, an intracellular causative proteobacteria of typhus, where the mitochondrial genome revealed high similarity that had not been recognised before (Andersson *et al*., 1998). However, the close relation between these two has also allowed the assumption to be made that since the initial endosymbiosis and during the long course of evolution mitochondrial DNA (mtDNA) from some organisms must have either been lost (non-coding DNA) or translocated to the nucleus (a reduction genome evolution) (Gray *et al*., 1999). Their loss from mtDNA contributed to reduction of the mitochondrial genome size and the stabilization of the symbiotic relationship. According to Andersson *et al.,* (1998) good candidates for such genes are especially those crucial for mitochondria including the genes involved in the biosynthesis of amino acids and nucleotides and their regulation or genes of anaerobic glycolyis. Now that many genes have been lost from the mtDNA, especially in humans and replaced by nuclear homologues, the present day mitochondria depend on their 'host' for the majority of the proteins that are required for correct function of the organelles. Thus, approximately 99% (Adams and Plamer, 2003) of the ~1500 proteins that are required to generate and maintain the mammalian mitochondrion are encoded by nucleus. The mitochondrion has now become an integral component of all nucleated eukaryotic cells and is responsible for or/and linked to wide variety of cellular activities, which are crucial for cell survival, some of which are described below. Moreover, it has been shown recently that the loss of the mitochondrial genome results in growth rate reduction, cell-cycle arrest and nuclear instability (Veatch *et al*., 2009).

Mitochondrial size, morphology, number and position in cells can vary and depends on energy demand of a tissue (Forner *et al*., 2006; Johnson *et al*., 2007). They are very dynamic organelles, which undergo constant fusion and fission events (Youle and Bliek, 2012; Hoppins and Nunnari, 2012).

1.1.2. General Structural Characteristics of mitochondria

Mitochondria have a number of unique features compared to other mammalian organelles, including a dynamic structure, possession of a genome that is essential for multiple mitochondrial functions, together with specific translation apparatus responsible for intraorganellar translation of mt-mRNAs that differs from the cytosolic proteins. The organelle is divided into a number of compartments (as depicted in Figure 1.1) and described here. It is enclosed by two membranes, the outer mitochondrial membrane (OMM), which separates it from the cytosol, contains porin forming channels and Translocase of the Outer Membrane (TOM) complexes to transport mitochondrial targeted polypeptides through the lipid bilayer, which makes OMM permeable to molecules smaller than 1500 Daltons. The inner mitochondrial membrane (IMM) plays a role in maintenance of the electrochemical potential and is more selectively permeable due to the different molecular composition including the presence of cardiolipin. It therefore contains various membrane transporters, such as TIM23 and the five oxidative phosphorylation (OXPHOS) complexes. The inner membrane is invaginated and so forms cristae with cristae junctions that are contacts sites with

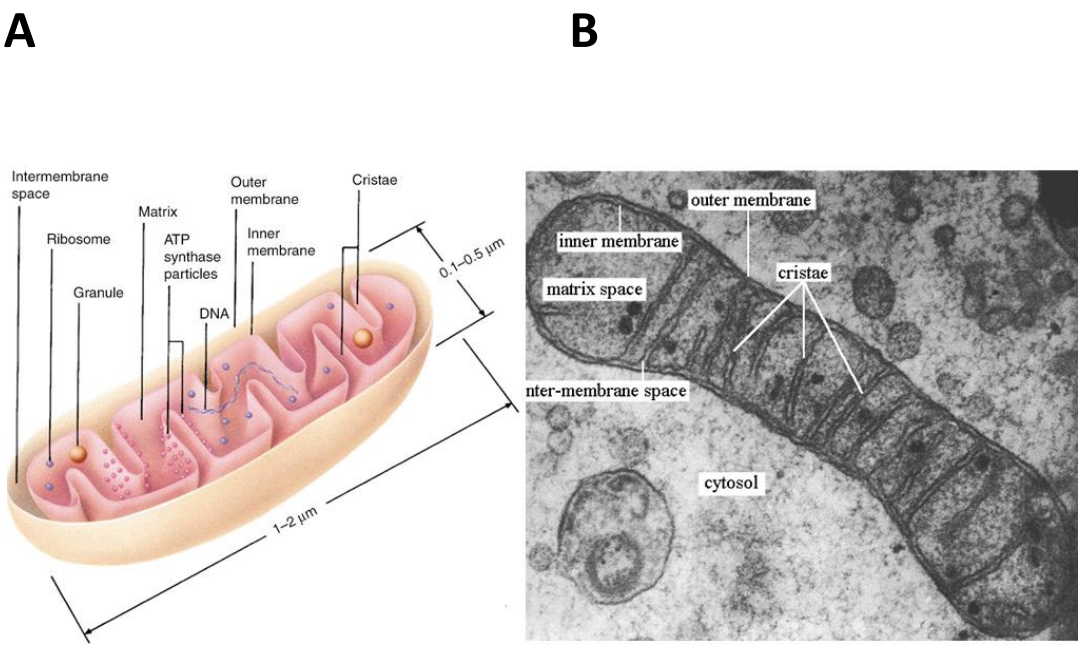

Figure 1. 1. Mitochondrial structure.

(A) The schematic of mitochondria indicates the different compartments and position of intramitochondrial particles (Frey and Mannella, 2000). **(B)** Similar features are shown in an electron microscopy image of a chick embryo mitochondrion (taken from **http://www.bmb.leeds.ac.uk/illingworth/6form/index.htm).**

the outer membrane, illustrated in Figure 1.1.

The inter-membrane space (IMS) harbours, among others proteins, cytochrome *c*, whereas the compartment surrounded by the inner membrane, matrix, hosts most of the mitochondrial proteins responsible for metabolic processes including fatty acids beta-oxidation, Krebs cycle and the intraorganellar protein synthesis, performed on specific mitochondria translation apparatus (all briefly reviewed by McBride *et al*., 2006). Moreover, the matrix of each mitochondrion contains 2-10 copies of circular mtDNA (Anderson *et al.,* 1981) and factors involved in maintenance and its gene expression.

1.1.3. Mitochondrial Functions

A central contribution of mitochondria to the cell is in energy transduction in the form of ATP generated by harnessing oxidative phosphorylation. Metabolic substrates such as carbohydrates are oxidised by the tricarboxylic acid cycle (Krebs cycle), and fats are broken down by the enzymes of the beta-oxidation cascade. Both of the processes result in the production of reduced cofactors i.e. NADH and FADH2, and are re-oxidised by the transfer of electrons to the mitochondrial electron transport chain. Following the oxidation of those cofactors by Complex I and II, electrons reduce Coenzyme Q (CoQ) to ubiquinol (QH_2) and protons are pumped into the IMS by Complex I (Galkin *et al*., 2006). Then, the electrons are transported further by QH_2, which is oxidised to ubiquinone. The electrons now are transferred from Complex III to IV by the cytochrome *c* and finally to ½ O_2 and $2H^+$ by Complex IV (with water as the end product). Protons are pumped into the IMS by Complexes I, III and IV generating the electrochemical gradient. Thus, with the oxygen as a final electron acceptor and by the *trans*-membrane electrochemical gradient formation, together with a subsequent ADP and Pi condensation, ATP is produced (Figure 1.2). Then, the adenine nucleotide translocator (ANT), a mitochondrial protein, exchanges mitochondria-generated ATP for the cytosolic ADP. The amount of ATP released from the organelle is about 10 fold greater than the production from glycolysis in the cytosol and thus mitochondria tend to be referred to as ‘the power house of the cell’ (Ballerd *et al*., 2004). However, apart from ATP production when respiring, mitochondria convert about 1% of oxygen to generate reactive oxygen species (ROS), such as hydrogen peroxide, superoxide or hydroperoxides. Despite the low level, which is believed

Complex:	I	II	III	IV	ATP synthase
mtDNA:	7	0	1	3	2
nDNA:	38	4	10	10	14

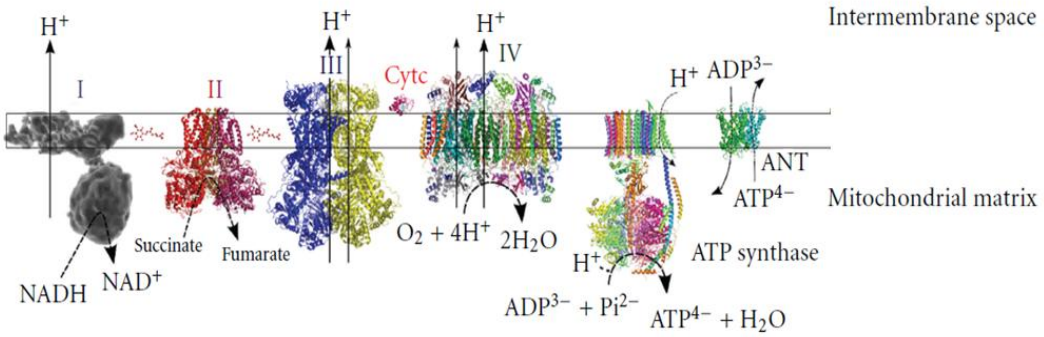

Figure 1. 2. A cartoon depicting the mitochondrial oxidative phosphorylation complexes.

The schematic is taken from Yoboue and Devin, 2012. Four respiratory complexes (I, II, III, and IV) are indicated. The largest, 980kDa **Complex I** (NADH:ubiquione oxidoreductase) consists of a hydrophobic membrane arm and hydrophilic matrix arm. Seven proteins (ND1, ND2, ND3, ND4, ND4L, ND5 and ND6) are mitochondrially encoded and 8 iron-sulphur clusters mediate the electron conduction**. Complex II** (succinate:ubiquinone oxidoreductase) has four subunits and delivers electrons to ubiquinone. **Complex III**, ~ 480 kDa (ubiquinol:cytochrome *c* reductase) forms a stable dimer, together 22 subunits, of which only cytochrome *b* is mitochondrially encoded. Complex III requires electron carriers and each electron transferred to cytochrome *c* results in two protons being pumped into the IMS. **Complex IV** (cytochrome *c* oxidase) also forms a dimer, 26 subunits make up ~ 408 kDa. Subunits COX1, COX2, each of which contains copper centres promoting the electron transfer, and COX3, a part of a structural core, are mitochondrially encoded. **Complex V** (the ATP synthetase) is composed of 5 subunits and forms a hydrophobic transmembrane part and a hydrophilic head. (Complexes described in review: Vogel *et al*., 2006; Rutter *et al.*, 2010; Saraste, 1999; Yoshida *et al*., 2001).

to be minimised by uncoupling of respiration ('uncoupling to survive' theory) (Speakman *et al*., 2004), these toxic radicals cause oxidative damage to DNA, proteins and lipids. ROS production increases with age and thus mitochondria have been implicated to play an important role in ageing process (reviewed by Lesnefsky and Hoppel, 2006).

Other important processes in which the organelles have been shown to be significant, include calcium buffering (Rizzutto *et al*., 2003; Hopper *et al*., 2006; reviewed by Glancy and Balaban, 2012), FeS cluster formation (Stemmler *et al*., 2010; Veatch *et al*., 2009) and programmed cell death, where released cytochrome *c*, one of the electron transport chain proteins, contributes to apoptosis (Phaneuf and Leeuwenburgh, 2002). Due to the fact that

mitochondria are not static in the cell as they move, fuse and divide, the involvement in a wide range of cell signalling cascades as well as in cell cycle control (Veatch *et al*., 2009) is strongly supported and connects those important organelles to development biology but also to abnormal responses such as in disease (reviewed by McBride *et al.*, 2006).

1.1.4. The human mitochondrial genome, its maintenance and transcription.

Even though the genetic role is universally conserved, mtDNA shows quite incredible variation in size, conformation and even gene content (Gray *et al*., 1998). Many mtDNA are circular, however linear molecules were found as well (reviewed by Nosek *et al*., 1998). Mitochondrial genome size can range from 6 kbp in the human malaria parasite to 367kbp, which is the largest mitochondrial genome sequenced (Unseld *et al*., 1997). Human mtDNA is quite distinct in its form and size. It is a double stranded, closed covalent circular genome that is relatively small in size, 16 596bp and encodes 13 polypeptides, ribosomal RNA 16S and 12S, and 22 tRNAs (Figure 1.3). All the protein encoding genes that

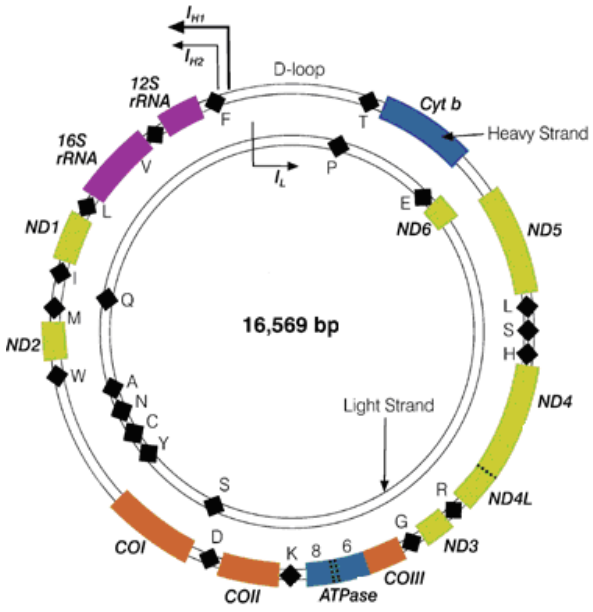

Figure 1. 3. Organisation of the human mitochondrial genome.

The guanine-rich *heavy* strand encodes most of the mitochondrial genes, 2 rRNAs (purple bars), 14 tRNAs (black diamonds, with single letter code) and 12 ORFs (green = complex I, blue = complex III, orange = complex IV, grey/blue = complex V). The guanine poor *light* strand encodes 8 tRNAs and 1 ORF (ND6). The genome lacks introns and harbours the displacement loop (D-loop or 7S DNA), the only triple stranded regulatory non-coding region. Transcription initiation promoters (I_{H1}, $I_{H2,}$ I_L) and their directions are indicated by bent arrows. The image was adapted from Kyriakouli *et al*., 2008.

are transcribed from mtDNA and the transcripts subsequently translated generate components of complexes involved in oxidative phosphorylation. The mitochondrial genome is protected by DNA-binding proteins that help compact the structure and form nucleoids. Due to its dynamic characteristic, the composition of nucleoids in mitochondria is debated as additional factors may be recruited when genome is copied and expressed. Moreover, there is no physical barrier between transcription and translation in mitochondria and these processes may be linked (Wang *et al*., 2007; Rorbach *et al*., 2008). Enriched preparation of mammalian mtDNA has given a number of nucleoid proteins, which could be peripheral (Bogenhagen *et al*., 2008; He *et al*., 2007; Reyes *et al.,* 2011). This may suggest that such packaging functions as an important regulator of gene expression containing all the key factors required for the replication, transcription of the mtDNA and possibly translation, however it is not agreed upon in the field (Bogenhagen, 2012; Kukat *et al*., 2011; He *et al*., 2012). Moreover, nucleoids association with IMM facilitates the import, complex assembly and coordination with cytosolic translation and nuclear encoded proteins insertion. Peripheral nucleoid proteins were suggested to provide intertalk between ER-bound cytosolic ribosomes and mitochondrial transcription/translation that occurs close to the assembly point (Spelbrink, 2010). Mitochondrial transcription is initiated in the D-loop region, where two promoters (I_{H1} and I_{H2}) are located only about 100 bp away from each other and transcribe in the same direction (illustrated in Figure 1.4). The third transcription initiation site (I_L) is also situated in the D-loop and transcribes in the opposite direction (Figure 1.4) (reviewed by Falkenberg *et al*., 2007; Peralta *et al*., 2012). Transcription initiation requires cooperation of three proteins: mitochondrial transcription factor A (TFAM), mitochondrial transcription factor B (TFB1M and TFB2M) and mitochondrial RNA polymerase (POLRMT) (Falkenberg *et al*., 2002; McCulloch and Shadel, 2003; Metodiev *et al*., 2009; Sologub *et al*., 2009; Litonin *et al*., 2010). TFAM as the main component of the nucleoids, without sequence specificity binds, unwinds and bends DNA, playing a function in both mtDNA maintenance and transcription (Parisi and Clayton, 1991; Dairaghi *et al*., 1995; Kukat *et al*., 2011). For transcription, TFAM forms a dimer and recognises specific sequences upstream of I_{H1} and I_{H2} promoters, unwinding DNA to provide access for the other components. TFB1M was shown to methylate the two adenines at the 3' terminus of 12S RNA (Metodiev *et al*., 2009) and TFB2M

acts as a heterodimer with the RNA polymerase, POLRMT. This protein is a single subunit protein (140kDa) composed of a C-terminal domain exerting conserved catalytic activity and N-terminal domain containing two putative

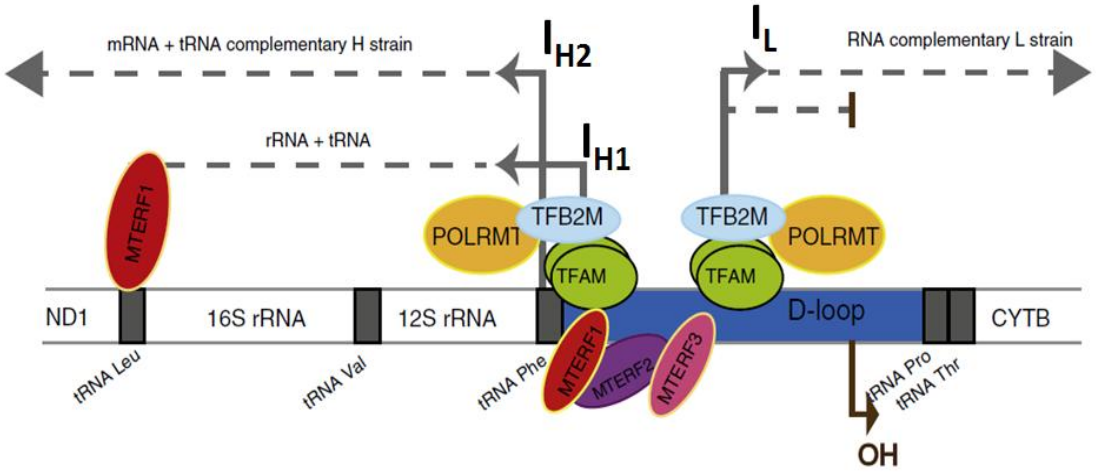

Figure 1. 4. mtDNA transcription machinery in the D-loop.

Initiation from I_{H1} promoter results in transcription of only 2 rRNAs and two tRNA (Val and Phe) terminating at the MTERF1 bound to the tRNA (Leu). I_{H2} and I_L originated transcripts represent the full length of mtDNA. The position of the origin of replication on the heavy strand (OH) is also indicated. The proteins MTERF1, MTERF 2 and MTERF3 bind to the promoter region and play modulating functions. The image was adopted from Peralta *et al,* 2012.

pentatricopeptide repeat (PPR) motifs. The family of MTERF proteins have roles, not only in initiation, termination, but also in modulation of transcription by replication pausing and translation. In vertebrates there have been four members identified, MTERF1-4 (Kruse *et al*.,1989; Linder *et al*., 2005; Yakubovskaya *et al*., 2010; Wenz *et al*., 2009; Pellegrini *et al*., 2009; Camara *et al*., 2011; Peralta *et al*., 2012). The transcribed polycistronic transcripts are punctuated with the tRNAs that are assumed to signal for the 5' endonucleolytic cleavage by RNase P (Ojala *et al*., 1981) and 3' end cleaving by RNase Z type protein ELAC2 (Vogel *et al*., 2005; Rossmanith, 2011) of the tRNAs. This processing of transcription units results in separate species of rRNAs, tRNAs and mRNAs. Further maturation is required for all but the mt-rRNAs and includes the addition of the CCA triplet to the 3' end of tRNAs by the ATP(CTP):tRNA nucleotidyltransferase (Rossmanith *et al*., 1995) and subsequently the addition of an amino acid by the specific aminoacyl-tRNA

synthetase. Mitochondrial mRNAs are finally matured by addition of either oligo- or poly(A) and their 3' ends.

1.2. Mitochondrial protein synthesis in human organelles

There are aspects of protein synthesis in mitochondria that differ from the cytosol, however the process is still divided into three steps as in other systems; initiation, elongation, and termination followed by ribosome recycling. In order to synthesise the 13 mtDNA encoded proteins, human mitochondria use their own translational apparatus that is different from the one found in the cytosol. First of all, the mammalian mitochondrial ribosomes (mitoribosomes) responsible for protein synthesis differ extensively from the counterpart found either in cytosol, bacteria, chloroplasts or indeed a number of mitochondrial ribosomes from yeast and other species (Suzuki *et al*., 2001a and 2001b; Koc *et al*., 2001a; Chrzanowska-Lightowlers *et al*., 2011).

Second, mammalian mitochondrial mRNAs are either monocistronic transcripts as in the majority of cases (9 of 13 ORFs) or present as bicistronic transcripts. This situation occurs only twice where there are overlapping reading open frame within *RNA14*, the transcript encoding ATP8 as the upstream ORF with ATP6 as the second ORF. There is a similar arrangement in *RNA7*, with ND4L at the 5’ end and ND4 as the more 3’ ORF. The typical Shine-Dalgarno sequence, found in prokaryotes for recognition and determinant of the correct selection for the start side on the ribosome, is absent in mitochondrial mRNAs. Instead the majority of start codons are found at the very 5' terminus or within 3 nucleotides of this (*MTND1*, *MTCO1* and *MTATP8*). The exceptions are the downstream ORFs of the bicistrons (Anderson *et al*., 1981). Analysis using SHAPE chemistry by (Jones *et al*., 2008) suggests that the majority of the mitochondrial transcripts are highly unstructured at the 5’ end but that two of them (*MTCyB* and *MTND5*) predict stem loop structures near the start site or closer to 3' terminus, respectively. Therefore it is posited that recruitment of ribosomes in mitochondria starts directly at the 5’ terminus, which in most cases is accessible within single stranded regions (Liu and Spremulli, 2000). A further unusual feature relevant to translation is the absence of 3' untranslated (UTR) regions in the majority of transcripts (described in Temperley *et al*., 2010a). This feature is derived from the compactness of the genome and means that for

seven mt-transcripts the 3' stop codons are generated only upon polyadenylation where the poly(A) tail completes the UAA stop codon (Temperley *et al*., 2010b). Apart from the stop codon formation the function of poly(A) tail addition in mitochondrial transcripts is not clear (Gagliardi *et al*., 2004). Poly(A) tails extensions can have different length between the transcripts and between different cell types, reports of which show conflicting data concerning poly(A) function in mt-transcripts stability or a function as translation modulator (Temperley *et al*., 2003; Tomecki *et al*., 2004; Nagaike *et al*., 2005; Slomovic *et al*., 2008, Wydro *et al*., 2010).

Due to the essential lack of UTRs on human mitochondrial mRNAs, there must be other mechanisms that promote and maintain stabilization and translation of transcripts, which is essential for gene expression. In *Saccharomyces cerevisiae* expression of each mitochondrial mRNA is regulated by individual, well characterised translational activators and most of them bind to 5' UTRs (reviewed in Herrmann *et al*., 2012). Very little is known about translation regulation in mammalian mitochondria and to date only the synthesis of cytochrome *c* oxidase subunit I have been shown to have translational activator, TACO1 (Weraarpachai *et al*., 2009). Its mutation results in cytochrome *c* oxidase deficiency, even though the mRNA levels remain normal. The COX synthesis and assembly could be restored by expression of the wild type TACO1 in patient fibroblasts. Yet, exact molecular mechanism remains elusive. Human mitochondrial poly(A) polymerase (hmtPAP) has also been identified and shown to be responsible for polyadenylating 3' termini of mitochondrial transcripts (Tomecki *et al*., 2004, Nagaike *et al*., 2005). However the mutated hmtPAP has been shown to accompany short tails but the effect on stability is not the same for all the transcripts (Crosby *et al*., 2010; personal communication with W.C. Wilson), which was also seen in Tomecki *et al*., and Nagaike *et al*., data. Recent characterisation of the first poly(A)-specific exoribonuclease in mitochondria, PDE12, also supported the observations that there is no universal rule in the behaviour of mt-mRNAs in the absence of a poly(A) tail. The over-expression of this deadenylating enzyme in cultured cells resulted in levels of three transcripts being unregulated (*MTND1*, *MTND2* and *MTND5*) and other three tested showed a decrease (*MTCO1*, *MTCO2* and *RNA14*) (Rorbach *et al*., 2011).

All the data thus shows that there is no single behaviour common to all transcripts in the absence of a poly(A) tail. Moreover, there may still be an uncharacterised mitochondrial poly(A) binding protein, that is required for correct translation efficiency (Wydro *et al*., 2010), whether those enzymes (i.e. hmtPAP, PDE12 and mtPABP1) themselves contributes to the stability of mitochondrial messengers and whether other factors are involved to contribute to the translation process via poly(A) tails remains an open question.

Understanding the regulation of mitochondrial transcript metabolism is still far from complete and many other factors need to be identified and for those that have been reported the molecular mechanism of action requires to be further characterised. Recent years studies on mechanisms underlying mitochondrial diseases hugely contribute to our understanding. Associated with a mitochondrial disease, Leigh syndrome French Canadian, a leucine-rich pentatricopeptide-repeat containing protein (LRPPRC) has been shown to be involved in translational control of mitochondrial mRNAs. The latest conditional *Lrpprc* knockout mice studies showed that in mammalian mitochondria LRPPRC not only is necessary for maintenance and stability of non-translated mRNAs pools via an RNA-independent complex formation with a stem-loop interacting RNA binding protein (SLIRP)(Sasarman *et al*., 2010), but also controls polyadenylation, thus affecting translation (Ruzzenente *et al*., 2012). Moreover, its post-translational regulation role together with SLIRP has been connected to its ability to bind mRNA coding sequences and suppress 3' degradation by exonucleolytic PNPase (Chujo *et al*., 2012).

Finally, for many years one of the most characteristic and striking features in the mitochondrial translation mechanism has been the predicted changes to its genetic code (Anderson *et al*., 1981). These centred on the termination codons, the standard UGA is now decoded as tryptophan. The UAA termination triplet is used by 9 of the 13 mitochondrial open reading frames (*MTCyt b*, *MTATP6*, *MTCO3*, *MTND1*, *MTND2*, *MTND3*, *MTND4*, *MTND4L* and *MTND5*) whilst both *MTCO2* and *MTATP8* use UAG. The three nucleotides following the final coding triplet in mitochondrial transcripts *MTCOI* and *MTND6* were identified as AGA and AGG respectively (Anderson *et al*., 1981). None of mitochondrial tRNAs has a capacity to decode these triplets that would normally be recognised as arginine. Therefore these were interpreted and became accepted as termination

signals and the literature described human mitochondria as employing 4 stops; UAA, UAG, AGA and AGG.

However recently, human mitochondrial ribosomes have been shown to frameshift when either AGA or AGG reach the A-site during translation (Temperley *et al*., 2010a). In such a position those codons cannot be recognized by either mt-tRNA or any release factor and the stable secondary structure generated downstream of the triplet blocks forward movement of the ribosome. The analysis of *MTCOI* and *MTND6* transcripts has shown that each of the codons is directly preceded by a 'U', which could now be shifted from the P-site and localised to the 5'-most position in the A-site. Therefore, by performing one nucleotide shift ribosomes position a standard stop triplet, UAG in the A-site, which now can be recognised by mtRF1a and the termination followed by recycling can continue (Lightowlers and Chrzanowska-Lightowlers, 2010).

1.2.1. Characteristics of the mammalian mitochondrial ribosome

There are highly conserved morphological regions accurately reflecting the tight functional and structural constraints on all ribosomes, based on several 3D cryo-EM maps. Analysis of bovine 55S mammalian mitoribosomes reveal an evolutionary divergent form of ribosome compared to all known ribosomal structures (Sharma *et al*., 2003; Koc *et al*., 2001a; Koc *et al*., 2001b).

The mammalian mitoribosomes consist of a small 28S subunit (mt-SSU), which contains the 12S rRNA, and the large 39S subunit (mt-LSU) with 16S rRNA. When together as a complete monosome they have relatively small sedimentation coefficient of 55S compared with bacterial ribosomes 70S (Figure 1.5), eukaryotic 80S and even yeast mitoribosomes that are also 70S. They do, however, have a slightly larger molecular mass of 2.71MDa than the ribosomes from *E. coli* (2.49MDa), suggesting a more porous structure to the mitoribosome. Another unusual feature is the loss of significant regions of rRNA. Perhaps the most dramatic and striking feature is the reversal of the RNA:Protein ratio. While in bacteria ribosomes there is conventionally 70% rRNA with 30% protein, the mammalian mitoribosomes has removed various regions of sequence from the rRNA and acquired a larger repertoire of proteins to generate 70% protein and only 30% rRNA (Sharma *et al*., 2003 and 2009). It appears that during the course of evolution a number of proteins, some of which

are novel proteins without bacterial ortologues, have taken over some of lost rRNA functions (O'Brien, 2003 includes a table of human mitochondrial

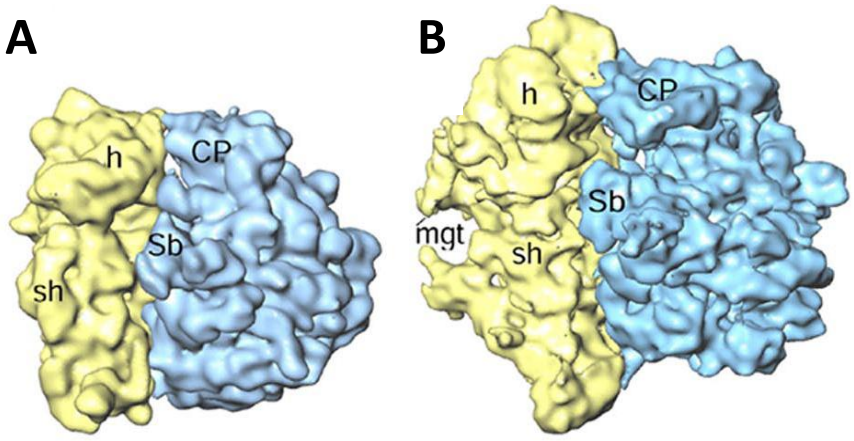

Figure 1. 5. Cryo-EM map of ribosomes adopted from Sharma *et al*, 2009.

(A) *E. coli* 70S ribosome. **(B)** Mammalian 55S ribosome. For both panels LSU is indicated in blue and SSU in yellow. The map shows characteristic features of a ribosome: central protuberance (CP), stalk base L7/L12 (Sb) on the LSU and the head with the shoulder of the SSU, mRNA gate (mtg).

ribosomes, compared to *E. coli* ribosomal proteins). As opposed to the cytosolic ribosomes, subunits of which are mostly connected via RNA-RNA bridges, truncation of several helices of mt-rRNA in both mt-SSU and mt-LSU are structurally replaced with proteins affecting intersubunit space, which gives rise to a wider opening in this region that is crucial for tRNAs and translation factor access.The two proteins that mainly cause this alteration are S4 and S20, which are missing in mt-SSU, but in bacteria are placed close to tRNA in A- and P-site (Koc *et al*., 2010). This is the region of the subunit that interacts with the central protuberance of the mt-LSU (Koc *et al*., 2010). As a consequence the mt-SSU and mt-LSU are held by seven protein-protein bridges, two protein-RNA bridges, five RNA-RNA bridges and one connection that recruits both components of both subunits (Sharma *et al*., 2003). In this altered composition of ribosomal proteins there are 12 prokaryotic ribosomal proteins absent from mitoribosomes (Koc *et al*., 2001a, Koc *et al*., 2001b). There are also additional proteins that have no bacterial orthologues causing the reversed RNA to protein ratio. This additional protein mass quite heavily shields the major part of mt-rRNA.

The secondary structure of 12S rRNA (Figure 1.6) (950 nucleotides compared with 1542 in *E. coli*) lacks an anti-Shine-Dalgarno sequence, reflecting the

specific characteristics of mt-mRNAs, also fifteen helices are missing and several of existing ones are shorter (Koc *et al*., 2001a; Sharma *et al*., 2003).
The 3' terminus of 12S rRNA has two highly conserved dimethylated adenines and the disruption of the methyltransferase TFB1M (TFB1M and TFB2M are the only rRNA modifying enzymes known in mitochondria to date) responsible for this modification was shown to be embryonic lethal due to the impaired ribosomal assembly and defective mitochondrial translation (Metodiev *et al*., 2009). Most of the lost fragments are situated on peripheries or away from the decoding centre (DC) of the mt-SSU. The only protein in the DC left that is the

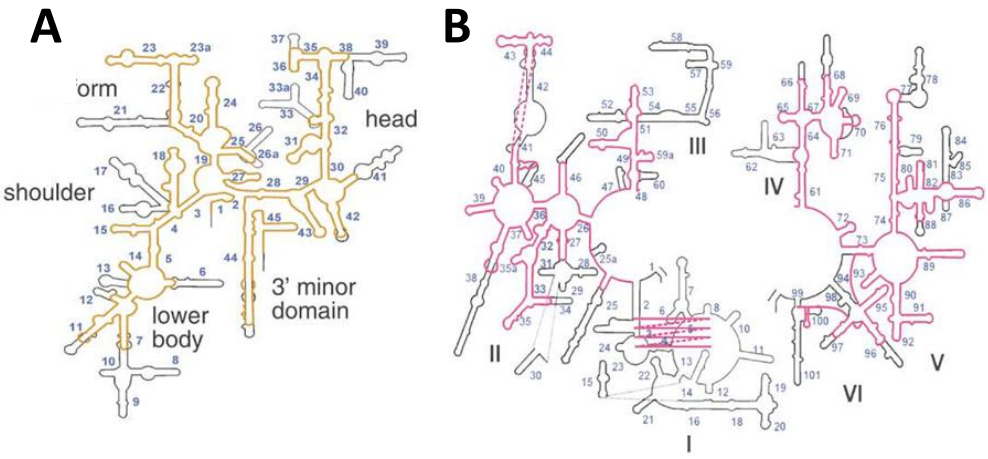

Figure 1. 6. The diagram of small and large subunit RNA of bovine mitoribosome adopted from Sharma *et al*, 2003.

(A) Secondary structure of mitochondrial SSU rRNA (yellow) with characteristic features indicated and **(B)** mt-LSU rRNA (purple) with six domains of the structure numbered. In both panels the fragments absent from 55S, but present in bacterial 70S are indicated in black.

most conserved is MRPS12. It makes the direct contact with the tRNA at the subunit interface (Koc *et al*., 2010). The cryo-EM map also reveals that only 19% of the lost rRNA has been replaced by protein mass (Sharma *et al*., 2003), Therefore the mt-SSU is longer, but significantly narrower in the midbody than bacterial 30S (Sharma *et al*., 2003). Currently the literature describes the mt-SSU as containing 29 proteins, 14 of them have bacterial homologues, each of which is 4-25 kDa larger than and only 20-40% identical to bacterial equivalent, whereas the 15 remaining proteins are specific to mitochondria only (Koc *et al*., 2001). Some of the new mitochondrial proteins also have adopted supplementary roles for the cell, this includes DAP3 (MRPS29), which as the TNF-α and FAS positive mediators together with MRPS30 have been reported

to play a role in apoptosis (Suzuki *et al*., 2001). MRPS36 also influences cell cycle and cell growth (Koc *et al*., 2010).

The structural organisation of one of the most remarkable features of SSU is a triangular gate like structure allowing the mRNA to enter, which has evolved to recognise unusual mitochondrial mRNA. In bacteria it is surrounded by 3 proteins S5, S3 and the S4 protein, which has been shown to be important in proofreading during translation (Van Acken, 1975). Loss of S3 and S4 is compensated by mitoribosome-specific proteins and by S5 being larger (Sharma *et al*., 2003). Moreover, as this structure is situated on the solvent side of the mt-SSU it is ideally positioned to play a part in regulating mitochondrial translation initiation.

Another significant structural feature is a central platform of mt-SSU. The mt-SSU proteins that contribute to formation of the P-site in the complete monosome are well conserved and one of these is MRPS18. In human mitochondrial there are 3 variants, whilst in bacteria there is a single orthologue that is located in the middle of the platform and changes conformation upon mRNA binding (Koc *et al*., 2001a). The 3 mt-isoforms are only 25-30% identical and originate from different genes, which again may implicate for the existence of mt-SSU sub-populations or other possible specific mitochondrial translation roles in different cells or tissues.

Similarly to the mt-SSU, the mt-LSU is also larger than the bacterial large subunit. It consists of ~48 proteins, 28 of which have bacterial homologues, all more than 75% identical, but due to structural differences between bacterial 50S and mt-39S, 5 of the bacterial proteins could not be localised on the cryo-EM mitoribosome map (Sharma *et al*., 2003). Twenty of remaining proteins are specific to mitochondria only and mostly located on the porous subunit surface (Koc *et al*., 2001b). The mt-rRNA 16S of the large subunit is 1571 nucleotides long and is highly truncated relative to the bacterial equivalent (Cannone *et al.,* 2002). The truncations mainly affect i) secondary structures outside the main body of the subunit, ii) a domain situated below the L7/L12 stalk that is involved in the GTPase activities of several of translational factors and iii) crucial helices involved in the peptidyl-transferase centre (PTC) function. The highly variable stem-loop region just outside PTC is lost in 16S in the peptidyl-transferase loop, and the loss of which has been shown to slow the protein release extremely (Das *et al*., 2011). This lost region in mitoribosomes, in bacteria is responsible

for releasing the folding competent state (FCS) of proteins transformed from unfolded state by PTC. Overall about 28% of the 'lost' regions of 16S are replaced by mitochondrial proteins (Koc *et al*., 2010), some of which again may have overtaken functions of lost rRNA to maintain the protein synthesis efficiency.

The most striking and debatable RNA loss locates to the central protuberance of mt-LSU. In bacteria it is formed by 5S rRNA and MRPL1, both of which are missing in mitoribosomes. However the mitochondrial genome does not code for 5S rRNA, a prokaryotic 5S rRNA binding protein homologue, MRPL18, has been found in 55S suggesting its translocation from the cytosol. Investigations by Koc *et al.* in 2001 on possible incorporation of 5S into mitoribosomes from cytosol showed that after extracting rRNA from bovine mitochondria, cytosolic and bacterial ribosomal subunits, no 5S or other corresponding RNA species could be found in 55S compared to 80S and 70S ribosomes (Koc *et al*., 2001b). These findings were also supported by the fact that the MRPL18 lacks the typical arginine rich N-terminal part, responsible for binding 5S in bacteria. Further attempts to detect 5S rRNA in mitochondrial ribosomes were unsuccessful (Sharma *et al*., 2009; Sharma *et al*., 2003). Therefore its function inside the organelles and the import processes provoked a debate until Smirnov *et al.*, (2010 and 2011) decided to readdress the question of 5S presence in mitoribosomes. It has been then claimed that the association of 5S rRNA with the core of mt-LSU is rather fragile. Thus using milder and more rapid isolations of mitoribosomes, via co-immunoprecipitation of FLAG tagged versions of either the mt-LSU protein, ICT1, or mt-SSU protein, MRPS27, 5S could be detected in mitochondrial ribosomes. Moreover, two new factors have been reported to participate in redirecting this rRNA from cytosol to mitochondrial matrix, namely MRPL18 via formation of non-canonical complex with S5, and rhodanese (Smirnov *et al*., 2010; Smirnov *et al*., 2011).

Other regions of mt-16S rRNA that have been lost compared with bacterial ribosomes are mapped to two domains, I and III, which most importantly focus around polypeptide exit tunnel. These rRNA regions are dramatically shorter, making it difficult to predict the secondary structure (Figure 1.6.). Reconstitution of mitoribosomal exit tunnel by cryo-electron microscopy revealed a substantially different structure with additional mass and protuberances

compared with other ribosomes (Sharma *et al*., 2009; Sharma *et al*., 2003). Moreover it was shown to be wide enough to allow an access to the solvent via the polypeptide accessible site (PAS), provoking a hypothesis that there may be two different pathways for newly synthesised polypeptides to leave the mitoribosome (Koc *et al*., 2010). The detailed yeast analysis of chemically cross-linked mitoribosomal proteins and mass spectrometry characterised a unique complex network of interacting proteins found in this region that are specific to mitochondria (Gruschke *et al*., 2010). In yeast mitoribosomes there are four proteins (MRPL4, MRPL40, MRP20, and MRPL22) that form the rim of the mitochondrial exit tunnel and make a direct contact with nascent polypeptide chain. MRPL27, MRPL13 and MRPL3 were found in close proximity to the tunnel indirectly supporting the formation and stability of the structure.

Similarly, the portion of L7/L12 stalk tertiary structure is lost implying alternative mitochondrial organisation of this region in order to be retained on the peripheries of the subunit, as observed on cryo-EM (Sharma *et al*., 2009; Sharma *et al*., 2003).

The interface part of mt-LSU also lacks several helical segments and as a consequence the tRNA binding sites on the mt-LSU have been altered. Apart from the A-site finger that contacts the D- and T loop of tRNAs, both structures of which are significantly smaller in mt-tRNA, the rest of this pocket has been conserved. Mitochondrial P-site however, with most tRNA contact points preserved, exhibits additional and unique P-site finger composed entirely of unidentified proteins and possibly providing stronger or additional interaction with tRNAs or specific mitochondria translation factors (Koc *et al*., 2010). Most of the E-site tRNA contacts found in bacterial LSU have been either lost in mitochondria or the region significantly altered with only one contact point present. This essentially means that no E-site exists in mammalian mitoribosomes (Koc *et al*., 2010).

The initial observation of ribosomes inside mitochondria (O'Brien *et al*., 1967, O'Brien *et al*., 1971) and further detailed proteomics analysis carried out by Koc, Spremulli, Suzuki and Watanabe has contributed to an immense progress in understanding of the structure and function of mammalian mitoribosomes. However, due to conformational heterogeneity and low abundance of the

mitoribosomes and therefore lack of high- resolution structural information much remains to be learned. Not only is the list of ribosomal proteins still growing (Richter *et al*., 2010b), but also the list of the nuclear encoded partners interacting with mitoribosome, which are involved in a variety of processes ranging from the biogenesis and modifications through processing and assembly to activity.

It has long been suggested that in order to perform translation mitoribosomes interact peripherally with the inner membrane, in part due to the hydrophobicity of the synthesised proteins (Liu and Spremulli, 2000). Recent studies have identified partners that are in close association with the rim of the large subunit exit tunnel proteins and act to facilitate co-translational insertion of the nascent polypeptide chains in to the mitochondrial inner membrane. The most studied protein of the insertion machinery is Oxa1p in yeast. It has been shown that Oxa1p is an integral membrane protein with its hydrophilic C-terminal tail exposed to mitochondrial matrix space, supporting the protein-ribosome interaction (Jia *et al*., 2003; Jia *et al*., 2009). Further analysis has shown that Oxa1 lies in a close proximity with MRPL20 and MRPL40, components of the exit tunnel, all of which can be chemically cross-linked and affinity purified with each other and emerging nascent chain (Hell *et al*., 2001). MRPL40 also contains a mitochondrial specific C-terminus that is crucial for the accurate translation and assembly of synthesised products (Jia *et al*., 2009). Additionally to Oxa1p, there are a number of yeast proteins identified to play a role in insertion machinery and some of them, such as Mba1 and Mdm38, directly interact with mitoribosomes and are responsible for inner membrane insertion of different specific OXPHOS proteins (Bauerschmitt *et al*., 2010, Gruschke *et al*., 2010, Gruschke *et al*., 2011, Lupo *et al*., 2011). To date however only three yeast homologues have been reported to be represented in mammalian mitoribosomes, i.e. Oxa1L as a homologue of Oxa1p, LETM1 (Mdm38 in yeast) and Cox18 (Oxa2 in yeast) (Gaisne and Bonnefoy, 2006, Haque *et al*., 2010, Piao *et al*., 2009). In addition, mitochondrial elongation factor-Tu has been hypothesized to also have some chaperone properties based on its *in vitro* ability to enhance protein folding and prevent thermal aggregation of proteins. It can, therefore, be a candidate to contribute to insertion/ folding of newly synthesised protein but further investigation is required (Suzuki *et al*., 2007).

Human Oxa1L, like its yeast homologue, binds mitoribosomes via C-terminal tail (CTT), but unlike Oxa1p, the tail of mammalian protein forms different structure. This cross-links to mitochondrial specific ribosomal proteins, MRPL48, 49 and 51 that are present at the back of the mammalian mt-LSU but do not exist in yeast mitoribosomes (Haque *et al*., 2010). Oxa1L-CTT does not seem to interact directly with the exit tunnel, but rather with the solvent side of the mammalian mt-LSU close to PAS and is part of a larger complex, the composition of which is unknown (Stiburek *et al*., 2007). As mentioned before methylation of small ribosomal subunit RNA is not the only post transcriptional modification found in mitochondria. Another three modification positions have been found on both 12S and 16S rRNA, which need to be confirmed and no responsible enzymes have been found (reviewed by (Rorbach and Minczuk, 2012). Another well-known modification involving ribosomes is post-translation phosphorylation of ribosomal proteins that also regulates a variety of other mitochondrial processes such as oxidative phosphorylation, mitochondrial induced apoptosis via DAP3 and MRPL40 or translation elongation (He *et al*., 2001). The pilot study by (Miller *et al*., 2009) identified 24 mitoribosomal proteins that are phosphorylated at serine, threonine or tyrosine residues. Proteins involved in these regulatory processes were found mainly in ribosomal functional sites, such as the polypeptide exit tunnel and mRNA binding regions, but also the L7/L12 stalk region. It has been suggested that phosphorylation may introduce conformational or structural changes altering protein-protein and protein-RNA cross-talk during stages of translation (Miller *et al*., 2009).

Even though remarkable progress has been made in the past decade concerning function and structure of 55S, the knowledge about the transcription of rRNA genes encoded by mtDNA and its coordination with the transcription, translation and the import of ribosomal proteins encoded by nuclear genome is limited, therefore very little is known about biogenesis, assembly of mitoribosomal subunits and the control over those processes. Detailed investigation of ERAL1, a GTP-ase RNA binding mitochondrial protein, has demonstrated that it binds a stem loop at 3' of 12S mt-rRNA, where dimethylation of two adenines was identified in ribosome maturation events. Since ERAL1 depletion results in decreased protein synthesis with lost stability of mRNA due to rapid decay of the 12S mt-rRNA it has been characterised as a

mitochondrial RNA chaperone that protects mt-SSU rRNA during formation of subunit (Dennerlein *et al*., 2010; Metodiev *et al*., 2009; Uchiumi *et al*., 2010). ERAL1 is the only factor characterized to play such a role to date. However, another protein, pentatricopeptide repeat domain protein 3 (PTCD3), has been shown to associate with rRNA of the small subunit and to regulate mitochondrial translation, its exact role and underlying mechanism of the process remains unknown (Davies *et al*., 2009). In contrast, there are a number of proteins implicated to play a role in the biogenesis and assembly of 16S mt-rRNA. First of all, mTERF4 that is a member of transcription factors family has been unexpectedly shown to have a direct role in ribosomal biogenesis in mitochondria (Camara *et al*., 2011). The depletion of mTERF4 results in increased levels of both subunits, however they are unable to assemble a monosome, and so reduce translation. It exerts its action due to its ability to bind 16S rRNA. It forms a stoichimetric complex with NSUN4, which belongs to m5C RNA methyltransferases, but lacks the targeting domain, thus needs to be recruited to the large mitochondrial subunit. However its contribution in ribosome maturation remains unclear. Inaccurate ribosome assembly was also observed in the absence of nitric oxide-associated-1 (NOA1) knock-out mouse embryonic fibroblasts cells (MEFs). Apart from the fact that the loss of this GTP binding protein impairs the protein synthesis it also caused aberrant migration of mt-LSU observed by sucrose gradient centrifugation, indicating that NOA1 has a role in correct assembly of 55S (Kolanczyk *et al*., 2011). Another GTPase, Mtg1, has been localised to mammalian mitochondria (Barrientos *et al*., 2003). It is a homologue of a yeast GTPase protein family, three members of which have been identified to regulate the assembly of LSU (Paul *et al*., 2012) and even though Mtg1 has been shown to partially rescue the respiratory deficiency in a yeast *mtg1* mutants, its exact function in mammalian mitochondria again has not been characterised. A different mitochondrial protein, C7orf30, however has recently been shown to associate with the 55S and thereby directly regulates the formation of mitochondrial monosomes (Rorbach *et al*., 2012, Wanschers *et al*., 2012).

Finally, a detailed mechanism of action contributing to ribosomal biogenesis and involved in regulation of ribosomal integrity has been reported in (Bonn *et al*., 2011). Here the *m*-AAA protease that is present in the IMM is involved in a

quality control of proteins by processing and mediating protein maturation during mitochondrial biogenesis. The maturation of imported ribosomal proteins is essential for assembly of ribosomes and one example is MRPL32. The final processing and folding of this depends on *m*AAA protease and unusual MRPL32 features. It demonstrates presequence-assisted folding after the import into the matrix space, which differs to the majority of presequence-containing proteins that are processed upon import by the mitochondrial processing peptidase (MPP). The integrity of a tightly folded cysteine containing domain of MRPL32 ensures its folding and inhibits the proteolysis initiated at the N terminus by *m*AAA of newly imported proteins.

1.2.2. Initiation of mitochondrial protein synthesis

Since the mt-SSU has been demonstrated to have GTP binding activity it is probable that this subunit is involved in the initiation step of translation (Suzuki *et al*., 2001) and requires recruitment of the mt-mRNA. With the exception of the 2 bicistronic transcripts, mammalian mitochondrial mRNAs generally do not possess either 5’ (maximum of three nucleotides preceding a start codon) or 3’ untranslated regions, which in other systems often contribute to mRNA recognition and ribosome binding (Liu and Spremulli, 2000). Thus, translation in mitochondrion is essentially assumed to start directly at the 5’ terminus. Mitochondrial ribosomes have been shown to be highly inefficient in recognising mRNAs containing more than 3 nucleotides prior to the start codon (Montoya *et al*., 1981). The formation of a stable initiation complex was decreased by 80% when the transcript encoding subunit II of cytochrome *c* oxidase was extended by 12 nucleotides at 5' end. This emphasised the leaderless nature of mitochondrial transcripts (Christian and Spremulli, 2010). Despite two initiation factors having been characterised (Koc and Spremulli, 2002) initiation factor 2 (IF2) promoting the binding of fMet-t-RNA to the small subunit and IF3, which facilitates dissociation of 55S ribosomes stimulating initiation complex formation, the exact mechanism behind directing mitoribosomes to the initiation codon is not known. The mitochondrial IF3 interacts with 55S particles to loosen subunits interactions to promote disassociation, maintain the subunits in the dissociated state and facilitate subsequent binding of fMet-tRNA in the presence of mRNA and mtIF2 (reviewed in Christian and Spremulli, 2010). After

the subunits have been disassociated mtIF3 has been shown to have the ability to remove prematurely bound fMet-tRNA and mtIF2 in the absence of mRNA from 28S. When the mRNA is bound however, mtIF3 has no effect on further interactions (Bhargava and Spremulli, 2005). This has led to a conclusion that the formation of the initiation complex requires a specific order, in which first mRNA is positioned randomly on the mitochondrial small subunit entering via the protein-rich mRNA entrance gate and only binding of mtIF3 can mediate 5' start codon to be positioned correctly in the P-site. Also, the binding of this initiation factor to the platform region of 28S is achieved in a way that the intersubunit bridges cannot be physically formed when mtIF3 is bound (Haque *et al*., 2011). The latter protein consists of two domains, N-domain and C-domain, separated by a flexible linker. The C-domain shows a strong affinity for the 28S SSU and the contacts are slightly facilitated by the linker. This was identified by studying mutations that were introduced in this region and that resulted in the loss of complex formation and subunit disassociation activity (Christian and Spremulli, 2009). The N-domain of the protein is positioned near the anticodon stem-loop of the initiator tRNA in the P-site suggesting a role reducing the binding of fMet-tRNA when no mRNA is present on the small subunit or in facilitating the correct positioning of mRNA (Haque and Spremulli, 2008). Toeprint analysis of the mitochondrial initiation complex revealed that after the first 17 nucleotides of the transcript have bound the 28S, the subunit pauses to inspect the mRNA and this also occurs in the absence of start codon (Christian and Spremulli, 2010). Moreover, it shows that the mitochondrial ribosomes can discriminate between the 5' terminus or internal AUG, and so when the start codon is not present at the 5' –end, the mRNA continues sliding off without associating. The binding of fMet-tRNA to the ribosome and codon-anticodon interaction is mediated by the mtIF2-GTP. In mtDNA there is only one gene coding for Met-tRNA that takes part in both initiation and elongation and formylation of the Met-tRNA. This allows it to bind mtIF2 and the elongation factor shows no detectable affinity to fMet-tRNA and the participation of the tRNA between phases occurs by a competition between the transformylase and the elongation factor (mtEF-Tu) (Spencer and Spremulli, 2004). The binding of mtIF2 is influenced by GDPNP, the non-hydrolyzable analogue, and is organized into four domains. These include the N-terminal domain that interact with the small ribosomal subunit, a central G-domain (G1, G2 and G3) that

organises the structure of the protein, thus facilitating binding and contact with the LSU, and two C-terminal domains, involved in binding the initiator tRNA (Spencer and Spremulli, 2005). Interactions between mRNA, mtIF3, mtIF2 and fMet-tRNA with the 28S SSU are followed by the large subunit joining, hydrolysis of GTP to GDP, release of the initiation factors and the full 55S initiation complex formation, which is then ready to move to the next step of synthesis.

1.2.3. Elongation of mitochondrial translation

Limited information is available regarding translation elongation, where to date only three factors are known to be involved, mitochondrial elongation factor-Tu (mtEF-Tu), Ts (mtEF-Ts) and G1 (mtEF-G1). Elongation factors are very abundant and highly conserved throughout evolution and because of the high sequence similarities it is believed that elongation in mitochondria proceeds in a similar fashion to bacteria. This involves the EFs introducing aminoacylated tRNAs to the ribosomal A-site thus facilitating formation of the translation complex (Jeppesen *et al*., 2005). However, the mechanism of the process consists of at least seven separate steps, recurrence of which leads to formation of full-length newly synthesized proteins. In contrast to prokaryotes factors mtEF-Tu does not appear to be present is a free form and can only be isolated from mitochondrial extracts of a bovine liver as a complex with mtEF-Ts, therefore it was postulated that the ratio of two factor in mitochondria is 1:1 (Woriax *et al*., 1997). This is in contrast to *S. cerevisiae* where only EFTu is present (Rosenthal and Bodley, 1987). During elongation the EF-Tu is known to interact with guanine nucleotides, however in mitochondria the mtEF-Tu-Ts complex do not disassociate even at high concentrations of guanine nucleotides and its stability depends on the aa-tRNA (Cai Yc Fau - Bullard *et al*., 2000). Moreover, the dissociation constant for the mtEF-Tu-GDP and for mtEF-Tu-GTP was shown to be more than two orders of magnitude and about 60-fold higher, respectively, than in prokaryotes (Cai Yc Fau - Bullard *et al*., 2000). The crystal structure of the bovine mitochondrial EF-Tu was obtained and has showed that the protein is organized in three domains as in the bacterial counterpart and they share up to 60% similarity (Woriax *et al*., 1995). Mitochondrial domain I and domain II interact with the small subunit of the ribosome also providing the binding site for aa-tRNA and guanine nucleotides,

while domain III also interacts with the 5' end and the acceptor stem loop of aa-tRNA organizing the structure in a pocket for the tRNA (Jeppesen *et al*., 2005). When the mtEF-Tu forms the complex with the mtEF-Ts its structure is changed and differs extensively from either the EF-Tu GTP or GDP-bound isolated from bacteria. There are three points of contact between the factors, which are G-domain and domain III of mtEF-Tu that mostly contact the core of the mt-EF-Ts and the region of both factors contribute to nucleotide exchange process. In contrast, the role of mtEF-Ts is mostly to promote guanine nucleotide exchange with mtEF-Tu. It shares only ~ 30% of sequence conservation with bacterial factors and the most striking difference is the loss of the majority of the coiled-coil domain, which in bacteria has been shown to promote the ability to compete guanine nucleotide binding (Karring *et al*., 2003). The core of the protein consists of β-sandwich in bacteria, whilst in mitochondria its organization differs by the number of β-strands and their arrangement, the N-terminal domain folds in a very similar way (Jeppesen *et al*., 2005).

The translocation step in elongation of protein synthesis depends on an EF-G (Bhargava *et al*., 2004). The protein consist of 5 domains, domains II, III and IV interact with SSU proteins whereas domain I and V with LSU. During translocation the movement of domains III-V inserts in to the decoding centre causing movement of tRNA, while the domains I-II exert the activity of the protein (Shoji *et al*., 2009). In mitochondria, surprisingly 2 forms of this protein have been identified, mtEF-G1 and mtEF-G2 (Hammarsund *et al*., 2001). It is mtEF-G1 that is involved in elongation step. This has been verified by cloned and purified preparations being active on both bacterial and mitochondrial ribosomes (Bhargava *et al*., 2004).

The current model for the elongation of translation in mammalian mitochondrial system (Christian and Spremulli, 2012) begins with the GTP-bound active form of mtEF-Tu. This complex is able to bind aminoacyl-tRNA (aa-tRNA), protecting it from degradation by forming a ternary complex that is now able to enter the ribosome. If cognate codon-anticodon interactions occur to dock the complex in the acceptor site, GTP is hydrolysed to GDP and EF-Tu-GDP is released. Then subsequent interaction with mtEF-Ts and the formation of intermediate complex with mtEF-Tu mediates the transition of GDP to GTP bound to mtEF-Tu for another cycle. Meanwhile, the peptide bond formation between aa-tRNA in the

A-site and the last amino acid on the nascent polypeptide chain bound to the tRNA in the P-site, catalyzed by the ribosome results in the deacylated tRNA in the P-site and one residue longer peptidyl-tRNA in the A-site. The translocation of the peptidyl-tRNA to the P-site occurs with the help of EF-G1 and the deacylated-tRNA is removed from the translating ribosome. Elongation is followed by termination and ribosome recycling.

1.2.4. Termination of mitochondrial translation

In terms of translation termination and identification of the proteins involved, the matter seems to be more complex and less studied compared with initiation and elongation. Unlike sense codons that are recognized by tRNA anticodons during elongation, when stop codons reach the decoding site in the ribosomal A-site, the recognition is mediated by a group of proteins termed class I release factors (RFs), the elongation is ceased and nascent polypeptide released from post-translational complex. Efficient termination of protein synthesis requires participation of two classes of RF. Class I RFs have sequence specificity and bind only to A-site stop codons to promote release of nascent polypeptide by triggering hydrolysis of the ester bond between the completed protein and the terminal tRNA. This hydrolysis occurs in the peptidyl-transferase centre (PTC) where the configuration of the rRNA and RF is critical to facilitate translation termination. Subsequently, class II RFs that a codon independent, but can enhance class I activity and/or act as GTPases dissociate class I RF from the translation complex (Youngman *et al*., 2008, (Martin *et al*., 2005).

In bacteria codon recognition is facilitated by two class I proteins. RF1 is able to bind UAA and UAG, while RF2 shows activity with UAG but also functions with UAA (Youngman *et al*., 2008). In contrast, the same three codons are used but are recognised by a single protein eRF1 in eukaryotes and aRF1 in archaea. The crystal structure analysis of bacterial RF1 has revealed the specific regions required for the release function (Laurberg *et al*., 2008; Petry *et al*., 2005). It has been shown that there are three RF domains (domain 2, 3 and 4) that can occupy the ribosomal A-site. Domain 2 contains a conserved tripeptide motif of proline and threonine separated by variable amino acids (PXT) in RF1 types and serine, proline and phenylalanine (SPF) in RF2 types, which in concert with the tip of the α5 helix interact with the stop codon bases in the decoding centre of the ribosome. This recognition is accompanied by conformational

rearrangement between domains 3 and 4 to mediate the position of another conserved region, Gly-Gly-Gln (GGQ), extending it towards the peptidyltransferase center (PTC) in the large subunit. Brought to the close proximity with the ester bond linking the P-site terminal tRNA with the newly synthesized polypeptide chain, the GGQ motif promotes the hydrolysis and consequent polypeptide release (Seit-Nebi *et al*., 2001).

In mitochondria there is only one protein that has been shown *in vitro* and *in vivo* to be active on all mitochondrial stop codons, directly recognizing UAA and UAG while promoting rather indirect termination through programmed ribosome frameshifting on mt-ORFs that are followed by with AGG and AGA triplets. Due to its greater similarity not only in sequence but also in length to RF1-type proteins in both prokaryotes and eukaryotes, the human mitochondrial factor was named mtRF1a (Soleimanpour-Lichaei *et al*., 2007, Temperley *et al*., 2010a). The amino acid sequence alignments of all mitochondrial factors indicate similarities with only RF1-type proteins rather than with RF-2, thus up to date mitochondria are not known to have or need an RF2 counterpart.

1.2.5. Ribosome recycling in mitochondria

The 55S with deacylated tRNA and mRNA is targeted for the last step of translation. The post-translational complex requires to be disassembled so that all the components of translation can be reused for the next rounds of synthesis. It was only few years ago that a candidate protein proposed by bioinformatics analyses has been biochemically characterized and shown to be involved in the mechanism of ribosome recycling (Rorbach *et al*., 2008). The mtRRF was shown to strongly bind mitoribosomes *in vivo* and depletion of the factor resulted in reduction of free ribosomal subunits and an increase in monosome formation. Moreover, the expression of human mtRRF was shown to suppress the partial deletion of *rrf1* gene in fission yeast *in vivo*.

Even though mtRRF is an essential protein for cell viability and its depletion caused general mitochondrial dysfunction, it was reported that the efficient disassembly process requires mtRRF to work in conjugation with mtEF-G2, thus the latter was renamed for mtRRF2 (Tsuboi *et al*., 2009). In contrast with bacterial systems, where a single protein had been assumed to be required for both elongation and recycling process, it was unusual to observe two separate

factors for tRNA translocation step and for disassociation of subunits. Now, however, there have been a number of bacterial EF-G2 proteins identified. mtEF-G2 has no significant translocation activity, however its over-expression in patient fibroblasts habouring a mutation in mtEF-G1 slightly elevates levels of fully assembled oxidative phosphorylation complexes suggesting to some extent its dual function (Coenen *et al*., 2004). The domain swapping between mt-EF-G2 revealed that the different function of the factors depends mostly on domains III and IV. Moreover, mtEF-G2 has strong ribosome-dependent GTPase activity and unlike bacterial systems the mitochondrial subunit recycling does not require GTP hydrolysis, but rather the GTP hydrolysis take place after the monosomes split and release mtEF-G2 and mtRRF bound from the large subunit (Tsuboi *et al*., 2009). In order to prevent factor free ribosomal subunits from reassembling mtIF-3 binding to the SSU is required (Christian and Spremulli, 2012).

1.2.6. Human mitochondrial release factor family

In 1998 bioinformatic analyses revealed a mitochondrial RF protein candidate based on sequence similarities with other RFs. This was termed mtRF1 (Zhang *et al*., 1998) and was referred to in the literature as the only translation termination factor in mammalian mitochondria that was anticipated to have RF activity on all 4 predicted stop codons. No release function, however, has been detected in *in vitro* studies of mtRF1 on bacterial ribosomes against UAA, AGA and AGG (Soleimanpour-Lichaei*et al*., 2007; Nozaki *et al*., 2008) or any other triplet tested (personal communication Z. Chrzanowska-Lightowlers) nor did an *in vivo* approach in yeast yield any detectable activity (Soleimanpour-Lichaei *et al*., 2007). In the latter investigation the overexpression of human mtRF1 could not rescue the respiratory deficiency caused by deletion of endogenous yeast MTRF1. A further candidate, mtRF1a, was then characterised and demonstrates activity only in response to UAA and UAG but not to AGA and AGG (Soleimanpour-Lichaei *et al*., 2007) or other codons tested (personal communication Z. Chrzanowska-Lightowlers). Both mtRF1a and mtRF1 have the conserved GGQ motif, but their amino acid sequences in the regions conferring codon recognition differ slightly. Across the tripeptide domain mtRF1a has PKT, conforming to the PXT consensus. In contrast, mtRF1

displays an extended hexapeptide motif, PEVGLS. At the tip of the α5 helix of domain 2 both proteins differ slightly from the *E. coli* proteins but again mtRF1a shares greater similarity than mtRF1. A consequent bioinformatics search revealed further 2 new members of the family, ICT1 and C12orf65. These two new predicted members of the mitochondrial release factor family, however, lack the sequences spanning codon recognition although they do retain the GGQ motif required for hydrolysis of nascent polypeptide chain.

The GGQ motif is present in all class I RFs and it is conserved in all eubacterial, archeal and eukaryotic release factors. The mutations of any of three residues results in significant decrease of its catalytic activity or in complete loss of function with poor ability to be even expressed in *E. coli* (Frolova *et al.* 1999; Mora *et al*., 2003). In both bacterial factors (RF1 and RF2) Gln residue is post-translationaly methylated, which contributes to the activity (Heurgue-Hamard *et al*., 2002). The same modification is made to yeast eRF1 (Heurgué-Hamard *et al*., 2005) and to the Gln of tripeptide motif in mtRF1a is believed to the modified by HMPrmC, a methyltransferase that is targeted to mitochondria (Ishizawa *et al*., 2008).

Richter *et al*. (2010) has already shown that ICT1 is able to immunoprecipitate the whole mitochondrial monosome, it co-sediments with both 39S and whole 55S articles. Ribosomes lacking ICT1 cannot be fully assembled, indicating it to be an integral part of the large subunit. Even though ICT1 has been tested for activity on *E. coli* ribosomes and was shown to act as a ribosome-dependant codon-independent peptidyl-tRNA hydrolase regardless of the codon presence or absence in the A-site, it is not possible to test this activity directly on mitoribosomes. Due to its known characteristics it is proposed to be involved in a mitochondrial strategy of dealing with mRNA that has lost the translation termination codon. When mitochondrial ribosomes encounter a 3' end of a non-stop mRNA, ICT1 is predicted to cleave the peptidyl-tRNA freeing the nascent chain allowing the ribosome and the tRNAs to undergo proper recycling.

Furthermore, structural differences between active domains of ICT1 and RFs have been implicated and linked to a specific function of ICT1 other than the translation termination mediated by RFs (Handa *et al*., 2010). The solution structure reveals a β1–β2–α1–β3–α2 topology (Figure 1.7 A) and the catalytic domain, including the mobile 15 residue GGQ loop of mouse ICT1 has been shown by to be identical in structural framework and length with domain 3 of

bacterial RF2. The only difference observed was in the region bridging β2 and β3, where ICT1 has 10-residue α-helix (α-1) that is sandwiched between the α-2 and β-sheets and its existence influences a different angle of α-2 against β-sheets, which is not present in bacterial RF2. The last α-helix is followed by

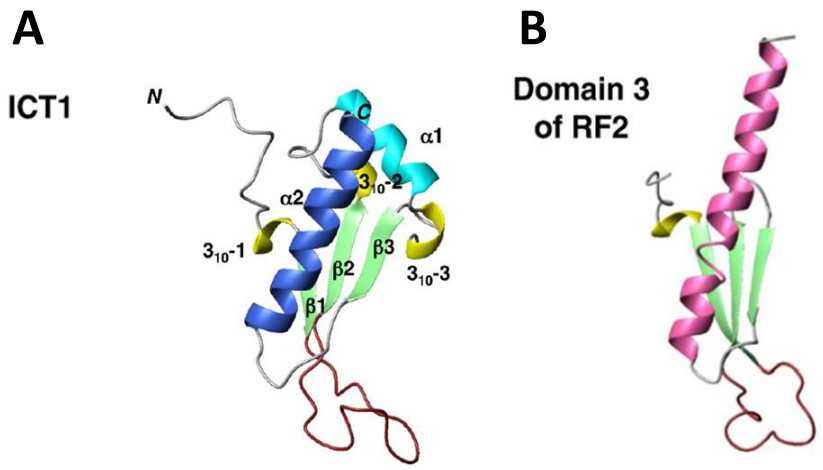

Figure 1. 7Ribbon diagrams of ICT1 and domain 3 of RF2.

The structures have been taken from Hanada *et al.,* 2010. See description in the main text. (A) The structure of ICT1 where, the α-helix 1 is coloured in blue and α2 is shown in cyan. The 3_{10} helices are indicated in yellow, β-strands in green and GGQ loop in brown.

rather unstructured C-terminal region of basic residues, which could be involved in direct ribosome binding or sensing stalled ribosomes as has been shown in the *E. coli* ICT1 homologue, YaeJ (Handa *et al*., 2011).

Following on from Richter *et al*. (2010) findings and trying to elucidate the function of mtRF1 in mitochondria, its 3D structure has been modelled in the ribosome. The structural differences between mtRF1a and mtRF1 developed a hypothetical function of the factor. Based on the structural implications, mtRF1 is only likely to bind to the A-site of the ribosome and exert its function if there is no mRNA present (Huynen *et al*., 2012). The translation of truncated, stop-codon less mRNA would result in such an empty A-site and stalled ribosomes.

As mentioned above, mechanism of recycling stalled ribosomes is not known in mammalian mitochondria, therefore ICT1 and now mtRF1 became positional candidates to release this biological dilemma. The last member of the mitochondrial release factor family is the C12orf65 protein. Even though mutations in this protein has been found in two patients diagnosed with an encephalomyopathic mitochondrial disease (Antonicka *et al*., 2010), and the solution structure of a mouse form has been determined (Kogure *et al*., 2012)

its physiological function remains unknown. C12orf65 was also characterised by the presence of a GGQ motif, the structural topology of which more resembles that of RF than ICT1. NMR shows that β2 and β3 in C12orf65 are connected by 6 residue turn that is similar to ICT1, an unstructured C-terminal extension (see chapter 7.1).

Homozygosity mapping and DNA sequence analysis identified two different 1bp C12orf65 deletions in two patients, both resulting in premature truncation of the protein. The molecular phenotype was mirrored in a decrease in complex I, IV, V and III assembly. Steady state levels of mitochondrial transcripts, tRNAs, rRNA as well as ribosomal proteins and elongation factors were not reduced. The assembly of complex I, V, III and IV could be only partially rescued by over-expression of ICT1, but not by mtRF1 or mtRF1a. C12orf65 does not show any detectable peptidyl-tRNA hydrolase activity when tested on bacterial ribosomes using any codon or no codon in the *in vitro assays* (Antonicka *et al*., 2010).

Since it has now been shown that there is only one human mitochondrial release factor, mtRF1a, that is both necessary and sufficient to terminate translation of all 13 open reading frames, the presence of the 3 remaining family members is an intellectual dilemma as they are left with uncharacterised activity (mtRF1, ICT1 and C7orf65). Even though ICTI 1 has already been shown to be an integral part of 55S (Richter *et al.,* 2010) its exact function in this context along with that of C12orf65 and, more importantly, mtRF1 still remains unanswered.

1.3. Overview of gene expression quality control

Unlike the distinguishable aberrant mRNA, such as those lacking a 5' cap or 3' poly(A) tail that are highly unlikely to be introduced into a translation process, mRNAs with more subtle errors are more difficult to be easily discriminated. Thus, in order to minimize those errors and the detrimental effects that translation those aberrant transcripts may have, cells have evolved the mechanism to monitor transcripts for degradation during translation (Keiler *et al*., 1996 and reviewed by Nicholson *et al*., 2012). Most of those mechanisms, termed mRNA surveillance, directly implicate translation in the process, due to the fact that factors involved act directly on the ribosome itself. In bacteria there are three distinct pathways, the most characterized depends on a functional RNA, tmRNA (transfer-messenger RNA) and others less studied pathways

depend on release factors homologues (Pech and Nierhaus, 2012). Eukaryotes have been identified to have three distinct surveillance pathways each of which act on different aberrant mRNA substrates (Isken and Maquat, 2007). Even though the mechanism of ribosome rescue differs between the prokaryotes and eukaryotes, the outcomes of the pathways are conserved.

1.1.1. Prokaryotic mRNA surveillance pathways

1.1.1.1. Trans translation

The most universal and best characterized system in bacteria to rescue stalled ribosomes at the end of non-stop mRNA is the classical tmRNA/SmpB system (Keiler *et al*., 1997). It mostly depends on action of bi-functional transfer-messenger RNA (tmRNA) that is also known as SsrA or 10Sa RNA and is highly structured with properties of both tRNA and mRNA. It also recruits other molecular partners such as EF-Tu, SmpB protein and alanyl-tRNA synthetase. The essential parts of the tmRNA for its function are its 5' and 3' ends. The folding of these domains forms tRNA-mimic and an mRNA strand (Felden *et al*., 1997; Komine *et al*., 1994). The tRNA domain does not contain anticodon loop, like conventional tRNAs, but includes an acceptor arm that can be aminoacetylated at its 3' terminus, with recognition sites for EF-Tu and SmpB, D loop and a T arm. The connector stem links the tRNA mimic domain with the rest of the molecule, mRNA-linker domain, which contains between several pseudoknots (PKs) and helical stems, a short internal open reading frame (ORF) that functions as mRNA template (Figure 1.8 B). While the function of the pseudoknot is controversial and has been suggested to play a role in overall folding, maintaining correct geometry or slowing down the degradation of the molecule, the ORF plays a crucial role in tmRNA function (Williams *et al*., 1999). It is the sequence of this ORF that when translated acts as a tag and dictates which proteases are going to degrade the protein. When a truncated or otherwise defective transcript, such as rare codons, a highly structure mRNA or strong interaction between nascent peptide and exit tunnel, causes the ribosome to stall and both elongation and termination are prevented, pausing is observed for long periods and subsequent pausing-dependent mRNA cleavage together with the poor occupancy of the A-site seem to direct the recognition of the stalled complex (Hayes and Sauer, 2003; Sunohara *et al*., 2004a and 2004b). The trans-translation events, i.e. SmpB-tmRNA-EF-Tu by changing the

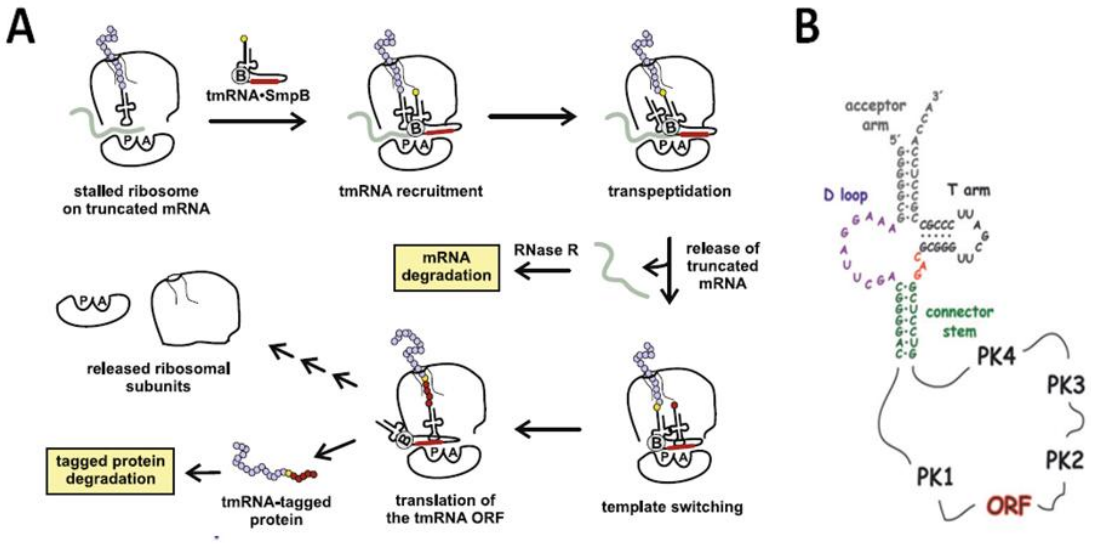

Figure 1. 8. Trans-translation process in bacteria.

(A) The model shows stalled ribosome rescue by tmRNA- mediated tagging.(Hayes and Keiler, 2009) **(B)** Simplified tmRNA structure includes tRNA-mimic domain connected (the connector stem is not complete) to the pseudoknots and ORF part. Adopted from (Moore and Sauer, 2007)

mRNA template, allow translation to continue. EF-Tu binds the acceptor and T arm of the tmRNA, protecting the ester from hydrolysis, as during normal translation, and delivers it to the A-site of the stalled ribosome mediating the addition of the nascent peptide on to the alanine at tRNA- mimic domain of tmRNA (Figure 1.8 A). The binding of tmRNA to the stalled ribosome is facilitated by two SmpB proteins that have been shown to bind 23S RNA of 50S and 16S close to the anticodon regions of P-site and E-site simultaneously with EF-Tu (Valle *et al*., 2003, Barends *et al*., 2001). Recent crystal structures of tmRNA, SmpB in complex with EF-Tu and the ribosome have shown that SmpB mimics codon-anticodon in the absence of mRNA in the A-site (Neubauer *et al*., 2012) and upon binding, the conformational changes on the ribosome as well as on the tmRNA occur. Consequently, the peptidyl-tmRNA is translocated into the P-site, then the first codon of tmRNA ORF is positioned into the A-site allowing the addition of the first encoded tag residue and translation resumes as with mRNA. The main event facilitating the correct translocation and positioning of the tmRNA ORF is the unique extra-large swivel movement of the 30S head (Ramrath *et al*., 2012). The hybrid protein product is eventually degraded by proteases, e.g. ClpXP and tm-RNA rescued ribosomes are ready for common recycling for further circles of translation (Gottesman *et al*., 1998).

Apart from the pausing-dependent cleavage there are also other mechanisms in bacteria by which active and stalled ribosomes with no mRNA or short 3’ end

extensions are discriminated (Ivanova *et al*., 2004). If the A-site is unoccupied or incompletely filled, basic residues of 30S will not interact with the mRNA, and so the mRNA entrance tunnel, due to conformational changes, stays open allowing tmRNA ORF access. The opening also seems to be partially accompanied by the actions of EF-Tu (Ramrath *et al*., 2012). In the scenario where a ribosome stalls at the 3' end that is about 20 bases and it emerges from the mRNA tunnel, ribosome pausing occurs triggering the cleavage by RelE toxin. That enzyme is then able to cleave A-site codon, but action of this is normally regulated by ReLB antitoxin expression. It has been shown that RelE cleavage can create more active substrates and increase tmRNA recognition (Ivanova *et al*., 2004). Such pausing-depended cleavage by RelE has been only shown by *E. coli,* whereas other strains lacking toxin-antitoxin systems can still cleave stalled mRNA and rescue ribosomes with tmRNA. It is possible, therefore, that after a long translational pause the ribosome itself is able to cleave mRNA in the A-site or that another rescue pathway resolves such problems.

1.1.1.2. Other ribosome-rescue pathway

In addition to the tmRNA/SmpB system there are other two rescue mechanisms found in bacteria that free stalled ribosomes and seem to be mostly dependent on release factor homologues. The first such novel protein characterised in *E. coli,* YaeJ, has been shown *in vitro* to hydrolyze peptidyl-tRNA from stalled ribosomes on non-stop mRNAs as well as on rare codons occupying the A-site. This action would block the ingress of Ala-tmRNA/SmpB. *In vivo, yaej* as a multicopy gene, it is also able to suppress the lethal phenotype of ssrA arfA double mutant (Chadani *et al*., 2011, Handa *et al*., 2011). YaeJ is a small basic protein that is similar in sequence and structure to domain 3 of the class I type RF (ICT1 is its mitochondrial orthologue)(Richter *et al*., 2010a). It contains the GGQ motif and missing domains 2 and 4 are replaced with unstructured C-terminal basic residue-rich extension. It therefore functions as a codon independent factor and has been renamed ArfB, an alternative ribosome factor B. It was shown to bind ribosomes tightly and mutations in the GGQ and deletion of C-terminal tail eliminated the ribosome rescue activity (Chadani *et al*., 2011). Recent crystal structure of the protein bound to 70S reveals

mechanism by which the ribosomes are rescued. The C-terminal was shown to bind the mRNA entry channel downstream of the A-site, between the head and the shoulder of small ribosomal subunit, which suggested that it samples the pocket to discriminate between active and stalled ribosomes (Figure 1.9A) (Gagnon *et al*., 2012). In addition, it was shown to function *in vitro* on stalled ribosomes with an empty A-site as well as on stalled ribosomes with mRNA of sufficient length (Shimizu, 2012).

The synthetic lethality screening by (Chadani *et al*., 2011) have shown that *E. coli* cannot survive simultaneous deletion of SsrA (tmRNA) and YhdL (novel rescue factor) genes. The latter has been named accordingly ArfA and was demonstrated to rescue stalled ribosomes *in vivo* and *in vitro* on non-stop mRNAs. Moreover, ArfA associates with the large subunit, but it does not have the typical GGQ motif to mediate peptidyl hydrolysis. Thus ArfA functions in collaboration with RF2 (Figure 1.9 B), which can only bind to the stalled ribosome with an empty A-site in the presence of ArfA (Shimizu, 2012; Chadani *et al*., 2012). Thus, it was suggested that the ArfA binds an empty A-site first, possibly associating with tRNA in the P-site and recruits RF2, which in turn catalyses the hydrolysis to release the polypeptide chain in a codon-independent manner.

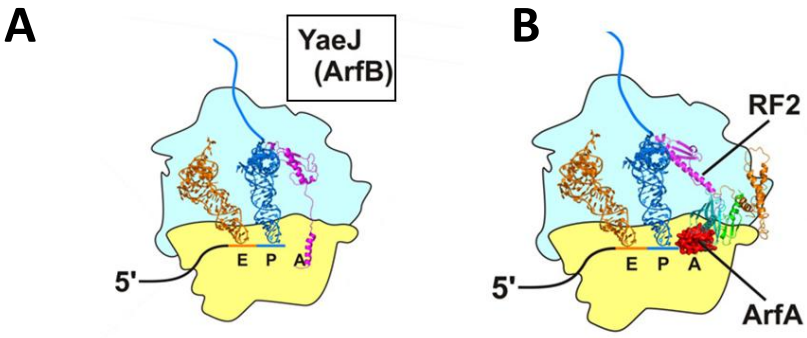

Figure 1. 9. Structure and ribosomal binding of alternative ribosomal rescue factors.

(A) Binding of the ArfB to the ribosome according to Gangon *et al.,* (2012). **(B)** Proposed arrangement of ArfA with RF2 on the ribosome. Both images adopted from (Pech and Nierhaus, 2012)**.**

1.1.2. Eukaryotic mRNA surveillance pathways

1.1.2.1. Nonsense-mediated mRNA decay (NMD)

The NMD pathway specifically recognizes mRNAs with premature termination codons (PTC). There are two models for the mechanisms that define the substrate in such cases. Normal stop codons are typically located at the end of the most 3' exon of mRNAs and are recognized by exon junction complexes (EJC). The close proximity of such junctions to the poly(A) tail and its cognate binding proteins act as a positive influence on peptide release under physiological conditions. When the close interaction between eRF3 and PABP is disrupted by a PTC that is upstream of the normal stop site, ribosome stalls. The normal communication between termination factors and the EJC is affected so that NMD is invoked and is coordinated by key factors including the UPF (upstream frameshifting) proteins, 1, 2 and 3 that modify canonical termination (Maquat *et al.*, 2010). The second model proposes that the Upf1 directly coats the 3'UTR of the defective mRNA way before it reaches the ribosome providing clear target for other factors involved in the process (Hogg and Goff, 2010) (Figure 1.10).

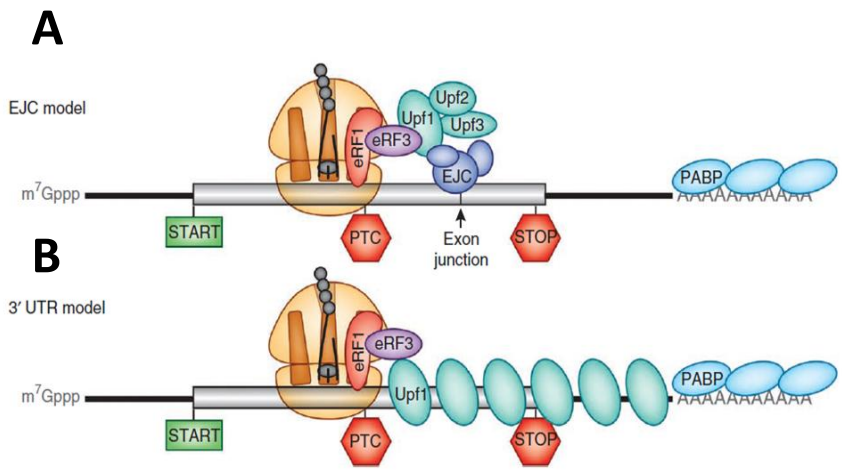

Figure 1. 10. Models for Nonsense-mediated decay.

(A) First EJC model and **(B)** 3'UTR model, both described in the main text.

All key NMD factors (Upf1, Upf2, Upf3) are conserved in eukaryotes, but the direct catalytic activity and interaction with termination factors (eRF3 and eRF1) has been ascribed only to Upf1 (Weng *et al.*, 1996), whereas Upf2 and Upf3 have been thought to provide scaffolding for Upf1, thus modulating its activity

(He *et al*,. 1997). In terms of ribosome recovery and ribosome reinitiation Upf1 also seems to be involved, however it is possible that the canonical recycling factors may be recruited by the NMD factors (Ghosh *et al*., 2010). Nevertheless, PTC recognition and the mechanism of its downstream events, as well as competition between stimulators of NMD mRNA decay and canonical termination factors are not well defined.

1.1.2.2. Nonstop mRNA decay (NSD)

This pathway functions on mRNA without in-frame stop codons, in which the ribosome translates to the end of the transcript due either to its truncation and lack of poly(A) tail or if the tail is present the translation runs through the poly(A) tail potentially generating a poly-lysine tag (Ito-Harashima *et al*., 2007; Frischmeyer *et al*, 2002). It has been shown that by translating adenosine nucleotides into positively charged lysines there is an interaction with negatively charged regions of the ribosomal exit tunnel that results in transient arrests during the elongation phase (Lu and Deutsch, 2008). Therefore, poly(A) tail read-through is rather referred to peptide-mediated internal stalling, based on recognized substrates classified as NoGoDecay (see 1.1.2.3.). Stalls from 'end of nonstop messages' in yeast are recognized by Ski7p, that specifically binds to an empty aminoacyl- site on the ribosome stalled at a transcript's 3' end, and promotes the exosome and the Ski complex to rapidly degrade the truncated mRNA (van Hoof *et al*., 2002). The C-terminus of Ski7 factor is closely related to a translational GTPase, such as EF1a and eRF3 and is believed to promote ribosome binding, whereas the N-terminus is thought to promote exosome recruitment to the ribosome. The poly(Lys) peptides in the exit tunnel arrest translation and due to the strong electrostatic interactions it can even stay associated after ribosomes disassemble. Such stalling causes Ltn1, an E3 ubiquitin ligase, to interact with the ribosome and its RING domain is able to recruit ubiquitin-charged E2s that in turn mark the nonstop protein with ubiquitin for proteolytic degradation by the proteosome (Bengtson *et al*, 2010). It is not known what is the exact signal that allows recognition of the stalled ribosome by Ltn1, whether the nonstop mRNA decay machinery components are required for this or whether the Ltn1 begins ubiquitylating substrate on stalled 80S and

promotes immediate disassociation staying attached to 60S as was mostly observed.

Once the NSD targets mRNA, the transcript is endonucleotically cleaved upstream of the stalled ribosome (Gatfield and Izaurralde, 2004). Messenger RNA decay is typically slow, tightly regulated and usually occurs either as 5'->3' or 3'->5' degradation. The process is initiated with deadenylation mediated by the CCR4-POP2-NOT complex (Chen *et al.*, 2002). This is followed by degradation in the 5'-3' that starts with the mRNA cap structure being removed by the decapping enzyme Dcp2. The degradation then proceeds with 5' exonuclease activity by Xrn1 (Hsu and Stavens, 1993). In 3'->5' degradation, deadenylation is followed by the exosome activity, which is a pore-like structure and its core domain exerts its exoRNase function (Dziembowski *et al.*, 2007). Ski7 has been shown to have a dual role in the pathway and apart from recognition of an empty ribosomal A-site, together with Ski2, Ski3 and Ski8 it can binds the cytoplasmic exosome (Araki *et al.*, 2001).

1.1.2.3. No-go decay (NGD)

NGD specifically targets ribosome stalls caused by mRNA with structural features such as damaged RNA bases, GC-rich sequences, pseudoknots or stable stem loops. More subtle mRNA characteristics such as strings of certain codons (mRNA mediated targets) or certain peptide sequences (peptide mediated targets) as mentioned above, may also stimulate NGD (Doma and Parker, 2006) (Reviewed by Doma and Parker, 2007).

If NGD complex stalls at the 3' end containing only a limited number of aberrant mRNA nucleotides downstream of the P-site, it is recognized and recycled by two interacting proteins Dom34 (yeast)/ Pelota (mammals) and Hbs1 (Pisareva *et al.*, 2011). Both factors are structurally related to the canonical termination factors and they mimic the complexes of eRF1 and eRF3 or even eEF and tRNA, supporting the fact that Dom34-Hbs1 complex binds to the ribosomal A-site (Becker *et al.*, 2011). Dom34 resembles eRF1 and both proteins share the sequence similarity of the central and C-terminal domains (CTDs), but differ in their N-terminal domains (NTDs). The NTD of eRF1 contains conserved NIKS loop that recognizes the stop codon in the ribosomal A-site, whereas NTD of

Dom34 harbours an RNA-binding Sm fold that was suggested to trigger cleavage (Doma and Parker, 2006; Lee *et al.*, 2007), which in turn would initiate mRNA degradation. Therefore Dom34-Hbs1 dissociates stalled ribosomes in a codon independent manner. Some further studies could not support that, where endonucleotic cleavage is not well understood and the nuclease that mediates it is not known (Passos *et al.*, 2009). Hbs1 belongs to the family of eEF1A-like GTPases and resembles eRF3. Both proteins share conserved G, II and III domains, but differ in NTD (Inagaki and Ford Doolittle, 2000; Tsuboi *et al*., 2009). Similarly to eRF3, the direct binding to the ribosome of Dom32 and Hbs1 increases Hbs1's affinity to GTP and the formation of Dom34-Hbs1-GTP or Pelota-aEF1a-GTP complexes promotes the Dom34 and Pelota to adopt conformation similar to tRNA, which increases the A-site binding affinity (Kobayashi *et al.*, 2010). Further structural studies (Becker *et al.*, 2011) demonstrated that upon binding Dom34 together with N-terminal of Hbs1 directly interact with rRNA and proteins of the tunnel-like mRNA entry site, thus possibly monitoring the length or mRNA in this position or marking the complex for subsequent events. Despite the similarities to eRF1 Dom34 does not contain a conserved GGQ motif. Therefore it is thought that the Dom34-Hbs1 binds to the ribosome and by destabilization of mRNA-tRNA interactions it recruits both mRNA degradation and additional factors in order to rescue stalled complexes. Following the endonucleolytic cleavage of mRNA targeted for NDG, the 3' and 5' termini are then degraded by Xrn1 and the exosome respectively (Doma and Parker 2006).

Ski7p was originally implicated in Non Stop Decay (van Hoof *et al.*, 2002) but since it is found only in a subset of yeast (Atkinson *et al.*, 2008) some data suggest that Dom34 and Hbs1 may be involved in release of ribosomes that are stalled at the 3'-ends of non-stop mRNAs (NSD) (Kobayashi *et al.*, 2010).

1.1.3. Release factors and protein quality control

Examination of eRF1, eRF3 and their evolution by sequence similarity, multiple alignment and phylogenetic analysis (Atkinson *et al.*, 2008) has revealed that it is possible that the three eukaryotic mRNA decay systems have arisen by duplication of *erf1* and *erf3* genes. It has been hypothesized that Dom34-mediated NGD was present in the last common ancestor of eukaryotes and

archaea, then in early eukaryotes eEF1A was duplicated giving rise to eRF3-like factor, which as a eRF1 partner was recruited for translation termination and from which from NMD have evolved. Further duplication of eRF3 may have given rise to Hbs1, which assists Dom34 in NGD. The last gene duplication in small subset of yeast may have led to Ski7p possibly as a specialized factor for Hbs1 in NSD.

1.4. The aims of this study

Since it is now clear that human mitochondria exploit the phenomenon of ribosomal frameshifting and therefore mtRF1a is both sufficient and necessary for release activity in mitoribosomes, this study aims to investigate the possible function of mtRF1 in quality control in relation to rescue of stalled ribosomes or aberrant translation in human mitochondria. This work will build on the current understanding and the characterization of mtRF1a data along with structural knowledge of mtRF1 and surveillance mechanisms in other species.

In mitochondrial RF1 and RF1a there are versions of the α5- helix sequence and the tripeptide (PXT) motifs that have been described as important for recognition of termination triplets but these differ from bacterial counterparts (not shown) and also from each other (Figure 3.1, chapter 3 sequence alignment). Outside these regions much of the amino acid sequence is similar possibly providing scaffolding for the crucial motifs. Those similarities could facilitate binding of mtRF1 and its possible function on the same ribosomal site as mtRF1a has been shown to do (Soleimanpour-Lichaei *et al*., 2007). Moreover, the fact that the highly conserved motifs present in all release factors in mtRF1 are extended making the protein larger, i.e. 445aa, than mtRF1a (380aa) leads to the assumption that mtRF1 could still interact with A-site. However this would only happen if there is more space for it to fit, for instance in an absence of mRNA in the decoding centre (DC) (Huynen *et al.,* 2012).

Truncated mRNA may occur in mitochondria as a result of incorrect transcription, misprocessing of polycistronic RNA precursors or/and due to exonucleases cleavage (Borowski *et al*., 2010). If the mt-mRNA transcript is truncated the subsequent addition of poly(A) tail fails to generate a termination signal. Eventually this results in truncated ORF, stalled ribosome with peptidyl-

tRNA in P-site and an empty A-site. Therefore an obvious question arises: how can mitochondria cope with such a problem?

In bacteria stalled ribosomes are rescued by tmRNA (Hayes and Keiler, 2009), a specialised RNA with properties of both mRNA and tRNA that tags the nascent polypeptide chain for degradation and releases it from ribosomes enhancing higher efficiency of ribosomal usage. Further, another factor ArfA (alternative ribosome-rescue factor), essential for the viability of *E. coli* in the absence of SsrA (tmRNA)-mediated *trans*-translation has been identified (Chadani *et al.,* 2010). It has since been shown that the combination of synthetically lethal *ssrA* and *arfA* mutations can be suppressed by overexpression of another protein YaeJ (Chadani *et al.,* 2011), which is a putative RF and ICT1 homologue that also contains a GGQ motif indicative of ribosome dependent peptidyl hydrolase activity. Taken all together bacteria maintain at least 3 distinct mechanisms by which stalled ribosomes may be rescued. However, to date no such mechanisms have been characterised in mitochondria

mtRF1 is of interest as it has been demonstrated to be mitochondrial and also its depletion affects not only organelles but cell growth, indicating it to be an essential protein (Soleimanpour-Lichaei*et al*., 2007). Furthermore, purified mtRF1 shows no activity on 70S ribosomes with any of tested codons and yet it is still highly similar to the main mitochondrial release factor, mtRF1a. This was in stark contrast to the RF assays performed with ICT1 where release activity was observed with any codon in the A-site. Thus, we hypothesised that mtRF1 as a mitochondrial protein crucial for cell survival is a good candidate to play a role in the rescue of aberrant transcripts or stalled mitoribosomes.

mtRF1, C12orf65 and ICT1 are interesting candidates for such quality control mechanisms as they have been demonstrated to be mitochondrial and also their depletion affects not only organellar function but cell growth, indicating them to be an essential proteins. Furthermore, purified mtRF1 or C12orf65 show no activity on 70S ribosomes with any of tested codons and yet they both retain motifs that are highly conserved for release factors as are retained in the main mitochondrial release factor, mtRF1a. This was in stark contrast to the RF assays performed with ICT1 where release activity was observed with any

codon or indeed no codon in the A-site (Richter *et al.,* 2010). Consequently, the current hypothesis is that mtRF1, together with C12orf65 and ICT1 are mitochondrial proteins that are crucial for cell survival and are candidates to function in the rescue of aberrant transcripts or stalled mitoribosomes analogous to factors involved in ribosome rescue in bacteria.

This investigation will focus on the main following aspects:

- What is the effect of mtRF1 or C12orf65 depletion in human cell lines?
- Is GGQ important for the function of these proteins?
- Does mtRF1 or C12orf65 associate with the monosome?
- And if it does, can it recognise and bind an empty A-site allowing subsequent recycling after stalled mitoribosome state?

Chapter 2

Materials and Methods

Chapter 2. Materials and Methods

2.1. Plasmid manipulations and use of DNA oligonucleotides.

Generation of FLAG-tagged constructs in pcDNA5/FRT/TO (i.e. C12orf65-WT-FLAG, mtRF1a-WT-FLAG, mtRF1-WT-FLAG, mtRF1-GSQ-FLAG and mtRF1-AGQ-FLAG) was kindly carried out in my host lab prior to the start of the mtRF1 project. The glutathione-S-transferase (GST)-tagged variant (C12orf65Δ26) was kindly prepared by Dr Paul Smith. (GST)-tagged and FLAG- tagged release factors GGQ mutants (i.e. mtRF1-AGQ; mtRF1-GSQ; C12orf65-AGQ and C12orf65-GSQ) were generated by Site-Directed Mutagenesis using QuikChange II Kit (Stratagene Catalog #200523). The fragments of interest were amplified by polymerase-chain-reaction (PCR) using the primers in Table 1. The PCR fragments of tagged ORFs of all targeted genes were cloned into BamH1 and Not1 restriction sites of pGEX-6P-1, an E. coli expression vector. pcDNA5/FRT/TO with mtRF1/1a GGQ or C12orf65 GGQ-FLAG tagged mutants incorporated, were used as templates in both PCR amplification in order to clone constructs into E. coli expression vector pGEX-6P-1 and in QuikChange II Site-Directed Mutagenesis PCR reaction to generate silent mutations (SM) across the siRNA targeting region (primers and siRNAs indicated in Table 1.). For bacterial expression of the recombinant matured protein, the mitochondrial targeting sequence was removed, hence the ORF of the wild type mtRF1a as well as mtRF1 wild type and the mutants lack the N-terminal 32 and 49 amino acids respectively (designated as RF1a Δ32; RF1 Δ49; RF1 Δ49-GSQ; RF1Δ49-AGQ). Similarly the open reading frame of the wild type and mutant C12orf65 lack 26 amino acids at the N-terminus (C12orf65Δ26; C12orf65 Δ26-GSQ; C12orf65Δ26-AGQ). Additionally, cleavage of these amino acids removed hydrophobic stretches so that the protein was not only corresponding to the mature form but was more likely to be obtained in a solution form.

Table 2. 1. The primers used for formation of the wild type and mutants constructs for this study.

	_For - 5' to 3'	_Rev - 5' to 3'	Accession No./Image clone No.
mtRF1Δ49 pGEX6.1	5'tctctcggatccttcatctgttaagtaagaattgg3'	5'Ctctccgcggccgcttattttgctgatttaaggtg3'	BC042196
mtRF1a-AGQ	ccagtggagctgcggggcagcatgtaaatacc	ggtatttacatgctgccccgcagctccactgg	BC011873
mtRF1a-GSQ	ccagtggagctgggtcgcagcatgtaaatacc	ggtatttacatgctgcgacccagctccactgg	BC011873
mtRF1-AGQ	ccaaaggagcagcagggcagcatgttaataaaactg	cagttttattaacatgctgccctgctgctccttgg	BC042196
mtRF1-GSQ	ccaaaggagcaggatcgcagcatgttaataaaactg	cagttttattaacatgctgcgatcctgctccttgg	BC042196
mtRF1-SM	gctagactctaccaacaaataatagaaaaggacaagcgtcag	ctgacgcttgtccttttctattatttgttggtagagtctagc	BC042196
C12orf65-AGQ	ggacacggtccagcgggccaggcaaccaac	gttggttgcctggcccgctggaccgtgtcc	BC062329
C12orf65-GSQ	cacggtccagggtcccaggcaaccaac	gttggttgcctgggaccctggaccgtg	BC062329
C12orf65- SM	ctccggctttgggaaaaattaacatttgttatccccaggaa	ttcctggggataacaatgttaatttttcccaaagccggag	BC062329

Restriction sites are indicated in **green (BamH1)** and **blue (Not1).** **Red** nucleotides mirror the GGQ motif and **bold** indicate the introduced mutations. All primers were ordered form EUROGENTEC S.A.

2.2. Cell culture

2.2.1. Cell culture maintenance, storage and microscopy

Hek293 cells used in this study were cultured in 75cm² tissue culture flasks with 15ml Dulbecco's Modified Eagle's Medium (DMEM, Sigma D6429) supplemented with 10% (v/v) foetal bovine serum (FBS), 1x non essential amino acids and 50µg/ml uridine. HeLa cells and fibroblasts were cultured in Earle's Minimal Essential Medium (EMEM) (Sigma, product M0643) with 10% FBS, 1x non essential amino acids, 50µg/ml uridine and 1mM sodium pyruvate. The cells were grown under stable conditions of 37°C and humidified 5% CO2 in the presence of 10 µg/ml blasticidin S to maintain the tet represor on pcDNA6/TR vector that was already independently integrated into the host cell line of HEK293T and the media were changed every 3 days. When the monolayer of cells reached 80% confluency the media was removed and the cells were harvested in 1mM EDTA/PBS. After pelleting at 230 xg (bench centrifuge) for 4 minutes, cells were resuspended in 2 ml of fresh media and for genral maintenance 1/10 of the cells were transferred to a new flask (with 15ml fresh media). In order to store the cells for later use they were harvested as for splitting and resuspended in 0.5ml FBS with 10% DMSO. The resuspension was transferred to the cryostorage vials, which were then transferred to -80°C in a container that would gradually lower the temperature and after 24h were transferred to liquid nitrogen.

All tissue culture manipulations were performed in a class II cabinet and cells were inspected daily under Inverted microscope Axiovert25 (Zeiss). To induce protein expression, the cultures were grown in the presence of 1µg/ml tetracycline unless otherwise indicated.

2.2.2. Cell counting

The cells were cultured in 75cm² flasks containing 15ml as described above, or in medium lacking glucose but with 0.9 mg/ml galactose. After 3 days an equal number of cells were transferred to individual wells in a 6-well plate. The following day was designated day 0, and remaining wells were induced with tetracycline. Cells were counted by taking 10µl of harvested and resuspended cells and adding to a haemocytometer, where 8 peripheral squares were counted and in order to obtain the amount of cells per ml, the average value was multiplied by 10,000.

2.2.3. Mycoplasma testing

Cells were kindly tested for Mycoplasma infection every 3 months by Debra Jones. MycoAlert® Mycoplasma Detection Kit (Lonza) was used following the manufacturer's instruction. In case of an infection, cells were treated with Plasmocin (1:1000) for minimum 2 weeks and the Mycoplasma test was repeated.

2.2.4. Forward and reverse siRNA transfection of HeLa and HEK293T cell lines.

The transfection of HEK293-Flp-In™ with siRNA was carried out in 6-well plates or 75cm² flasks. For each transfection for 6 well-plate or 75cm² one tube was prepared with 250µl or 1.5ml Opti-MEM® I+Glutatmax™I (Gibco 51985-026), 2.5µl or 15µl desired siRNA and 2µl or 12µl Lipofectamine RNAiMAX (Invitrogen), respectively. Such a mix was added to an empty flask and incubated for 10 to 20 min at room temperature. During this time cells were counted and 30,000 in volume of 1.25 ml added to each well or 900,000 in volume of 7.5 ml per a 75cm² flask. After 3 days the cells were harvested or retransfected. For further treatment forward transfection was carried out. The old media was removed and the same volume of fresh one replaced with the same amount of siRNA and transfections reagents.

All siRNAs were custom synthesised by Eurogentec (Table 2.2) and stored as 20 µM or 100 µM stocks in RNase free water at -20°C.

Table 2. 2. All siRNAs sequences used for this study.

siRNA-mtRF1#3	CCA GCA GAU UAU UGA GAA ATT
siRNA- C12orf65	GGG AGA AGC UGA CGU UGU U
siRNA NT	siRNA non-targeting negative control duplex OR-0030-NEG05

2.2.5. Stable Transfection of HEK293-Flp-InTMT-RexTM cells.

In order to generate a stable cell line with pcDNA5/FRT/TO Tetracycline inducible expression vector (Hygromycin and ampicillin resistance, Invitrogen) containing the gene of interest, HEK293-Flp-In^{TM}T-REx^{TM} were co-transfected with pcDNA5/FRT/TO and pOG44 (Ampicillin resistance) using the ration of 1:7.5 and following the protocol

from Qiagen (Superfect Transfection Reagent Handbook). Stable inducible transfections of HEK293T cells for mtRF1-GSQ and mtRF1-AGQ were kindly carried out by Ricarda Richter.

2.3. Bacterial strains and general bacterial culture

All bacteria were grown on LB (Table 2.3) agar plates or LB media. For amplification of plasmids bacteria were grown in suspension with appropriate antibiotics at 37°C, usually overnight. For a longer storage bacteria were frozen in LB media containing 15 % (v/v) glycerol at -80°C.

Table 2. 3. The buffers and media components used.

Luria- Bertani (LB) medium –pH 7.5	'Rapid lysate Buffer'
-1% Bacto- tryptone -0.5% Yeast extract -1% NaCl -(for plates – 2% agar)	-50 mM NaOH -0.5% SDS -5 mM EDTA -10% Glycerol -0.025% bromocresol green

2.3.1. Transformation of bacterial strains with plasmids.

Transformation of chemically competent cells with pGEX-6P-1 (Amersham Bioscience), an IPTG inducible expression vector used for production of N terminal GST fusions of proteins of interest was carried out following manufacturers' instructions (Bioline α-select chemically competent cells, BIO- 85025). *E. coli* expression strain Rosetta (DE3 pLysS, for inducible overexpression of recombinant GSTfusion protein, Novagen) was transfected with 100 ng of DNA and further steps were followed as recommended by the manufacturer. For longer storage bacteria with the plasmid of interest were immortalised as described earlier.

2.3.2. Colony screening

In order to find colonies with a desired plasmid, bacteria were lysed in 25µl 'rapid lysate cracking buffer' (Table 2.3). The clone and buffer were mixed by short vortexing,

incubated for 30 minutes in 68°C followed by another mixing by vortex. The lysed bacteria were pelleted at 13,000 *g* for 8 minutes and 18µl of supernatant was dry-loaded on a 0.75% agarose gel (without ethidium bromide), followed by the electrophoresis at 65V for 40 minutes. The gel was then stained with 0.2µg/ml ethidium bromide for 15 minutes and washed twice in dH_20 for 5 minutes and analysed under UV light.

2.3.3. Plasmid DNA purification

Once colonies with plasmids of interest were identified, the bacteria were grown in 5ml LB-ampicillin overnight at 37°C. The plasmid DNA was isolated from bacteria using the Wizard PlusSV Minipreps kit (Promega A1460). The plasmid DNA was finally eluted in 50µl of dH_20 and used to transform Rosetta Cells.

2.4. DNA manipulation

2.4.1. Polymerase chain reaction (PCR)

All PCR reactions for cloning purposes used proof-reading DNA polymerase, and were carried out in 0.5 ml thin-walled tubes with final volumes of 50µl for each reaction. All reaction preparations were performed in a UV- sterilised cabinet. Components and conditions under which both PCR were carried out are listed in Table 2.4

Table 2. 4. PCR components and conditions.

<table>
<tr><td></td><td>PCR for cloning (Novagen)

-proof-reading KOD DNA polymerase</td></tr>
<tr><td>PCR thermal conditions</td><td>Initial denaturation - 95°C: 2 min.

<table><tr><td>Denaturation - 95°C: 30 sec.

Annealing - 55°C: 30 sec.

Extension - 70°C: 45 sec.</td><td>30 cycles</td></tr></table>
Final Extension - 70°C: 5 min.

Storage - 4˚C until stopped</td></tr>
<tr><td>Components and final concentrations per reaction</td><td>-1x buffer for KOD HotStart DNA Polymerase

-1.5mM $MgSO_4$

-0.2mM dNTPs

-1U KOD Hot Start DNA Polymerase

-1µM primer – forward

-1µM primer – reverse

-50ng DNA template</td></tr>
</table>

2.4.2. Purification of PCR products

PCR products were purified either straight from PCR reaction (if there was single DNA product of the correct size when analysed by agarose gel electrophoresis) or excised and extracted from 1% low melting agarose gels. In both cases the centrifugation procedure was carried out as described in QIAquick PCR Purification Kit (QIAGEN Catalogue #28106) or QIAquick Gel Extraction Kit (QIAGEN Catalogue #28706), respectively.

2.4.3. Restriction enzyme digestion

The digestion reactions were incubated at 37°C for 5h or overnight. 1 U of restriction enzyme was used to digest 1µg of DNA in the final volume of 10µl to 25µl where the amount of DNA varied from 0.2µg to 10µg. The enzymes used in this study were NotI and BamHI that were provided by either BioLabs or Roche and the conditions for each reaction were followed as recommended by the manufacturer.

2.4.4. Dephosphorylation of linearised vectors

Vectors were 5' dephosphorylated with 1U Alkaline Phosphate in 1x dephosphorylation buffer, both of which were supplied by Roche. Samples were incubated at 37°C for 1h.

2.4.5. Phenol/chloroform extraction and precipitation of DNA

DNA samples were diluted up to 100µl with dH_2O to which 100µl (equal volume) of phenol was added. The solution was vigorously mixed by vortexing and to separate the phases it was centrifuged for 2 minutes at 14,000 *g*. The upper aqueous phase was carefully removed to a new tube and 50µl of phenol and 50µl of chloroform/isoamylalcohol (24:1) was added. The mixture was vortexed and centrifuged again. At this stage the aqueous phase was again retained in a new tube and in order to ensure complete precipitation of the DNA, 1µl of linear acrylamide was added as a carrier with 10µl (1/10 of the total volume) 3M sodium acetate and 250µl (2.5 volumes) 100% ethanol, followed by at least 1h of incubation in -80°C. This was then centrifuged at 20,000 g, 4˚C for 30 minutes and resulted in pelleted DNA. The ethanol was removed and the pellet was resuspended in 10µl of sterile dH_2O.

2.4.6. Ligation

The ligation reaction of linear DNA fragments i.e. digested PCR product with a vector was catalysed by T4 DNA ligase in a presence of 1x ligation buffer (both provided by Roche) and 1mM ATP in a total volume of 10µl. The molar ratio of insert to vector for each sample was 1:3 and 1:6. The samples were incubated at 16°C overnight.

2.4.7. Electrophoresis

0.7% - 1 % agarose gels and 1% - 3% low- melt agarose gels were prepared by dissolving agarose in 1x TAE buffer (40mM Tris acetate, 1mM EDTA pH 8.0) using a

microwave. After the gel was dissolved ethidium bromide (0.5µg/ml final concentration) was added to facilitate DNA visualisation with UV light. The prepared gel was placed in the electrophoresis chamber with 1xTAE buffer, the samples (containing 1x loading buffer) and the 1kb ladder (as a molecular weight marker) were loaded and the electrophoresed at constant voltage (60 – 80V).

10x loading buffer:

- 0.25% bromophenol blue
- 0.25% xylene cyanol FF
- 30% (v/v) glycerol

2.4.8. Site Directed Mutagenesis

To introduce specific mutations into genes of interest the QuikChange II Site-Directed Mutagenesis Kit (Stratagene 200523) was used and the manufacturer's protocol followed. The plasmids with mutated genes were used to transform XL1-Blue supercompetent cells (Stratagene) also following the manufacturer's protocol.

2.4.9. DNA concentration measurements and sequencing

The concentration of DNA samples was measured with Nano-drop Spectrophotometer ND-1000, using a molar extinction coefficient of 33 for single stranded DNA and 50 for double stranded DNA (40 for RNA). All required sequencing of constructs was kindly performed by Agata Rozanska.

2.5. RNA manipulation

For all RNA work and solutions used water was 0.1% DEPC treated and autoclaved.

2.5.1. Extraction

All RNA was isolated from human cells using Trizol Reagent from Invitrogen following the manufacturer's protocol. In order to resuspend the harvested pellet 0.5ml of Trizol was added and it was incubated for 5min at room temperature. Then, after 0.1ml of chloroform was added, each sample was shaken by hand for 15s and incubated for 3min at room temperature prior to 15min centrifugation at 12,000 xg (4°C). A clear supernatant was collected and transferred into a fresh tube, to which 250µl of isopropanol was added, tubes were gently inverted to mix, then incubated at room

temperature for 10min and centrifuged at 12,000 xg for another 10min at 4°C. The final pellet was washed with 75% (v/v) ethanol and finally resuspended in 10-20µl of DEPC treated water containing 1U of RNAguard per 1µl, then left on ice for at least 30min in order to fully dissolve the RNA pellet before freezing.

If RNA was isolated form gradient fractions (80µl) 240µl of Trizol LS was used and all the steps followed the same. Accordingly, 48µl of chloroform and 0.15 ml of Isopropanol (to which 1.5µl linear acrylamite was added) were used in further steps.The final RNA pellet was resuspended always in 10µl of DEPC treated water containg 1U of RNAguard per 1µl.

2.5.2. Northern blotting

The RNA samples were prepared in 20µl, which contained 1-4µg in 8µl H_2O, 1x MOPS, 35 % (v/v) formamide and 5.5 % (v/v) formaldehyde.The samples are incubated at 55°C for 15min, cooled down on ice and ethidium bromide (0.1 µg/ µl final) and 1x RNA loading buffer were added before loading the samples on the 1.2% (w/v) denaturing agarose gel (1x MOPS and 0.9% formaldehyde). The samples were separated at 50 V and after 6 to 7 h of elctrophoresisthe gel was rinsed in 5 volumes of DEPC water and transferred on a GeneScreen Plus membrane over-night in 10x SSPE buffer. After the transfer was completed the membrane was rinsed in 2x SSPE and vacuum baked at 80°C for 2h followed by prehybridisation in 10ml of 50 % (v/v) formamide, 5x SSPE, 1% (w/v) SDS and 5x Denhardt's solution for minimum 2 h at 42°C.

The RNA was then labelled with 50-100ng of DNA fragment, which was denatured in 9µl DEPC water at 95°C for 4 min. When cooled down on ice3 µl random hexamer mix, 5U Klenow DNA polymerase I and 2 µl of 32P dCTP (~ 10-20 µCi, PerkinElmer NEG513H) were added and probe incubated at 37°C for 1 h. In order to purify the probe, it volume was increased up to 100µl and added to a Nick column to completely enter the bed of it. The addition of another 400µl of DEPC water allowed to enter the column and the first flowthrough was discarded, while the second flowthrough (the final probe) after addition of further 400µl of DEPC water was collected in a fresh tube. The activity of the probe was measured by a Cerenkov counter and minimum of 500,000cps were added to 10 ml of hybridisation buffer to incubate over night at 42°C. Then, the membrane was washed twice for 15min. with 2x SSPE at room temperature and one 15min washing with 2xSSPE/2%(w/v) SDS at 65°C. If further washes were not necessary the membrane was exposed to a screen in the Phosphor-Imager cassette. The radiolabelled RNAs were visualised and analysed using Phosphor-Imager and Image-Quant software (Molecular Dynamics, GE Healthcare). If reprobing

was required the membrane was washed twice in boiling 0.1x SSC and once with 0.1x SSC/ 0.1% (w/v) SDS for stripping the old singals. Then the membrane was pre-hybridised again as described above.

2.5.3. Reverse transcription

In order to synthesise a cDNA form isolated RNA from cells the reverse transcription was used (SuperScript™ First-Strand Synthesis System for RT-PCR from Invitrogen). Following the random primer protocol, first the RNA (up to 0.5µg) was mixed with 50ng of random hexamers, 1µl of 10 µM dNTP (final concentration 0.5

µM) to a final volume of 10 µl. The mix was then incubated at 65˚ C for 5 min., on ice for 1 min. to add 2 µl of 10x buffer, 2mM MgCl**2** (4 µl), 0.1M DTT (2 µl) and RNA guard (1 µl). Before 2 min incubation at 25˚C 50 U of Superscript was added to the reaction for further incubation at 25˚C (10 min.), 42˚C (50 min.) and finally 70˚C for 15 min.

2.6. Protein manipulation

2.6.1. Cell lysate preparation

Following the cell harvesting, the pellets were washed with PBS, and 50µl of cold lysis buffer (Table 2.5) was added to ~10mg of wet pellets. If the lysis buffer containing Triton X-100 was used then the samples were incubated for 30 min at 4°C on rotating wheel. Finally, lysed cells were centrifuged for 10 min at 12,000xg at 4°C and the supernatant collected into a new pre-chilled tube. If the lysis buffer contained Nonidet P-40 detergent, the samples were vortexed for 30sec and centrifuged for 2 min. at 2.300 rpm (1100g) at 4°C, then the supernatant was collected in a new pre-chilled tube. Samples were snap frozen in liquid nitrogen and kept in -80°C for longer than few week storage and in -20°C for more immediate use.

Table 2. 5. Lysis buffers used in this project.

Triton X-100: - 50 mM Tris/HCl pH 7.4 - 150mM NaCl - 1mM EDTA - 1% Triton X-100 - PI-Mix, (Roche) -1mM PMSF and 10mM $MgCl_2$ (added before use)
Nonidet P-40 : - 50 mM Tris/HCl pH 7.4 - 130mM NaCl - 2mM $MgCl_2$ - 1mM PMSF - PI-Mix (Roche), 1% Nonidet P-40 - benzonase (added before use)

2.6.2. Mitochondrial isolation by differential centrifugation

The cells for this procedure were seeded, induced with tetracycline where applicable, and grown for 2 days in 225 cm^2 flasks until they reached 80-85% confluency. They were harvested and the pellet was resuspended in 2 ml of Homogenisation Buffer (0.6 Mannitol, 10mM Tris pH 7.4 and 1mM EGTA) with 0.1% BSA and 1mM PMSF. This was then homogenised at 4°C in a Glas Col Homogeniser (15 passes) using a drill and then the suspension was centrifuged at 4°C, 400 *g* for 10 minutes. The supernatant was saved in a new tube and the remaining pellet underwent the step again followed by another centrifugation for 5 minutes. To pellet mitochondria supernatants were centrifuged at 11,000 *g* for 10 minutes, and then washed in 100µl homogenisation buffer lacking BSA and

centrifuged again for 5 minutes to be finally resuspended in 100µl homogenisation buffer lacking BSA. The obtained mitochondrial suspension was treated with 1µg proteinase K per 100µg of mitochondria to reduce contamination from cytosolic proteins. Following 30 minutes incubation on ice the reaction was terminated with PMSF (2mM final concentration) and washed twice with homogenisation buffer.

2.6.3. Protein concentration measurement by Bradford assay

Protein concentration was estimated by Bradford Assay. 1µl of each sample was added to the total volume of 800µl (including 200µl of Bradford- BioRad), mixed by vortexing and 2x 200µl aliquots of the solution were loaded onto 96 well-plate (flat bottom) to be measured in Microplate Reader (Elx800) at the absorbance of 595nm. The standard curve was generated by using different BSA (bovine serum albumin) concentrations ranging from 0, 2, 5, 10, 15 to 20mg/ml. BSA standard samples were loaded in duplicate and their concentration was measured together with proteins samples.

2.6.4. SDS-PAGE

Proteins in this study were separated by SDS-PAGE with a 12% or 14% resolving gel and 3.75% stacking gel (Table 2.6). The components of the first were mixed at room temperature and transferred to the casting apparatus (Hoefer/Amersham) with dH_2O applied on the top to prevent air inhibiting polymerisation and to obtain a level gel interface. After the gel polymerised the water was removed and stacking gel was poured in. Before loading, the samples were incubated in 1x(final) dissociation buffer (6.25mM Tris-HCl pH 6.8, 2% SDS, 10% Glycerol, 0.01% Bromophenol Blue and 100mM DTT) for 3 minutes at 95°C and centrifuged for 1 minute at room temperature. Proteins were separated in 1x running buffer (192mM Glycine, 25mM Tris and 0.1% SDS) at 80V through stacking gel and 120V through resolving gel. Post electrophoresis the acrylamide gels were either stained or used for immunodetection.

Table 2. 6. SDS-PAGE gel components (for 1 8x10cm gel with 0.75mm spacers)

	12% Resolving Gel	3.75% Stacking Gel
29:1 30% Bisacrylamide	2 ml	0.625ml
3.75 M Tris/HCl pH 8.5	0.5ml	----
dH_2O	2.395ml	3.02ml
0.5 M Tris/HCl pH 6.8	-----	1.25ml
10 % SDS	50µl	50µl
TEMED	5µl	5µl
10% APS	50µl	50µl

2.6.5. Coomassie blue and silver staining of polyacrylamide gels.

For Coomassie Brilliant Blue (CBB) staining, gels were incubated for 15 minutes in CBB solution (45% (v/v) methanol, 10% (v/v) acetic acid and 0.2% (w/v) Coomassie Blue R) then destained for 2 x 10 minutes in the CBB destaining solution (45% (v/v) methanol and 10% (v/v) aceticaAcid). For detection of, as low as 5ng proteins, SimplyBlue Safe Stain was used (following the invitrogen – LC6060, instruction manual for the most sensitive detection).

For silver staining the gel was incubated in 50 %(v/v) methanol for 1 h, followed by the incubation in staining solution (8% (w/v) $AgNO_3$, 1.4% (v/v) NH_4OH 0.075% (w/v) NaOH) for 15 min. Staining solution needs to be make up fresh and it is important to prepare it in a spotless glass vessel to notice the change in color before it is overstaurated. Before development with 0.055% (v/v) formaldehyde and 0.05% (w/v) citric acid (which also need to be make up fresh) the gel was washed 5 min for 3 times with dH_2O, then the reaction was stopped using fixer (45% (v/v) methanol and 10 % (v/v) acetic acid).

2.6.6. Western blotting and immunodetection

For western analysis proteins were immobilised on PVDF membrane (Immobilon-P, Millipore Corporation) by wet transfer. Before the gel and membrane were placed in between 2 layers of Whatman paper and transfer sponges, the separated proteins were equilibrated in 1x transfer buffer (25mM Tris, 192mM Glycine, 0.02% SDS and 15% methanol). The PVDF membrane was activated in 100% methanol and washed in water and then transfer buffer. The transfer was carried out at 100V for 2 h at 4°C in 1x transfer buffer with constant mixing. Next, the membrane was blocked in 5% milk in TBS (20mM Tris, 0.5 M NaCl) for a minimum of 1 hour at room temperature and proteins were decorated with primary antibodies (Table 2.7) at 4°C overnight in the same buffer. Following 3 washes in TBS with Tween 20 (TTBS) (each wash for 15 min.), secondary HRP- conjugated antibodies (DAKO Cytomation) were added for 1h incubation at room temperature. The membrane was washed again as before and signals detected with the ECL+ kit (Amersham) following instructions and visualised using both X-ray Films and PhosphoImager, where signal was quantified with ImageQuant programme.

Table 2. 7. Antibodies used in this study

Antibodies	Working dilutions	Produced in
Anti-Mouse/HRP(Dako Cytomation P0260) secondary	1:2000	Rabbit (polyclonal)
Anti-Rabbit/HRP(Dako Cytomation P0339) secondary	1:3000	Swine (polyclonal)
Anti-Goat/HRP (Dako Cytomation P0449) secondary	1:2000	Rabbit (polyclonal)
Anti-NDUFB8/20 kDa SU complex I (Mitosciences MS105)	1:1000	Mouse (monoclonal)
Anti-Cox II (Molecular Probes A6404)	1:1000	Mouse (monoclonal)
Anti-porin (Molecular probes A31855)	1:10000	Mouse (monoclonal)
Anti-mtRF1 (Eurogentec)	1: 2000	Rabbit (polyclonal)
Anti-mtRF1a (Eurogentec)	1:1000	Rabbit (polyclonal)
Anti-mtRRF (Eurogentec)	1:1000	Rabbit (polyclonal)
Anti-FLAG (Sigma F1804)	1:2000	Mouse (monoclonal)
Anti-MRPS18B (ProteinTech Group 6139-1-AP)	1:4000	Rabbit (monoclonal)
Anti-DAP3 (Abcam ab11928)	1:1000	Mouse (monoclonal)
Anti-MRPL3 (Abcam ab39268)	1:2000	Goat (monoclonal)
Anti- MRPL12 (Eurogentec)	1:1000	Rabbit (polyclonal)

2.6.7. Overexpression and purification of GST-fusion proteins from bacteria for release assay or *in vitro* ribosome binding

Transformed Rosetta colonies were grown overnight in 5 ml LB media with appropriate antibiotics. To express the proteins 500 ml media containing the antibiotics were inoculated with 2x 5ml of overnight culture and incubated for 2-2.5 h at 37°C. When the A_{600} was between 0.4 and 0.5, 1 mM (final concentration) of IPTG (isopropyl-1-thio-b-D-galactopyranoside) was added to the large bacteria cultures and incubated overnight at 16°C. To harvest cells the large cultures were centrifuged at 5,000 rpm (GSA rotor), 4°C for 15 minutes and PBS (containing 1 tablet of protease inhibitor cocktail mix, 1mM PMSF-

final concentration and 1µl Benzonase) was added to the pellet, which was then resuspended by vortexing and incubated on ice for 20 minutes. This was followed by 15 pulses of 10 seconds sonication (Soniprep 150) with 18 microns amplitude and hard centrifugation at 30,000g in 4°C for 30 minutes. The supernatant was filtered (0.45µm filter) and applied to the column (0.5ml of Glutathione Sepharose 4B beads). The column was washed with sterile dH_2O and PBS, and after incubation overnight on a rocking table at 4°C it was washed again 5 times with 50 ml PBS containing PI-Mix and 1mM PMSF and then washed 5 times with 50 ml PBS. Finally, to release the proteins from GST, the column was washed with 600µl of PBS containing 25µl PreScission Protease, 1mM EDTA and 1mM DTT. This was followed by collection of elution fraction, which was to be used for release assay. The aggregation state of purified proteins was measured by dynamic light scattering (Zetasizer 1600). The release assay was kindly performed by Professor Zofia Chrzanowska-Lightowlers.

2.6.8. Dynamic light scattering

Small aliquots of protein samples (20µl) were measured in low-volume glass cuvettes using a commercial Zetasizer 1600 (Malvern Instruments) equipped with a He–Ne laser (633 nm, 5 mW). Measurements were carried out at 25°C for 70s for 5 times.

2.6.9. Antibody purification

After the recombinant GST protein was successfully purified as described above in section 2.6.7, it was run on the 14% SDS-PAGE and the band of interest was cut out of the gel to be used for the Immunisation (performed by Eurogentec using their Speedy protocol for Custom Anti-protein Polyclonal Antibody Production). After the final bleed was obtained Antibody purification was procceded using 'NHS-activated Shepharose 4 Fast Flow' (GE Healthcare Life Sciences). After the sepharose beads were added to 10ml BioRad Column to a final volume of 0.6ml, they were washed 3 times with cold 1mM HCl.

Then, the purified earlier protein of interest (1-2mg in elution buffer) was applied to the column and incubated overnight at 4°C. The next day the flowthrough

was saved and the beads on the column incubated with 0.1M Tris/HCl (ph7.4) again overnight. After the blocking was finished, the column with the beads was washed 5 times with PBS and 7ml of filterised (using 0.45µm and 0.2µm filters) serum with 3ml of PBS were added to the column for overnight incubation on the rocker at 4°C. Then, the flowthrough was saved again and the beads washed 2 times with PBS, once with Tris-buffer of pH 8.0 (50mM Tris/HCl pH8.0, 0.1% Triton X-100, 0.5M NaCl), once with Tris-buffer of pH 9.0 (50mM Tris/HCl pH 9.0, 0.1% Triton X-100, 0.5M NaCl) and once with Sodium-phosphate-buffer pH 6.3 (50mM Sodium phosphate pH 6.3, 0.1% Triton X-100, 0.5M NaCl). Finally, in order to elute the antibodies from the column, 5ml of Glycine-buffer of pH 2.5 (50mM Glycine pH 2.5, 0.1% Triton X-100 and 0.15M NCl) was added to the column and immediately neutralized by adding 1ml of 1M Tris/HCl of pH 9.0. In order to concentrate the affinity purified antibodies the buffer exchange for PBS was performed using concentration centrifugal devices (Millipore). The antibodies were stored in 10% Glycerol and 0.02% of sodium azide in 50µl aliquots in - 20°C.

2.6.10. Immunoprecipitation via FLAG moiety

Cells for this experiment were prepared in 3 x 300cm² flasks and induced for 3 days with tetracycline as described above. The mitochondria were isolated as described above. The pelleted mitochondria were then lysed with 500µl Sigma lysis buffer (supplemented with 10mM MgCl2; 1mM PMSF and RNAguar) and further steps were performed as described by Sigma (FLAG Tagged Protein Immunoprecipitation Kit).

2.6.11. Isokinetic sucrose gradient analysis

0.5ml of 10% sucrose in 1x buffer (Table 2.8) was added to the Ultra Clear plastic tube (for 1ml volume with an open top, Beckman 343778). Using a needle with 1ml syringe, 0.5ml of 30 % sucrose in 1x buffer was loaded under 10 % sucrose being careful not to mix the two. The linear gradient was formed by a 55 seconds process called tilted tube rotation (Biocomp Gradient Maker instrument; using programme for TL55, 10-30% S1/1 0:55/85.0/22). Such gradients were then incubated at 4°C for an hour prior to use. Meanwhile the cells were harvested and depending on the pellet size resuspended in 100-

300µl lysis buffer (Table 2.8). After the cell lysate was incubated for 30 minutes on rotating wheel at 4°C it was centrifuged (10 minutes, 12,000g, 4°C) and 700µg of totlat cell lysate of supernatant was loaded on to the top of the gradient. The centrifugation was then performed for 2h 15 min at 4°C at 39,000 rpm (Beckman bench ultra rotor TLS 55, acceleration 1 and deceleration 4) and ten fractions were collected to separate tubes (frozen in liquid nitrogen and kept at -20°C until required).

Table 2. 8. Buffers required for the isokinetic sucrose gradient

	Components
10x gradient buffer	- 0.5 M Tris-HCl pH 7.2 - 0.1 M MgOAc - 0.4 M NH_4Cl - 1 M KCl - 1mM PMSF and 50µg/ml chloramphenicol (the stocks were prepared in 100% ethanol and stores at -20 °C) (both added before use)
Lysis Buffer	*Triton X-100*: - 50 mM Tris/HCl pH 7.4 - 150mM NaCl - 1mM EDTA - 1% Triton X-100 - PI-Mix, 1mM PMSF and 10mM $MgCl_2$ (added before use)

2.7. Statistics

The standard deviation of all the means obtained from the data in this project were calculated using a t-test available on the webpage:

http://www.graphpad.com/quickcalcs/ttest1.cfm. The differences of the significance in the results were specified as:

to be not statistically significant when $p > 0.05$,

as significant (*), when $p = 0.01$ to 0.05,

as very significant (**) with $p = 0.001$ to 0.01,

and as extremely significant (***) with $p < 0.001$.

Chapter 3

Depletion of mtRF1 in human cells – Does this affect cell viability and what are the consequences on mitochondrial metabolism?

3. Chapter 3: Depletion of mtRF1 in human cells – Does this affect cell viability and what are the consequences on mitochondrial metabolism?

3.1. Introduction

Mitochondrial Release Factor 1 (mtRF1) is one of four members of the mitochondrial release family and one of three factors whose role in translation has not yet been characterised. Previous preliminary studies have demonstrated that a mtRF1-GFP fluorescence signal that overlapped with the mitochondria stained with mitotracker CMH_2X-Ros, confirming its mitochondrial colocalisation (Soleimanpour-Lichaei *et al*., 2007). After its original identification *in silico* (Zhang and Spremulli, 1998) mtRF1 was consistently referred to in the literature as the only release factor present in the mitochondria. The first biochemical characterisation, therefore, attempted to elucidate the function. These studies focused on testing mtRF1's ability to recognise termination signals and hydrolyse the ester bond between a P-site tRNA and its amino acid moiety *in vitro*. The substrate was generated with *E. coli* ribosomes loaded with a synthetic AUG start triplet and f[^{3}H]Met-tRNA^{MET} in the P site. To this was added a triplet corresponding to the perceived mitochondrial stop codon (UAA, UAG, AGA and AGG) and finally the recombinant RF of choice. When mtRF1 was assessed against the panel of triplets, no free f[^{3}H]Met could be detected to indicate any release activity. Moreover, mtRF1 failed to suppress the respiratory deficiency caused by loss of endogenous mitochondrial RF1 (*Δmrf1)* from both model yeasts *in vivo.* Those findings led to a search for the second human mitochondrial release factor. The revealed candidate, mtRF1a, was then characterised as a mitochondrial factor capable of terminating translation at UAA and UAG as demonstrated via the *in vitro* release assay described above. It was also capable of *in vivo* restoration of yeast (*S. pombe* and *S. cerevisiae*) *Δmrf1* phenotype (Soleimanpour-Lichaei *et al*., 2007). Further discovery of the ability of human mitoribosomes to -1 frameshift proved that mtRF1a is the only ribosome-dependent peptidyl-tRNA hydrolase with sequence specificity required to terminate all 13 mitochondrial ORFs (Temperley et al., 2010). Another member of the mitochondrial release factor family, ICT1, has been reported as a codon independent peptidyl-tRNA hydrolase and a mitoribosomal protein (Richter et al., 2010). It has been suggested to be involved in a quality control mechanism of resolving non-stop mRNA in mitochondria, however,

direct examination of such function and further experimental confirmation is required.

The precise function of the fourth family member, C12orf65, remains unknown and is the subject of the second part of this thesis. All four factors have been classified based on their sequence homology with class I RF.

Analysis of the mtRF1 sequence and comparison to bacterial release factors revealed sequence similarities so that mtRF1 was initially identified as a class I sequence specific RF1 type protein (Zhang and Spremulli, 1998). mtRF1 is a polypeptide of 445 amino acids with a molecular mass of 52,153 kDa and as indicated above, it more closely resembles the prokaryotic RF1-type factors rather than lower eukaryotic mitochondrial factors (Zhang and Spremulli, 1998). All known class I RFs have a GGQ motif that catalyzes the hydrolysis of the ester bond between nascent polypeptide chain and tRNA in the P site (Seit-Nebi et al., 2001). This motif is also present in mtRF1. There are 2 regions that are important in codon recognition. The PXT motif and region of α5 helix in a linier alignment separated from each other (Figure 3.1 A) need to come together to recognise the A-site codon (indicted by the blue boxes in Figure 3.1 B). mtRF1 has extensions in both of these domains and you will need to extend the alignment in the figure above. The sequence spanning codon recognition motifs, even though highly conserved in mtRF1a, varies in mtRF1 where it contains a hexapeptide PEVLGS. The fact the mtRF1 has arisen from a duplication of mtRF1a early in vertebrate evolution and that both genes can now be found in a number of vertebrates suggests that both are equally essential (Young et al., 2010). Moreover the fact that there is high sequence homology with mtRF1a, particularly within domains 2, 3 and 4 that are predicted to occupy the A-site ribosomal pocket, implies that both factors would occupy the same site in the ribosome. This also could be substantiated by the fact that when the ribosome was immunoprecipitated by mtRRF, it did not contain bound mtRF1a as both factors recognize the same A-site and only 1 could be present at any one time (Rorbach et al, 2008). This could also be the reason for mtRF1 not being found on those immunoprecipitated ribosomes. Further 3D molecular modelling of mtRF1 bound to the ribosome has highlighted the structural implications of the differences between mtRF1a and mtRF1, which will be

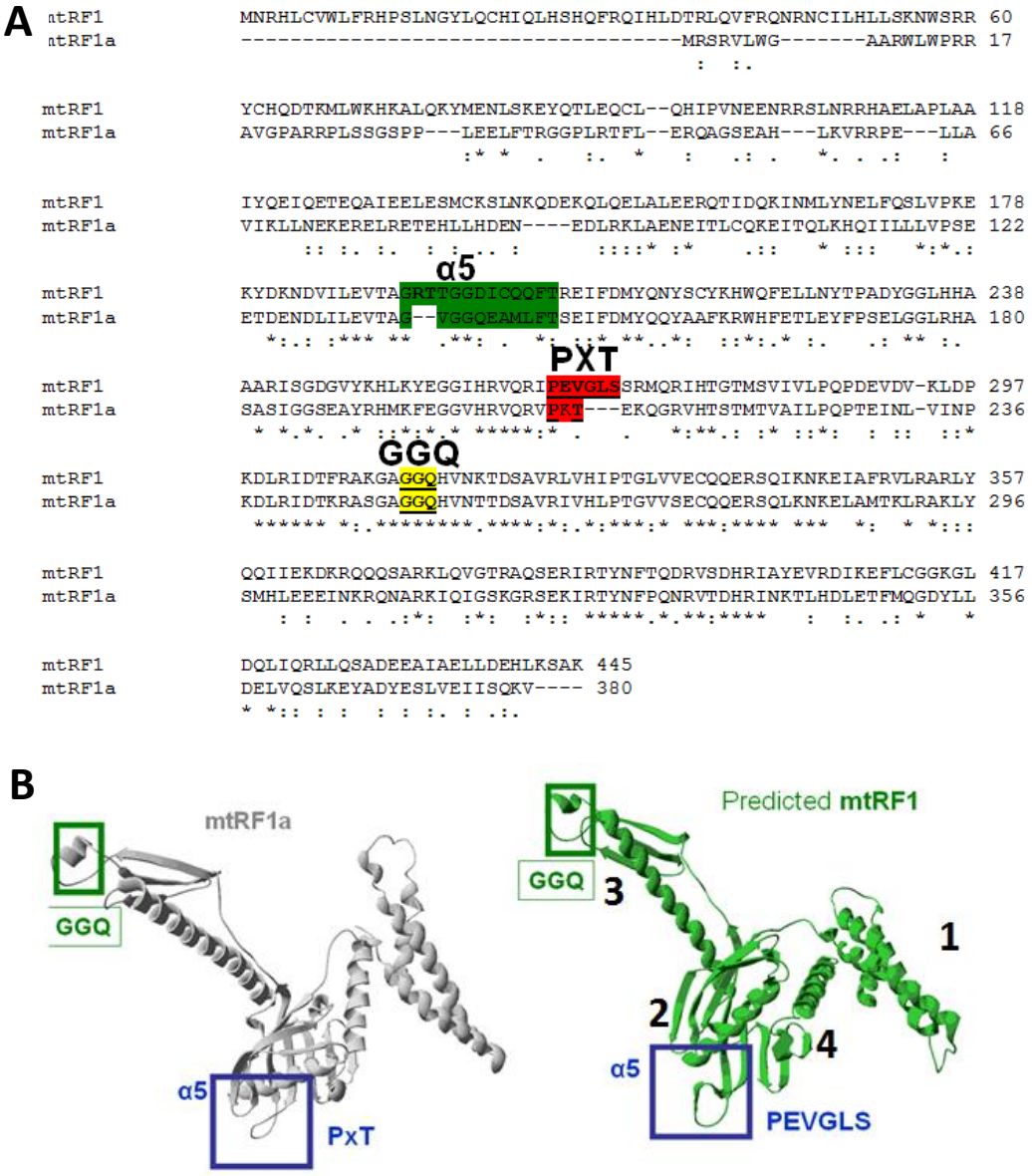

Figure 3. 1Structural comparison between mtRF1a and mtRF1 with their sequences alignment.

(A) The amino acids sequences of mtRF1 and mtRF1a were aligned with CLUSTAL 2.0.12 multiple sequence alignment. The fully conserved RF residues of functional regions between the proteins are indicated in **bold**. Conservations in all three proteins are indicated by an asterisk. Three crucial motifs described in the text are coloured, α5 in green, PXT in red and GGQ in yellow.**(B)** Both structures were modelled using SWISS-PDB-Viewer based on available crystallised models from PDB through blast selection against ExPDB and show open comrofmation upon ribosome binding of mtRF1a and mtRF1. Domains 4 and 2 interact with ribosomal SSU (via sequence recognition motives, boxed in blue) and once they are docked domain 3 swings away to deliver GGQ (green boxes) at the distal tip of the protein to the PTC on the LSU.

discussed later. The models serve to predict that mtRF1 is able to function on ribosomes with an empty A-site (Huynen et al., 2012).

Taken all together, mtRF1 has been described as a member of mitochondrial release factor family and given that mtRF1a is sufficient for all translation

termination, it makes searching for a function other than canonical translation termination for mtRF1 an interesting, but also challenging study. This first results chapter therefore focuses on investigating whether mtRF1 is an essential protein that is required for maintaining viable cells and fully functional mitochondria and what are the consequences of its loss.

3.2. Effect of mtRF1 depletion on cell growth

First to answer whether mtRF1 is required for cell viability, transient mtRF1 gene silencing by siRNA was performed (as described in methods 2.2.4). Three siRNA duplexes were designed and synthesised but after initial experiments to determine specificity, efficacy and reproducibility, duplex # 3 was chosen to be used throughout this investigation. In this project the final concentration used was 0.33 µM and the targeting specificity was optimised in my host lab prior to the start of my studies.

A known number of Hek293 cells and HeLa cells were treated with siRNA against mtRF1 (si-RF1) then grown in the presence of galactose, rather than glucose, to force respiration. Cells were maintained in this medium and after 3 days examined, after 4 days they were counted or retransfected to maintain 7 days of depletion. The western blot analysis of isolated mitochondria lysates (5 and 10 µg) from Hek293T clearly shows depletion of endogenous mtRF1 to non detectable levels after 3 days and this very significant depletion was maintained over 7 days (Figure 3.2 A). Similarly, mtRF1 was effectively depleted in HeLa cells after 3 days of treatment as determined by western blot analysis of 10 µg of mitochondrial lysates (Figure 3.2 D).

The number of the cells decreased dramatically as a consequence of mtRF1 depletion. After 4 days of treating HEK293T cells, there were twice as many control si-NT cells as si-RF1 cells (Figure 3.2) and this effect became even more striking after 7 days ($p=0.0061^{**}$) indicating reduced growth rate. A similar, but less profound effect was observed in the experiment with HeLa cells, where the number of cells also decreased significantly compared with control after 4 days ($p=0.0165^{*}$) and 7 days ($p=0.0250^{*}$). Due to the fact that the HeLa cell growth defect is less dramatic further investigation focused primarily on HEK293T cell line. The morphology and cell phenotype was examined after 3 days of siRNA treatment and the mtRF1 depleted cells show a significant

change (Figure 3.2 B). The mtRF1 depleted cells are elongated and do not grow close to each other, which contrasts with the cells treated with siRNA that does not target (NT) any transcripts. Together with the decreased cell number, the morphology data suggest mtRF1 to be crucial and essential for cell viability. This corresponds with earlier findings (Soleimanpour-Lichaei *et al*., 2007).

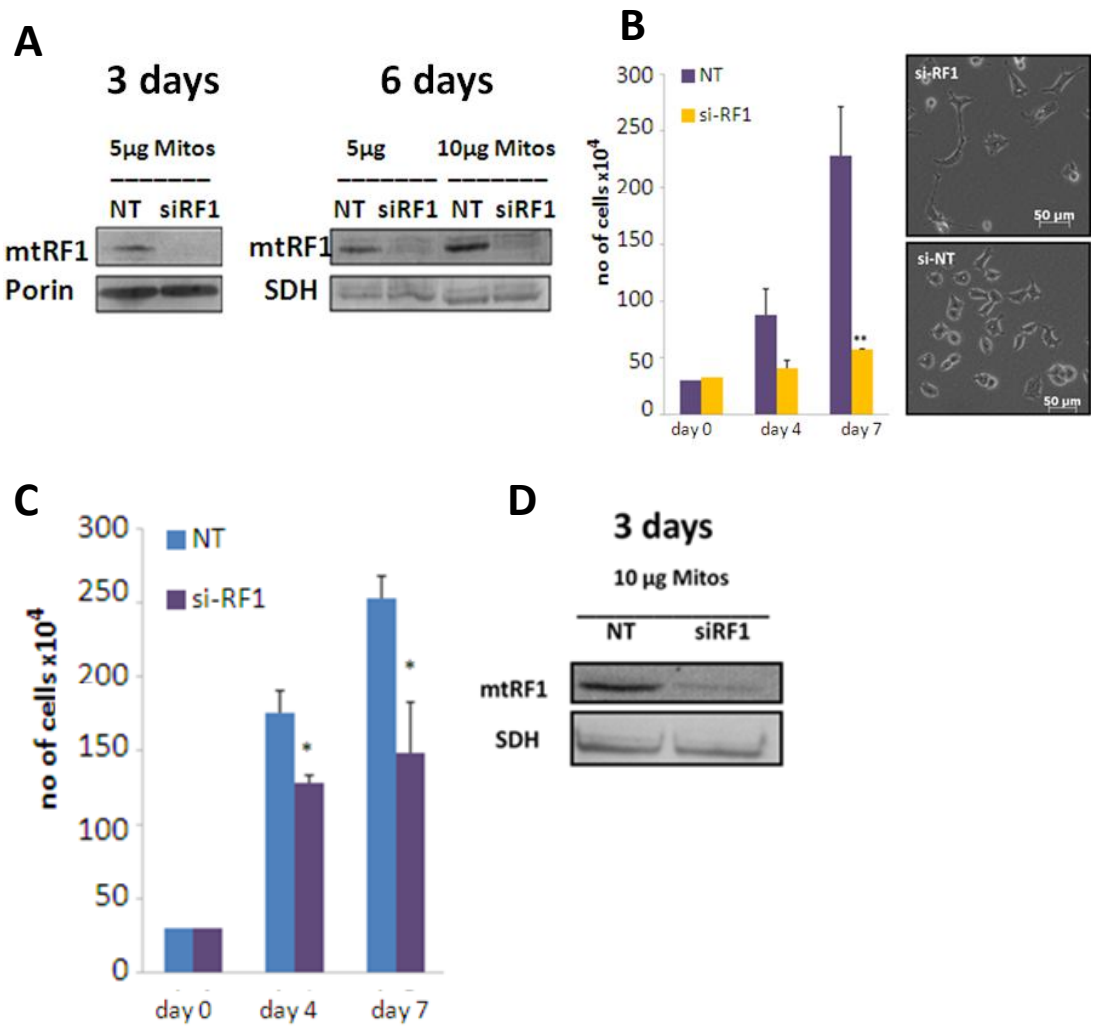

Figure 3. 2. mtRF1 depletion in HEK293T and HeLa cells.

Mitochondrial lysate (5 or 10µg) was separated by 12% SDS-PAGE, proteins were transferred to PVDF membrane and western blots performed with antibodies against mtRF1 to confirm depletion (si-RF1) in HEK293T cells **(A)** and in HeLa cells **(D)** after 3 and 6 days compared with non-targeting control (NT). Porin and 70kDa subunit of SDH were used as a loading control. The blot accurately reflects three experiments. **(B)** The doubling time in galactose medium of HEK293T (left panel of B, panel right shows morphology of HEK293T cells after 3 days of depletion) and HeLa cells **(C)** treated with siRNA directed against endogenous mtRF1 (si-RF1) or non-targeted (NT) siRNA was monitored after 7 days (day 0 represents initial starting cell number). The mean numbers with standard deviation represents three independent experiments (n=3; HeLa day 4 p=0.0165*, day 7 p=0.0250*; HEK293T: day 4 p=0.0834; day 7 p=0.0061**).

3.3. Effect of mtRF1 loss on mitochondrial morphology.

Following on robust decrease in cell growth rate and the overall change in phenotype upon mtRF1 depletion, mitochondrial morphology was also investigated. In order to assess any changes that might occur in mitochondrial organisation following siRNA transfection after either 3 or 6 days HEK293 and HeLa cells were stained with two fluorescent dyes. TMRM will enter mitochondria in a membrane potential dependent manner and Pico Green, which fluoresce upon binding to dsDNA. Staining of DNA with this dye hugely depends on DNA conformation, where supercoiled DNA produces lower signal as opposed to relaxed circles of this milecule (Reyes et al., 2011). Combined staining allows visualization of, the mitochondrial network as well as the nucleus and mt-nucleoids. As seen in my previous experiments cells become elongated and the mitochondria network of HEK293T cells after 3 and 6 days mtRF1 siRNA treatment (Figure 3.3 B and C) appear disrupted and more punctate, almost granules being placed more at the peripheries of the cells compared with mitochondria of HEK293T transfected with NT siRNA (Figure 3.3 A). HEK293T cells tend to be more loosely attached to the flask surface when in culture and their shape is more round making it more difficult to focus the zoom on one plane, therefore HeLa cells, which are generally more flat in culture, were incubated with the same dyes for better network visualisation. Mitochondria of HeLa cells treated with NT siRNA represent a characteristic reticular mitochondrial network evenly distributed within normal healthy cells (Figure 3.3 D). This network becomes disrupted into small fragmented units, seen clearly after 6 days, which tend to accumulate around nucleus. The experiment was performed in non quench mode, where lower dye concentrations were used in order to avoid dye aggregation or quenching in mitochondria. Thus the prediction would be that the lower fluorescence reflects depolarized mitochondria, which seem to be the case with mtRF1 depletion in this experiment. However, the directional changes in mitochondrial fluorescence cannot be interpreted here as no agent that would affect the membrane potential and confirm dye behaviour was used.

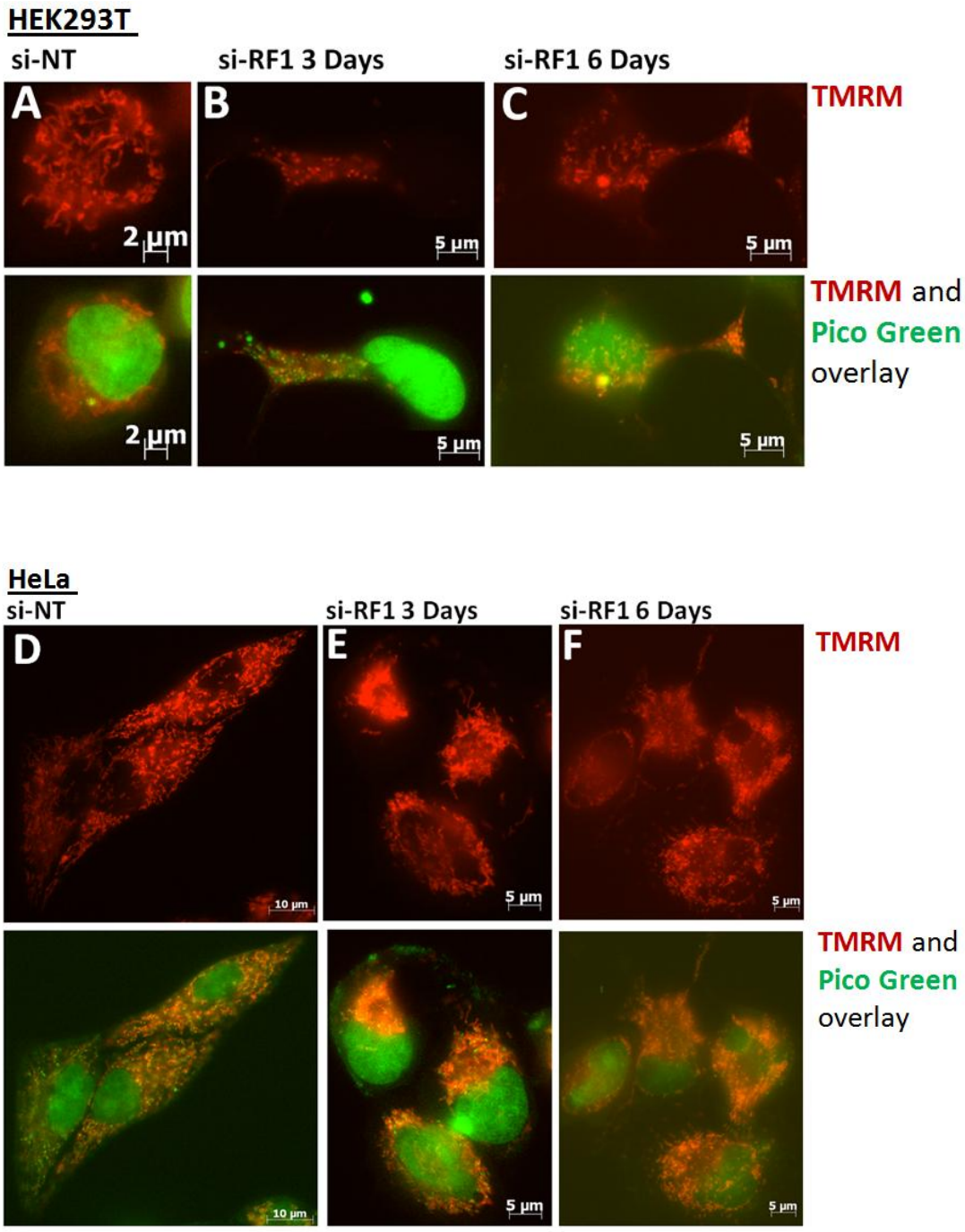

Figure 3. 3. Morphological changes of mitochondria upon mtRF1 depletion.

Representative fluorescent images of HEK293T **(A** to **C)** and HeLa cells **(D** to **F)** after 3 and 6 days of mtRF1 depletion with siRNA. Mitochondria were treated with TMRM to detect mitochondrial network (red) and *mitochondrial DNA* was visualised with PicoGreen, which stains both mitochondrial nucleoids and nuclear DNA green. siRNA targeted to mtRF1 led to visible deformation in mitochondrial network morphology in both cell lines after 3 and 6 days based on TMRM.

3.4. Investigating the steady state levels of mitochondrial proteins

With the evidence that mtRF1 is an essential protein, the next aspect that needed to be considered was: why do cells grow more slowly without this protein? With the assumption that mtRF1 plays a role in translation, its termination or the quality control of the process, and to further investigate the consequences of mtRF1 depletion and the cause of such a robust effect on cell growth rate, the effect of the depletion on the steady state levels of mitochondrial synthesised proteins, was analysed by western blot.

Hek293 cells were treated with either siRNA- mtRF1 or siRNA-NT for 4 and 6 days and 50µg of total cell lysates were separated by SDS-PAGE, followed by a transfer and immunodetection of the proteins of interest. The Figure 3.4 B (top panel) shows that the transfection with siRNA was efficient and after 3 days

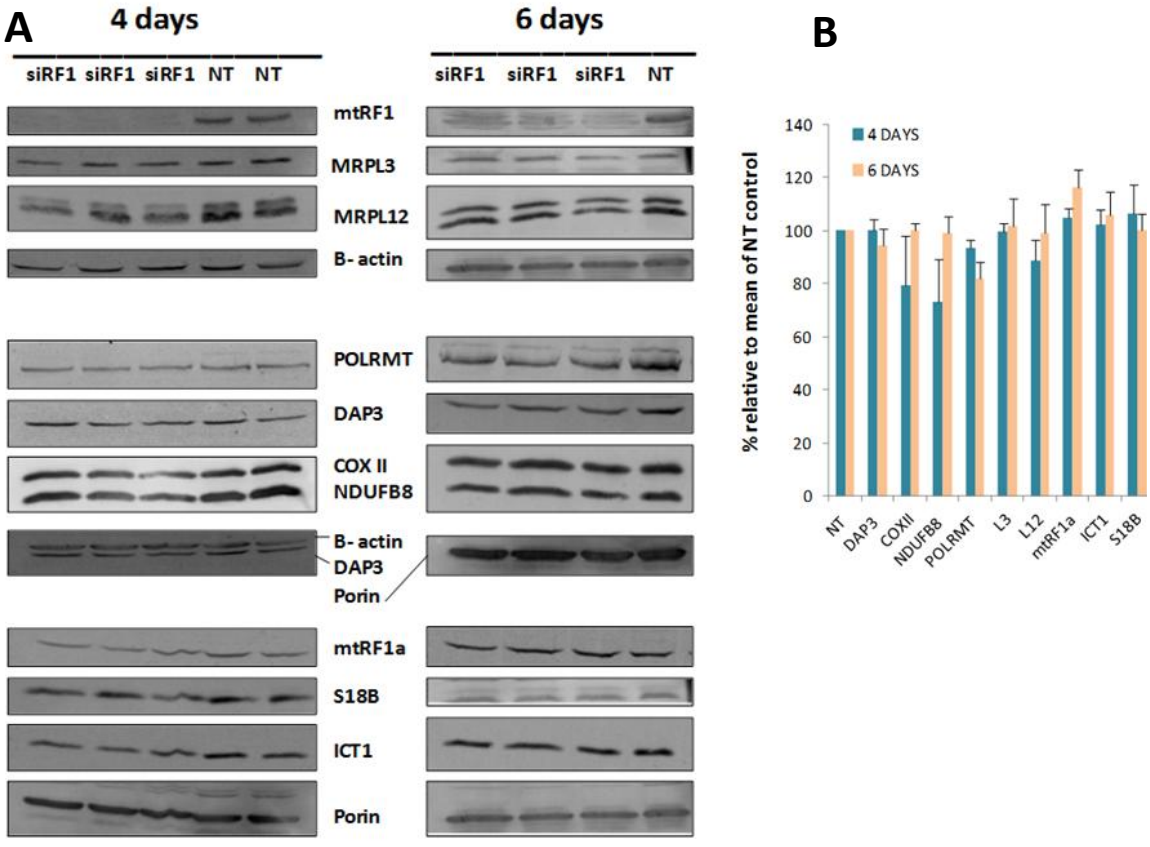

Figure 3. 4. Steady state levels of proteins after mtRF1 depletion.

(A) Western blot analysis of cell lysates (50µg) after 4 and 6 days of siRNA (siRF1 or NT) treatment with antibodies against proteins sensitive to mitochondrial translation inhibition (complex I subunit NDUFB8 and COX II), mitochondrial ribosome proteins (DAP3, MRPS18B, MRPL3, ICT1 and MRPL12) and other mitochondrial proteins including mtRF1, POLRMT and mtRF1a. Nuclear-encoded Porin and β-actin were used as loading controls. **(B)** Signals from panel B were quantified with Image-Quant software and the diagram represents three repeat experiments.

there was no detectable signal for mtRF1 (indicated by an arrow in Figure 3.4). Apart from this there were not any significant changes in mitochondrial encoded protein (COX II) in comparison with the control. There was also no defect in other, nuclear encoded, important mitochondrial proteins including mtRF1a, POLRMT or NDUFB8. In the absence of antibodies to all the mt-encoded proteins, NDUFB8 is used as a highly sensitive marker to defective assembly and stability of complex I that occurs in the absence of mt-encoded ND polypeptides. Components of the mitoribosome such as MRPL3, DAP3, MRPS18B and ICT1 remain stable, but interestingly MRPL12 consistently decreased.

Due to the fact that the results after 3 days of depletion do not directly correlate with the severe growth defect observed, a longer 6 day siRNA transfection of HEK293 cells was carried out. Since the number of cells (Figure 3.2) after 7 days treatment was significantly decreased one would predict this defect would be reflected on crucial proteins participating in mitochondrial processes. After 6 days of siRNA treatment, whole cell lysates were again separated by SDS-PAGE. The level of mtRF1 was dramatically decreased consistent with the growth curve data from 7 days of treatment. However, level of mitochondrial encoded COX II seems unchanged, with mitoribosomal proteins also being stable (MRPL3, ICT1, MRPS18B and DPA3). Whilst the depletion of mtRF1 for 3 days resulted in a noticeable decrease of MRPL12, the 6 days treatment did not show such a profound change. This could be due to the level of mtRF1 that was still present in the organelles after treatment and decay rate, as the level is clearly higher than seen after 3 days of depletion. This may directly reflect the relation between levels of mtRF1 and MRPL12 in cells, which needs to be investigated in more depth. One should note here, that since the western blots are only semi-quantitative, the signals were measured and histogram plotted only in order to confirm the visual inspection that indicated no significant differences between signals.

3.5. Effect of mtRF1 depletion on mitoribosomes

In light of the observation that depletion of mtRF1 may cause a direct down regulation of one of mitoribosomal proteins, MRPL12, as seen in the previous section the hypothesis that mtRF1 can really interact with monosomes to rescue aberrant translation became stronger. This would predict that loss of mtRF1

would result in accumulation of stalled mitoribosomes, which could be detected by western blotting of sucrose gradients as an increased signal corresponding to the monosome fraction. Such an arrest may have been sufficient to cause the growth defect. To assess whether this was indeed the case, HEK293T cells treated with mtRF1 or NT siRNA for 6 days were lysed and separated on 10-30% isokinetic sucrose density gradient. Separated proteins of interest were visualised by western blot with antibodies against polypeptides in the small (DAP3) and large (MRPL3 and MRPL12) mitochondrial ribosomal subunits. The same whole cell lysate preparation that was used for the gradient analysis was also separated independently on SDS-PAGE and analysed using anti-mtRF1 antibodies, with anti-SDH antibodies as a loading control. As seen in Figure 3.5 B the depletion was effective as the mtRF1 signal cannot be detected compared to siRNA-NT control. The result (Figure 3.5 A) clearly shows a similar pattern of distribution of MRPL3 and DAP3 in both experimental (Figure 3.5 A, bottom panel) and control gradients (upper panel), after 6 days of knockdown (Figure 3.5 C) In both cases the SSU, detected by anti-DAP3, migrated to and

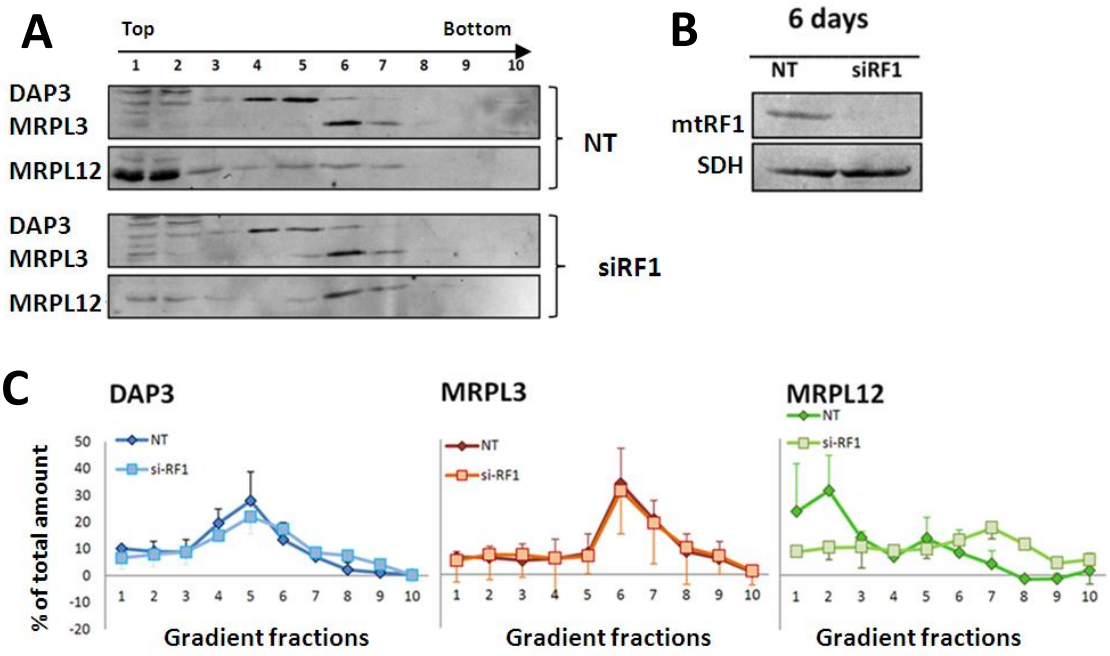

Figure 3. 5. Depletion of mtRF1 does not affect mitoribosome composition.

(A) HEK293T cells were treated with mtRF1 (siRF1) or non-targeted (NT) siRNA for 6 days and lysates (700µg) separated on 10-30% isokinetic sucrose gradient followed by fraction analysis by western blots using antibodies against the small (DAP3) and large mitochondrial subunits (MRPL3, MRPL12). **(B)** In order to confirm mtRF1 depletion in this experiment 50µg of cell lysates (prior to sucrose gradient centrifugation) were collected and analyzed separately by Western blot using antibodies against endogenous mtRF1 and SDH as loading control. **(C)** Western blot signals from (A) were quantified via ImageQuant software and presented in graphs showing the mean with standard deviation for each of 3 mitoribosomal proteins, from 3 independent experiments.

accumulated mostly in fractions 4 and 5, while a member of LSU, MRPL3, migrated to fractions 7, but mostly accumulated in fraction 6. Therefore, based on this data mtRF1 depletion did not contribute to detectable accumulation of monosomes. Interestingly, the decreased levels of MRPL12 did not affect the composition of monosome as visualised by the sucrose gradient, where there is still a signal detected in fraction 7 (Figure 3.5 A) in both samples siRF1 and NT treated. The free form of MRPL12, however, as seen in fractions 1 and 2 in the siRNA-NT (Figure 3.5 A, top panel) is present at a very low level after 6 days of mtRF1 depletion.

3.6. Investigating the steady state levels of mitochondrial mRNA

The existence of a pool of non-ribosome associated MRPL12 has been shown previously (Surovtseva et al., 2011). Its function, however outside ribosomes is not yet known but it has been shown to directly interact with POLRMT and believed to contribute to activation or increase of transcription (Surovtseva et al., 2011). Therefore, due to the decrease of ribosome free MRPL12 upon 6 days of mtRF1 depletion and in the further search for the cause of growth defect seen earlier (section 3.2) steady state levels of mitochondrial mRNAs were analysed by Northern blot after 4 and 6 days mtRF1 depletion in HEK293T cells, as well as 4 and 7 days mtRF1 depletion in HeLa cells. Overall the 4 days depletion of mtRF1 in both cell lines resulted in no loss of stability of all tested transcripts. With the exceptions of bicistronic *RNA14* (*MT-ATP6* in Figure 3.6) that is not significantly lower in HeLa cells after 4 days depletion. The rest of the steady state transcript levels oscillate around the control levels of mRNAs seen in 'healthy' mitochondria, which are within experimental error. After 6 day of mtRF1 depletion HEK293 cells do not show any significant loss of mRNA stability, in fact they show a slight increase of two transcripts (*RNA14* and *MT-ND1*) and ribosomal RNA (*MT-RNR1* and *MT-RNR2*) with *MT-COX1* remaining unaffected (Figure 3.6 B). HeLa cells, in contrast, as seen on the histogram (Figure 3.6 B, left panel) show a significant loss of stability of *MT-COX1*, mt-rRNAs (*MT-RNR1* and *MT-RNR2*) and an increase of *MT-ND1* with *MT-RNA14*.

However, the signals were measured by Image-Quant software, then calculated relative to the controls and resultant histograms are not fully quantitative. These

are included to indicate any subtle changes that might exhibit a trend. Moreover, it is clear that the northern blot does not reflect such dramatic changes in mRNAs levels. Therefore, apart from the subtle increase of several RNAs, there was no obvious pattern that could be detected between the different transcripts or treatments.

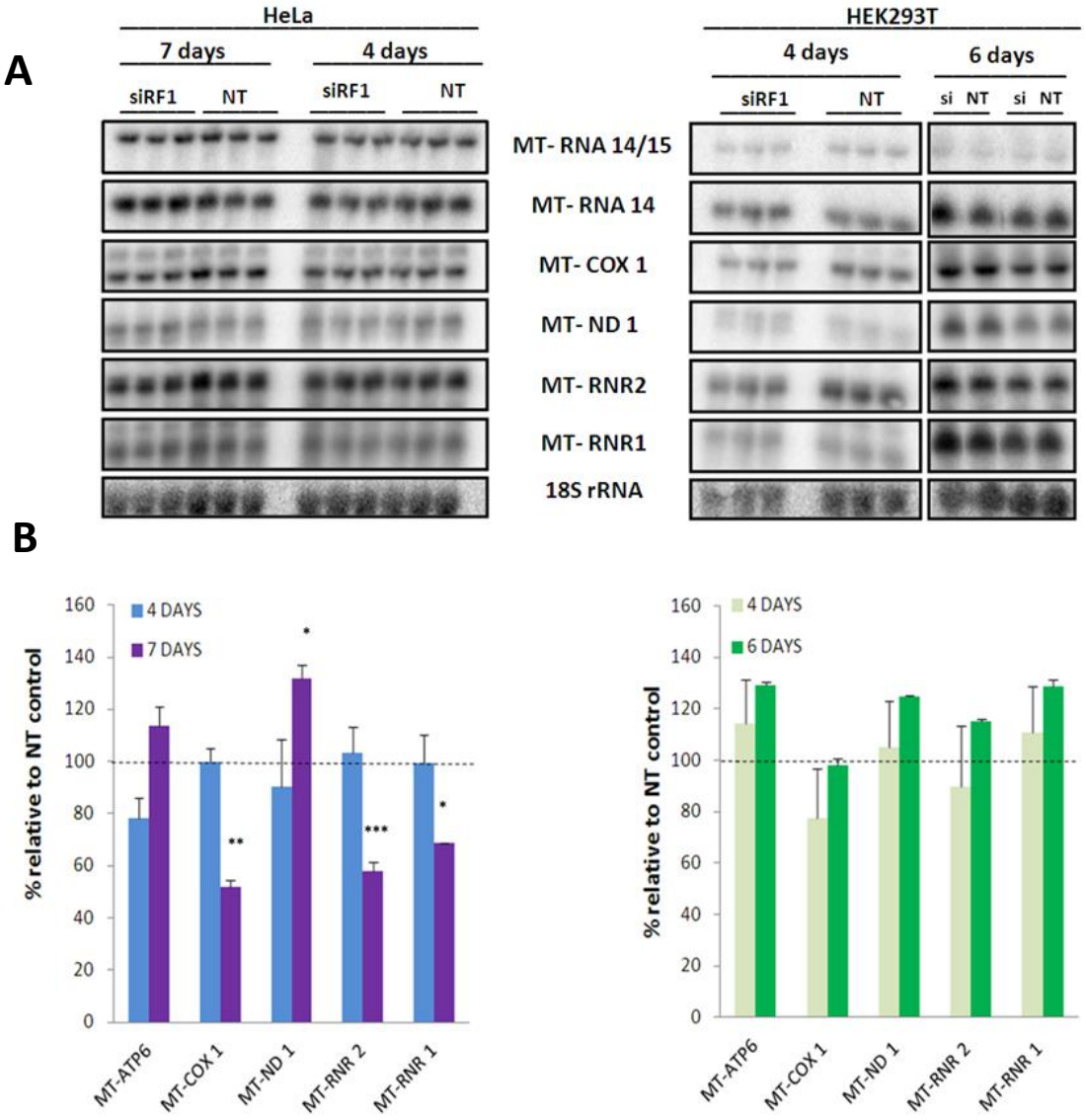

Figure 3. 6. Steady state levels of mitochondrial RNA after mtRF1 depletion.

(A) Northern blots of total RNA extracted from HeLa cells (3 µg RNA) and HEK293T (4 days -1µg RNA, 6 days- 6 µg RNA) treated with non-targeting (NT) or targeting endogenous mtRF1 (siRF1) siRNA. The blots were hybridised with probes to mitochondrial mRNAs (*RNA14*, *MTCO1* and *MTND1*), mt-rRNAs 16S (*MT-RNR2*) and 12S (*MT-RNR1*) as well as human 18S rRNA for quality and loading control. **(B)** The signals were quantified and the graph presents mean and standard deviation of three independent experiment repeats, which are relative to the mean of non-targeting control, a dotted line (*p <0.05, **p<0.01,***p<0.001).

3.7. Investigating the mitochondrial mRNA distribution on isokinetic sucrose gradients at steady state.

A further aim was to test whether mtRF1 knock-down would facilitate an accumulation of the increased mRNA species (seen in previous section) on ribosomal subunits or the fully assembled monosome. I aimed to detect this by analysing sucrose gradients that would allow RNA distribution, which, if affected could reflect the stalled mitoribosome status. This was analysed by preparing a lysate from HEK293T cells that had been subjected to siRNA treatment for 6 days. The lysate was separated though an isokinetic sucrose density gradient followed by a western and northern blot analyses of the protein and RNA fractions respectively. In order to detect the migration of the mtSSU, mtLSU and monosome two probes specific to each rRNA were used (MT-RNR1 and MT-RNR2) in the northern blot. The signal for mtSSU first appears in fraction 4 and distributes evenly down to the bottom of the gradient, where fraction 11 represents the gradient pellet (Figure 3.7 A). The 16S rRNA partitions to fraction

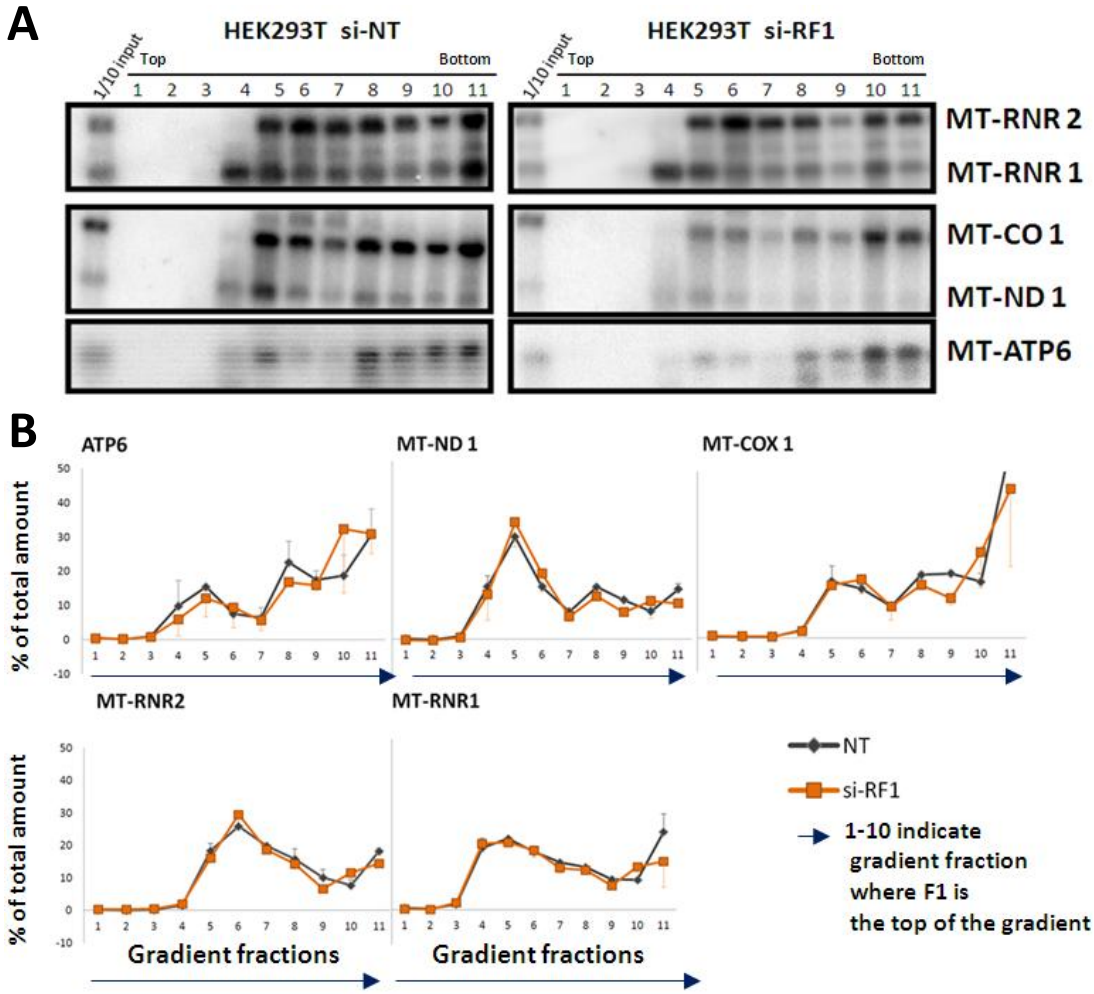

Fiure 3. 7. Northern blot analysis of mitochondrial RNA distribution on gradient after mtRF1 depletion.

(A) HEK293T cells were treated with mtRF1 (siRF1) or non-targeted (NT) siRNA for 6 days and lysates (700µg) separated on 10-30% isokinetic sucrose gradient. RNA was extracted from each fraction (1-11 and 1/10 of an input) and analysed on a northern blot using probes to mitochondrial mRNAs (*RNA14, MTCO1* and *MTND1*) and 16S (*MT-RNR2*) with 12S (*MT-RNR1*), mt-rRNAs. **(B)** The signals were quantified and presented as the graph of mean and standard deviation from three independent experiment repeats (**p* <0.05, ***p*<0.01, ****p*<0.001).

5, then distributes to the bottom of the gradient. The signals in earlier fractions (4-6) represent the free uncomplexed state of each individual subunit, whereas signals in fractions from 8 represent the presence of monosomes. This pattern of monosome is also seen by the distributions of mRNA, signals of which become more intense again, where trapped by the monosome (fractions 8). The histogram plotted based on detected signal on northern blot clearly reflects this even distribution of both rRNA and mRNA tested between the sample (si-RF1) and control (NT in Figure 3.7). Therefore, based on this piece of data 6 days of mtRF1 depletion does not appear to affect the migration of the mitoribosomes. This recapitulates protein distributions seen in section 3.5. In neither case was there strong evidence that mitochondrial transcripts accumulate on monosomes following mtRF1 depletion with these conditions.

3.8. Discussion

In this chapter that aimed to determine the function of mtRF1, siRNA were used to deplete this target protein from human cell lines. As part of this initial characterisation, which resulted in a decrease in growth rate after only 3 days and was even more dramatic after 6 days, both the cell morphology and mitochondrial network were also changed. The approaches undertaken in this chapter could not uncover the molecular mechanism responsible for such dramatic effects.

It is commonly known that significant mitochondrial morphological changes can be induced by various stress conditions. Moreover, because mitochondrial dynamics regulates many specific cell functions, the changes in their morphology, such as fragmentation, can play an important role in a variety of processes including apoptosis (Youle and Karbowski, 2005), Calcium transfer (Park *et al*., 2001), mitochondrial quality control (Ashrafi and Schwarz, 2012) and cell-cycle regulation (Mitra *et al.*, 2009). In addition, mitochondria have

been shown to be much less likely to fuse in a depolarized state and could undergo autophagy (Twig *et al*., 2008).

Mitochondrial quality control and autophagy/mitophagy machinery is a broad subject and out of the scope to this thesis. However, it has been shown that as a response to the depolarisation of electrochemical potential across the IMM (achieved experimentally by addition of the commonly used mitochondrial uncoupler CCCP), a complete recruitment of Parkin to the fragmented and uncoupled mitochondria occurs, which together with PINK1 eventually leads to autophagy (Narendra *et al*., 2008; Park *et al*., 2006). Parkin is an ubiquitin E3 ligase, the activity of which increases when accumulated in mitochondria and mediates the formation of 2 polyubiquitin chains. One (K48) is associated with proteosomal degradation of a substrate and the second (K63) is associated with autophagic degradation (Chan *et al*., 2011). Parkin is not the only E3 ligase that has been linked to mitochondrial dynamics. There is also MULAN, a RING finger protein and the small ubiguitin-like modifier (SUMO) E3 ligase (MAPL), both of which have been shown to be translocated to mitochondria and influence mitochondrial fragmentation (Li, *et al*., 2008; Braschi *et al*., 2009), however their detailed role is not clear.

There is growing evidence that the cytosolic ubiquitin/proteasome system (UPS) is also a part of mitochondrial surveillance pathways. Accumulation of elevated levels of mitochondrial ubiquitinated proteins have been observed when proteosome activity was inhibited and many proteins have been identified as UPS substrates, such as mitofusin 1 and 2, Mcl1, but also VDAC1, Tom20 and Tom70 (Livnat-Levanon *et al*., 2011; Margineantu *et al*., 2007; Tanaka *et al*., 2010; Chan *et al*., 2011). In addition to the mitochondria's own proteolytic system in the IMM that degrades unfolded proteins (AAA proteases) (Langer *et al*., 2001) and the proteosome directed degradation of proteins from different mitochondrial compartments, another pathway was recently reported. In this route mitochondrial derived vesicles transport selected mitochondrial proteins to the lysosome. This process does not require depolarization and complements mitophagy (Soubannier *et al*., 2012). However, there is no evidence of the fate of proteins that have been stalled on the ribosomes and needs to be degraded. In yeast, there has been a specific ribosome-associated E3 ubiquitin ligase

characterised that specifically marks nonstop proteins for proteosome degradation in the cytosol (Bengtson *et al*., 2010).

Given mtRF1 structure and the prediction that it functions on the ribosome as part of a mechanism exerting quality control in mt-protein synthesis, it cannot be excluded that it may have similar function or at least be indirectly involved. Loss of mtRF1 by siRNA depletion would be predicted to unbalance the system. If it participates in mitochondrial surveillance pathway, its depletion would result in nascent polypeptides being stalled on ribosomes that need to be degraded and ribosome recycled. In the data presented in this chapter the accumulation of such proteins and ribosome stalling was not observed when monitoring either steady state levels of proteins or RNA, or on gradient fractions of proteins or RNAs. Also in previous preliminary experiments performed in HeLa cells prior to my involvement in the project only a very subtle, not significant increase was seen in ^{35}S *de novo* mitochondrial protein synthesis (data not shown) after 3 day of mtRF1 depletion. The unaffected steady state levels of mitochondrial proteins after depletion of mtRF1 could be explained by the fact that even if mtRF1 takes part in translation termination it is not until the stop codon/no codon is present in the A-site. Thus, the synthesised polypeptide chain is already fully elongated when RF1 may exert its action, and the level of synthesised proteins most probably reflects the elongation step rather than termination or rescue. By using only western blot analysis it is not possible to determine whether the proteins seen on the membranes are folded correctly, not truncated or whether they are fully active and able to form complexes. Moreover, at this stage it was not possible to assess whether the mitochondrial encoded proteins are being trapped in the mitoribosomes and not being released and able to be chaperoned properly and inserted into the inner mitochondrial membrane.

Despite the lack of robust effect on the proteins analysed, the superoxide, peroxide and mitochondrial mass (all part of the preliminary studies in my host lab) were all shown to be elevated upon mtRF1 depletion. Increased ROS can cause oxidative damage to mitochondria (mtDNA, lipids, proteins) (Reviewed by Parsons and Green, 2010), which in turn can cause release cytochrome *c* and high levels of Ca^{2+}. The changes in Ca^{2+} signalling can affect mitochondrial normal strategic positioning within the cells and result in groups of separate

mitochondria grouped in different regions within a cell (Park *et al*., 2001), which was seen in this chapter, i.e. fragmented mitochondria accumulated around the nucleus in HeLa cells (Figure 3.3). Increased ROS can also affect membrane potential and this can trigger recruitment of E3 ligase to mitochondria to target initially proteins stalled on the ribosomes to degradation.

In order to assess whether such a scenario is plausible, the mtRF1 depleted cells would have to be tested for accumulation of E3 ligases, e.g. Parkin. Although potentially interesting, more importantly for this thesis, this would not shed any new light on the possible mtRF1 function. For this it is necessary to produce the candidate substrate or to try and demonstrate the occurrence of blocked ribosomes and truncated/ stalled proteins, which is the focus of the following chapters.

It is difficult to link the mt-RF1 depletion induced mitochondria fragmentation with any of the processes mentioned above that would justify the substantial decrease in growth rate. This finding has shown that mitochondrial RF1 is essential for cell viability, which confirms its important role for both mitochondrial and cell biology. Even though there was no significant difference in steady state level of most mitochondrial proteins after 3 days of depletion, surprisingly, the mitochondrial ribosome protein MRPL12 (MRPL12) does seem to be down regulated at this stage and potentially the levels of mtRF1 could reflect or influence the levels of this ribosomal protein.

The second function of MRPL12 outside the ribosome in mitochondrial gene expression and regulation of transcription is still debated. It has been shown that some proteins from the mtSSU, MRPLS29 and MRPS30 play a part in apoptosis, connecting the mitochondrial translation with cytosolic processes (Surovtseva *et al*., 2011; Koc *et al*., 2001; Shutt and Shadel, 2010). Based on this it is tempting to hypothesize that MRPL12, as suggested earlier (Surovtseva *et al*., 2011), could play similar function to that in bacteria (Ramagopal *et al.*, 1976), where accumulation of non-ribosome associated L7 and L12 can bind RNA sequences inducing ribosome biogenesis. It is possible that accumulation of free MRPL12 upon mtRF1 depletion could be an indication of similar mechanism, where in principle ribosome stalling events can shift the balance between ribosome associated and free pools, in turn signal, either

through POLRMT binding or possibly to the nucleus that ribosome biogenesis is required to compensate for impaired mitochondria.

Chapter 4

Is human mtRF1 a ribosome dependent peptidyl-tRNA hydrolase?

4. Chapter 4: Is human mtRF1 a ribosome dependent peptidyl-tRNA hydrolase?

4.1. Introduction

Two mitochondrial proteins, mtRF1a and mtRF1 have been shown to be localised to mitochondria, however only mtRF1a has been experimentally ascribed to have the release factor function and to recognise the two mitochondrial termination signals UAA/UAG, which are sufficient to terminate translation of all human mitochondrial open reading frames (Soleimanpour-Lichaei *et al*., 2007, Temperley *et al*. 2010). So why do mitochondria still retain the other release factors such as mtRF1? It is therefore hypothesised that mtRF1 may still function on the A-site of ribosomes but instead of recognising specific codons sequences it would only bind there if mRNA is missing from the site mediating the rescue of stalled ribosomes.

Structural studies of bacterial RF1 (Petry *et al*., 2005) have demonstrated that the characteristic loop containing the PXT motif of bacterial RFs faces the second and third bases of stop codon, whereas the tip of alpha 5 helix is parallel to the first nucleotide of codon, forming 'molecular tweezers' facilitating codon specificity. Significantly, mtRF1a shows high levels of similarity when compared with bacterial counterpart sequence. In addition both of them possess i) the GGQ tripeptide found in all release factors that is known to promote peptidyl- tRNA hydrolysis (PTH) in the peptidyl-transferase centre (PTC) located deep in the large ribosomal subunit, ii) the tripeptide PXT motif and iii) share similar alpha 5 domains. By analogy, mtRF1 would use the different, PEVGLS hexapeptide motif together with the extended and different tip of alpha 5 helix that would be positioned within the decoding centre in A-site. This would allow for the prediction that mtRF1 may still act on the ribosomal A-site. A fundamental aspect of my project was to identify if human mtRF1 can act as a peptidyl tRNA hydrolase and whether its conserved GGQ domain is functional and therefore required to maintain cell viability.

The presence of the evolutionarily conserved GGQ motif is a strong theoretical indicator that mtRF1 should have retained PTH activity. Frolova *et al.* (1999) have shown that mutations in the highly conserved GGQ motif, present in all release factor family members, result in the loss of peptidyl-tRNA hydrolysis activity. I therefore decided to use this information to design mutants that would

enable me to determine whether the GGQ motif is still significant for mtRF1 function. The following set of experiments were designed to generate stable cell lines that could inducibly express mtRF1-wild type GGQ, mtRF1-AGQ or mtRF1-GSQ as FLAG-tagged proteins in human HEK293-Flp in cell lines. The cells would be induced to express the relevant protein for 3 days so that a growth curve could be plotted to allow me to assess changes in cell metabolism caused by a dominant negative effect due to expression of the mutants. Moreover, these constructs were designed so that silent mutations would be incorporated in to the gene sequence to render these transcripts insensitive to the siRNA that is effective against endogenous mtRF1. This strategy allowed to me to deplete the endogenous protein and express the mutant at wild type levels to avoid any phenotype being only the consequence of over-expression of an exogenous protein. Assuming the motif preserves its function, and the expressed proteins are localized to mitochondria, mutations in this region would be predicted to have the same consequence as depletion (as reported in chapter 3) including reduced growth on galactose. One hypothesis was that the mtRF1 mutants may engage in the A-site but fail to elicit PTH activity and so might remain in the A-site rather than being only transiently associated. To test this, the expression of the mutated proteins was induced *in vivo* for 6 days followed by a sucrose gradient analysis to examine the mtRF1 mutants ability to associate with the monosomes.

4.2. Generation of stable inducible cell lines expressing mtRF1-GGQ-SM-FLAG wild type or mutant proteins.

The aim was to determine whether the presence of a mutated GGQ motif can have a dominant negative when expressed in cultured cells. It was important, however, to make sure that any effect was due to the mutant form of mtRF1 and not simply due to the presence of high levels of overexpressed protein. For this reason it was necessary to titrate the levels of the FLAG-tagged mtRF1 proteins to ensure it was equivalent to the levels of the endogenous mtRF1 that is constitutively present in untransfected HEK293T cell lines. Initial experiments treated cells for 3 days simultaneously with different concentrations of siRNA-RF1 (5-50nM), which targets both endogenous and expressed forms, and tetracycline to induce expression of exogenous FLAG-tagged mtRF1 proteins.

This was intended to deplete the endogenous protein and at the same time keep the exogenous protein level low. The latter could be detected by western using anti-FLAG antibodies to discriminate between endo/ and exogenous protein. Frustratingly, the range of siRNA dilutions tested did not control the FLAG-tagged protein to a level comparable to the endogenous amount of mtRF1 (Figure 4.1 A). mtRF1 decreased gradually as the concentration of siRNA used increased from 5nM to 15nM, however mtRF1 levels were still ~50% higher than the control untreated HEK293T. Despite increasing the siRNA concentration in the range of 30 - 50nM, the level seems to become fixed and did not decrease further (Figure 4.1 A). It was clear from this result that a different approach needed to be carried out. Thus, to determine whether the presence of a mutated GGQ motif can have a dominant negative effect when expressed in cultured cells, constructs were generated that would allow expression not just of FLAG-tagged versions of mtRF1-GSQ and mtRF1-AGQ but versions that would be insensitive to the siRNA. Thus, FLAG-tagged versions of each mutant and of wildtype mtRF1-GGQ were generated so that each construct included a site directed synonymous silent mutation (SM) in the region covered by the siRNA. For simplicity these SM-FLAG variants of mtRF1 will be described as **WT**, **GSQ** or **AGQ** hereafter unless otherwise specified. The endogenous gene would still be targeted but translation of the exogenous transcripts would still occur. Inducible HEK293T cell lines were generated for each construct. As described above, the expression of the FLAG-tagged proteins needed to be titrated to ensure that levels were equivalent to those of the endogenous mtRF1 normally present in untransfected HEK293T cell lines. To achieve this, the cells were treated as before with siRNA-RF1 (33nM). In this fashion the levels of FLAG-tagged mtRF1 could be now regulated by different tetracycline concentration added to the cells whilst depleting the endogenous proteins, with an overall expression level that reflects the physiological condition.

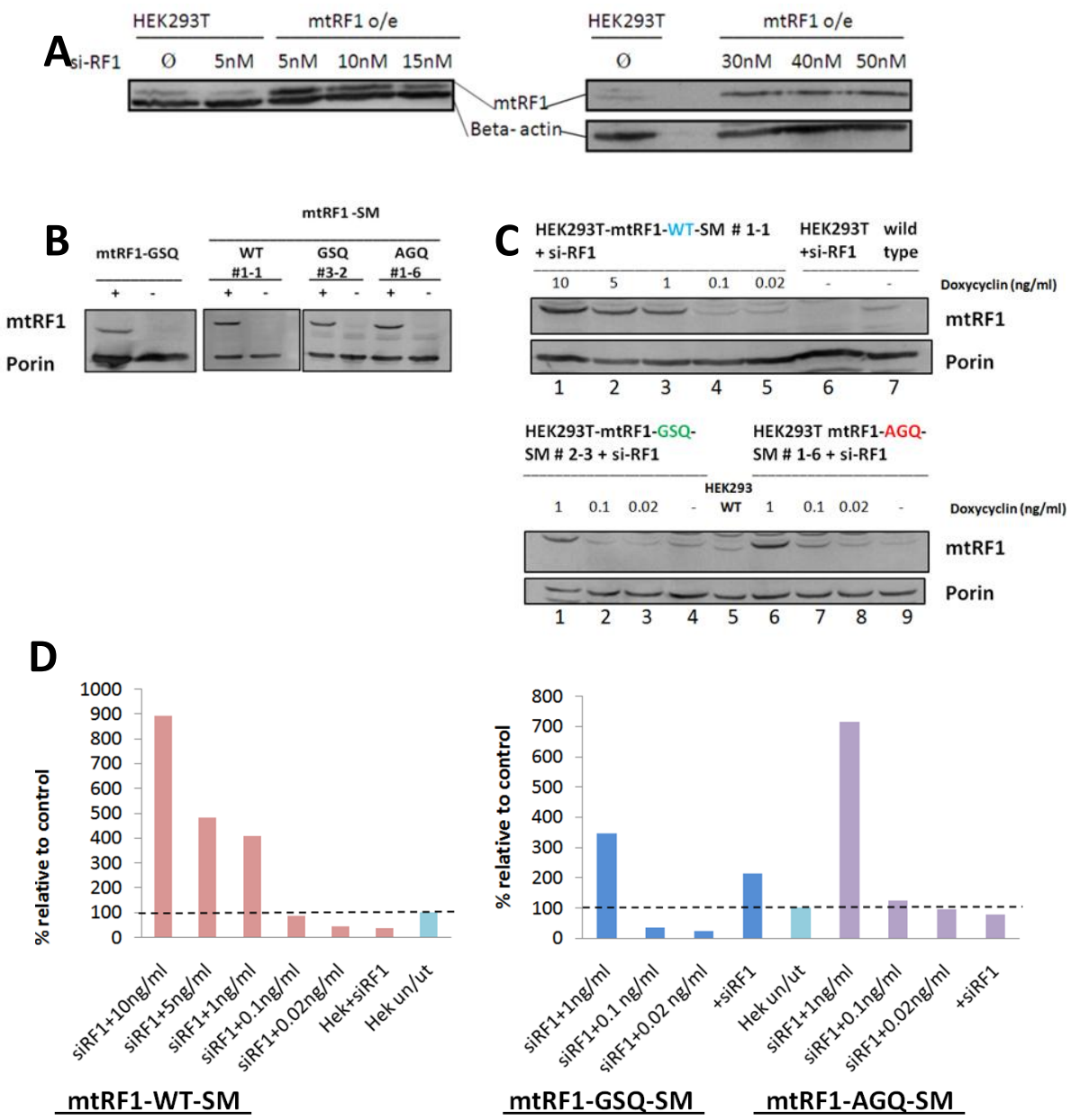

Figure 4. 1. Regulating the levels of overexpressed mtRF1.

(A) HEK293T untransfected or transfected with mtRF1-FLAG and tetracycline induced (3 days) were treated with different amounts of siRNA for mtRF1 (0-50nM) for 3 days. Each cell lysate (50µg) was analysed by western blot. To show the level of overexpression, anti-mtRF1 antibodies were used along with anti- β-actin antibodies as a loading control. **(B)** Expression was tested in three HEK293T cell lines stably transfected with mtRF1 gene containing siRNA resistant mutations and **mtRF1-WT** (clone # 1-1), **mtRF1-GSQ** (clone # 3-2) and **mtRF1-AGQ** (clone #1-6). MtRF1-GSQ-FLAG lacking the silent mutation (left panel), used previously, was used here as an overexpression control; and porin as a loading control. **(C)** Different concentrations of doxycycline were used to titrate expression of mutant FLAG-tagged mtRF1 proteins, whilst depleting with siRNA and levels were analyzed by western blot (50µg of cell lysates). HEK293T untransfected wild type (lane 6 and 7 in upper panel; lane 5 bottom panel), **mtRF1-WT** (lanes 1 to 5 top panel), **mtRF1-GSQ** and **mtRF1-AGQ** (lanes 1-4 and 6-9 respectively, bottom panel) cells were cultured for three days in glucose in the presence of both 33nM siRNA-RF1 and different amounts of doxycycline. **(D)** The levels of mtRF1 proteins were measured via ImageQuant software.

Hek293-FlpIn TRex cells were transfected for a stable integration of the

constructs containing the mtRF1-GSQ, mtRF1-AGQ and mtRF1 wildtype variants all with the silent mutation in the siRNA targeted region. Successful transfectants were selected over a 2 week period using Hygromycin^{B} (100ug/ml). Once a population of resistant cells was established a small culture was induced with tetracycline for 24 hours to analyse for expression. Cells were harvested, a cell lysate prepared and western blot analysis performed with anti-FLAG antibodies (Figure 4.1 B). Effective expression of mtRF1-WT and both mutants was observed and the levels of FLAG-tagged mtRF1 variants could be now regulated by addition of different doxycycline concentrations (10ng/ml, 5ng/ml, 1ng/ml, 0.1ng/ml and 0.02ng/ml) whilst depleting the endogenous protein. This way expression could be regulated to only that of the variant and only at physiological levels. In Figure 4 where the doxycycline titration experiment is presented (Figure 4.1 C), there is clear depletion of mtRF1 (Figure 4.1 C, lane 6) compared with control (untransfected wild type HEK293T, Figure 4.1C lane 7). There is also controlled doxycycline induction of all three expressed proteins: using concentrations ranging from 10 to 0.02ng/ml for mtRF1-WT (Figure 4.1C, top panel, lanes 1-5), and <1 to 0.02ng/ml for mtRF1-GSQ (lanes 1-3) and mtRF1-AGQ (lanes 6-8). Based on the western results and the quantification of the signals (Figure 4.1 D) it was decided that the closest resemblance to endogenous levels of mtRF1 and thus optimal for the purposes of this investigation was with induction using 0.1ng/ml of doxycycline in all three cases.

4.3. Mitochondrial import of mtRF1-GGQ-SM-FLAG mutants.

Before testing the functionality of the conserved GGQ motif in mtRF1 using the newly defined induction conditions, it was necessary to determine whether the expressed variants were translocated to mitochondria. Cells expressing each of the variants were treated with 1µg/ml of tetracycline for maximum induction for 3 days, then the organelles were isolated and following western blot analysis the expressed proteins could be detected via anti-FLAG antibodies. Clear expression (Fig. 4.2, lane 1) and efficient translocation of each of the proteins to a mitochondrial compartment was shown. This was demonstrated as the FLAG-tagged proteins were protected from proteinase K treatment (1µg and 4µg; lanes 2 and 4 respectively in figure 4.2). However, when the organelles were

lysed with 1%Triton X-100 the proteins lacked protection and were efficiently digested in all cases with 4µg of proteinase K (Figure 4.2, lane 5).

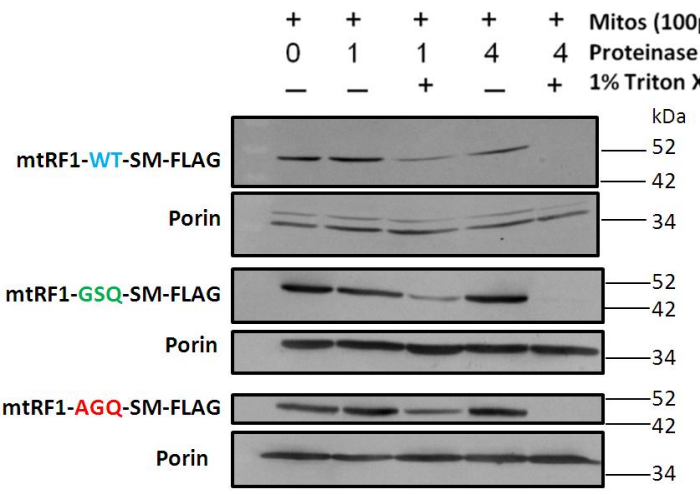

Figure 4. 2. Mitochondria import of mtRF1-GGQ-SM-FLAG mutants.

Western blot analysis was performed on 10µg of isolated mitochondria from HEK293T cell lines expressing each of the gene constructs. Isolated mitochondria were treated with proteinase K (1 or 4µg per 100µg mitochondria, lanes 2-5) and with 1% Triton X-100 (lanes 3 and 5), to confirm PK activity or untreated control (lane 1). Anti-FLAG antibodies were used to confirm the presence of overexpressed protein in each sample. Porin was used as a loading control.

4.4. Expression of mtRF1-WT-GGQ is required for healthy mitochondria and normal cell growth.

Since the stable transfection of all 3 gene variants and their translocation to mitochondrial was successful, the analysis of whether the GGQ of mtRF1 was functional could now be performed. Therefore for the following investigation 0.1ng/ml of doxycycline was used to induce expression of each of the mtRF1 variants; wild type or GGQ mutants. The cells were simultaneously depleted of mtRF1 over 3 days then harvested, cell counts performed, followed by a western blot analysis of the cell lysates.

As seen in the graph (Figure 4.3 B) the depletion of mtRF1 resulted in significant growth defect compared with HEK293T-mtRF1-WT treated with NT siRNA (Figure 4.3, for RF1-WT+NT vs RF-WT+siRF1 p=0.0059) as observed before in chapter 3. If doxycycline was added to bring about the simultaneous expression of mtRF1-WT, the cells showed a significant rescue of mtRF1 depleted cells phenotype (RF-WT+si vs RF-WT+si+0.1 p=0.0006). The cell morphology also reflected the rescue. Wild type HEK293T cells (Figure 4.3 A, panel a) show the characteristic shape and distribution of healthy cells in culture, which is also seen in transfected but uninduced HEK293 treated with NT siRNA (A panel b). The depletion of mtRF1 resulted in changed phenotype,

cells became elongated and did not grow close to each other, as seen previously in chapter 3 (A panel c). After inducing expression of wild type mtRF1 in those cells, where endogenous has been depleted, the cell shape more resembled healthy HEK293 cells than those after mtRF1 depletion (A panel d). This was also consistent with the relative steady state levels of mtRF1 as analysed by western. The levels are comparable between endogenous protein (with or without NT siRNA) and expressed forms (Figure 4.3 C, lanes 3,

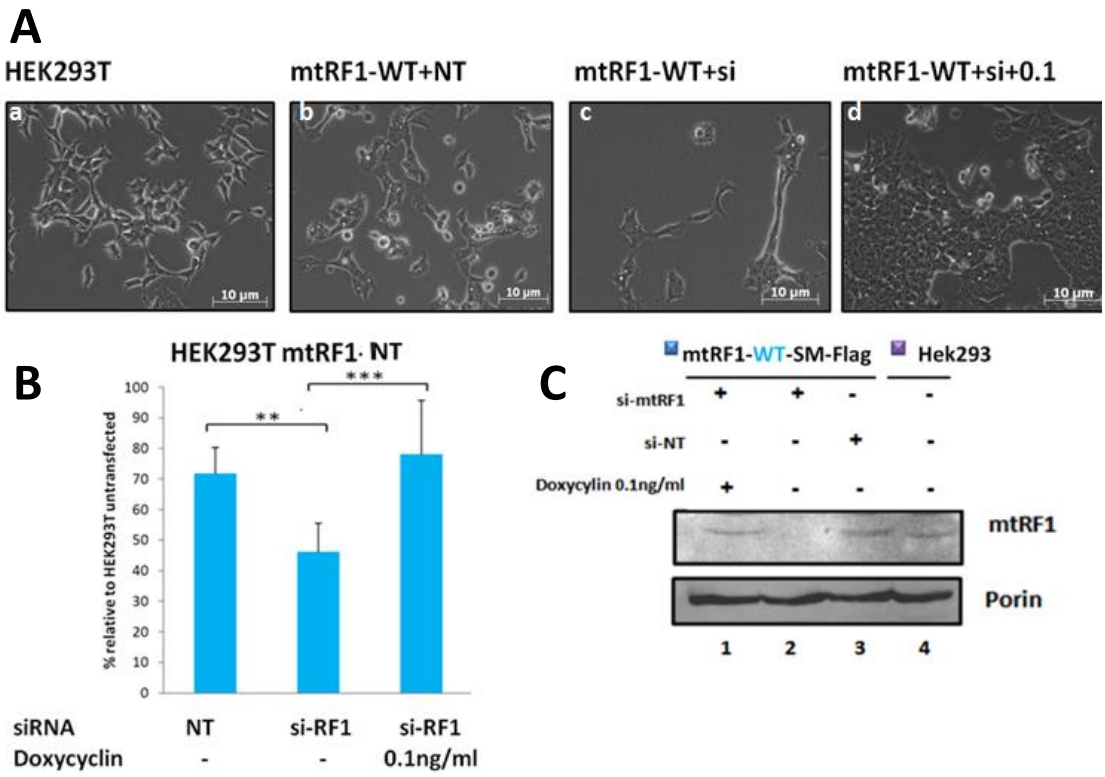

Figure 4. 3. Expression of mtRF1-WT-SM-FLAG is required for normal cell growth.

HEK293Tcells expressing mtRF1-WT were treated with 33nM of either NT-siRNA or siRNA-RF1 and induced with 0.1ng/ml of doxycycline where indicated. **(A)** After 3 days cells images were taken to show cell morphology of:- untreated and untransfected cells (a); uninduced mtRF1-WT cells treated with non-targeting siRNA (b); or siRNA specific to endogenous mtRF1 (c); and (d) cells depleted for endogenous mtRF1 simultaneously expressing mtRF1-WT. **(B)** To monitor the growth, the cells were counted and data presented as a mean ± standard deviation based on three independent experiments (**p<0.01, ***p<0.001). **(C)** Cell lysates (50µg) were analysed via western blot to compare the levels of mtRF1 expression in all cell lines. Porin was used as a loading control.

4 and 1, respectively), while the signal for mtRF1 is undetectable where cells were treated with siRNA to mtRF1 (Figure 4.3 C, lane 2).

The same format of experiment was performed for each of the two GGQ mutant versions of mtRF1 (AGQ and GSQ). This was done to confirm the specificity of

the rescue described above. The phenotype caused by the depletion was not suppressed by expression of either the mtRF1-AGQ or mtRF1-GSQ mutant. The HEK293T cells transfected with mtRF1-GSQ, but not induced seem to be firmly attached to the surface and show characteristic shape of HEK293T cells (Figure 4.4 A, panel a).Growth rate as determined by cell counts shows that uninduced HEK293T-RF1-GSQ+NT – labelled NT, had decreased growth

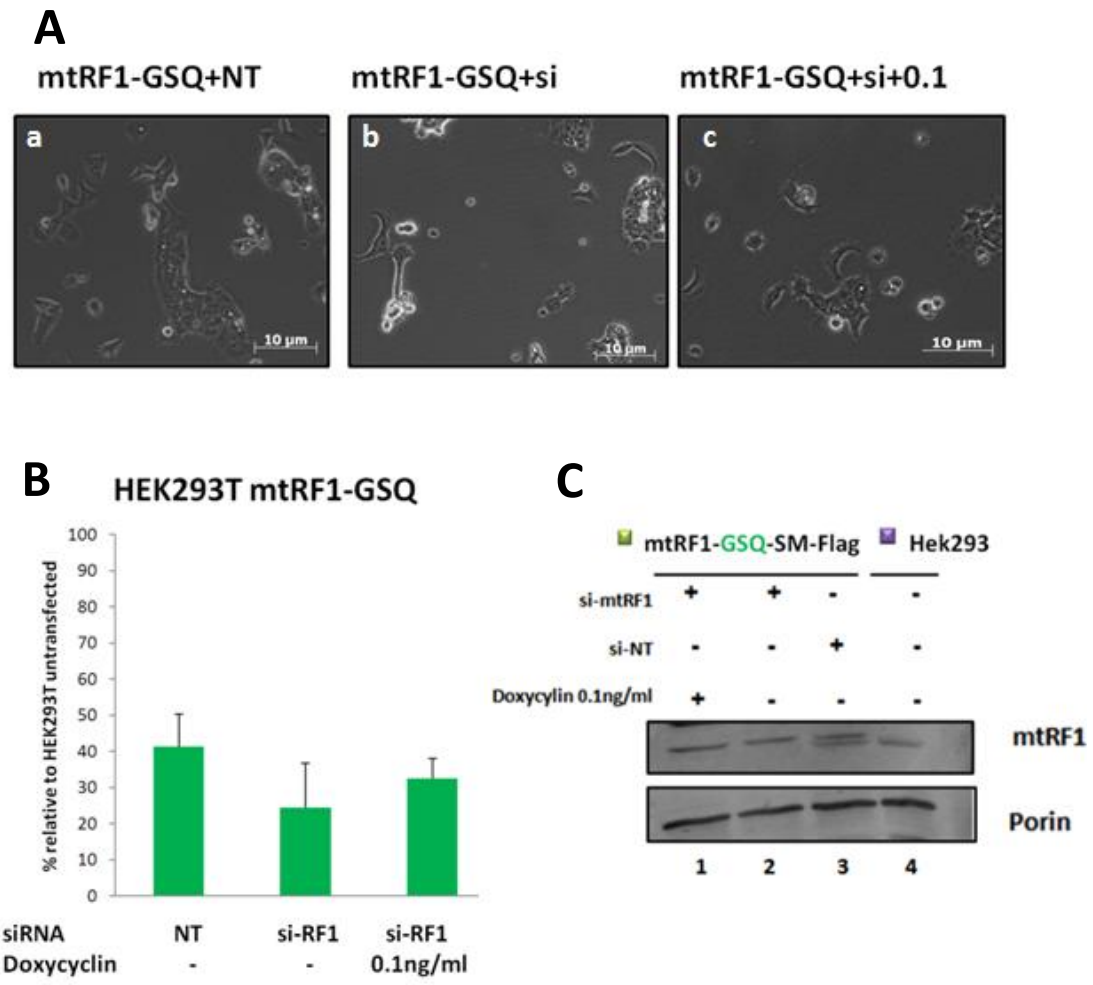

Figure 4. 4. Expression of mtRF1-GSQ-SM-FLAG mutant does not restore normal cell growth following mtRF1 depletion.

HEK293T cells expressing mtRF1-GSQ were treated with 33nM of either NT-siRNA or siRNA-RF1 (+NT or +si, respectively) and induced with 0.1ng/ml of doxycyclin (+ 0.1) where indicated. **(A)** After 3 days cell images were taken to show the morphology of (a) non-targeting or (b) specific to endogenous mtRF1 siRNA treatment of transfected but not induced cells; or (c) cells depleted for endogenous mtRF1 and simultaneously expressing mtRF1-GSQ. **(B)** To monitor the growth, the cells were counted and the result presented as a mean with standard deviation based on three independent experiments. **(C)** 50µg of cell lysates were analysed via western blot to compare the levels of mtRF1 expression in all cell lines. Porin was used as a loading control.

(Figure 4.4 B) when compared with uninduced HEK293T-WT+NT that is represented by 100%. This was due to leaky expression (see discussion) of

FLAG-tagged protein, as can be seen on western blot in lane 2 and 3 (Figure 4.4 C), where the lower of the two mtRF1 bands corresponds to the endogenous form of the protein; the upper corresponds to FLAG-tagged mutant. The endogenous mtRF1 could be successfully depleted (Figure 4.4 C, lanes 1 and 2) and the levels of expressed GSQ mutant correspond to the levels seen in wild type HEK293T cells (Figure 4.4 C, lane 4). The leaky expression of the mutant GGQ motif in the NT treated control indicated a negative effect even without depleting the endogenous form. Upon depletion of mtRF1 in uninduced mRF1-GSQ cells the negative effect was more apparent on both the morphology and number (Figure 4.4 A, panels b and B). Further, upon subsequent induction of mtRF1-GSQ mutant both the phenotype or cells number remained lower than NT treated controls (Figure 4.4 A, panel c and B). Similarly, the leaky expression of FLAG mutant also occurred here prior induction (Figure 4.5 C, lanes 2 and 3) explaining the decreased growth of uninduced HEK293T-RF1-AGQ+NT (Figure 4.5 B).

Also the expression at endogenous levels of mtRF1-AGQ mutant (Figure 4.5 C, lane 4 compared with lane 1) failed to restore the normal cell growth (Figure 4.5 B) or healthy HEK293T cells phenotype (seen in figure 4.5 A, panel a) following the depletion of mtRF1 endogenous form. Therefore, these findings confirm the dominant negative effect of both mutants on cell viability and show the functional importance of conserved GGQ motif in mtRF1.

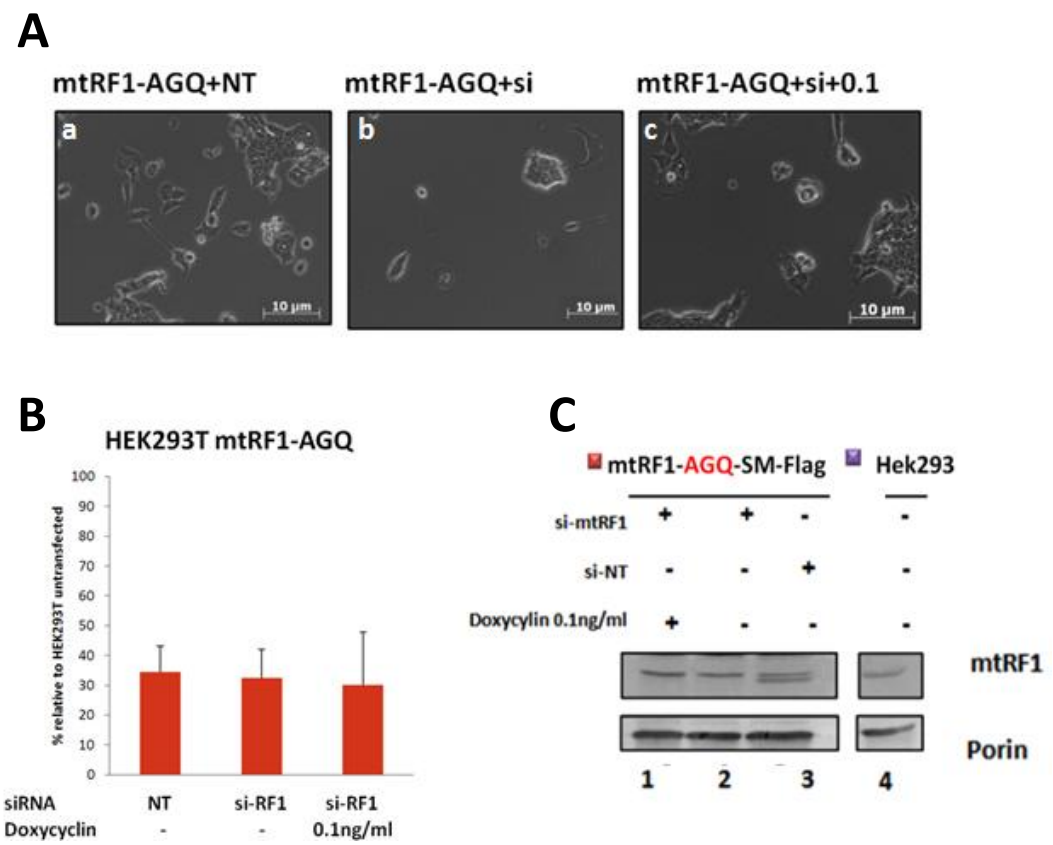

Figure 4. 5. Expression of mtRF1-AGQ-SM-FLAG mutant does not restore normal cell growth following by mtRF1 depletion.

HEK293Tcells expressing mtRF1-AGQ were treated with 33nM of either NT-siRNA or siRNA-RF1 (+NT or +si, respectively) and induced with 0.1ng/ml of doxycycline (+ 0.1) where indicated. **(A)** Morphology is depicted after 3 days cells of (a) non-targeting or (b) specific to endogenous mtRF1 siRNA treatment of transfected, but not induced cells and (c) cells depleted for endogenous mtRF1 and simultaneously expressing mtRF1-AGQ. **(B)** To monitor the growth, the cells were counted and result presented as a mean with standard deviation based on three independent experiments. **(C)** 50µg of cell lysates were analysed via western blot to assess and compare the levels of mtRF1 expression in all cell lines. Porin was used as a loading control.

4.5. Expression of mtRF1-GGQ mutants does not affect mitoribosomal profile.

To further analyse any possible effect of the mtRF1 variants, lysates prepared from cells expressing each variant were subjected to isokinetic sucrose density gradient and the collected fractions were analysed by western blot. I was previously unable to detect any evidence of mitoribosome accumulation during earlier mtRF1 depletion. It was still possible that mtRF1 acts as a peptidyl-tRNA transferase, as the previous results strongly suggested that the GGQ is required for protein function. One possibility was that the mutated protein would still be able to enter A-site but that this mutation may prevent ester bond cleavage and so prevent the aberrant polypeptide chain exiting and blocking the ribosome

and its recycling, potentially with the mutated protein still in the A-site. If so this would allow detection of mutated mtRF1-FLAG proteins associated with the monosomes by western blot. Such blockage of mitoribosomes with mutants would be sufficient to affect the system, limit the availability of charged tRNAs and explain the cause of the growth defect described here from the negative dominant effect of expressed mutants prior to induction and as described in the previous chapter.

As seen in figure 4.6 the majority of endogenous mtRF1 is localised to the top gradient fractions, 1-4, (Figure 4.6 A). The position of mitoribosome subunits were identified using MRPL3 antibodies for mtLSU and MRPS18B for the mtSSU. Free mtSSU migrates mostly in fractions 8-10, while mtLSU is present in fractions 11-12. The majority of all 3 expressed mtRF1 proteins (detected by the anti-FLAG antibody) remained in the 'free' fractions (1 - 4, trailing to 6) and not in mitoribosome associated fractions 12 - 15. Both the wild type mtRF1 (Figure 4.6 D) and mtRF1- AGQ mutant (Figure 4.6 B) are tailing up to fractions 9, whereas mtRF1-GSQ migrates up to fraction 6 where the strongest signals are detected within fractions 1-4 (Figure 4.6 C). Despite the presence of the expressed wild type protein or mutated variants the ribosomal profile on the gradient was not significantly affected. In all four cases the majority of MRPS18 can be observed in fractions 8 and 9 with the overlap of MRPL3 in fractions 10 - 13 indicating monosome. All membranes were also incubated with antibodies against MRPL12 to test its distribution as a response to the mutated expressed proteins. The levels of non-ribosome associated MRPL12 are almost undetectable in each mutant, mtRF1-AGQ or mtRF1-GSQ. When the wild type mtRF1 is expressed the free MRPL12 can still be detected at the top of the gradient (fractions 1 - 3, figure 4.6 D), however the signals are decreased compared with the control (Figure 4.6 A). This also demonstrates that the expression of the mutated forms of mtRF1 negatively affects the levels of MRPL12 as seen upon initial depletion in previous chapter and thus confirms the functional importance of the conserved GGQ motif in mtRF1.

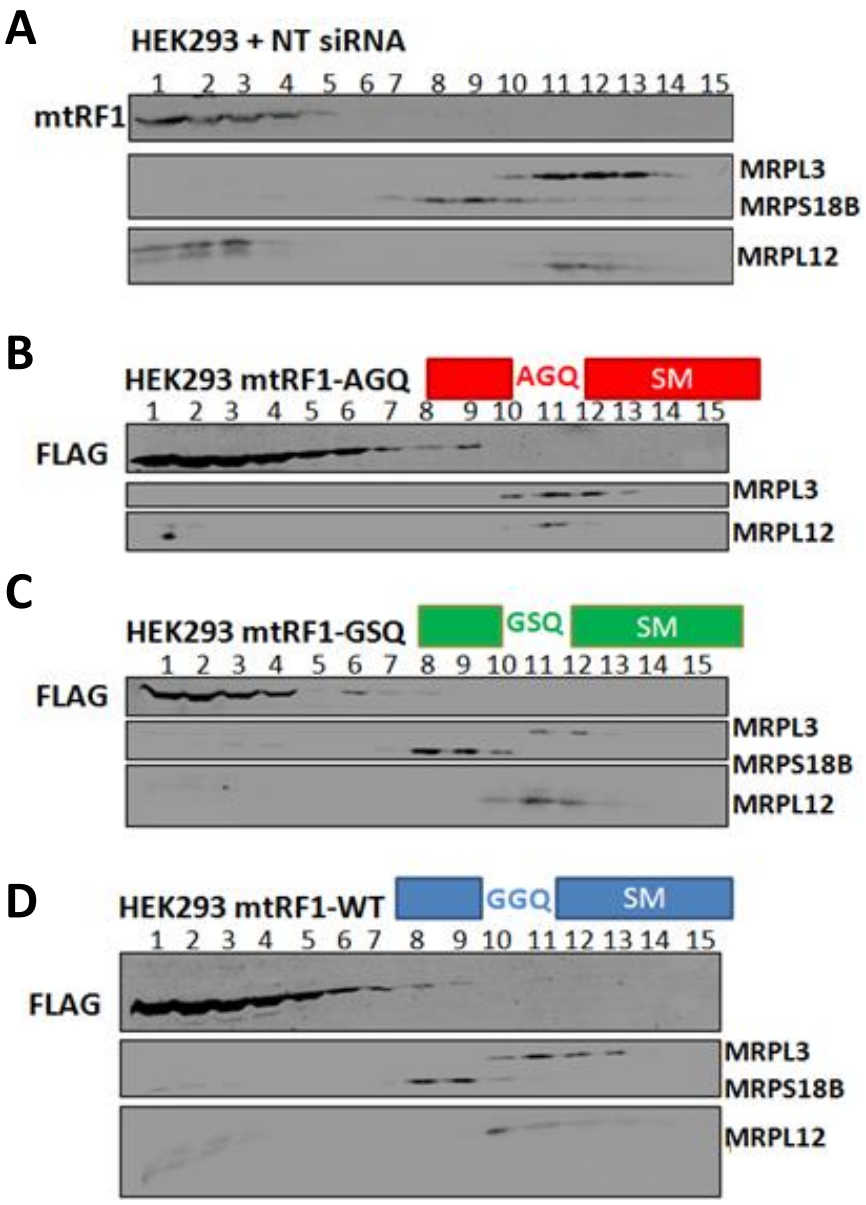

Figure 4. 6. Sucrose gradient analyses of the GGQ mutants.

(A) HEK293T wild type or **(B, C, D)** expressing (induced with 1µg/ml tetracycline for 3 days) the mtRF1 variants as well as the wild type protein were lysed and proteins separated by 10-30% isokinetic sucrose gradient. Fractions were then subjected to western blot analysis. To determine migration of the small, large and 55S monosomal particles, antibodies against the small (MRPS18B) and large (MRPL3, MRPL12) mitochondrial ribosomal polypeptides were used. Signals were visualised in fractions 1- 15 (collected from top to bottom). Anti-FLAG antibodies were used to detect expressed recombinant proteins.

4.6. Discussion

This project aims to investigate recognition of mRNA-free A site on the ribosome by mtRF1, thereby providing some insights into the still unknown function of mtRF1. The GGQ tripeptide that is known to promote peptidyl-tRNA

hydrolysis in PTC (Schmeing *et al*., 2005) is characteristic of all release factors and an indicator of ribosome dependence, as this motif requires the ribosomal environment for activity. It was therefore important to first establish whether this motif in mtRF1 was required for function, as this would also confirm the interaction of mtRF1 with the mt-ribosome. This chapter demonstrates that the GGQ motif in mtRF1 is essential for mtRF1 function. The expression of the proteins with mutations within this highly conserved motif failed to suppress the phenotype caused by the siRNA depletion of endogenous mtRF1 (Figure 4.4 and 4.5). In contrast the expression of the wild type FLAG-tagged variant was able to rescue the dramatic growth defect (Figure 4.3). The expression of both variants, mtRF1-AGQ and mtRF1-GSQ, appeared to be 'leaky' in the main experiment of this chapter (Figure 4.4 and 4.5), but was not observed either in the initial examination of the expression of the mutants shortly after transfection or when expression was titrated with the range of doxycycline concentrations (Figure 4.1).

It is often the case that cells, which have been stably transfected to inducibly express a gene of interest, demonstrate a basal expression or leakiness. This is especially true in tetracycline/doxycycline inducible expression systems (Mayer-Ficca *et al*., 2004). One of the causes of the high basal expression under noninduced conditions can depend on the site of chromosomal integration, as an important factor in Tetracycline promoter regulation, as well as false or cryptic promoters (Garrick *et al*., 1998; Johansen *et al*., 2002). However, the Flp-In System used for this project allows the integration of the gene at a specific genomic location. The co-transfection of cells with pcDNA5/FRT/TO-MTRF1 variant and pOG44 plasmids allows the integration of the gene in a specific Flp Recombination Target (FRT) site on the genome of the host cells, catalyzed by Flp recombinase from pOG44. The Tet- repressor protein expressed by the host cells binds Tet operator and represses the expression of the gene until the tetracycline is added to the culture medium. Thus, the mis-integration in to the genome under controlled condition is unlikely in this case. The leaky expression of the 2 mtRF1 mutants however could possibly be due to tetracycline traces present in culture media, which cannot be ruled out since tetracycline is widely used in veterinarian medicine. It may also result from insufficient Blastocidin^{S} treatment resulting in the loss of the Tet repressor.

The leaky expression of those genes however can strengthen the finding presented here. The presence of mtRF1-GSQ prior to induction (Figure 4.4 C, lane 3) has a dominant negative effect on HEK392-mtRF1-GSQ+NT cell growth and results in poor morphology of these control cells (Figure 4.4 A, panel a). The same effect can be observed in transfected but not induced HEK293-mtRF1-AGQ+NT control, again due to the leaky expression of mtRF1-AGQ mutant. The growth of both cell lines is decreased down to 35-40% relative to untransfected HEK293T control, while the growth of HEK293T-mtRF1-GGQ+NT (Figure 4.2 B) shows ~71% on average. This confirms that the conserved GGQ motif is required for protein function, but also shows that continuous presence of not functional mtRF1 in mitochondria can be toxic to some extent. Even though the expression of mtRF1-GGQ prior to induction cannot be detected on western blot (Figure 4.2 C, lane 2), the growth of those cells after mtRF1 depletion seems increased (on average the growth of HEK293T-mtRF1-GGQ cells was decreased by 36%, figure 4.2 B) compared with the mtRF1 depletion in HEK293T-wilde type in chapter 3, where the cell growth was decreased by 51% after 4 days of depletion (Figure 3.1 B). Since all cell lines were cultured and treated in the same way, it cannot be excluded that the trace of mtRF1-GGQ may still be present in cells prior to induction and therefore it is possible that the increase was due to leaky expression of functional mtRF1-GGQ upon depletion of endogenous form. Moreover, the morphology of HEK293T-mtRF1-GGQ in culture was observed to become more affected with time until the cells were aggregating, could not grow in monolayer and it was not possible to distinguish single cells. Those cells were harvested, lysed and then tested for the leaky expression by western blot (data not shown). The levels of basal expression of all 3 variants of protein were detected and appear higher compared with the initial experiment presented in this chapter. This suggests that not only the presence of non-functional mtRF1 may be toxic, but also the presence of functional GGQ at constant low levels without regulating it. As a consequence of constant leaky expression of mtRF1-GGQ could result in such affected morphology of HEK293T-mtRF1-GGQ over long time. As presented in this chapter the basal expression of the mutants was titrated so that they were not that different to the levels of the endogenous mtRF1. Although not accurately estimated (this was not the priority for the progress of the project), the levels of endogenous mtRF1 seem low on western blots, as compared with other

proteins, investigation of which this lab is focused on and it is possible that these low levels are regulated by physiological conditions. The negative feedback mechanism that regulates its level may depend on and reflect the rate of formation and accumulation of stalled ribosomes. This can be connected to the MRPL12 function outside the ribosomes as discussed in previous section (3.8).

The toxic consequence of mutant mtRF1 in cells is with agreement with some of my previous data. One of the aims of my Masters degree project (MRes) was the investigation of the other mtRF1 domains that corresponds to the tripeptide and $\alpha 5$-helix motif involved in codon recognition. In order to demonstrate the functional activity of 'molecular tweezers' in mitochondrial release factors mtRF1 and 1a, 2 chimeric proteins were designed. The sequence of the functional recognition domains of mtRF1a were exchanged into the backbone of mtRF1. This resulted in a chimeric mtRF1 containing the tripeptide PXT (rather than PEVGLS) and the $\alpha 5$-helix sequence from mtRF1a (mtRF1-PKT+α). In a reciprocal manner the functional domains of mtRF1 were substituted into mtRF1a such that it now contained the hexapeptide PEVGLS of mtRF1 and its α5 helix (mtRF1a-PEV+α). These chimeras were designed to test whether the mtRF1a domains were sufficient to support RF activity when placed in a different backbone or whether there were other regions apart from these conserved motifs that were required to facilitate the codon recognition. The results demonstrated that not only the substitution of PEVGLS into mtRF1a caused the loss of UAA/UAG recognition *in vitro*, but also overexpression of both chimeric proteins resulted in a dramatic growth defect (A. Pajak MRes thesis) similar to that seen in both GGQ mutants presented in this chapter (NT samples in figures 4.4B and 4.5B).

Interpretation of the data presented in this chapter has its limits. It was, however, possible to determine that similar to the wild type protein, the GGQ mutants were not able to bind to ribosomes more than transiently. The sucrose gradient experiment also confirmed the fact they were not trapped at the A-site of the complex, and confirmed that mitoribosomes were not 'blocked' and unable to be recycled. Hence stalled mitoribosomes were not the cause of impaired growth due to the presence either mutants or wild type FLAG tagged proteins. Even though none of the FLAG-tagged expressed proteins co-

sedimented with large mitoribosomal subunits, one mutant i.e. mtRF1-AGQ and wild type mtRF1-GGQ form a type of tail up to fraction 9, where it overlaps with signal for mtSSU (Figure 4.6 B and D). If mtRF1 associates with the ribosome transiently and only 'samples' the A site for possible recognition of stalled ribosome it is likely that the situation observed in Figure 4.6 represents the state after the A-site has been sampled by expressed proteins whilst the majority of mtRF1 proteins end up at the top of the gradient as they are dissociated from the monosome as the whole complex migrates down the gradient. It is unlikely that figure 4.6 represents the actual state and that mtRF1-GGQ and mtRF1-AGQ mutant bind the free mtSSU, because the majority of the A-site pocket is formed by the mtLSU. Moreover, there is no structural and functional rationale for release factor to bind mtSSU, which in fact would have initiation factors associated (mtIF3 posterior to active 55S disassociation or mtIF2 or both prior translation initiation). It could be that those FLAG-tagged proteins (detected in fractions 8 and 9 in both figures 4.6 B and D) bound a proportion of the monosome population, i.e. those with empty A-sites. This could be explained by the mutation in the GGQ motif obliterating the catalytic function (signal in fraction 9 of mtRF1-AGQ suggests more mtRF1 at this position compared with mtRF1-GGQ in D) and in the absence of the peptide being released, mtRF1 is not recognized by factors that would remove it from the ribosome. The overlapping signals of mtRF1-GGQ or mtRF1-AGQ in the fractions reflecting mtSSU, may suggest some sort of rather not physiological interaction. As mtRF1-AGQ is not able to exert its function and due to the extended region corresponding to the 'codon recognition', it could have been 'locked' into the decoding center of mtSSU (see section 5.1). Then as a result of monosome disassociation (with the mutant still bound), the mtRF1-AGQ signal is detected in fraction 9 together with mtSSU. The disassociation of the subunits can be forced during sucrose gradient centrifugation or by buffers components and very often the balance between monosome and free subunits is shifted towards the free subunits. This is an unlikely explanation in this case as experiments in my host lab have shown that immunoprecipitated 55S do not separate if subsequently processed on the same format of isokinetic sucrose gradient. It is however a phenomenon that is observed on most of our experiments performed from whole cell lysates, and by comparison with published literature suggests

that there is a difference between tissues and cells in culture in the proportion of free subunits to monosome.

The above indication of mtRF1 interaction with monosome can be supported by the fact that the 'tail' of expressed proteins discussed above is absent in mtRF1-GSQ mutant (Figure 4.6 B) which reassembles more the migration pattern of the endogenous mtRF1 (Figure 4.6 A), levels of which are much lower than expressed protein. This difference indicated that the association of mtRF1-AGQ and mtRF1-GGQ or their 'tails' were not simply due to an increased amount of the protein present in mitochondria at that time. Importantly, it has been shown that the mutation of second glycine in the GGQ motif of bacterial RF1 resulted in a 3300 fold decrease in catalyzed peptide release rate, but only 800 fold decrease was observed when the first glycine was replaced (Shaw and Green, 2007). Second, within the same study it was demonstrated that mutation of the universally conserved nucleotide (G2553) of 23S bacterial rRNA, which directly interacts with CCA-end of the incoming aminoacyl-tRNA to promote the conformational changes in, and the activation of, the large subunit catalytic centre, mediated the 33-fold defect in the peptide release rates (Shaw and Green, 2007). It was thus suggested that the productive reorganization of PTC can be connected to properties of the GGQ motif in release factors, but the existence of other points in RFs to manage the activation of the PTC was also possible. The mutagenesis studies of ICT1 (Richter *et al*., 2010) were also in agreement with speculations here, and also with results on bacterial GGQ mutagenesis. The protein harboring GSQ mutation (ICT1-GSQ) failed to rescue the phenotype caused by the depletion of ICT1 endogenous protein, and ICT1-AGQ showed a similar level of rescue compared to the wild type ICT1. Consequently, if a conformational rearrangement in the active site of mitoribosomes is required for high rate hydrolysis and the second glycine facilitates this process, it could be that mtRF1-GSQ mutation inhibited the promotion of conformation change at this site completely and even the transient interaction was not possible, which, resulted in the shorter 'tail' seen in Figure 4.6. Accordingly, mtRF1-AGQ mutation could hydrolyse at a lower rate and the transient interaction with PTC occurs, resulting in a changed conformation therefore longer occupation of the mutant protein in the site is possible. The longer 'tail' seen in the sucrose gradient analysis may thus be due to this protein

coming off ribosomes as they progressed during centrifugation. However, this remains a hypothesis and the ability of mtRF1 to bind an empty A-site needs to be further investigated, which is the focus of the next chapter.

Chapter 5

Does mtRF1 associate with the A-site of mitoribosomes, which is vacant due to loss of mRNA?

Chapter 5: Does mtRF1 associate with the A-site of mitoribosomes, which is vacant due to loss of mRNA?

5.1. Introduction

The last chapter showed that mutations in the conserved GGQ motif cause a decreased growth rate leading to cell death. Hence, the data thus far clearly shows that mtRF1 is essential to maintain healthy cells and its GGQ motif is required for protein function. Therefore, it is reasonable to assume mtRF1 would be able to catalyse nascent polypeptide chain release. Based on the proposition that the expanded codon recognition domains of mtRF1 would enable it to recognize and bind an empty A-site of mitoribosomes my working hypothesis was that mtRF1 may play a role in rescue of aberrant transcripts or stalled ribosomes.

This hypothesis is supported by recent studies (Huynen *et al*., 2012) using a combination of bioinformatics and modelling. The authors used a bioinformatics systematic strategy, where a possible differentiation of function in mtRF1 has taken place after *mtrf1a* gene has been duplicated in the course of evolution. Most of the identified differences between mtRF1 and mtRF1a were localised to the domain 2, which clusters around the codon recognition region. This region brings together in space 2 features (PXT tripeptide motif and the α-5 helix) that are separated by over 60 amino acids in the linear molecule (Figure 5.1) but act in concert to discern A-site mRNA sequences. Hence these 2 regions harbouring the most critical differences have been selected to create three-dimensional models of each of those two proteins bound to the A-site of a bacterial ribosome.

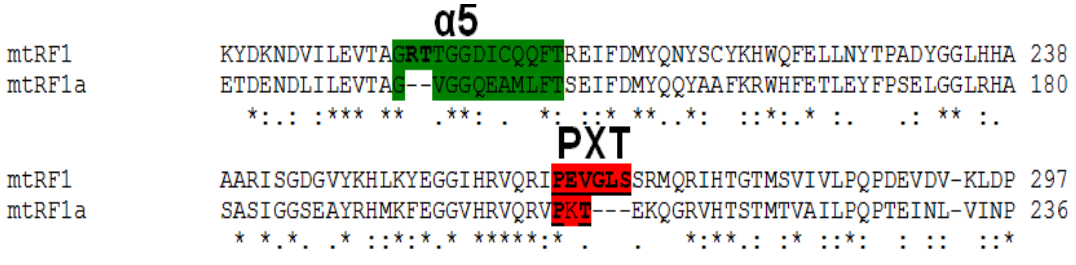

Figure 5. 1. A fragment of human mtRF1a and mtRF1 sequence alignment.

Two motifs α-5 in green and PXT in red interact to form codon recognition in the secondary structure of the protein. The crucial differences described in text are in **bold**.

There are amino acids insertions in mtRF1 at each of these two sites that alter the conformation of the codon recognition loop significantly. First of all, the α-5 helix is extended by the addition of 'RT'. This threonine points inwards into the mRNA binding pocket and in combination with compensatory changes in mtRF1 causes a complete blockage of the A-site preventing any mRNA binding Moreover, the 'RT' insertion has taken place in mtRF1 exactly between two residues that in RF1 and mtRF1a interact with stop codons and decoding centre of the ribosome. As a consequence, this 'RT' insertion provides the key stabilization of the catalytic conformation of RF1 upon correct stop codon recognition (Huynen *et al*., 2012). The second addition is in the tripeptide motif that is altered to PEVGLS. The consequence is that the threonine side chain of PXT motif is replaced with valine in mtRF1, which is not able to make any hydrogen bonding with stop codon. The 'GLS' insertion extends the recognition loop towards the rRNA to possibly provide stronger stabilization with mitoribosome (Huynen *et al*., 2012).

According to this model mtRF1 is able to bind at decoding centre of a stalled ribosome that lacks A-site mRNA. In this no-mRNA state mtRF1 then stabilises itself via interactions caused by the 'RT' insertion to mediate the active open conformation of mtRF1, which extends to the PTC and catalyses hydrolysis of a 'stalled' polypeptide chain. This phenomenon, however, could not be shown in my previous chapters either by accumulation of stalled product and monosomes upon mtRF1 depletion nor did overexpressing wild type form or mtRF1-GGQ mutants produce clear results. Therefore it is important to ask how common ribosome stalling and subsequent rescue can be in mitochondria?

As a result of defective or prematurely truncated messenger RNAs, either elongation or normal termination is prevented usually due to absence of complete codon in the A-site of the ribosome. In bacteria this is rescued by tmRNA, ArfA or YaeJ. It has been estimated that during normal exponential growth of *E. coli* ~0.4% of all protein synthesis terminates with ribosome rescue by tmRNA and the capacity of that system seems to be 3 or 4-fold greater than required for normal ribosome rescue demands (Moore and Sauer, 2005). Thus, at the frequency of 1 in every 250 translation reactions resulting in *trans*-translation during normal bacterial culture growth, every ribosome in the cell translates tmRNA once per cell cycle. Therefore, if there were no way of rescuing translational stalls, the blocked ribosomes would be excluded from

active pool and eventually all would be queued and trapped on each defective mRNA. The half life of paused ribosomes *in vivo* has been estimated for $T_{1/2}$ = 22sec. ± 2.2sec. based on ribosome recycling and peptidyl-tRNA turn over in the presence of tmRNA (Brian and Hayes, 2009).

It is possible that in mitochondria the ribosome stalling and ribosome rescue/ recycling are at similar rates, but the 3 or 6 day mtRF1 depletion was not long enough to produce detectable results, as shown in earlier chapters. Therefore, in order to test the hypothesis that mtRF1 is a candidate to play a role in rescue of stalled ribosomes with empty A-sites, this chapter aims to generate a substrate for mtRF1 i.e. a vacant A-site on mitochondrial ribosomes *in vitro* to investigate direct interaction with mtRF1.

5.2. Immunoprecipitation of mtRF1-WT-SM-FLAG to test for interaction with mitoribosomes

It has been demonstrated that mtRF1 was not present in ribosomes immunoprecipitated (IP) by either mtRRF-FLAG (Rorbach *et al*., 2008) or ICT1-FLAG (Richter *et al*., 2010). In the first case the A-site is occupied by mtRRF, presumably preventing entry of mtRF1. In the second case, ICT1 was suggested to be integrated at the surface cavity on the mt-LSU near the exit tunnel, which was described as polypeptide-acessible site (PAS), leaving its A-site accessible. It could therefore potentially act as a tool of testing mtRF1 binding to isolated mitoribosomes. However, it was first necessary to test whether mtRF1 could be seen to interact with ribosomal subunits by IP using FLAG-tagged mtRF1 as data suggested in section 4.5 and as predicted by Huynen *et al*., (2012).

For this expression of mtRF1-FLAG (not containing silent mutations across siRNA targetting region) was induced in HEK293T cells for 3 days, then the cells were used for immunoprecipitation via the FLAG tag. In order to control for any unspecific binding, mitochondrial targetted luciferase-FLAG was used as a control under the same conditions. The IP eluate of mtRF1-FLAG (Figure 5.2, lane 4) clearly shows that after removing all material that did not bind FLAG-tagged protein (SNs in Figure 5.2, lanes 3 and 6) mtRF1-FLAG was succesfully immunoprecipitated (Figure 5.2, lane 4, indicated by an asterisk) from mitochondrial 'input' (Figure 5.2, lane 1). The other bands that can be detected

by silver staining in the mtRF1-FLAG eluate are also present in eluted fraction of mtLuc-FLAG, where luciferase is indicated with asterisk. Taken together this indicates only unspecific interactions since no other proteins could be detected with mtRF1-FLAG IP. This suggests as do data presented in earlier chapters, that mtRF1 does not interact with mitoribosome more than transiently.

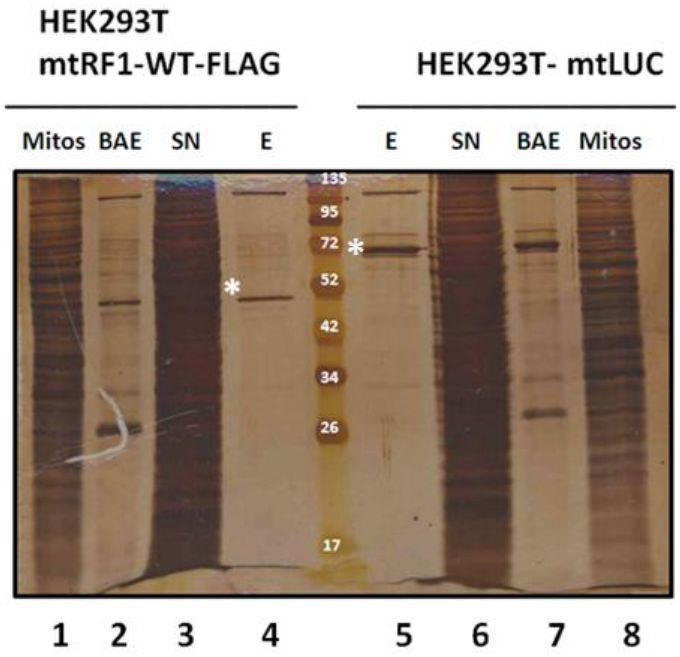

Figure 5. 2. Immunoprecipitation of mtRF1 to detect whether there is a tight association with other mitochondrial components.

HEK293T cells expressing either wildtype mtRF1-FLAG (lanes 1-4) or control mtLuc-FLAG (lanes 5-8) were induced with 1µg/ml tetracycline. After 3 days cells were harvested and mitochondrial lysates (2mg) were used for immunoprecipitations via the FLAG-tag. 5µg proteins of mitochondrial lysates (Mitos), 5% of beads after elution (BAE), 10% of supernatant that did not bind to beads (SN) and 10% elution fraction (E) of each sample were separated on 12% SDS-PAGE and visualized by silver stain. MtRF1-FLAG and mtLuc-FLAG are indicated by *.

5.3. Analysis of RNA content of ICT1-FLAG immunoprecipitation.

It has been demonstrated that overexpressed and immunoprecipitated (IP) ICT1-FLAG can pull down the mitoribosomes (Richter *et al*. 2010), therefore it is used here as a tool for isolating mitoribosomes and generating a substrate mtRF1 could recognize and interact with. In the ICT1 pull-down, however, mtRRF was detected at low levels suggesting that some of those immunoprecipitated ribosomes could still have mRNA attached. In order to increase the degradation of mRNA in those mitoribosomes to facilitate formation of an empty A-site, the incubation step of mitochondrial lysates with anti-FLAG

beads was extended to 3h. During the procedure the mitochondrial content is diluted by the lysis buffer, and so are all the components required for subunit disassociation, or association inhibitors such as mtIF3 or mtEFG2. In addition to mRNA degradation this extended IP incubation step (3h), was predicted to allow free subunits to reform into monosomes, which have no mRNA associated and mRNA-free A-sites. In order to test this possibility, ICT1 IP was performed (as described in methods section 2.6.10) and prior to 3h incubation divided into 3 equal samples, which were eluted after 1h, 2h or 3h of incubation with anti-FLAG-beads. The protein and RNA content of elution fractions (10% and 80% respectively) as well as input and supernatant were assessed by western and northern blot. The 3 h incubation elution was also assessed to monitor monosome reformation on density sucrose gradient.

The result as shown by western blot (Figure 5.3 B) was that the majority of both mtSSU and mtLSU, marked by DAP3 / MRPS18B and MRPL3 / MRPL12, respectively, did not immunoprecipitate after 1h and were washed off and discarded in supernatant (Figure 5.3 B, lane 2). However, what was present in the 1h IP elution, showed that the proportion of both subunits is clearly shifted towards mtLSU compared to the mitochondrial lysate, where proportions are fairly equal (Figure 5.3 B, lane 3 and 1, respectively). The MRPS18B signal indicating the presence of mtSSU in this elution is barely detectable, suggesting that 1h IP was not enough to form monosomes and mostly free mtLSU was isolated in this case. After 2h of incubation, the elution contained greater amounts of mtSSU (Figure 5.3 B, lane 5), since the IP was via a large subunit protein this result indicated increased monosome reformation. There are also less free subunits excluded from binding, as seen in the 2h supernatant fraction (Figure 5.3 B, lane 4). Finally, after 3h incubation the monosome formation did not seem to increase significantly over 2h, however judging from the weaker MRPL12 signal in 3h SN (lane 6) compared with 2h SN, there was less free mtLSU. Next, northern analysis of RNA content of the same fractions in figure 5.3 A shows that the 3 mRNAs tested (*RNA14, MTCOI* and *MTNDI*) are already severely degraded after 2h of IP elution (Figure 5.2A, lane 3), although feint bands can still be noticed for all 3 transcripts. Although the levels of rRNA (*MT-RNR1* and *MT-RNR2*) seem to decrease after 3h incubation (Figure 5.3 A, lane 5), its quality is comparable with that one from input fraction (lane 1 of the same

figure) and more importantly the signals corresponding to transcripts are not detectable after 3h in elution fraction (Figure 5.3 A, lane 5).

This together shows that during the IP procedure, especially with the 3h incubation time, mt-mRNA is degraded promoting the reformation of now mt-mRNA-free monosomes. These were analysed by sucrose density gradient and were seen to migrate and accumulate in fractions 7 and 8 (Figure 5.3 C, lowest panel) and providing the putative substrate that may be recognisable by purified mtRF1.

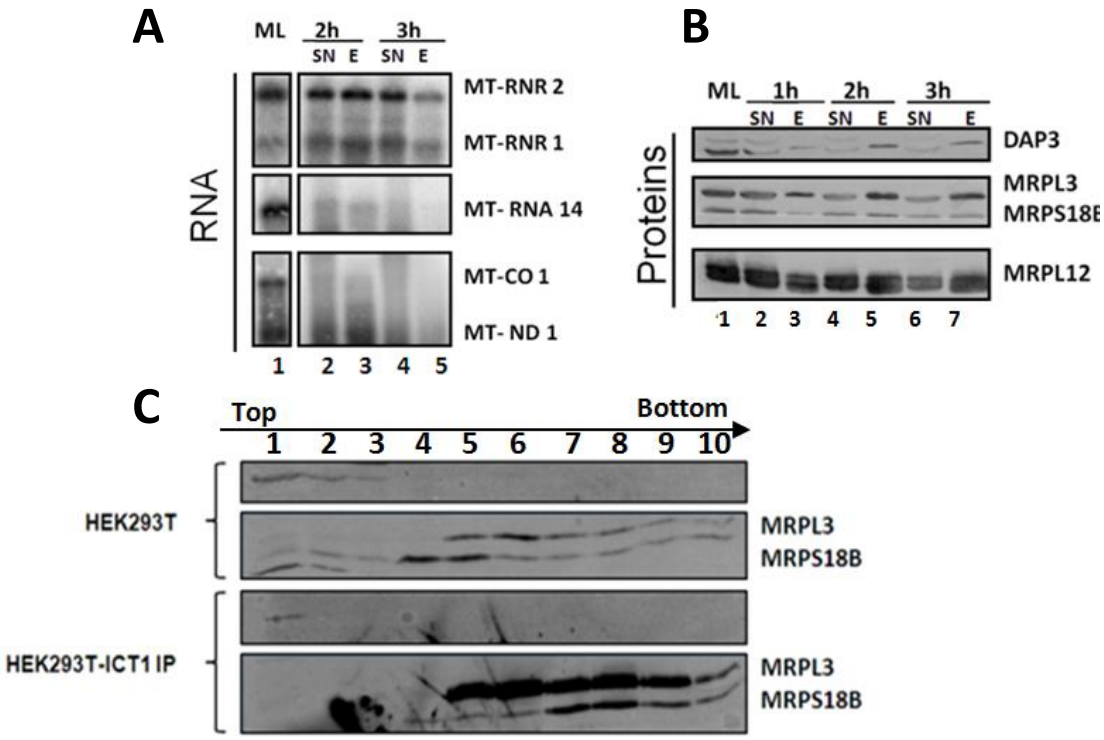

Figure 5. 3. Analysis of RNA/protein content and migration of ICT1-FLAG immunoprecipitated material by isokinetic sucrose gradient.

HEK293T cells capable of expressing ICT1-FLAG were induced with 1µg/ml tetracycline for 3 days. The cells were harvested, mitochondria isolated and lysed (mitochondrial lysate [ML] panel A lane 1; panel B lane 1) 2.75mg of which was used for immunoprecipitation via the FLAG tag. The final elution fractions were collected after 1, 2 or 3h of incubation. **(A)** mitochondrial lysate (~800ug, lane 1) prior to IP, together with 'flowthrough' (lanes 2 and 4) and 80% of each elution (lanes 3 and 5) were subjected to RNA extraction prior to analysis by northern blot. Probes to mitochondrial mRNAs (*RNA14*, *MTCO1* and *MTND1*); and to mt-rRNAs 16S (*MT-RNR2*) and 12S (*MT-RNR1*) indicate the RNA content before (lane 1) and after IP (lanes 2-5). **(B)** 10% of each elution fraction was analysed by western blot, where antibodies against MRPL3, MRPL12 and MRPS18B determined the level of co-immunoprecipitated 39S LSU and 28S SSU respectively. **(C)** HEK293T total cell lysate (700µg) (Top panel) and 80% of the final elution fraction after 3h of incubation (bottom panel) were separated by isokinetic sucrose gradient. The fractions (1-10) were analysed by western blot, where antibodies against MRPL3 and MRPS18B determined the level of co-immunoprecipitated 55S monosome (F 7 and 8).

5.4. *In vitro* binding of mtRF1 to mitoribosomes

The mitoribosomes prepared in this way could now be used as a substrate for mtRF1 binding. For this Δ49mtRF1-GST fusion protein was succesfully overexpressed in Rosetta cells as seen in SN fraction in figure 5.3A, lane 1 indicated by an asterisks at size ~73 kDa. Binding of the GST-protein to the beads (beads before elution [BBE], lane 3) resulted in decreased levels of it in the flowthrough (FT) fraction in lane 2, shown in the same figure. After enzymatic cleavage of the GST, Δ49mtRF1 was released (Figure 5.4 A, lane 5) with a proportion of it still bound to the beads (BAE, beads after elution, lane 4). Once pure Δ49mtRF1 was eluted, 70pmol of it was then incubated for 40 minutes with mitoribosomes bound to FLAG-beads, then washed 3 times before the final elution of the immunoprecipitated mitoribosomes from the beads. It was shown that even though a proportion of purified Δ49mtRF1 (Figure 5.4 B, lane 5) was observed in the supernatant fraction that contained proteins that did not bind monosome/beads (figure 5.4 B, lane 2) together with low levels of both ribosomal subunits, mtRF1 was also present in eluate. The latter corresponded to the IP immobilised mitoribosomes (Figure. 5.4 B, lane 1) that were confirmed by western analysis signals for MRPS18B representing mtSSU, and MRPL3 and ICT1-FLAG representing mtLSU. This suggests the Δ49mtRF1 can bind mitoribosomes under those conditions.

The same elution fraction was separated by sucrose density gradient where Δ49mtRF1 appeared both as a free form on the top of the gradient and in fractions 6 and 7 (Figure 5.4 C, top panel), being colocalised with proteins of large 39S and small 29S mitoribosomal subunits (MRPL3 and MRPS18B, respectively, lower panel), where monosome can be only observed in fraction 7.

In order to estimate the actual amount of immunoprecipitated Δ49mtRF1 and identify specificity of molecules bound per ribosome, a serial dilution of 2-250ng of purified Δ49mtRF1 was used as a calibration standard and compared with amounts of Δ49mtRF1 and MRPL3 present in the elution fraction of the immunoprecipitated mitoribosome. Based on the amount of mtRF1 detected by western in both mito lysate and IP elution (Figure 5.4 D, lower panel) in comparison with the serial dilution of Δ49mtRF1, it can be estimated that there is approximately 2ng of mtRF1 per 10µg of ML, which represents 0.2% of all mitochondrial proteins. Unfortunately, without purified MRPL3 or any other

ribosomal protein, which were not avalible at that time in our lab, the precise ratio of mtRF1 to ribosomes could not be estimated. However, the signal for both mtRF1 and MRPL3 in the mitoribosome (ICT1 IP) aliquot appears similar on western (Figure 5.4 D), so if one assumes that the affinitiy of those two antibodies used are the same, it could be roughly estimated that the ratio of mtRF1 to monosomes in the IP eluate is not more than 1:1. Based on this

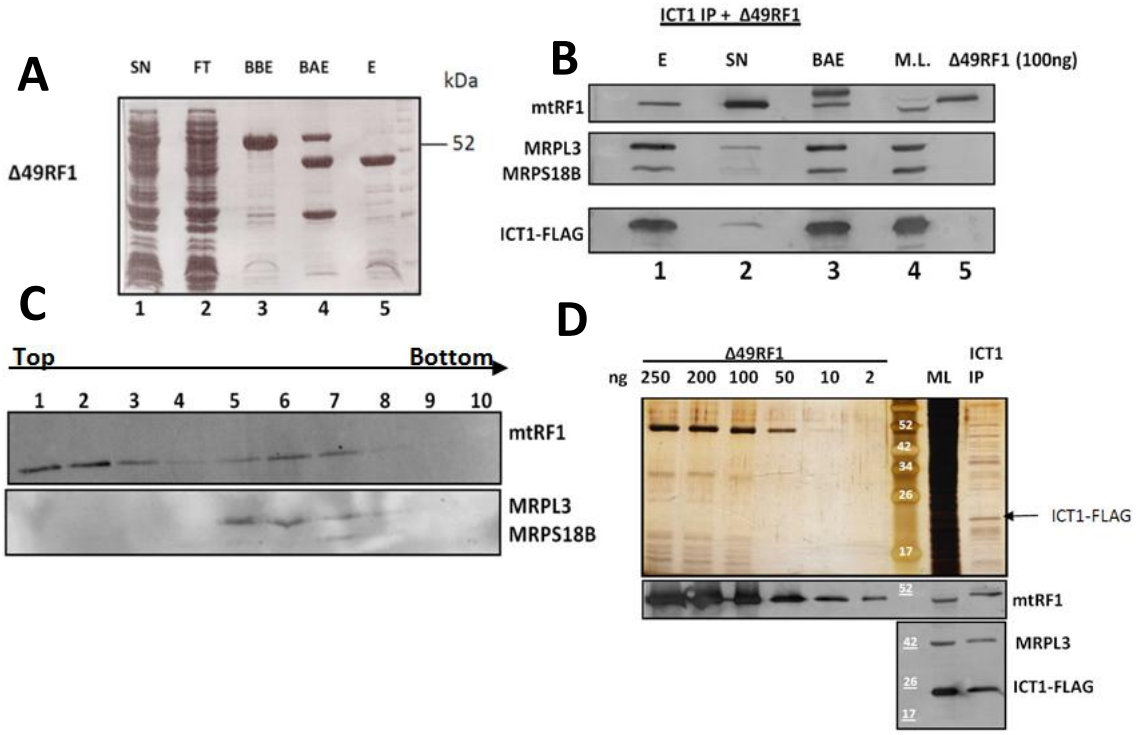

Figure 5. 4. Assay to determine if Δ49 mtRF1 can bind to ICT1-FLAG immunoprecipitated mitoribosomes lacking mt-mRNA.

(A) GST-purification of Δ49mtRF1. Transfected Rosetta cells were grown to OD_{600} 0.4-0.6 and induced to overexpress mtRF1-GST (~73 kDa) by 1 mM IPTG over-night at 16°C. Cells were harvested, sonicated and the soluble fraction was subjected to glutathione Sepharose beads (SN = post-centrifugation input to the column). After binding, the flow through (FT) was discarded and the beads (BBE; beads before elution) washed with PBS. By the addition of PreScission protease the GST-tag was cleaved off and mtRF1 protein could be eluted (E), whilst the GST-tag (~ 26 kDa) remained on the beads (BAE; beads after elution). **(B)** HEK293T ICT1-FLAG cell line was induced for 3 days with 1µg/ml tetracycline. After standard IP (where ~2.5mg of mitochondria lysate (ML) was incubated for 3h with the beads) 70pmol purified recombinant Δ49RF1 was added to ICT1-FLAG 55S particles still immobilised on the beads. This incubation proceeded for 40 min, before elution with 3xFLAG peptide (E = elution fraction). Supernatant was also collected (SN = all that did not bind ribosomes). Beads after elution (BAE) were included in the western blot analysis. **(C)** 80% of eluted fraction was subjected to 10%-30% isokinetic sucrose gradient, fractions 1 to 10 of which were analysed by western blot. Each blot was probed with antibodies against mitochondrial ribosomal proteins (MRPL3, as a mt-LSU marker; MRPS18B, as mt-SSU marker), FLAG and mtRF1. **(D)** To estimate actual amounts of protein, 5% of eluted mitoribosomes with Δ49RF1 bound, 5µg of starting mitochondrial lysate (ML) along with BSA (2 to 250ng) were separated on SDS-PAGE and silver stained. A parallel Western blot with the same samples was probed with anti-FLAG, anti-MRPL3 and anti-mtRF1 antibodies.

western there is approximately 2-4ng mtRF1 in the aliquot of ICT1 IP (Figure 5.4 D, far right lane 2ng lane of mtRF1) this amount could not be detected on silver stained gel (the signal for 10ng of Δ49mtRF1 is very weak on Figure 5.4 D, top panel). The fact that ICT1-FLAG, in this fraction being a part of either free mtLSU or monosome, is about 20ng also suggests that the ratio cannot be more than 1:1 in the total population of immunoprecipitated proteins. However, at this stage it was impossible to determine whether the binding was specific and whether some monosomes bound one, four or no mtRF1 in these conditions. Therefore further investigations followed.

5.5. *In vitro* binding of mtRF1a to mitoribosomes

Based on the fact that mtRF1a is the real realease factor and recognises mitochondrial stop codons in order to bind in the A-site, it can be predicted that if mtRF1a was purified in the same way as Δ49mtRF1 and incubated with similarly immunoprecipitated mt-mRNA free mitoribosomes, it should not interact. Purification of Δ32mtRF1a was therefore carried out using the same conditions as previously, where Δ32mtRF1a-GST was overexpressed in Rosetta cells (Figure 5.5 A, lane 1) as 75kDa fusion protein. Binding to the beads (BBE, lane 3) isolated it from the flowthrough (FT, lane 2), then cleavage of GST released ~49kDa Δ32mtRF1a (lane 5) from the column (lane 4).

After the monosomes were incubated with 70pmol of purified Δ32mtRF1a (Figure 5.5 B, lane 1), trace amounts could be detected in the final elution together with the expected mtSSU (MRPS18B) and mtLSU (MRPL3 and ICT1) markers (lane 6) but this was significantly lower than Δ49mtRF1 after elution (lane 7). To further examine the immunoprecipitated monosome and Δ32mtRF1a, distribution and migration of these polypeptides from the final eluate was examined by 10-30% sugrose density gradient. Figure 5.5 C shows that even though a low level of Δ32mtRF1a was pulled down with mitoribosomes, it was not associated with either free large ribosomal subunits (fraction 6) or monosome, which is clearly present in fractions 7 and 8. Δ32mtRF1a was only detectable in the top 2 fractions of the sucrose gradient, which suggests that the majority of immunoprecipitated mitoribosomes have, in fact, an empty A-site and Δ32mtRF1a does not stay bound to it.

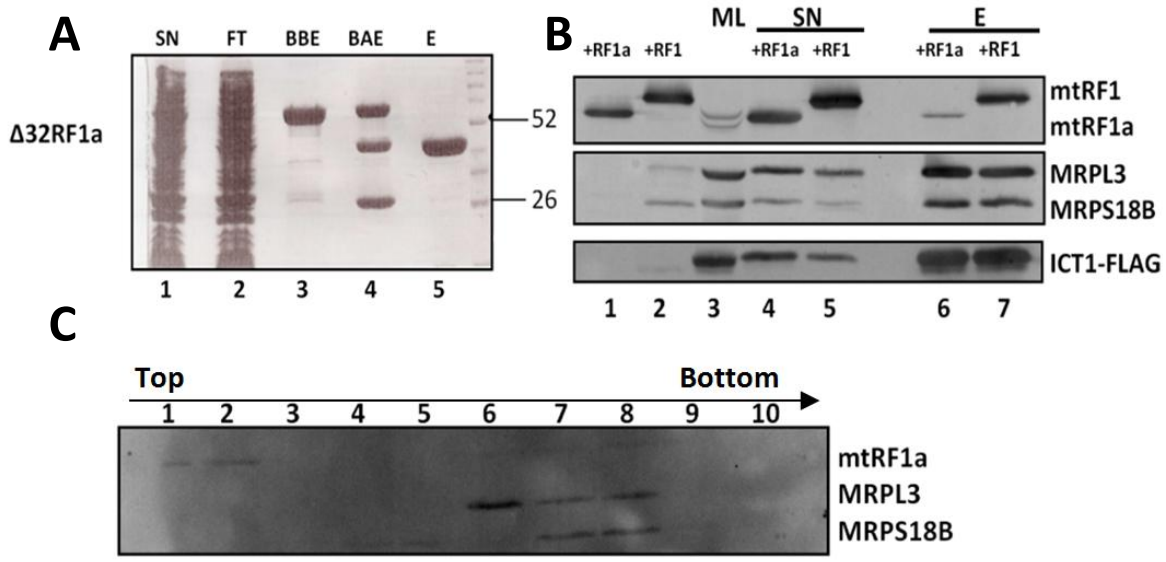

Figure 5. 5. Interactions of mtRF1 and mtRF1a with isolated 55S particles.

(A) GST-tagged Δ32mtRF1a was purified from transfected Rosetta cells cultured to OD_{600} 0.4-0.6, induced with 1 mM IPTG over-night at 16°C allowing overexpression of mtRF1a-GST (~75 kDa). Cells were harvested, sonicated and the soluble fraction exposed to glutathione Sepharose beads (SN = post-centrifugation input to the column). After binding the flowthrough (FT) was discarded and the beads (BBE) washed with PBS. Δ32RF1a was eluted (E) by the addition of PreScission protease leaving GST-tag (~ 26 kDa) immobilised on the beads (BAE). **(B)** The HEK293T ICT1-FLAG cell line was induced for 3 days with 1µg/ml tetracycline. After standard IP (as described in methods section 2.6.10) 70pmol purified recombinant Δ49RF1 or 70pmol purified recombinant Δ32RF1a were added to the ICT1 immobilised 55S/39S (beads) and incubated for 40 min. The supernatant was collected (SN = all that did not bind ribosomes) before elution with 3xFLAG peptide of ICT1 immobilised 55S/39S (E = elution fraction). SN and 10% of total elution were analysed by western blot using antibodies against MRPL3 as mt-LSU marker, MRPS18B for mt-SSU, FLAG, mtRF1 and mtRF1a. **(C)** Eluted mitoribosome IP (80%) incubated with Δ32RF1a was separated by sucrose density gradient (10-30-%) and obtained fractions (1-10)

5.6. Competition for binding of ribosomal A-site.

As shown before (section 5.3) Δ49mtRF1 interacted with immunoprecipitated mitoribosomes *in vitro*, however it was observed to migrate to fractions 6 and 7 and co-localised with signals for both, mtLSU alone and the monosome, which could suggest some level of unspecific binding or the binding in fraction 6 might represent low levels of monosome where the antibody is not strong enough to detect any small subunit present in that fraction. Therefore in order to exclude this possibility and to determine whether Δ49mtRF1 binds specifically it was necessary to block the A-site in the reformed monosomes to inhibit this interaction.

One of the methods to block the A-site under those conditions was to use synthetic UAG RNA triplet, which is also used for *in vitro* release assays to programme bacterial ribosomes. For this, another ICT1-FLAG immunoprecipitation was performed (as described earlier) with a 3h incubation of mitochondrial lysate with anti-FLAG beads. Bead bound mitoribosomes were

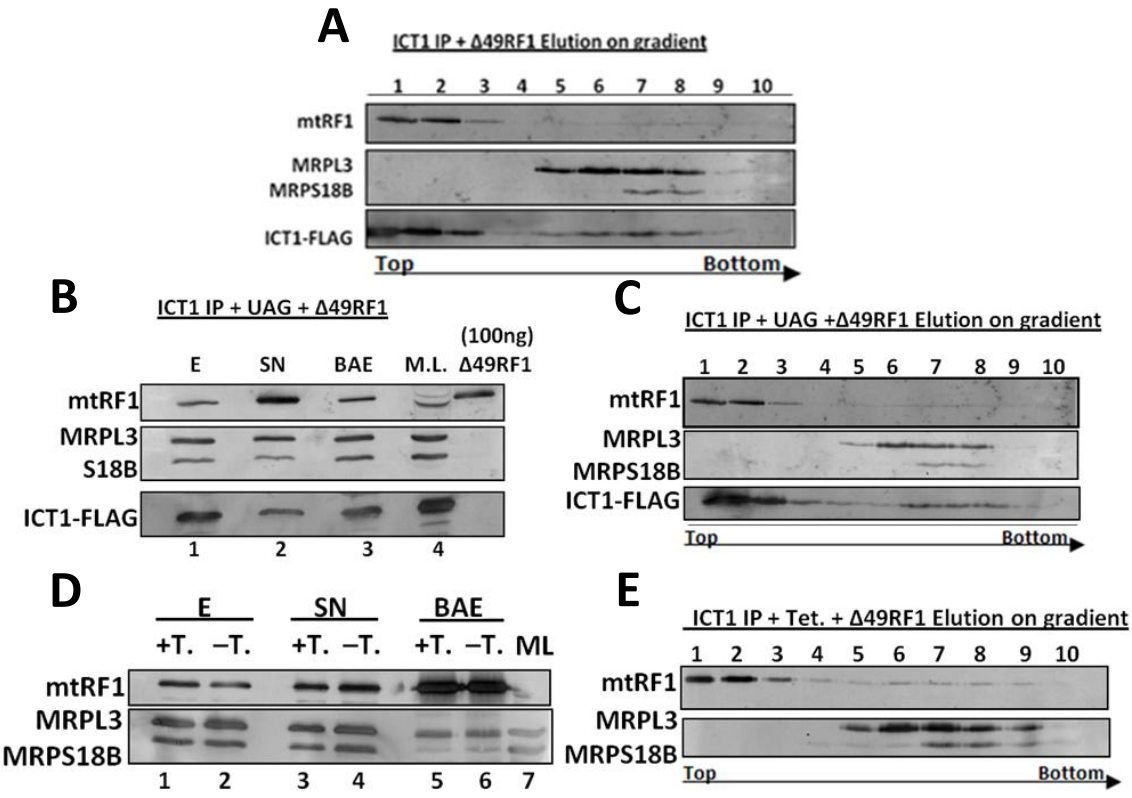

Figure 5. 6. Blocking the A-site of the immunoprecipitated mitoribosomes.

ICT1-FLAG was expressed in HEK293T cells for 3 days and standard IP performed. Mitochondrial lysates were initially incubated with anti-FLAG beads for 3h, Δ49mtRF1 recombinant protein was then added for a further 40 min (panel **A** shows 80% of the final elution separated by a sucrose gradient into 1-10 fractions). **(B)** Mitoribosomes were preincubated with 1nmol of UAG RNA triplet for 5 minutes prior to 40 minutes incubation with recombinant Δ49mtRF1 and 10% of a total elution, supernatant, BAE and mito lysate analysed by western. **(C)** 80% of total elution from **B** separated by a sucrose gradient (fractions 1-10). (**D)** Mitoribosomes were preincubated with 100μM tetracycline for 15 minutes prior to 40 minutes incubation with Δ49mtRF1, and elution. Content of 10% of the total elution, supernatant, BAE and mitochondrial lysate were analysed by western blot. **(E)** The total elution from D was separated by a sucrose gradient into fractions 1-10.

preincubated with 1nmol of UAG triplet for 5 min prior to addition of purified Δ49mtRF1 for another 40 min. Figure 5.5 shows the final elution fraction separated by sucrose density gradient (panel C), and for comparison, an experiment control where no triplet was present (panel A). The majority of Δ49mtRF1 remains uncomplexed in fractions 1-3, but in both cases trace

amounts co-migrate with monosome, seen in fractions 7 and 8. As described in the previous section the content of each fraction during the procedure was monitored by western blot. It shows that although mitoribosomes were preincubated with the RNA triplet, it did not successfully saturate all A-sites to block the interaction with Δ49mtRF1. In the final elution (Figure 5.6 B, lane 1) the signal for Δ49mtRF1 appears as do those of mitoribosomal markers (MRPL3, ICT1-FLAG or MRPS18B). This association is also reflected after the total eluate was separated by sucrose gradient (Figure 5.6 C). The Δ49mtRF1 signal accumulates at the top of the gradient in fractions 1-3, and is again detectable in fraction 6 to 8, suggesting direct interaction with monosome in this case.

It has been demonstrated that a broad-spectrum antibiotic, tetracycline (Tc) binds bacterial ribosomes. 30S ribosomal subunit-tetracycline crystal structures are avaliable (Brodersen *et al*.,2000; Pioletti *et al*., 2001) showing that Tc primarily targets bacterial ribosomes to prevent the binding of aminoacylated tRNA to the A-site of mRNA programmed ribosomes, thus blocking protein synthesis (Rasmussen *et al*., 1994; Aleksandrov and Simonson, 2008; and reviewed by Connell *et al*., 2003). Since the A-site and decoding centre in *E. coli* and mitochondrial ribosomes are highly conserved (Koc *et al*. 2010), it was highly likely that Tc may well bind to A-site of immunoprecipitated mitoribosomes thereby preventing binding of the recombinant, purified protein. The minimum inhibitory concentration for bacterial synthesis is 0.3-3 μM (Ross *et al*., 1998) and for crystallography studies the concentration used ranged from 4-80 μM (Brodersen *et al*., 2000; Pioletti *et al*., 2001). Unfortunately, as seen in figure 5.6 D despite the FLAG-immobilised mitoribosomes being incubated for 15min with 100μM tetracycline to saturate and block the ribosomal A-sites, this treatment did not affect the interaction of Δ49mtRF1 with mitoribosome (Figure 5.6 D, lane 1 compared with lane 2) and the binding was not inhibited.

As a consequence of Tc not being able to block the A-site of mitoribosomes a further strategy was devised. It was established in my host lab that mtRRF does not appear to be cleaved on import and that this full length protein occupies the A-site, and it is through this interaction that it is able to co-immunoprecipitate mitochondrial ribosomal proteins (Rorbach *et al.*, 2008). Mitoribosomes were again immobilised via ICT1-FLAG and purified a full length mtRFF-GST fusion protein added and expected to inhibit the binding interactions with Δ49mtRF1.

First, after the full length mtRRF (FL mtRRF) was successfully purified (Figure 5.7 A, lane 7), 70pmol of it were incubated with mitoribosomes for an additional 40 minutes and then the elution performed. As predicted, mtRRF bound mitoribosomes were detected in final elution fraction together with ICT1-FLAG the marker of mtLSU and control for successful IP (Figure 5.7 A, lane 1).

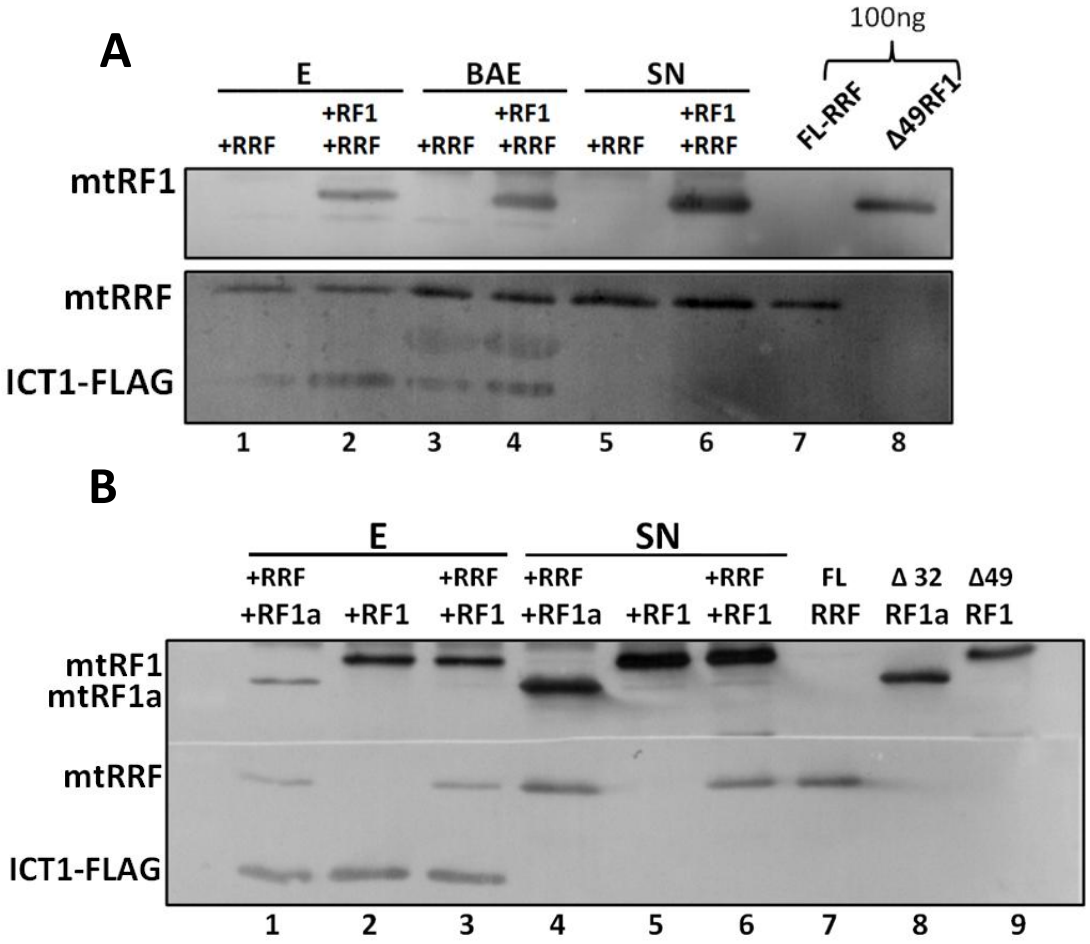

Figure 5. 7Blocking the A-site of the immunoprecipitated mitoribosomes with mtRRF.

(A) ICT1-FLAG was expressed in HEK293T cells for 3 days and standard IP performed. Mitochondrial lysates were initially incubated with anti-FLAG beads for 3h, to which either full length mtRRF or ∆49RF1 recombinant was added for 40 minutes incubation. To the latter addition of full length mtRRF proceeded for another 40 minutes, which was followed by the final elution in both cases (lane 1 and 2, respectively). 10% of a total elution, supernatant, BAE and mito lysate with recombinant Δ49RF1 and FL-mtRRF were separated by the western blot. **B,** isolated mitochondria were initially divided in three equal volumes and two of them preincubated with full length mtRRF for 40 minutes and one with ∆49RF1. These preincubated where then incubated with ∆49RF1 for another 40 minutes and eventually all three eluted. The content of 10% of a total elution and supernatant were then analysed by western.

However, according to the prediction that mtRRF and mtRF1 aim for the same site, when the mitoribosomes were preincubated with Δ49mtRF1, also for 40 minutes, prior to incubation with mtRRF, the content of the final elution

demonstrated that both added proteins bound simultaneously to the isolated mitoribosomes (Figure 5.7 A, lane 2) and mtRRF interaction was not inhibited. This could suggest either unspecific binding of one or another factor, lack of initial saturation of 55S particles with mtRF1 or it could be due to the constant transition state between both factors and mitoribosomes resulting in an equilibrium of two distinct populations of mitoribosomes, one containing mtRF1 and the other population interacting with mtRRF. Under such conditions absolute inhibition is not possible. Therefore, in order to examine this, the experiment was performed in a reciprocal manner, where the Δ49mtRF1-ribosome interaction was attempted to be decreased by presence of mtRRF in the mix (preincubated with mtRRF for 40 minutes prior to addition of Δ49mtRF1 or Δ32mtRF1a). If the interaction of Δ32mtRF1a and mitoribosomes seen earlier (section 5.5) was due to a small proportion of A-sites still being occupied with mRNA, mtRRF could occupy those too. Thus mtRF1a was used as another control to test whether the minimal level of interaction of mtRF1a can be eliminated by preincubation of mitoribosomes with mtRRF for 40 minutes. Lane 1 of Figure 5.7 B, however, still shows the presence of mtRF1a in the final eluate. Moreover, when the isolated mitoribosomes were pre-exposed to mtRRF (70pmol, for 40 min), then the amount of Δ49RF1 bound that could be detected in the eluate is comparable with the amount of Δ49mtRF1 bound without preincubation with mtRRF. Together this suggests that the binding of Δ49mtRF1 could not be inhibited by the presence of mtRRF in the sample and, similarly the binding of FLmtRFF to the mitoribosome could not be suppressed by the presence of Δ49RF1 in the samples. Therefore, the proposed hypothesis could not be either proved or disproved from those results and further investigation is required.

5.7. Discussion

The *in vitro* experimentation undertaken in this chapter aimed to investigate the recognition, binding and specificity abilities of mtRF1 towards isolated mitoribosomes with empty A-sites.

First, the data strongly suggests (Figure 5.2) that the majority of mitoribosomes immunoprecipitated via ICT1 have empty A-sites. This was determined by varying the incubation time and monitoring the mtRNA degradation over this

period. The 3h incubation period was determined to be optimal as the rRNAs remained intact while the mt-mRNAs degraded during this IP procedure.

Further, I have successfully shown that purified Δ49mtRF1 presented a level of interaction (Figure 5.3 B and C) with isolated mitoribosomes. It was also shown here that mtRF1a does not have the same affinity as mtRF1 for those isolated mitoribosomes, although an interaction still occurs, but it is much lower (Figure 5.5 B). It is possible that the detected interaction represents recognition of the small proportion of those ribosomes that have retained mRNA in the A site. Since the reaction contains no other factors that this site could be occupied by, mtRF1a samples for activity, and is therefore found in the eluate.

Why could this interaction not be detected *in vivo* with HEK293 expressed mtRF1 as described in previous chapter? First, the Δ49mtRF1 appears by its migration to be bigger than endogenous forms on westerns (Figure 5.4 B, compare lanes 4 and 5) and this additional length at N-terminal that corresponds to domain 1, exact function of which is still unknown, but it may 'lock' the protein on the ribosome for longer than the endogenous form interacts *in vivo.* Second, if there is a factor that facilitates the mtRF1 disassociation from ribosomes after it serves it function, it would not be present in these *in vitro* experimental conditions, therefore the process is prolonged and associated protein can be visualised.

The specificity of this ‘empty A-site’ binding could not, however, be determined in this experimentation. Neither of the selected potential inhibitors of mtRF1 binding could compete out mtRF1. The UAG synthetic triplet was chosen to block the A-site based on the fact that its addition is able to programme the bacterial ribosomal A-site for *in vitro* release assays. Even though the decoding centre is highly conserved between bacterial and mitoribosomes (Koc *et al.*, 2010) it cannot be excluded that the triplet did not associate and with the available techniques this could not be controlled for. There is also another possibility. The mitoribosomes that were used to obtain cryo-EM structures were purified with tRNA bound to a P-site (Koc *et al*., 2003). It is possible that the 55S ribosome isolated via overexpression and immunoprecipitation of ICT1 also has a tRNA still bound at the P-site. If there is no mRNA associated with the P-site tRNA in those ribosomes and if the UAG triplet actually bound the A-site as predicted, there would be no physical obstacles so that the addition of Δ49mtRF1 could potentially push the triplet forward to the P-site. The other A-

site blocker used was tetracycline, addition of which also did not inhibit mtRF1 binding to the mitoribosomes. There are at least two crystal structures of Tc bound to the *Thermus thermophilus* 30S that have been determined (Brodersen *et al*., 2000; Pioletti *et al*., 2001). Based on these, there are six different binding sites on the bacterial subunit are characterised, including the one close to the A site that is consistent with its inhibitory role. Even though this site was then reported (Aleksandrov and Simonson, 2007) to be a single, predominant binding site for Tc that is highly occupied and much stronger at physiological concentrations of Tc, on bacterial ribosomes, four of the other sites are identical and conserved in mitoribosomes. Therefore it is not known whether the affinity of those conserved sites on mitoribosome is different or stronger or which of them Tc would select to occupy under various conditions. There is also a study (Zhang *et al*., 2006) that reported tetracycline to have inhibitory effects that were similar on *E. coli* and mitochondrial ribosomes. However, the concentrations reported were calculated based on *in vitro* translation of both systems. The maximum inhibitory concentration required was much higher, i.e. approximately 100 times more to inhibit bacterial protein synthesis compared with the minimum inhibitory concentration from other studies, where this effect was measured on cultured cells (Ross *et al*., 1998). Further, Zhang *et al*., (2006) reported that in order to fully inhibit mitochondrial translation 340μM tetracycline was required which was over 110 times more than the reported minimum inhibitory concentration and 3.4 times more than the concentration that was used in this chapter's investigation, to block the A-site on ribosomes isolated via immunoprecipitation of FLAG tagged ICT1. If this is the case, then the approach required to be optimised and the concentration of 100μM Tc used in this study could simply not be sufficient to block A-site occupancy by incoming proteins.

Finally, the addition of the full length mtRRF to the isolated mitoribosomes in this study showed interaction with the ribosomes. However, this interaction could not inhibit binding of Δ49mtRF1 nor could the reciprocal arrangement prevent mtRRF binding 55S that was prebound with mtRF1. By doing so two different populations of ribosomes were generated, some mitoribosomes would have mtRF1 bound and some others mtRRF. The ribosome could not be saturated with either factor probably due to the constant on and off rate of each of those factors. The data is also not conclusive due to the limitations of

experimental material so that not all desired controls could be performed within one experiment. Each preparation yielded only enough mitochondrial lysate,

Table 5. 1. Outline of the proposed set of experiments to investigate the competition for A-site occupancy between mitochondrial translational factors.

Mitoribosomes +recombinant protein	I		II		III	
	Reaction 1	Reaction 2	Reaction 1	Reaction 2	Reaction 1	Reaction 2
1st step	+mtRF1	--	+mtRRF	--	+mtRRF	--
2nd step	+mtRRF	+mtRRF	+mtRF1	+mtRF1	+mtRF1a	+mtRF1a

which was incubated with the FLAG beads, to be divided into maximally three equal reactions, thus limiting the simultaneous controls that could be performed. The ideal approach would be to perform from the same mitolysate three pairs of reactions as presented in Table 5.1 below. The recombinant mtRRF would be added in the first step for incubation to one of each of the paired reactions of mitoribosome samples II and III whilst recombinant mtRF1 would be added to the one reaction of the pair I. Then, in the second step either the recombinant mtRRF, mtRF1 or mtRF1a would be added. In this way, if there was any effect of binding caused by the addition of a factor in first step, the changes in ratios of the interacting proteins between two ribosomes pools could be detected and compared.

Another way of answering the question of mtRF1 specificity on mitoribosomes and the A-site would be to use a crosslinking immunoprecipitation (CLIP) assay. This technique allows physiological RNA-proteins interactions to be determined. This is done by treating cells with UV light to facilitate *in vivo* crosslinking of an RNA species and a protein that it interacts with or is in close proximity to. The RNA and the protein are covalently bound to each other by UV- irradiation, and by using antibodies to the protein of interest the fragment of RNA that is protected by the protein can eventually be characterised (the procedure was adapted from Ule *et al*. [2005] and optimised in my host lab by Agata Rozanska). Most of the contacts between the rRNA in the ribosome A-site and bound tRNA are preserved (15 out of 18 contacts sites) (Koc *et al*., 2010), some

of which may be exposed as well when mtRF1 is bound and if this is the case and mtRF1 binds there it could be covalently bound by UV treatment to the fragments of rRNA. There was not enough time however, for me to explore this option of detecting interactions between mtRF1 and the mitoribosome. The next chapter instead concentrates on alternative approaches to generate potential substrates of mtRF1.

Chapter 6

Further approaches to generate an experimental system that reconstitutes ribosomes lacking A-site mRNA sequences in order to test mtRF1 specificity.

6. Chapter 6: Further approaches to generate an experimental system that reconstitutes ribosomes lacking A-site mRNA sequences in order to test mtRF1 specificity.

6.1. Introduction

As shown previously by Soleimanpour-Lichaei *et al*., (2007), mtRF1 does not show any peptidyl tRNA hydrolase activity on bacterial ribosomes *in vitro* with UAA, AGA, AGG codons. Therefore whilst determining whether the mtRF1 substrate proposed in this thesis' hypothesis, and as a follow up on the previous chapter, it was important to perform the release assay again but without programming the ribosomes with any codons for the A-site. The primary aim of this part of the *in vitro* investigation in this chapter is to compare whether there was a difference in activity of recombinant Δ49mtRF1 proteins expressed in *E. coli* compared to those that were expressed in human HEK293 cells. The importance of this is that differences in activity could result from possible differences in folding or more likely from differences in modifications.

However, in order to test whether mtRF1 could recognise and bind an A-site lacking mRNA thereby rescuing stalled mitoribosomes, both *in vivo* and *in vitro* approaches are required. Consequently, if the hypothesis is that mtRF1 acts as a rescue factor that prevents accumulation of mitoribosomes that have stalled at an empty A-site, then it is important to consider how often this event might occur under physiological conditions. My result so far suggest that this is either very rare or is relieved very quickly and so it has not been possible to capture mtRF1 'in flagrante'. If mtRF1 can recognise empty A-sites to potentially trigger release or recycling then generating an excess of this substrate *in vivo* may allow an otherwise rare event to be trapped, visualised and measured. In addition to the *in vitro* approach described in the previous chapter I aimed to test this hypothesis by increasing levels of potential substrate recognisable by mtRF1 *in vivo*. Two possible approaches were considered. The first would use a cell line generated in my host lab that expresses a mitochondrially targeted version of a cytosolic poly(A) specific 3' exoribonuclease (PARN) (Wydro *et al*., 2010). When full length PARN is targeted to mitochondria its activity is not restricted to only poly(A), but continues degradation into ORFs of most mitochondrial transcripts as shown in Wydro *et al*., (2010). It has been also

demonstrated that a C-terminal truncated version of PARN (mtPARN-N) reduces its processivity leaving most of the mt-transcripts stable but without termination codons. Therefore, this study will take advantage of this activity that should increase the level of transcripts that are predicted to migrate through the mitoribosome until the truncated 3' terminus leaves an empty or partially empty A-site, generating a potential substrate for mtRF1.

In mitochondria the physiological occurrence of an empty A-site may be low, moreover if there is more than one rescue system for different substrates as it is in prokaryotes, which could be the case with the three candidates for such a process (C12orf65, ICT1 and mtRF1), where the capacity for rescue of stalled ribosomes is greater than the demand (Moore and Sauer, 2005). Therefore, another, second approach was used in order to increase the demand and fulfil the capacity of potential rescue mechanisms in mitochondria. For this part of investigation, a bacterial endonuclease, RelE, was targeted to mitochondria (Temperley *et al*., 2010). In *E. coli*, RelE associates with the ribosomes and is part of toxin-antitoxin regulatory complex that specifically cleaves at the 3' end of mRNA in the A-site and targets all three bacterial stop codons, with the highest preference for UAG, but also shows some level of effectiveness on sense codons, such as CAG and UCG (Pedersen *et al*., 2003). Additionally, the cleavage occur either between 1 and 2 or 2 and 3 nucleotide of the codon (Hurley *et al*., 2010) and been shown specifically by Temperley *et al*., (2010) that in mammalian mitochondria all of the cleavage sites are between nucleotides 2 and 3 leaving 2 nt and only partially empty A-sites thereby providing a different substrate for mtRF1 than would be created by mtPARN-N. The stalled ribosomes generated by overexpressing in mitochondria each of those enzymes were challenged further by depletion of mtRF1, which would potentially, according to the hypothesis, minimise the rescue capacity of such treated cells allowing detection of the effect.

Finally this chapter investigated the potential involvement of mtRF1 in mitochondrial mRNA decay using patient's fibroblasts with a characterised pathogenic mtDNA microdeletion that results in removal of the stop codon from *MT-RNA14.* It was shown that an mRNA surveillance pathway requires translating mitoribosomes to recognize the target i.e. the transcript lacking the stop codon was rapidly degraded unless translation was inhibited (Temperley *et*

al., 2003). There is evidence in other translation systems that provide a clear link between mRNA surveillance pathways with ribosomes and show that proteins with similarities to release factors have a role in mRNA decay. It has been shown that stalling of yeast ribosomes during translation elongation is recognized by a pair of proteins Dom34 and Hbs1p that are evolutionarily conserved and related to the eukaryotic translation release factors eRF1 and eRF3 (Clement and Lykke-Andersen, 2006). Mammalian Pelota with Hbs1 (like their yeast counterparts Dom34 and Hbs1p) promote release of peptidyl-tRNA from stalled elongation complexes (Pisareva *et al.*, 2011). Therefore, there is a potential that mtRF1 is involved in degradation of the transcript in microdeletion patient fibroblasts and its depletion would 'protect', at least some of it.

The approach undertaken to characterise mtRF1 substrate and its binding site on the ribosome described in previous chapters was not conclusive and there was further need to design a different approach to identify the hypothesised function of this protein, which this chapter is going to be focused on. Also, due to the difficulties narrowing down mtRF1 function in mitochondria, this chapter describes testing for an alternative function of the protein.

6.1. *In vitro* Release assay with recombinant proteins

To this end I needed to generate constructs in vectors suitable for either i) overexpression in bacteria of GST tagged mtRF1 and then to purify it, ii) constructs that would direct stable and specific integration allowing inducible expression of FLAG tagged mtRF1 protein in HEK293 cells. Beads conjugated to anti-FLAG antibody then facilitated purification. Bacterially or human cell expressed mtRF1 could then be tested in an *in vitro* Release Assay. The assay simulates protein synthesis termination conditions, where bacterial ribosomes are pre-loaded with a synthetic AUG start codon and tritiated formylmethionine-$tRNA^{met}$ in the P-site, before the introduction of the specific termination codon in the A-site (or no codon added) and finally the purified protein of interest. If the protein exhibits a release activity by cleaving the ester bond between the tritiated methionine and the $tRNA^{met}$, the radioactive amino acid representing the polypeptide will be released into the supernatant and can be measured.

The aim of this investigation was to show release activity of mtRF1 *in vitro* assuming that the protein would occupy the A-site transiently and no mRNA is required for its function. It has been shown (chapter 5) that mtRF1 does not immunoprecipitate with any other proteins, therefore IP can be a good tool for purification of the protein, which should yield a relatively pure protein that can then be used for *in vitro* assays. The IP method uses FLAG antibodies that are specific to the FLAG tagged mtRF1 proteins to allow isolation of them. Such isolated mtRF1-FLAG proteins (Figure 6.1B, 1µl in lane 6 and 5µl in lane 7), believed to preserve its native folding and active size, along with mtRF1 recombinant protein GST-purified from bacteria (lane 10) (as described in method section 2.6.7) were tested in release assays. As shown in figure 6.1A compared with ICT1 control, which has been shown by Richter *et al*., (2010) to have codon-independent translation release activity on 70S ribosomes, both

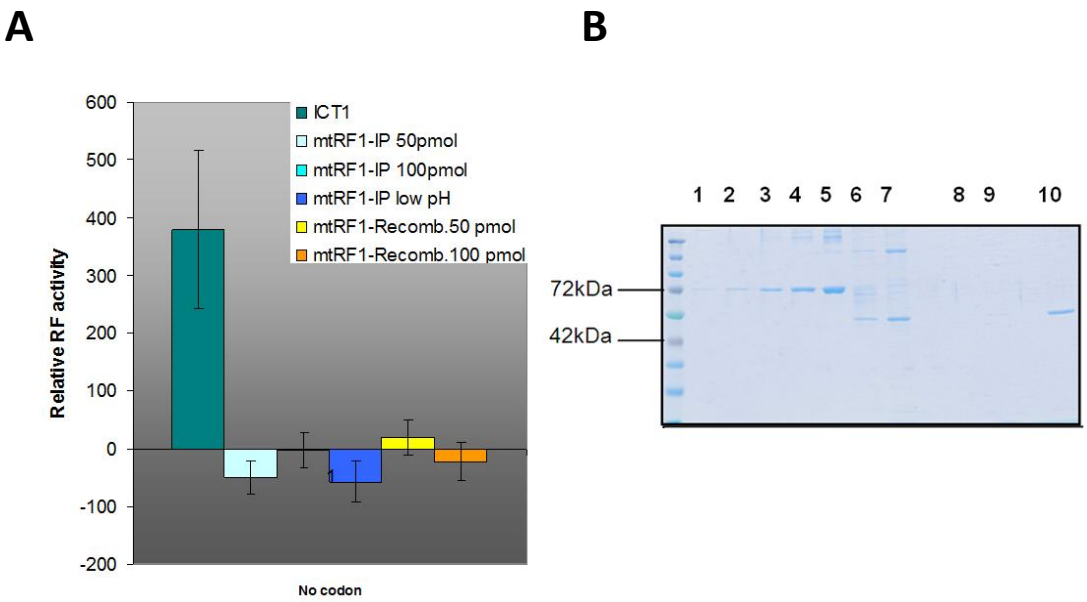

Figure 6. 1. mtRF1 and the *in vitro* Release Assay.

(A) The data presented in the histogram is from different amounts of mtRF1 protein either HEK293 or bacterially expressed and represents the mean of triplicate release assays. The relative release activity is measured in counts per minute shown on axis Y. Each assay was performed without any stop codon and ICT1, known to have activity under such conditions, was used as a positive control. **(B)** In order to estimate the amount of proteins, obtained from the IP described previously, to be used in release assay, elution fractions, BSA standard range (25, 50, 100, 250 and to 500ng, lanes 1-5) and GST-purified protein (237ng, lane 10) were separated by SDS-PAGE and visualised with SimplyBlue Safe stain. Samples in lane 6 (1µl of IP mtRF1 elution) and 7 (5µl of IP mtRF1 elution) were eluted under native conditions by competition with 3xFLAG peptide. Lanes 8 (1µl) and 9 (5µl) represent samples eluted under acidic condition with 0.1M glycine (pH 3.5), which were equilibrated with wash buffer to help preserve the protein structure and therefore function. The protein concentration in the elution fraction (lane 6) was estimated to be ~60ng/µl.

mtRF1-FLAG (mtRF1-IP) and recombinant Δ49mtRF1 were not able to promote release of fMet in *in vitro* conditions with the absence of stop codon. mtRF1-FLAG was also eluted in acidic conditions and then neutralised to preserve its structure (mtRF1-IP low pH), however using it in the release assay did not result in release of fMet either. The procedure was repeated using a double amount of ethanol to loosen the structure of bacterial ribosomes (data not shown), however this did not contribute to any increase in release activity detected. This data shows there is no difference in two tested variants of mtRF1 and neither recombinant mtRF1 nor mtRF1-FLAG isolated from human cells is active on bacterial ribosomes with an empty A-site as a substrate.

6.2. Can mtPARN-N generate the substrate for mtRF1?

Taken that truncated poly(A)-ribonuclease (mtPARN-N) expression results in removal of the termination codons from most of the mt-transcripts (Wydro *et al*., 2010), the exonucleolytic activity of mtPARN-N cleaves the transcripts from the poly(A) tail and extends into the stop codon leaving a complete open reading frame. As the elongation step of translation continues, migration of the ribosome eventually reaches the end of the transcript and leaves no codon in A-site to terminate. Depletion of mtRF1 in these circumstances should yield accumulated monosomes, assuming there is no particle that would recognise and rescue such complexes any more. HEK293 PARN-N expressing cells were transfected with siRNA-mtRF1 and siRNA-NT for 4 days, whereas the expression of truncated poly(A)-ribonuclease was induced for only 2 days prior to harvesting cells. Then followed sucrose density gradient separation of lysate, every fraction of which was subjected to western blot and northern blot analysis to determine if there is a change in behaviour of mitochondrial ribosomal proteins. Separated proteins of interest were visualised by western blot with antibodies against polypeptides in the small (DAP3) and large (MRPL3) mitochondrial ribosomal subunits. The same whole cell lysate preparation that was used for the gradient analysis was also separated independently on SDS-PAGE and analysed using anti-mtRF1 antibodies, with anti-porin antibodies used as a loading control. As seen in figure 6.2A the depletion was effective as the mtRF1 signal cannot be detected compared to siRNA-NT control. Unfortunately, the sucrose gradient results (Figure 6.2B) show no increase in accumulated ribosomes.

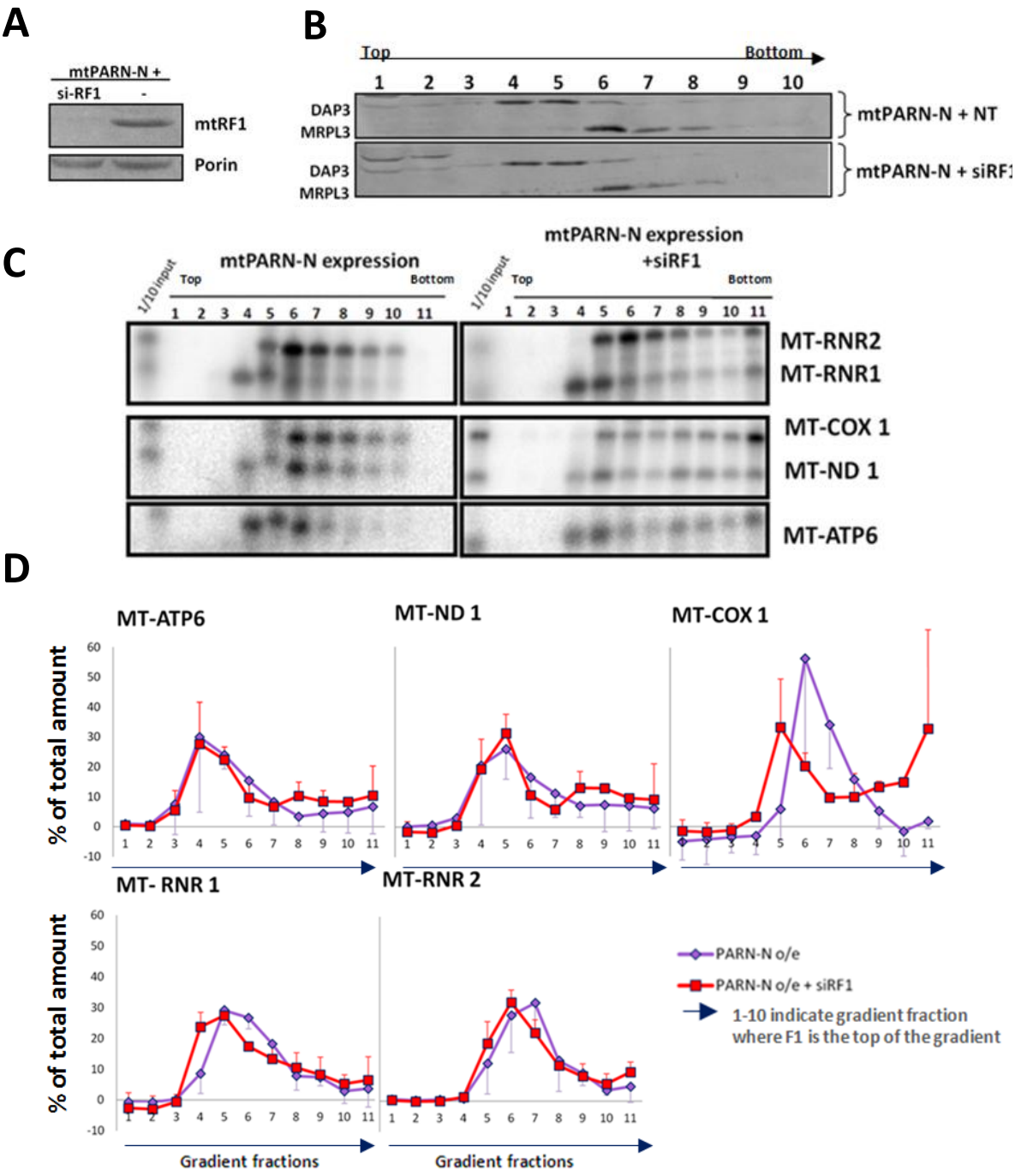

Figure 6. 2. Analysis of mt-RNA and mitoribosome components following mtPARN-N expression with and without concomitant depletion of mtRF1.

HEK293T mtPARN-N cells were induced with 1µg/ml tetracycline for 2 days and treated with mtRF1 (siRF1) or non-targeted (NT) siRNA for 4 days. The lysates (700µg) of each sample were separated on 10-30% isokinetic sucrose gradient. **(A)** In order to confirm mtRF1 depletion in this experiment 50µg of cell lysates (prior to sucrose gradient centrifugation) were collected and analyzed separately by western blot using antibodies against endogenous mtRF1 and Porin as loading control. **(B)** 10 % of each fraction were separated by SDS-PAGE and analysed using antibodies against the small (DAP3) and large mitochondrial subunits (MRPL3). **(C)** RNA was extracted from 80% of each fraction (1-11 and 1/10 of an input) and analysed on a northern blot using probes to mitochondrial mRNAs (*MTATP6* only, *MTCOX1* and *MTND1*) and 16S (*MT-RNR2*) with 12S (*MT-RNR1*) mt-rRNAs. **(D)** The signals were quantified and presented as the graph of mean and standard deviation from three independent experiment repeats (*p <0.05, **p<0.01, ***p<0.001).

A similar pattern of distribution of mtSSU and mtLSU is the same in the absence of mtRF1 (4 day depletion) or presence as in the control (top panel), after 2 days of mtPARN-N expression. In both cases the SSU, detected by anti-DAP3, migrated to and accumulated mostly in fractions 4 and 5, while a member of LSU, MRPL3, migrated to fractions 8, but mostly accumulated in fraction 6. In order to analyse RNA in those samples, 80% of each fraction had RNA extracted that was subjected to northern blot analyses. Two probes each specific to an rRNA were used (*MT-RNR1* and *MT-RNR2*) to detect the migration of the mtSSU, mtLSU and monosome in the northern blot. The signal for mtSSU first appears in fraction 4 and distributes evenly down to the bottom of the gradient, where fraction 11 represents the gradient pellet (Figure 6.2 C). The 16S rRNA partitions to fraction 5-7, then distributes to the bottom of the gradient. The signals in earlier fractions (4-6) represent the free uncomplexed state of each individual subunit, whereas signal in fractions from 7-8 represent the presence of monosomes. This pattern of monosome is also seen by the distributions of mRNA where mtRF1 was depleted, signals of which become more intense again, where trapped by the monosome (Figure 6.2C, right panel, fractions 8) and distributed evenly throughout the gradient. The distribution of mRNAs in the cells where mtRF1 was still present (Figure 6.2C, left panel) is focused more towards the top of the gradient. The histogram plotted (Figure 6.2D) based on detected signal on northern blot clearly reflects this distribution of both rRNA and mRNA tested between the sample (si-RF1) and control (NT). Even though the difference is very subtle, it seems that the mtPARN-N overexpression resulted in a peak of mRNA (purple line in figure 6.2D) concentrated to one fraction (*MT-COXI* to fraction 6, *MT-NDI* to fraction 5 and *MT-ATP6* to fraction 4) and declines with each later fraction to the last one. Depletion of mtRF1 'restores' the distribution to the one of control (Figure 3.6A, left panel), where the signal for mRNA comes back again in fraction 8 (and two peaks can be detected). Therefore, based on this data the overexpression of Poly(A)-ribonuclease and mtRF1 depletion did not contribute to significant accumulation of monosomes, however discrete change distribution of mRNA may suggest that the lack of mtRF1 promotes its accumulation on the monosome.

6.3. Can mtRelE generate the substrate for mtRF1?

Another way of looking at potential mtRF1 activity that would be reflected on distribution of mRNA and monosomes *in vivo* was using a mitochondrially targeted endoribonuclease, mtRelE that cleaves specifically between nucleotide positions 2 and 3 of a codon in A-site of the ribosome. It was shown that the expression of mtRelE in mitochondria results in cleaving more than 90% of the tested bicistronic *RNA14* transcripts (Temperley *et al*., 2010). In order to test this as an alternative substrate for mtRF1, mtRelE was overexpressed for 3 days, then cells were subjected to the same analysis as previously (in section 6.2). As previously, HEK293 cells but this time expressing mtRelE, were transfected with siRNA-mtRF1 and siRNA-NT for 4 days, while mtRelE was induced for 3 days prior cell harvesting and sucrose density gradient separation followed by western blot and northern blot investigation. The separated proteins were visualised by western blot with antibodies against polypeptides in the small (MRPS18B) and large (MRPL3) mitochondrial ribosomal subunits. Figure 6.3A shows the depletion was effective as the mtRF1 signal cannot be detected compared to siRNA-NT control, with anti-porin antibodies acting as a loading control. The expression of mtRelE resulted in a relatively normal pattern of distribution of MRPL3 and MRPS18B in both controls (Figure 6.3B, lower and middle panels). The mtSSU, detected by anti-MRPS18B, migrated to fraction 4 and extends evenly to fraction 7, which marks the monosome. This marker was somewhat stronger in fraction 4 and 5 in +mtRelE only sample depicted here (Figure 6.3B, lower panel), but multiple repeats of this experiment show that this is not a consistent phenomenon and is within experimental error of taking fractions. A member of mtLSU, MRPL3, migrated to fractions 7 in all three cases, but this signal in control with NT mostly accumulated in fractions 5 and 6 (middle panel of Figure 6.3B) while in the si-RNA for mtRF1 sample it was mostly in fraction 7 (upper panel). The pattern of both 'control' +RelE and ‘sample’ +RelE treated with siRF1 are reasonably comparable when viewed over multiple repeats, and due to the fact that the changes occur inconsistently are categorised as experimental error and no significant change in migration of tested proteins could be detected. This same distribution profile of ribosomal proteins was also seen in controls in chapter 3, where no treatment was introduced to HEK293T cells (Figure 3.4A, top panel).

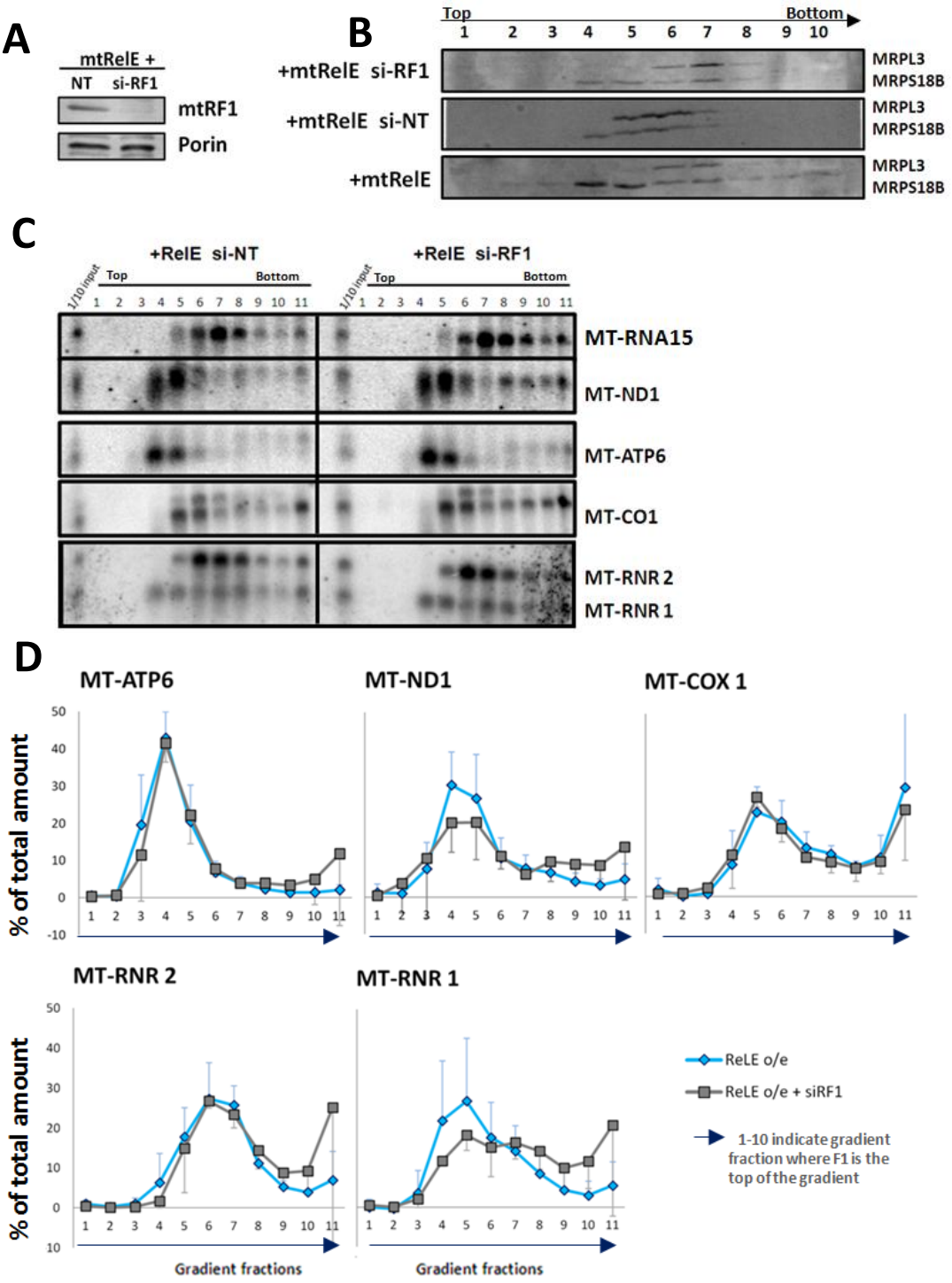

Figure 6. 3. Analysis of mt-RNA and mitoribosome components following mtRelE expression with and without concomitant depletion of mtRF1.

HEK293T cells expressing mtRelE were induced with 1µg/ml tetracycline for 3 days and treated with mtRF1 (siRF1) or non-targeted (NT) siRNA for 4 days. The lysates (700µg) of each sample were separated on 10-30% isokinetic sucrose gradient. **(A)** In order to confirm mtRF1 depletion in this experiment 50µg of cell lysates (prior to sucrose gradient centrifugation) were collected and analyzed separately by western blot using antibodies against endogenous mtRF1 and porin as loading control. **(B)** 10 % of each fraction were separated by SDS-PAGE and analysed using antibodies against the small (MRPS18B) and large mitochondrial subunits (MRPL3). **(C)** RNA was extracted from 80 % of each fraction (1-11 and 1/10 of input) and analysed on a northern blot using probes to mitochondrial mRNAs (*ATP6* only, *MTCOX1* and *MTND1*) and 16S (*MT-RNR2*) with 12S (*MT-RNR1*), mt-rRNAs. **(D)** The signals were quantified and presented as the graph of mean and standard deviation from three independent experiment repeats (**p* <0.05, ***p*<0.01, ****p*<0.001).

The fractions analysed were also subjected to northern blot analysis as in the previous section, to test whether the distribution of RNA reflected the state of stalled ribosomes. First of all, in the figure 6.3C it can be noticed that the signal for *MT-ATP6* predominantly accumulates in fraction 4 as a result of mtRelE cleavage of bicistronic *MT-RNA14*. A faint signal of the uncleaved transcript was also detected on the same panel, where is still associated with the monosome in fractions 8-11. This confirms that mtRelE was both, expressed successfully and it was functional. The signal for mtSSU (*MT-RNR1*) in samples, [+RelE +siNT] and [+RelE +siRF1] (left and right panel, respectively) first appears in fraction 4 and distributes evenly down to the bottom of the gradient, where fraction 11 represents the gradient pellet. The 16S rRNA partitions to fraction 5, then distributes to the bottom of the gradient, but is mostly in fractions 5-7/8. The signals in earlier fractions (5-6) represent the free uncomplexed state of the subunit, whereas signals in fractions from 7/8 represent the presence of monosomes. There is no difference in distribution of this transcript in two presented samples in Figure 6.3C. The only difference between the distribution of mtSSU that can be noticed with the mtRF1 being depleted is the lack of rapid decline of the *MT-RNR1* signal from fraction 5, which is seen it +RelE only sample. This rapid decline of the signal is the case for only mtRelE treated sample (quantified in Figure 6.3D, *MT-RNR1* panel, blue line) and is characteristic for all transcripts in the mtRelE overexpression sample. Comparing it with the gradient profile of all mRNA extracted from untransfected HEK293T (Figure 3.7 B, black line), where the signal increases back from fraction 7 for each tested transcript (for comparison see appendix 1.1 for those figures merged), which indicates the presence of the monosome, a trend can be noticed. This piece of data suggests that the mtRelE cleavage resulted in dissociation of monosomes to some extent, while the mtRF1 depletion sample represents more flat distribution of this transcript restoring the second peak seen in wild type HEK293T in *MT-RNR1* and *MTND1* transcripts. The other transcripts, *MT-ATP6*, *MT-COXI* and *MT-RNR2* remained the same with or without mtRF1 depletion. This result suggests that in spite of the minor differences caused by mtRF1 depletion in two tested transcripts, the overall trend remains unchanged, additional depletion of mtRF1 did not seem to be involved in generation of more blocked ribosomes resulting from mtRelE cleavage.

6.4. Is mtRF1 involved in mRNA decay pathway?

There was a subtle increase of steady state level of several RNAs upon mtRF1 depletion seen earlier in chapter 3 (Figure 3.5). An accumulation of transcripts can also be seen, when mt-protein synthesis is inhibited with thiamphenicol (Temperley *et al*., 2010). If mtRF1 is really involved in quality control of protein translation and its loss is able to inhibit translation, even if translation inhibition is only slight, this should be more pronounced and detectable in the patient-derived fibroblasts line that lacks the termination codon for the bi-cistronic *RNA14.* This is due to the mtDNA harbouring a microdeletion at bp 9204/5 (μΔ9205) that removes nucleotides that comprise part of the stop codon in the orf encoding ATPase 6. In order to investigate the potential involvement of mtRF1 in mitochondrial mRNA decay directly, mtRF1 was silenced with siRNA in those patient fibroblasts and in a non-diseased control primary fibroblast line (control) and after 7 days of treatment subjected for analysis. The western blot results shows that the protein was substantially depleted in both cell lines (Figure 6.4B) and, as seen before, this depletion correlated with the decreased levels of MRPL12 in both, μΔ and control cell lines.

The prediction was that the mtRF1 depletion in that patient's cell lines should inhibit degradation of μΔ*RNA14,* as a consequence of translational inhibition, at the same time restoring its levels to those seen in control as shown by Temperley *et al.*, (2003). The northern blot analysis in this investigation has confirmed that the levels of *MT-RNA14* are much lower in μΔ cell line (Figure 4.6A, lane 2) than in the control (lane 4), reflecting the rapid translation-dependant degradation of aberrant transcripts. The depletion of mtRF1 did not affect the translation process and thereby did not cause the restoration of steady state levels of non-stop transcript and so the μΔ*RNA14* still remains degraded (Figure 6.4A, lane 1). This suggests that mt-protein synthesis was not inhibited and that mtRF1 is not directly involved in liberating the nascent protein with polylysine extensions trapped on mitoribosomes in those cells. In order to be sure that depletion of a translation factor can inhibit mRNA degradation in this fashion, ICT1 was depleted alongside in both cell lines. The loss of ICT1 is known to affect ribosome assembly, therefore inhibit protein synthesis (Richter *et al*., 2010). Consistent with this, ICT1 depletion caused the stabilization of μΔ*RNA14* transcript (Figure 6.4A, lane 5), comparable with the control (lane 8)

confirming the same effect as thiamphenicol on mRNA decay and translation reported by Temperley *et al*., (2003). The steady state level of other transcripts tested, especially in control cell lines (Figure 6.4A, lanes 3-4 and 7-8) shows

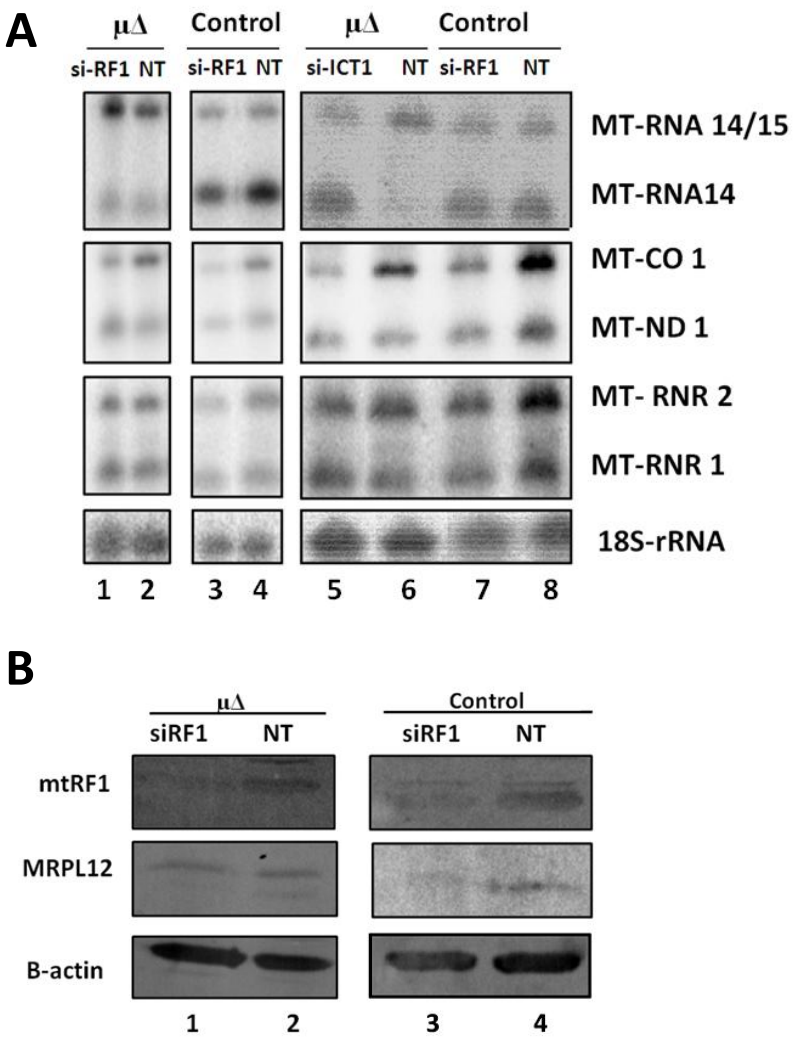

Figure 6. 4. Investigation of the effect of mtRF1 depletion in a patient fibroblast cell line carrying a microdeletion at the very 3' terminus of *RNA14* that causes the termination codon to be lost resulting in non-stop decay.

(A) The patient-derived cell line carrying an mtDNA microdeletion at the RNA14/15 processing site (μΔ, lanes 1, 2, 5 and 6) and non-disease control primary fibroblast line (lanes 3, 4, 7 and 8) were treated with siRNA against either mtRF1 (si-RF1, lane 1,3,7), ICT1 (si-ICT1, lane5) or non-targeting (NT, lane 4,8). Northern blot analysis reveals steady state levels of mt-mRNAs (*RNA14/15*, *RNA14*, *MTCO1* and *MTND1*), rRNAs (*MT-RNR2* and *MT-RNR1*). Cytosolic rRNA 18S was used as a loading control. **(B)** Total fibroblast lysates (50μg) from the same cell lines were separated on 12% SDS-PAGE, transferred to PVDF membrane and interrogated with antibodies against mtRF1, MRPL12 and B-actin (loading control).

rather opposite results than seen in HEK293T upon mtRF1 depletion (chapter 3). At this stage, it cannot be justified in more detail rather than a simple

explanation that it is due to the tissue specific cell types and it is has not followed up in this thesis.

6.5. Can increased expression of ICT1 rescue the phenotype caused by mtRF1 depletion?

The depletion of mtRF1 in the patient-derived fibroblasts, where the stop codon of *MT-RNA14* is lost (due to a 2 bp deletion), did not affect the translation-dependent degradation of the faulty transcript, suggesting that mtRF1 is either not involved at all or that its absence has been compensated for. The depletion of ICT1 in the same cell lines causes the lack of fully assembled mitoribosomes, therefore it was not possible to determine the independent roles of those two factors on mitochondrial quality control. ICT1 is a very small protein and if not integrally associated with ribosome it is presumed that it could easily enter the A-site of the ribosome and reach the PTC to hydrolyze the nascent polypeptide chain. When ICT1-FLAG is overexpressed in HEK293T cells, apart from a proportion of it being incorporated in newly assembled mitoribosomes, there is also a substantial amount of ICT1 that is free, which has also been shown to marginally affect the cells' growth (Richter *et al*., 2010). As shown in chapter 3 the loss of mtRF1 causes a growth defect in HEK293 and HeLa cells, which can be partly caused by the limited availability of mtRF1 derived GGQ activity. If that is the case, this deficiency could be partially rescued by overexpression of ICT1, which would provide some functional codon independent hydrolysis on all available substrates, also those that await recognition by mtRF1 activity.

To test this potential effect of ICT1 on mtRF1 depleted cells, three sets of HEK293T cells were prepared, all capable of expressing ICT1-FLAG: one set ICT-FLAG overexpressor only for 4 days, a second set targeted with NT siRNA for 4 days and a final set depleting mtRF1 for 4 days. In each of the 3 sets ICT1 expression was either induced for the full 4 days or no tetracycline induction was performed. The data are presented in the figure below. As shown in lanes 1 and 2, the overexpression of ICT1-FLAG only resulted in a minor drop in number of cells compared with a control, which was consistent with previous data. The depletion of mtRF1 on its own shows a severe defect on cell growth (lane 6 compared with lane 4) also seen earlier, but the simultaneous overexpression of ICT1-FLAG did not rescue the phenotype caused by mtRF1

depletion (compare lanes 5 and 6). This piece of data strongly implies that ICT1 cannot compensate for the loss of mtRF1 and despite the presence of functional GGQ motif in both proteins, their roles may be involved in recognition of different substrates, which is possibly determined by the rest of mtRF1 structure that ICT1 lacks.

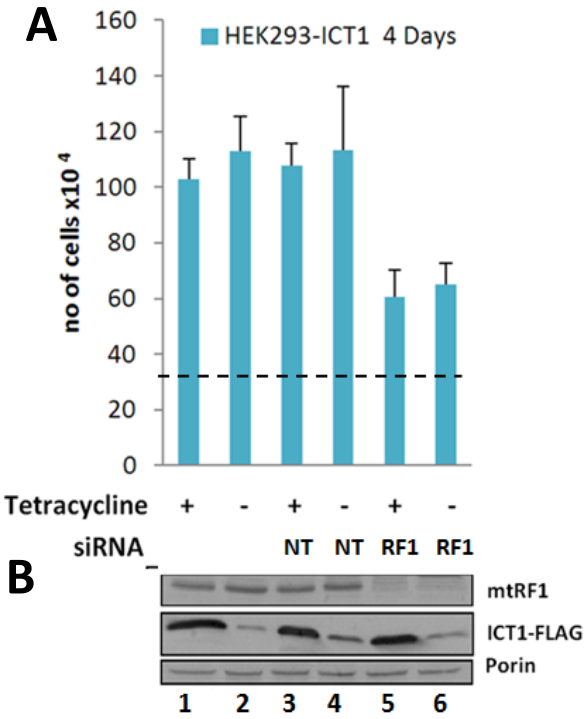

Figure 6. 5. ICT1 overexpression fails to rescue the deleterious phenotype caused by mtRF1 depletion as measured by cell growth.

(A) HEK293T cells capable of expressing ICT1-FLAG were treated with either 1µg/mg tetracycline, siRNA against NT or mtRF1 or both tetracycline and one of the siRNA reagents. After 4 days cell counts were performed and data plotted based on the mean and standard deviation of three independent experiments. **(B)** After counting, cells were lysed and 50ug subjected to western analysis to confirm depletion (lanes 5 and 6) or overexpression (lanes 1, 3 and 5) and to compare against lane 2 (cells not expressing ICT1-FLAG and containing mtRF1) by interrogation with antibodies against mtRF1 and FLAG, respectively. The dotted line indicates the initial number of cells seeded.

6.6. Does mtRF1 act as a scaffold for ribosome assembly?

Despite of all the efforts to confirm mtRF1 involvement in quality control of mitochondrial protein synthesis, the data presented so far could neither unequivocally confirm this fact nor exclude it. One of the alternative possibilities for the function of mtRF1 in mitochondria could be its involvement in maturation/assembly of the monosome. This hypothesis was considered since due to mtRF1 secondary structure being predicted to fold in a similar manner as

mtRF1a, coupled with the nucleotide extensions within mtRF1's codon recognition motifs, it is predicted to fill up the space of ribosomal A-site in the absence of mRNA. Such empty A-sites in ribosomes may not only be a result of translation of faulty transcripts, they could potentially also occur during ribosome assembly allowing a protein to occupy this cavity acting as a scaffold within what will become the A-site pocket. Ribosomal LSU and SSU subunits are recycled after translation to be used in a subsequent round of translation. If the monosomes assemble from ribosomal subunits that were already used in previous rounds of translation, the scaffolding function of mtRF1 can be also extended to this phase in between translation recycling and reinitiating. mtRF1 would bind in this case to an empty ribosome and its functional GGQ motif would efficiently assure that any aberrant situation where a tRNA still had a polypeptide chain attached, are removed and the extended codon recognition motif of this protein could evict any residual mRNA from the decoding centre allowing the 2 subunits to rejoin and form a 55S particle.

In order to test the first hypothesis a simple experiment was performed and adapted from (Dennerlein *et al*., 2010). The point was to assess if after mtRF1 depletion *de novo* formed 55S can be isolated via newly expressed FLAG tagged ICT1. When ICT1 is overexpressed, much of it is incorporated into *de novo* ribosomes, the rest remains free. For this experiment, mtRF1 was depleted with siRNA for 5 days, but after 3 days of siRNA treatment, the expression of ICT1-FLAG was induced for the remaining 2 days of the experiment. After 5 days of total treatment, cell lysates were subjected to sucrose gradient centrifugation, fractions of which were subjected to western blotting analysis. The induction and depletion were also assessed and as shown in Figure 6.6B both, ICT1 was successfully overexpressed in both samples and mtRF1 efficiently depleted in siRF1. The newly assembled ribosomes that were formed during the experiments were then visualised by the presence of ICT1-FLAG, clearly seen in fractions 7 and 8 of figure 6.6A top panel. This is consistent with monosome being formed from the signals of mtSSU protein, MRPS18B, and of mtLSU, MRPL3 observed mostly in fraction 7. A large proportion of overexpressed ICT1-FLAG remained free, mostly in fraction 1 and 2 in both samples, whereas the rest migrated to fractions 6/7 in both NT and siRF1 treated samples, where the LSU and monosome are expected to migrate. The amounts of ICT1-FLAG incorporated in newly

assembled monosomes however appears the same, despite the absence of mtRF1. This was, however, a preliminary attempt, but it suggests that there is no link between mtRF1 function and assembly of mitoribosomes, at least not directly.

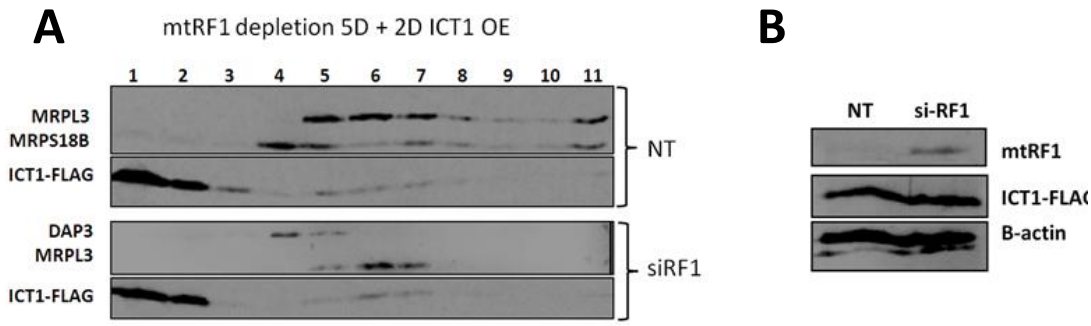

Figure 6. 6. Analysis of whether new mitoribosomes can be formed in the absence of mtRF1.

(A) HEK293T ICT1-FLAG cells were treated with siRNA targeted to either mtRF1 (siRF1) or control (NT) for 5 days. Two days before harvesting cells were induced with 1µg/ml tetracycline. Total cell lysate (700µg) was separated by isokinetic gradient centrifugation, prior to fractionation and western blot performed to analysis the integration of newly synthesised polypeptides into 55S monosomes (antibodies against MRPS18B and DAP3 for 28S mt-SSU, MRPL3 and FLAG for 39S mt-LSU). **(B)** Western analysis of 50µg total cell lysate probed with antibodies against mtRF1 and FLAG to confirm

6.7. Discussion

Due to the fact that genetic manipulations in mammalian mitochondria are limited and appropriate tools are not available yet, there are no models to study molecular mechanisms of mitoribosome stalling. Therefore, the aim of this chapter was to use all available techniques to investigate the substrate that mtRF1 may act on in regulating quality control (QC) of human mt-protein synthesis.

First, the release assay demonstrated that mtRF1 activity could not be detected on *E. coli* ribosomes that had an empty A-site. This absence of release activity may be due to the compulsory use of heterologous assay system (bacterial ribosomes and human mtRF protein), which, despite the similarities may not be compatible between those systems for assessing the quality control. The ribosomes used in the assay are not physically stalled and the absence of mRNA in A-site may simply not be the only feature of such bacterial ribosomes that would be recognized by mitochondrial factor, which would potentially

rescue blocked complexes. The ideal approach to overcome this problem would be by using mammalian mitoribosomes or as second best bacterial ribosomes that had been stalled beforehand in release assays, to test the QC function in orthologous systems or the compatibility of mitochondrial factors with bacterial systems. In the absence of such ribosomes for *in vitro* assays I tried to maximize the generation of stalled ribosomes *in vivo* by using two different enzymes, mtPARN-N and RelE, both of which act on mt-mRNA in different ways. The exonucleolytic activity of mtPARN-N cleaves outside the ribosome digesting into the poly(A) tail and leaves no complete codon in the A-site to allow termination and release when the translation of the ORF comes to an end. In contrast, mtRelE cleaves stop codons between nucleotide positions 2 and 3 specifically in the A-site of ribosomes.

The results generated by the overexpression of those two enzymes in mitochondria were rather complicated and it was difficult to make clear and unequivocal conclusions, mostly due to the lack of detecting any clear accumulation of blocked monosomes or accurate assessment of their presence. Even though there was a tendency towards accumulation of transcripts on ribosomes, the effect of mtRF1 depletion did not yield a dramatic effect. This could be due to the presence of other factors harbouring the crucial functional GGQ motif, which could potentially compensate for the loss mtRF1 under such stressful situations as truncation of the majority of mammalian mt-transcripts, due to either mtPARN-N or mtRelE activity. It was recently reported by Vivanco-Dominguez *et al*., (2012) that bacterial release factors (RF1, RF2, RF3), and also RRF together with tmRNA all collaborated *in vitro* to reduce accumulation of empty A-site stalled ribosomes and they proposed 3 different pathways involving those factors. Two of these pathways have been well accepted before, one of which involves a tmRNA activity following RelE cleavage, and then RRF/EF-G mediated ribosome recycling. The second proposes the 'drop off' of peptidyl-tRNA from the ribosome by RRF, RF3 and EF-G together. Their data however suggests a new concept of RF1, RF2 and RF3 participating in disassembly of ribosomes that have stalled with empty A-sites. If this is the case in *E. coli*, it is possible that a similar phenomenon can occur in mitochondria. In the later part of this chapter it was demonstrated that ICT1 is unlikely to be one of those factors that could compensate for the loss of mtRF1.

However, there are still mtRF1a, mtRRF and uncharacterized C12orf65, which could compensate and are going to be a focus of the next chapter. Those factors together could collaborate to be responsible for the mild effect seen in PARN-N/RelE experiments. Similarly, the experiment with depleting mtRF1 in μΔ patient's fibroblasts could not confirm the direct involvement of this protein in mRNA decay process. This could be because it was not possible to deplete mtRF1 completely in those cells and remaining traces of the protein even after 7 days might be sufficient to cope with the introduced ‘problem' or it is possible that there may be other factors involved.

Unfortunately, without having *in vitro* mitochondrial translation system to investigate the other partners, which potentially could take part in a mechanism of action together with mtRF1 to rescue mitochondrial stalled ribosomes, a simultaneous overexpression in HEK293T of at least two factors and silencing the others would be required, which was out of the scope of this investigation at the given time. Moreover, without a mitochondrial *in vitro* system or other suitable tool to investigate the interactions between mitochondrial transcripts and ribosomes during ribosomal stalling events, quality control may remain the least studied and understood phase of mitochondrial protein synthesis. One of the potential approaches to overcome this problem specific to the mammalian mitochondrial field would be use of a powerful technique, ribosome profiling, which is being optimized in my host lab by Maria Wesolowska. The aim of this technique is to investigate the mRNA fragments that are protected by the ribosome during protein synthesis. The analysis of them by deep sequencing methods will provide profiles of ribosome position on mRNA to reflect *in vivo* translation. Using this method to study the factors involved in quality control of protein synthesis will not only answer the question of which proteins are responsible, which could not be answered within this project using currently available techniques, but will also shed a new light on very important process in mitochondrial biology.

Chapter 7

Investigation of human mitochondrial protein C12orf65

7. Chapter 7: Investigation of human mitochondrial protein C12orf65

7.1. Introduction

C12orf65 is the 4th member of mitochondrial class I peptide release factor family, which was shown to play an important role in mitochondrial protein synthesis, however its exact function remains unanswered. Moreover, the gene that codes C12orf65 is conserved in various species (Antonicka *et al*., 2010). It was first reported as a gene with a mutation that causes a premature stop codon in this protein. The mutation in the gene was reflected in a molecular impairment of mitochondrial protein synthesis and defects in assembly of complexes I, IV, III and V, which in turn led to a Leigh Syndrome in two unrelated patients. Also recently, there was a different homozygous nonsense mutation identified in two related patients in Japan that could underlie autosomal recessive hereditary spastic paraplegias (AR-HSP) with optic atrophy and neuropathy. This mutation resulted in reduction of mitochondrial protein synthesis and defects in complexes I and IV (Shimazaki *et al*., 2012). This together proves that C12orf65, similar to other release factor family proteins, is an essential protein in mitochondrial biology.

C12orf65 contains a conserved GGQ motif, characteristic for all release factor family proteins but it lacks domains 2 and 4, where two codon recognition regions would be found. This truncation, similar to ICT1, makes it a relatively small protein of 166aa (~18 kDa). However, recent crystallographic structure has revealed that the conserved GGQ motif of C12orf65 is more similar to domain 3 of the bacterial RF2 than to ICT1 (Figure 7.1). The structure of C12orf65 forms a topology of a 3_{10}-β1–β2–β3–α1 with the GGQ being localized in the unstructured loop between β1 and β2 and it lacks, the characteristic for ICT1, α helix (α_i) found between β2 and β3 (Kogure *et al*., 2012). This difference together with the finding that the overexpression of ICT1 can partially rescue the phenotype resulting from C12orf65 mutation in patients' fibroblasts (Antonicka *et al*., 2010) may indicate that the two proteins, ICT1 and C12orf65 could have a similar role in maintenance of mitochondrial gene expression with partially overlapping functions. The study of Antonicka *et al*., (2010) demonstrated that C12orf65 is localized to mitochondria, but unlike ICT1, C12orf65 does not exhibit peptidyl-tRNA hydrolase activity on bacterial ribosomes tested *in vitro*. The aim of this part of my thesis, further to the crystal structure information and

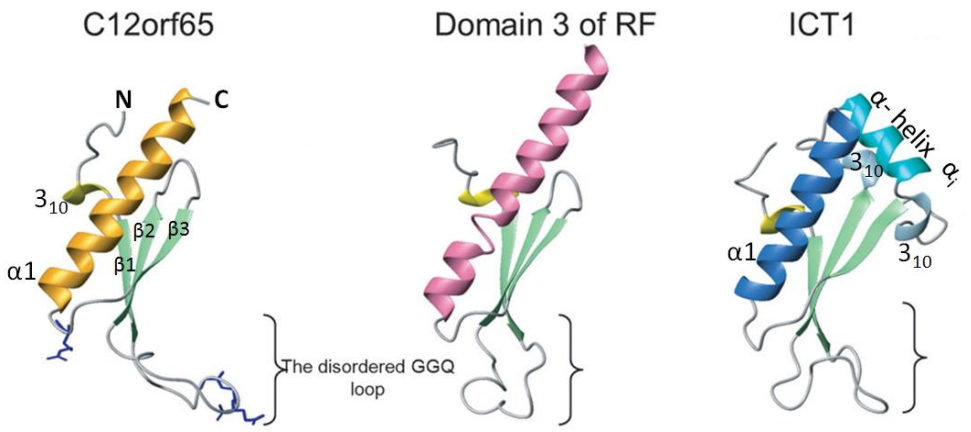

Figure 7. 1. Ribbon diagrams comparing the structures of the GGQ domain in class 1 Release Factor family proteins.

The β-strands and 3_{10} helix are coloured light green and yellow respectively in all presented structures. The main α helix (α1) is coloured orange in C12orf65, pink in domain 3 of RF (free RF2 from *E. coli*) and dark blue in ICT1 structure.

studies on patients' fibroblasts, was to investigate the real function of C12orf65 in mitochondrial gene expression and whether the hypothesis of it being involved in quality control of this process can be proven. This chapter particularly represents preliminary data obtained from experimentation on cultured human cells (HEK293T and HeLa). First, in order to detect the endogenous form of C12orf65 in cell lysates an antibody was required. To this end a recombinant protein was generated, purified and used for immunisation of two different rabbits. Then the specific antibodies were affinity purified from the final bleeds. Further investigation aimed to test the consequences of C12orf65 depletion in cultured human cells and whether it reflects the phenotype seen in patients' fibroblasts caused by the mutation in this protein. Finally the association of C12orf65 with mitoribosomes was to be tested, followed by generation of stable cell lines that could inducibly express wildtype C12orf65 or with two different point mutations across the conserved GGQ motifs.

7.2. Generation of a polyclonal antibody against C12orf65

7.2.1. Overexpression and purification of GST-fusion protein

Generation of C12orf65 construct and cloning it into the bacterial pGEX-6P-1 vector was successfully performed by a student Edward Carter as his MRes project in my host lab prior to the start of this project. For the purpose of generating the recombinant antigen C12orf65-GST fusion protein was

overexpressed in Rosetta cells, which can be seen in Figure 7.2, lane 1 at ~42kDa size marker. The GST-protein binding to the beads (BBE, lane 3) resulted in decreased amount of it being discarded in flowthrough (FT, lane 2 of the same Figure). The GST was cleaved away, releasing Δ26C12orf65 (Figure 7.2, lane 5). There was a proportion of both the cleaved version of the GST tag alone and also the still fused GST-C12orf65 bound to the beads (BAE, lane 4). Because the elution fraction (lane 5) apart from the protein of interest, which migrates consistent with a molecular weight ~17kDa (but of actual size 15kDa), also contained other proteins, the band of interest was cut out from the gel and sent to Eurogentec for immunisation of two rabbits.

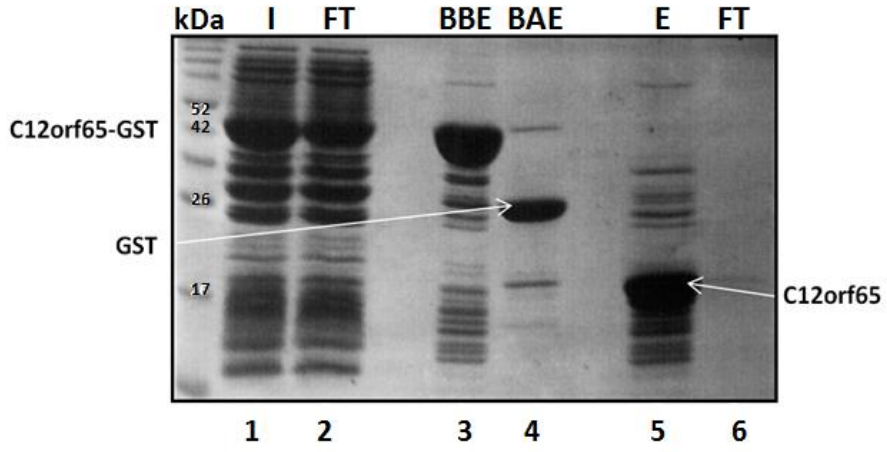

Figure 7. 2. Expression and purification of recombinant C12orf65 protein.

In order to overexpress the fusion protein C12orf65-GST (~ 41 kDa*) E. coli* Rosetta cells were cultured to OD_{600} 0.4-0.6, induced with 1mM IPTG and incubated overnight at 16°C before harvesting and sonication. The soluble proteins (input, lane 1) were loaded onto glutathione Sepharose beads. After incubation the flowthrough (FT, lane 2) was discarded and the beads (BBE, lane 3) washed with PBS. C12orf65 (~15 kDa) was eluted by the addition of PreScission protease and the beads (BAE, lane 4) analysed for residual bound material. The elution fraction (lane 5) was then loaded onto NHS-activated Sepharose 4 Fast Flow beads, to which the protein should covalently bind and the flowthrough (FT, lane 6) analysed to inspect efficiency of binding. Each sample was loaded on 14% gel, which was then Coomassie stained.

7.2.2. Antibody testing and affinity purification

After the final bleed from two different rabbits (#93 and #94) was received, they were tested on total cell lysates and mitochondrial lysates at a dilution 1:1000 (Figure 7.3A) prior to affinity purification. Both antisera gave similar results, with the only clear band being at approximately the right size of ~17kDa appearing in total cell lysates of HEK293T overexpressing C12orf65-FLAG (lanes 1 and 6,

band indicated by an arrow in Figure 7.3A). There is also a weak band at the approximately the same size present in total cell lysate of HEK293T (lanes 3 and 4). Due to the same intensity of the band recognized at around expected size, the antisera from both rabbits were used for affinity purification.

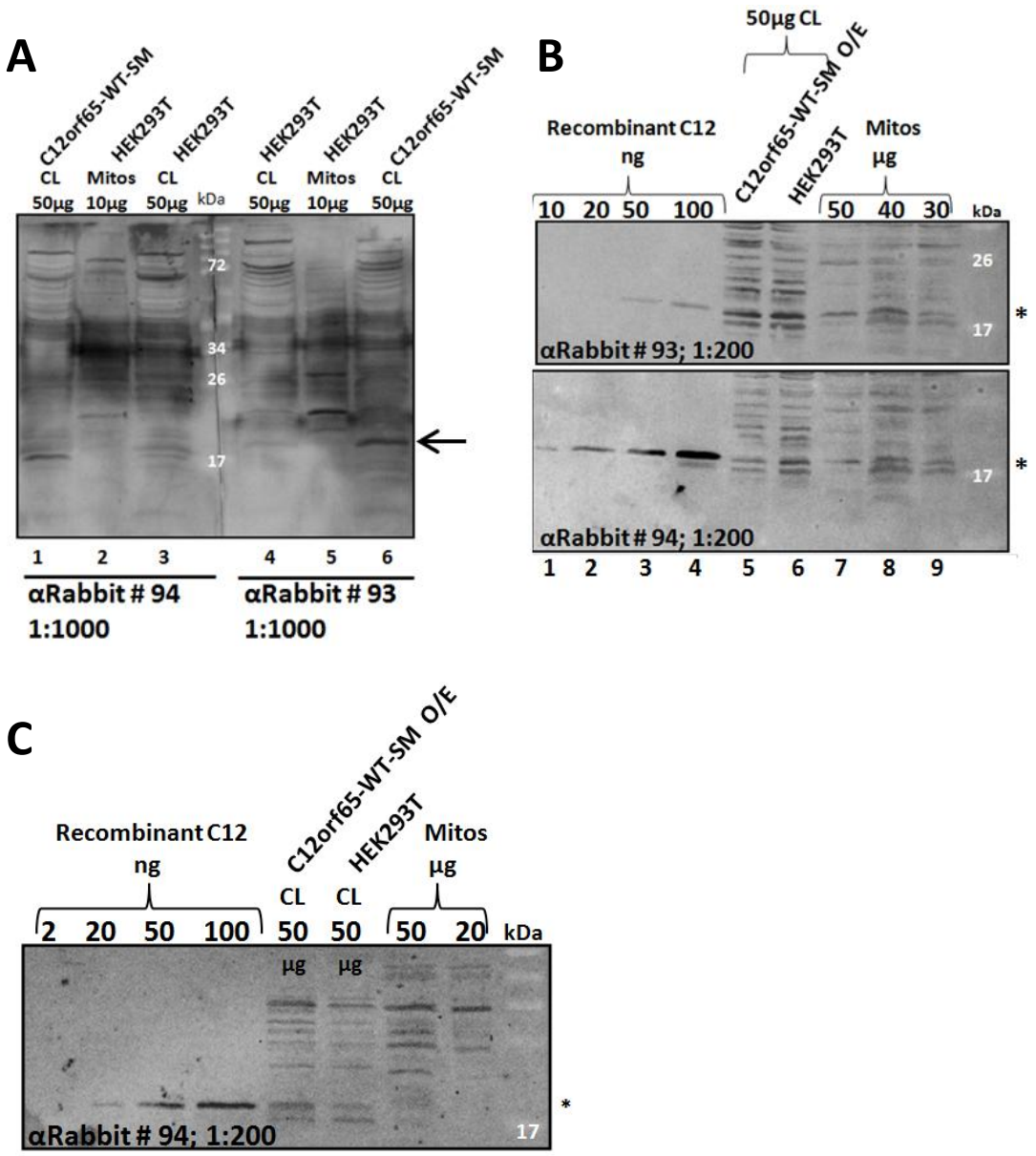

Figure 7. 3. Characterisation of rabbit anti human C12orf65 polyclonal antibodies - the initial affinity purifications.

(A) Western analysis of 50µg lysate of HEK293T cells (lanes 1, 3, 4 and 6) and 10µg of isolated mitochondria (lanes 2 and 5) probed with non purified final bleed serum from two different rabbits (#93 and #94), diluted 1:1000. An arrow indicates the expected size of C12orf65. **(B)** Western analysis of the first affinity purification of both antisera (top panel #93, bottom panel #94). A serial dilution of C12orf65 GST-purified recombinant protein (lanes 1-4), 50µg lysate of wild type (lane 6) or C12orf65-FLAG expressing (lane 5) HEK293T and different amounts of isolated mitochondria from HEK293T (lanes 7-9) were decorated with affinity purified C12orf65 antibodies from both rabbits (dilution 1:200).* indicates expected position of signal for C12orf65. **(C)** Second affinity purification of antiserum #94, dilution 1:200, where double the volume (14 ml) of antiserum was presented to the NHS-activated beads.

The antiserum of each rabbit was applied onto a previously prepared column with recombinant C12orf65 protein covalently bound onto NHS-activated Sepharose 4 Fast Flow beads. In order to analyse the efficiency of binding the flowthrough (Figure 7.2, FT, lane 6), after the protein was loaded onto the column, was separated on polyacrylamide gel and Coomassie stained. There is no band detected in lane 6 of Figure 7.2 indicating that all applied recombinant protein bound to the beads. Further antibody purification continued according to the common protocol used in the lab and described in section 2.6.9 of methods (chapter 2). The resulting affinity purified antibodies from both rabbits were tested (Figure 7.3B) at a dilution of 1:200 on serial dilution of 10-100ng of recombinant C12orf65 (lanes 1-4), total cell lysates with (lane 5) or without overexpression of C12orf65-FLAG tagged protein (lane 6) and different amounts of mitochondrial lysates (50, 40 and 30µg, lanes 7- 9 of Figure 7.3B). The first purification of antibodies from both antisera showed a proportion of unspecific bands of all sizes in total cell lysates and in mitochondrial lysates. Amongst the unspecific signals there was a distinctive band detected in all samples that was level with the size of recombinant C12orf65, especially the signal picked up in 50µg of mitochondrial lysate (Figure 7.3B, lane 7), which could potentially indicate the specific signal of C12orf65. However, this could not be conclusive at this stage because the band of the correct size did not seem to get any stronger where C12orf65 was overexpressed (Figure 7.3B, lane 5) compared with the signal of the same size in the total cell lysate from HEK239Tcells (Figure 7.3B, lane 6). Therefore, in order to make sure the amount of the purified antibodies was not limiting a second attempt was undertaken. As seen in Figure 7.3B lower panel, antibodies from rabbit #94 showed stronger affinity towards the recombinant protein and recognized 10ng of this protein (lane 1), therefore this antiserum was used for purification, but the volume of antisera initially added to the NHS-activated beads was doubled. Obtained antibodies were again tested on serial dilution of recombinant C12orf65 (2-100ng), HEK293T cell lysates with or without overexpression of C12orf65-FLAG tagged protein and on mitochondrial lysates (50 and 20µg). The lowest amount of recombinant protein detected this time was ~20ng and the band corresponding with the correct size appear stronger in sample where C12orf65 was overexpressed, but unfortunately cannot be recognized in the mitochondrial lysates at all. In additional to the increased amount of antisera

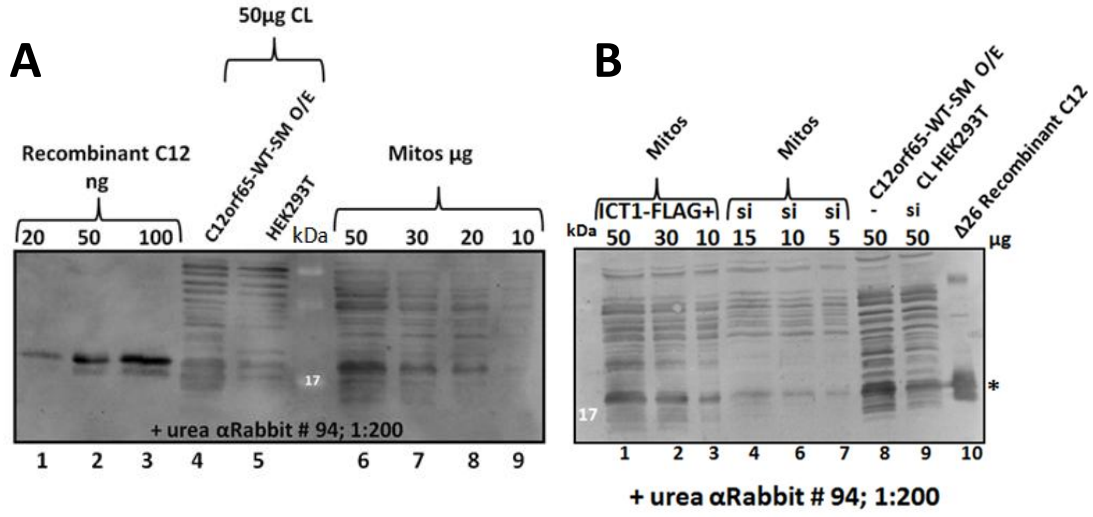

Figure 7. 4. Further characterisation of rabbit anti human C12orf65 polyclonal antibody.

(A) Third affinity purification of antiserum # 94, dilution 1:200: before double amount (14ml) of serum was added, NHS-activated beads with covalently bound C12orf65 were treated with 8M urea for 3h, then washed with PBS. **(B)** Western blot of isolated mitochondria from HEK293T cells either expressing ICT1-FLAG tagged proteins (lanes, 1-3) or depleted of C12orf65 for 3 days (lanes 4-7) and cell lysates of HEK293T either expressing C12orf65-FLAG tagged protein (lane 8) or depleted of endogenous C12orf65 protein for 3 days (lane 9).

added to the beads, the recombinant C12orf65 covalently bound with the beads was denatured to ensure that the epitope was exposed to antibodies on the column during the purification procedure. The resultant affinity purified antibodies (Figure 7.4A) recognized 20ng of recombinant C12orf65 (lane 1), potential endogenous form of the expected size in HEK293T cell lysates, where the signal is enriched indicating overexpression (lane 4) and most importantly the band of an expected size can be detected in 10µg of mitochondrial lysate (lane 9), which all together made it a promising result that the purified antibodies were specific. Therefore further analysis involved depleting the endogenous form of C12orf65 with siRNA, to test whether this loss of protein was reflected on the western blot using antibodies purified in this way. Tested on a similar set of samples, which include 5-15µg of mitochondrial lysates after 3 days of siRNA treatment, Figure 7.4B shows a clear band of the expected size in all samples, including 10ng of mitochondrial lysate (lane 3) and total cell lysates from HEK293T (lane 8). The siRNA treatment did not result in absolute disappearance of the candidate signal and the signal could still be detected in total cell lysate of HEK293T cells (lane 9). The sets of samples of mitochondrial lysates in the same panel shows similar results, where the siRNA treatment

resulted in decreased signal of interest between lysates without and with depletion (compare lane 3 and lane 6 of Figure 7.4B). Unfortunately, this promising result could not be repeated and the affinity purified antibodies seem to be very unstable after any time of storage in either -20°C or 4°C (data not shown). At this stage it is difficult to conclude whether the antibodies purified in for this investigation recognize a specific antigen. The mitochondrial lysates come from two different preparations and samples in lanes 1-3 have ICT1 overexpressed, which potentially could have an effect on levels of C12orf65. Thus, the fact that the result could not be repeated and that I would have liked to include more extensive controls on the western blot (Figure 7.4B) and also due to the time constraints, the use of these antibodies was not possible in this project and requires further optimisation.

7.3. Consequences of the depletion of C12orf65 in human cells

As a first part of investigation into C12orf65 function in mitochondrial gene expression it was necessary to answer whether C12orf65 is essential in cultured cells, such as HEK293T and HeLa. In order to do so, transient gene silencing by siRNA was performed using 3 different synthesised siRNA duplexes of which (# 2) was chosen for further studies. This selection was based on initial experiments by Dr Paul Smith, where siRNA # 2 had the most profound effect on mitochondrial protein synthesis at a concentration of 0.33μM. A known number of HEK293T cells and HeLa cells were treated with siRNA against C12orf65 (si-C12) then, in order to force respiration, grown in the presence of galactose, rather than glucose. Cells were maintained in this medium and examined after 3 days. The levels of protein depletion could not be analysed at this stage, due to the difficulties with the antibodies described above but transcript levels could be tested. This was done by semi-quantitative PCR amplification of reverse transcribed RNA isolated from cells after 3 and 6 days of siRNA treatment and reflected the levels of mRNA of interest present in tested cells. As seen in Figure 7.5B, the level of C12orf65 transcripts clearly decreased after 3 days and this effect was even more pronounced after 6 days of treatment compared to NT (not targeted) samples; 18S was used as an endogenous control. The number of the cells decreased dramatically as a consequence of C12orf65 depletion. After 3 days of treating HeLa cells, there

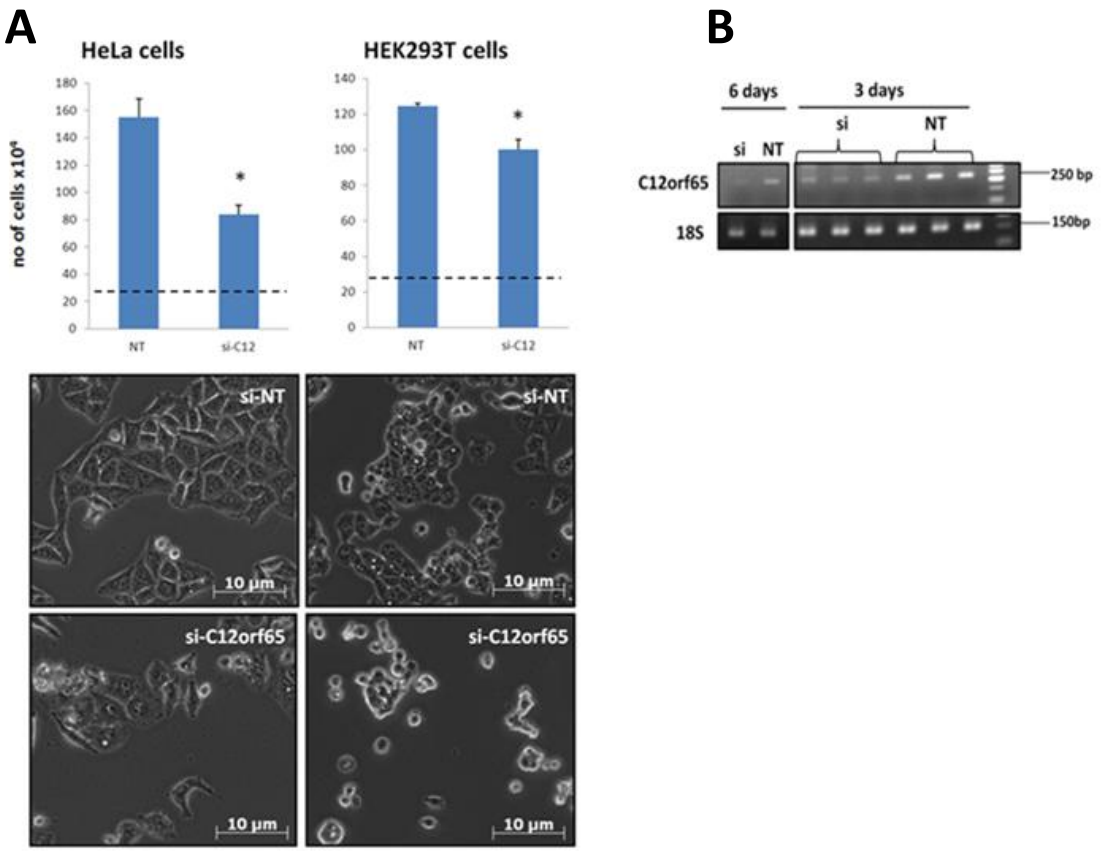

Figure 7. 5. Phenotypic characterisation of C12orf65 depletion in HEK293T and HeLa cells.

(A) Growth of HEK293T cells and HeLa cells, in galactose media in the presence of siRNA against either C12orf65 (lanes siC12) or a non-targetting control (NT), was monitored over 3 days. Cell number seeded at day 0 is indicated by the dotted line. Cells were counted and presented as a mean with standard deviation representing three independent experiments (HeLa p=0.0327*; HEK293T p=0.0125*)(top panel). Lower panels show morphology changes of cells after 3 days of depletion, HEK293T right and HeLa left panel compared to controls (si-NT). **(B)** At the time no antibody was available so the effect of C12orf65-targetted siRNA in HEK293T cells was monitored by PCR. Total RNA was extracted from cells treated with either non-targeting siRNA (NT) or targeted at endogenous C12orf65 and 1µg used in RT-PCR reaction as a template (random hexamers were used), then second step standard PCR amplified the *c12orf65* gene (product of ~250 bp). Products were separated on 2% agarose gel and stained with ethidium bromide. Nuclear encoded 18S-rRNA was used as endogenous control.

were twice as many control si-NT cells as si-C12 cells (Figure 7.5, left panels) indicating reduced growth rate.

A similar, but less profound effect was observed. in the experiment with HEK293T cells, where the number of cells also decreased significantly compared with control after 3 days right panels). Even though the effect of C12orf65 depletion on cell growth of HEK293T cells is not as striking as on HeLa cells, the treatment has equally dramatic effect on cell morphology and phenotype in both cases. The C12orf65 depleted HeLa cells (Figure 7.5A, left

lower panel) are shrunken, they have lost their characteristic 'star' long shape and do not make clear contact with other growing cells, as contrasted by cells treated with not targeting siRNA (NT)(left upper panel). Similar effect can be seen after 3 days of HEK293T treatment with the same siRNA. Those cells show even more rounded shape Figure 7.5 A right lower panel), which makes it difficult to recognize the type of cells. The cells seem to be very weakly attached to the surface of a culture flask. These data together suggest that C12orf65 is crucial and an essential protein for viability of cultured cells, which corresponds with the earlier report (Antonicka *et al*., 2010).

7.4. Effect C12orf65 depletion on cell growth and morphology

In order to assess any changes that might occur in mitochondrial organisation following C12orf65 depletion after either 3 or 6 days siRNA treatment of HEK293 and HeLa cells, two different fluorescent dyes were used. TMRM, which will enter mitochondria in a membrane potential dependent manner and Pico Green, which will fluoresce upon binding to dsDNA. Combined staining allows visualization of the mitochondrial network as well as the nucleus and mt-nucleoids.

Following the profound decrease in cell growth rate and the overall change in phenotype upon C12orf65 depletion seen in previous section, mitochondrial network morphology also changed. After 3 and 6 days C12orf65 siRNA treatment (Figure 7.6 B and C) HEK293T cell mitochondria appear more compact, almost enlarged granules being placed on top of each other more in the centre of the cells surrounding nucleus compared with mitochondria of HEK293T transfected with NT siRNA (Figure 7.6 A), where the network seems to be more spread through the cell body. This difference can be noticed even though HEK293T cells tend to be more loosely attached to the flask surface when in culture and their shape is more round making it generally more difficult to focus on one plane. HeLa cells are generally more flat in culture and easier to discern morphological changes. Mitochondria of HeLa cells treated with NT siRNA represent a characteristic reticular mitochondrial network evenly distributed within normal healthy cells (Figure 7.6 D). This network becomes clumped together into one large patch seen after 3 days of C12orf65 depletion. After 6 days, these patches of mitochondria seem to be more spread but also

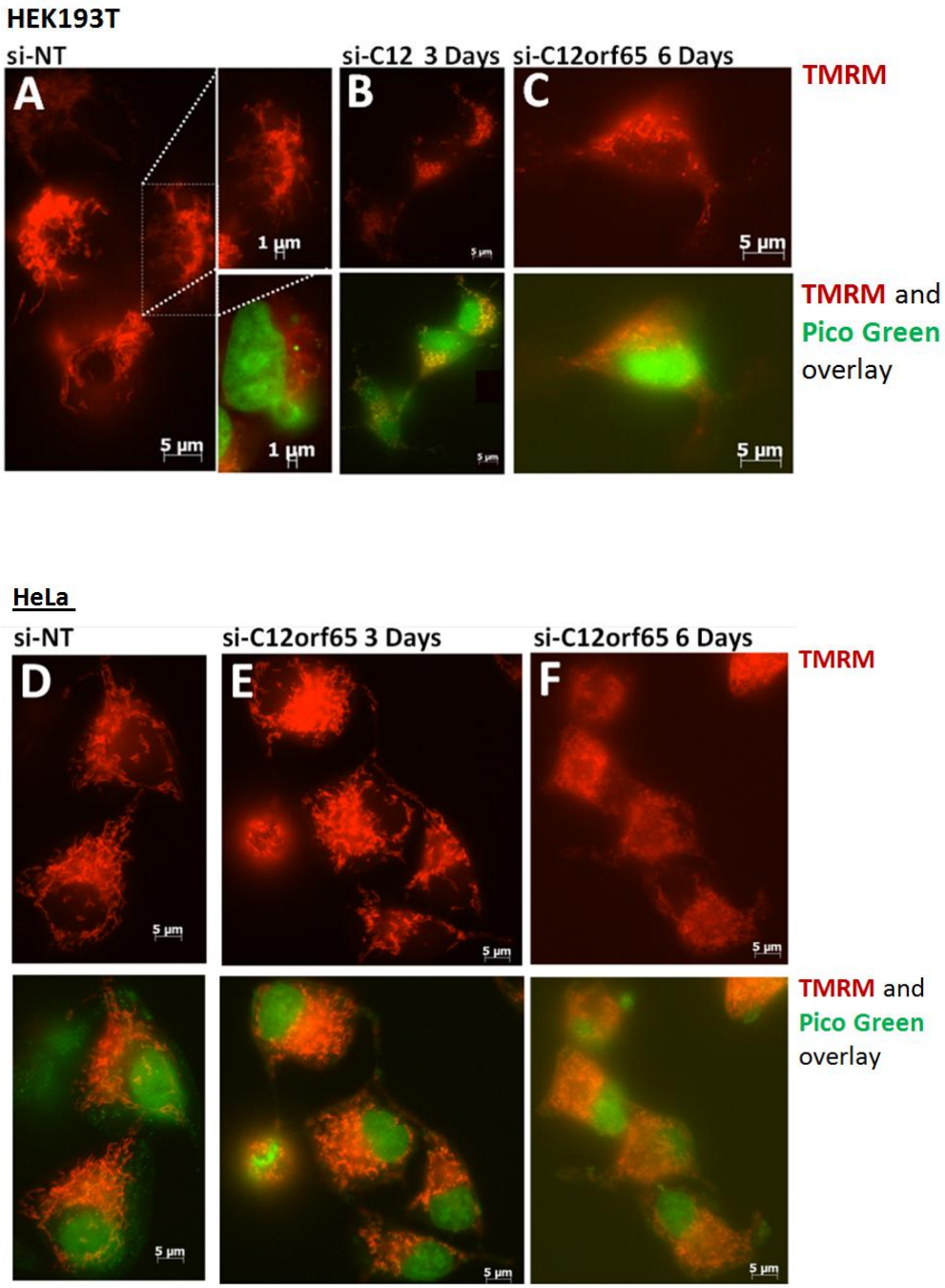

Figure 7. 6. Changes to mitochondrial morphology upon depletion of C12orf65

Representative fluorescent images of HEK293T (A to C) and HeLa cells (D to F) after 3 and 6 days of C12orf65 depletion with siRNA. Mitochondria were loaded with TMRM (red) and *mitochondrial DNA* was visualised with PicoGreen, which stains both mitochondrial nucleoids and nuclear DNA green. siRNA targeted to mtRF1 led to visible deformation in mitochondrial network morphology in both cell lines after 3 and 6 days based on TMRM.

more punctuate, however due to the shrunken morphology of treated cells it was difficult to clearly describe resulting changes.

The experiment was performed in non quench mode, where lower dye concentrations were used in order to avoid dye aggregation or quenching in

mitochondria. The prediction would be that the lower fluorescence reflects depolarized mitochondria, which seem to be the case with C12orf65 depletion in HeLa cells after 6 days of treatment. However, the directional changes in mitochondrial fluorescence seen here can be only provisionally interpreted as no agent that would affect the membrane potential and confirm dye behaviour was used. Thus this data can only be used as an estimate of changes confirming what has been presented in chapter above.

7.5. Effect of C12orf65 depletion on steady state levels of mitochondrial proteins

To further investigate the consequences of C12orf65 depletion on human cultured cells, its effect on steady state levels of protein was tested. For this HEK293T cells were treated with either siRNA- C12orf65 or siRNA-NT for 3 and 6 days and 50µg of total cell lysates were separated by SDS-PAGE, followed by transfer and immunodetection of the proteins of interest. As presented by Figure 7.7 A there were not any significant changes. The histograms, panel B, were generated from the densitometric measurements of the westerns in panel A and confirm the visual inspection. They indicate no significant difference in nuclear encoded, important mitochondrial proteins including the RNA polymerase (POLRMT) and a member of complex I (NDUFB8) after either 3 or 6 days of treatment. In the absence of antibodies to all the mt-encoded proteins, NDUFB8 is used as a highly sensitive marker of complex I assembly that is generally absent in the absence of mt-encoded ND polypeptides. This is in contradiction with the data presented by Antonicka *et al*., (2010), where ND polypeptides levels were affected and so was the assembly of complex I in the patients' fibroblasts. The stable level of NDUFB8 shown here could simply imply that the 6 day depletion was not enough to affect the assembly of stable respiratory complexes, and it cannot be excluded that a difference would be detected upon longer depletion. There was also no defect in mitochondrial encoded protein (COX II) in comparison with the control and, similarly to the earlier findings the components of the mitoribosome such as MRPL3, DAP3, MRPS18B and MRPL12 remain stable (lower band from the doublet), confirming that the growth rate defect in HEK293T is not due to the depletion of mitoribosomal proteins.

Since the number of cells after 3 days of HeLa treatment with C12orf65 siRNA was more dramatically decreased one would predict this defect could be significantly more detectable than in HEK293T cells. Therefore, again after 6

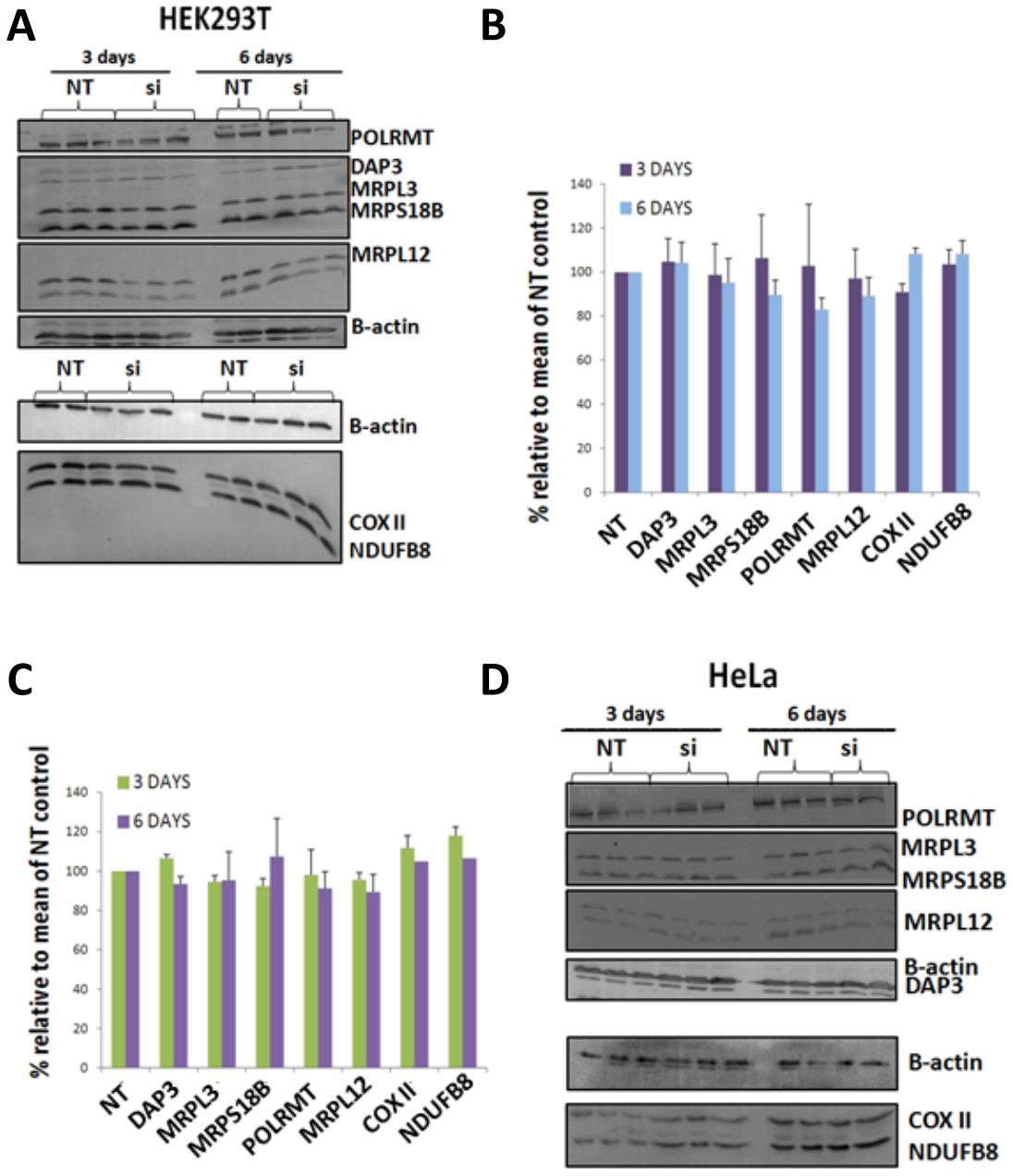

Figure 7. 7. Steady state levels of mitochondrial proteins after C12orf65 depletion.

Western blot analysis of HEK293T **(A)** and HeLa **(D)** cell lysates (50µg) after 3 and 6 days of treatment of siRNA against C12orf65 or non-targeting (si or NT, respectively). Levels of proteins sensitive to inhibition of mitochondrial translation (complex I subunit NDUFB8 and COX II), mitochondrial ribosome proteins (DAP3, MRPS18B, MRPL3 and MRPL12) and POLRMT were analysed. Nuclear-encoded β-actin was used as a loading control. Signals were quantified with ImageQuant software and the graphs represent three repeat experiments of HEK293T **(B)** and HeLa cells **(C).** None of the changes observed were statistically significant.

days of siRNA treatment of HeLa cells, whole cell lysates were separated by SDS-PAGE. However, similarly to HEK293T cells, the levels of mitochondrial encoded COX II seem unchanged, with mitoribosomal proteins also being stable (MRPL3, MRPS18B and DAP3). Since western blots are only semi-quantitative, the signal densities were measured and histograms plotted only in order to confirm the visual inspection that indicated no significant differences between signals.

7.6. Depletion of C12orf65 up-regulates mt-mRNA levels.

With the assumption that C12orf65 plays a part in mRNA decay or rescuing stalled ribosomes a further search for the evidence involved investigation of the steady state levels of mitochondrial transcripts. The steady state levels of mitochondrial RNAs were analysed by Northern blot after 3 and 6 days C12orf65 depletion in both HEK293T cells and HeLa cells. In general, the 3 days depletion of C12orf65 in both cell lines resulted in an increase of most of the tested transcripts in both tested cell lines. With the exception of rRNA, which appears more stable, in HeLa cells 6 day C12orf65 depletion resulted in a significant increase of *MT-RNA14* (probed with a fragment to *ATP6*), *MTND1, MTCOI, MT-RNA15* (Figure 7.8 A, top left panel).

The signals were measured with ImageQuant software, then calculated relative to the controls and resultant histograms although not fully quantitative, clearly reflect the tendency to increased transcript levels after C12orf65 depletion (Figure 7.8 B, left panel). After 6 days of depletion in HEK293T cells the effect is even more evident. The level of all mRNA and rRNA tested are significantly elevated (Figure 7.8 A and B, right panels). This data strongly implies that the accumulation of the transcripts relates to decreased C12orf65 and may contribute to the defective growth rate observed in previous section.

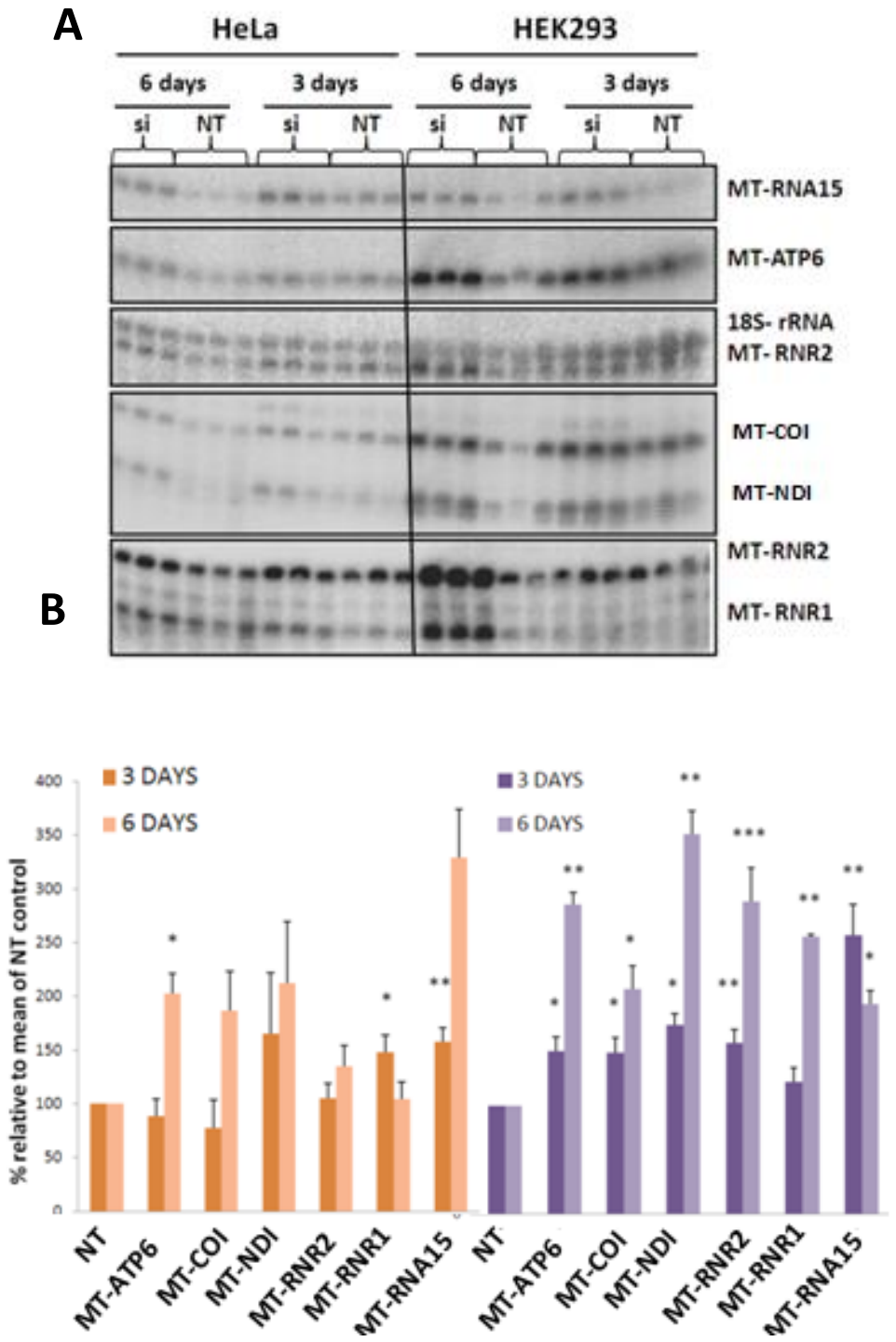

Figure 7. 8. Steady state levels of mitochondrial RNA after depletion of C12orf65.

(A) Northern blot of total RNA extracted from HEK293T (4µg, right panel) and HeLa cells (1µg left panel) treated with non-targeting (NT) or targeting endogenous C12orf65 (si) siRNA. The blots were hybridised with probes to mitochondrial mRNAs (*RNA14*, *MTCO1* and *MTND1*), mt-rRNAs 16S (*MT-RNR2*) and 12S (*MT-RNR1*) in addition to human 18S rRNA for quality and loading control. **(B)** The signals were quantified and the graph presents mean and standard deviation of three independent experiment repeats in HEK293T (right) and HeLa cells (left), which are relative to the mean of non-targeting control , NT (*p <0.05, **p<0.01,***p<0.001).

7.7. Where do the increased transcripts accumulate?

C12orf65, as a candidate protein for the quality control factor in mt-protein synthesis that may free stalled ribosomes on truncated mRNA in mitochondria, is essential to maintain healthy cells. The first characterised mutation in its gene causes Leigh syndrome, optic atrophy, and ophthalmoplegia (Antonicka et al., 2010). As demonstrated in the previous section, its depletion in cultured human cells results in a distinct increase of all tested mitochondrial transcripts. Thus, a further aim was to test whether C12orf65 knock-down causes an accumulation of the increased mRNA on individual ribosomal subunits or the fully assembled monosomes, and also whether the increased rRNA assembles into monosomes or remains free. Sucrose gradient analysis allows investigation of the RNA distribution, which, if affected, could reflect the stalled mitoribosome status and identify the distribution of mRNA. This was analysed by preparing a lysate from HEK293T cells that had been subjected to siRNA treatment for 6 days. The lysate was separated though an isokinetic sucrose density gradient followed by a northern blot analyses. In order to detect the migration of the mtSSU, mtLSU and monosome two probes were used in the northern blot, each specific to an rRNA (*MT-RNR1* and *MT-RNR2*). As seen on the gradient from HEK293T cells treated with non targeting siRNA (NT), the signal for mtSSU first appears in fraction 4 and distributes evenly down to the bottom of the gradient, where fraction 11 represents the gradient pellet (Figure 7.9 A, left panel). The 16S rRNA (*MT-RNR2*) partitions to fraction 5, then distributes to the bottom of the gradient. The signals in earlier fractions (4-6) represent the free uncomplexed state of each individual subunit, whereas signals in fractions from 8 onwards represent the presence of monosomes. This pattern of monosome is also seen by the distribution of mRNA, signals of which become more intense again, where trapped by the monosome (fractions 8). The histogram plotted based on detected NT control signal on northern blot reflects this distribution of both rRNA and mRNA across many fractions (NT in Figure 7.9A, left panel and black line in histograms). In contrast to the control, the 6 days C12orf65 depletion resulted in all mRNA tested being shifted towards the top of the gradient and accumulated mostly in fraction 5. The exception was *MT-RNR1*, distribution of which resembled that of the control, being localised mostly to fraction 5 and tailing down to the bottom of the gradient. This similarity is reflected in the histogram plotted from the detected signals (Figure 7.9 B pink squares). The increased

MT-RNR2 accumulate mostly in fractions 5 and 6 and the tail toward the bottom of the gradient is much weaker compared with the control, which is also reflected on the histogram (Figure 7.9 A right panel, and B). Therefore, based

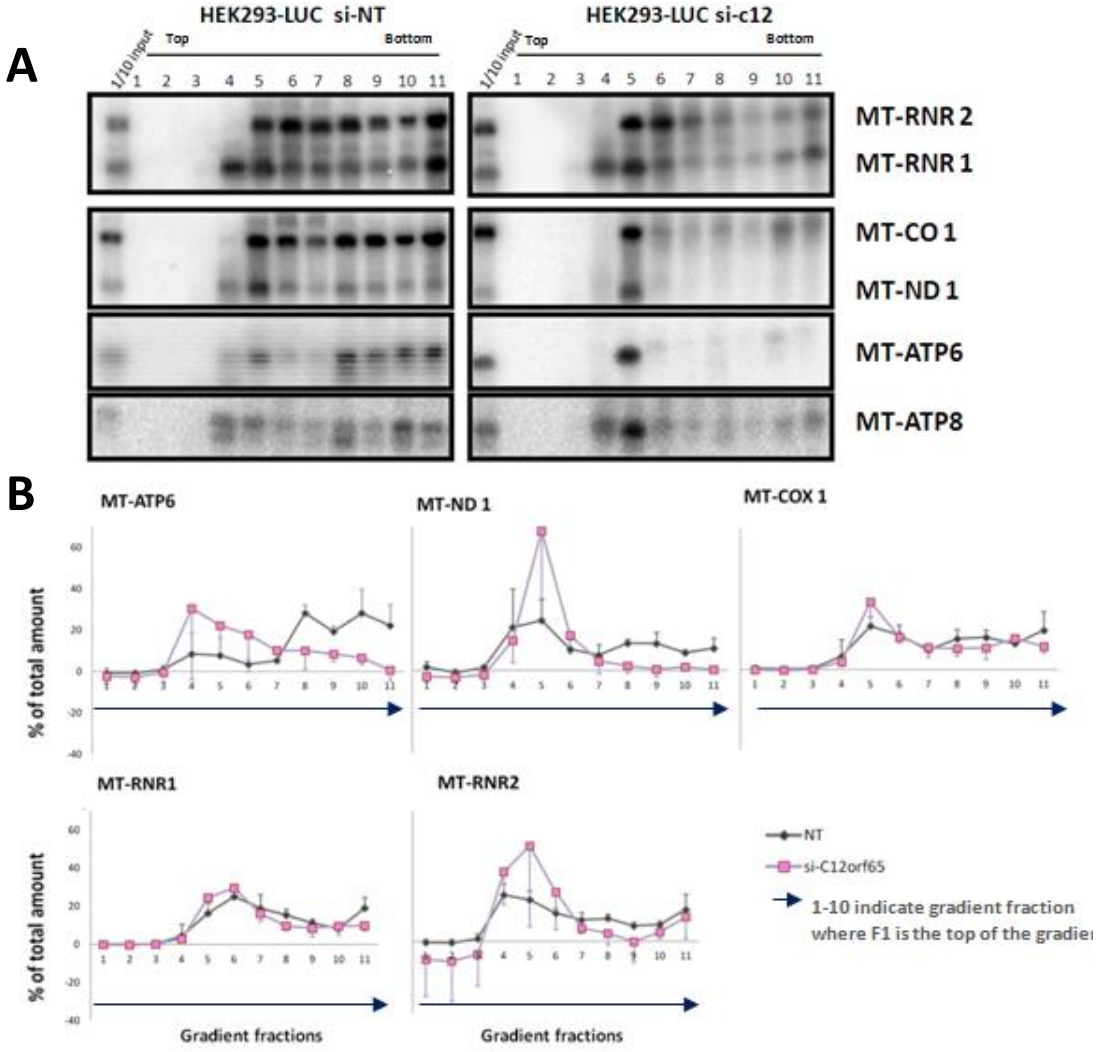

Figure 7. 9. Northern blot analysis of mitochondrial RNA on sucrose gradient after depletion of C12orf65.

(A) HEK293T cells were treated with C12orf65 (si-c12) or non-targeted (NT) siRNA for 6 days and lysates (700µg) separated on 10-30% isokinetic sucrose gradient. RNA was extracted from each fraction (1-11 and 1/10 of input) and analysed on a northern blot using probes to mitochondrial mRNAs (ATP6 and ATP8 , COX 1 and ND 1) and 16S (MT-RNR2), 12S (MT-RNR1) mt-rRNAs. **(B)** The signals were quantified and presented as the graph of mean and standard deviation from three independent experiment repeats (**p* <0.05, ***p*<0.01, ****p*<0.001).

on this piece of data 6 days of C12orf65 depletion does not appear to cause the accumulation of the increased transcripts on monosomes. In fact these data suggest that the composition of the monosomes is also affected, since there is hardly any strong signal in fraction 7-8 where the monosome is expected as seen in control. In neither case was there strong evidence that mitochondrial

transcripts accumulate on monosomes following C12orf65 depletion with these conditions, it rather suggests it associated with either free ribosomal subunit or with other, large complexes or an equal density.

7.8. Is the composition of 55S affected by the C12orf65 knock-down?

In light of the observation that depletion of C12orf65 causes striking increase of mt-mRNAs and a change in position on gradients, now mostly co-localised with free ribosomal subunits, it seems possible that the MRPs may have all clustered at the top of the gradient as well.

To assess whether this was indeed the case, HEK293T cells treated with C12orf65 or NT siRNA for 6 days were lysed and separated on 10-30% isokinetic sucrose density gradient. Separated proteins of interest were visualised by western blot with antibodies against polypeptides in the small (MRPS18B) and large (MRPL3 and MRPL12) mitochondrial ribosomal subunits. As seen in Figure 7.10 A the depletion resulted in a similar pattern of

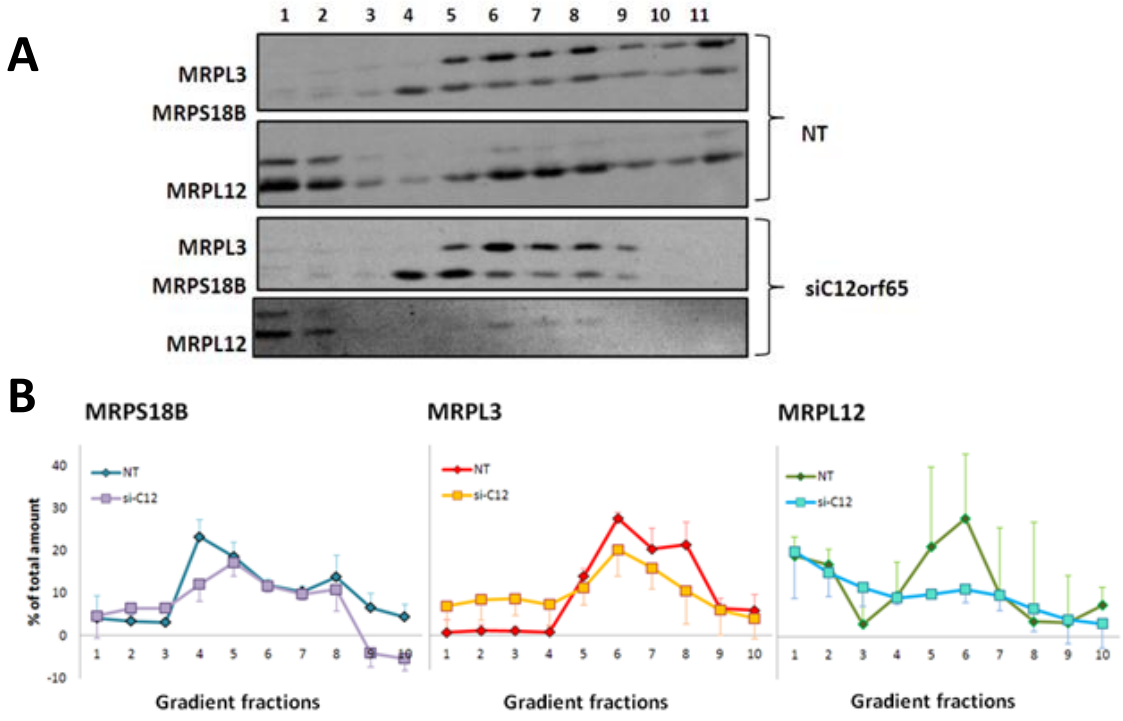

Figure 7. 10. Depletion of C12orf65 does not appear to affect mitoribosome composition.

(A) HEK293T cells were treated with C12orf65 (si-C12) or non-targeted (NT) siRNA for 6 days and lysates (700µg) separated on 10-30% isokinetic sucrose gradient followed by analysis of fractions by western blots using antibodies against MRPS18B, MRPL3 and MRPL12. **(B)** Western blot signals presented in panel B were quantified via ImageQuant software and presented in graphs below showing mean with standard deviation from three independent experiment repeats of gradients after depleting C12orf65.

distribution of MRPL3 and MRPS18B in both experimental (Figure 7.10 A, si-c12 bottom panel) and control gradients (NT, upper panel), after 6 days of siRNA treatment. In both cases the SSU, detected by anti-MRPS18B, migrated to and accumulated mostly in fractions 4 and 5, while a member of LSU, MRPL3, migrated from fraction 5 to F8/9, where signal indicates monosome. Although similar the distribution is slightly different for these 2 polypeptides as with C12orf65 depletion neither protein appeared to migrate significantly beyond F9. Therefore, based on this data C12orf65 depletion did not contribute to detectable accumulation of free ribosomal subunits at the top of the gradient as seen in mRNA profiles in the previous section. Interestingly, the distribution of MRPL12 changed. This was the same MRP that was sensitive to levels of mtRF1, such that depletion of mtRF1 was accompanied by a decrease in MRPL12. This was seen in fibroblasts, HEK293 and HeLa cells. The free form of MRPL12 as seen in fractions 1 and 2 in the siRNA-NT (Figure 7.10 A, top panel) is still present but at lower level after 6 days of C12orf65 depletion (lower panel). The form that is associated with the mitoribosome, however, migrates in fractions 6-8 in the NT control, whilst in the treated sample the level of this form is almost undetectable. This shows that the overall distribution of mtSSU and mtLSU is not affected by the C12orf65 depletion and that the general MRP distribution does not reflect that of the mt-RNAs after C12-siRNA treatment. However, even though the steady state level of MRPL12 appears stable (Figure 7.7), when tested in section 7.5, the depletion of C12orf65 caused the levels of MRPL12-ribosome associated form to decrease (Figure 7.10, lowest panel), suggesting it affected the correct assembly of MRPL12 into the LSU and probably monosomes.

7.9. Can C12orf65-GGQ-SM-FLAG associate with mitoribosomes?

It has been demonstrated in previous sections that C12orf65 depletion causes increased accumulation of mRNA on ribosomal subunits but a decrease of ribosome associated MRPL12. As a putative member of the mitochondrial release factor family C12orf65 remains a protein of unknown function, and so it was necessary to determine whether C12orf65 directly interacts with the ribosome.

To test this inducibly expressing C12orf65-FLAG HEK293T cells were used. The expression was induced for 3 days, then the cells were used for immunoprecipitation with the FLAG tag according to the protocol described in methods section (2.6.10) As can be clearly seen on Figure 7.11 A in the IP eluate (E) C12orf65-FLAG was succesfully immunoprecipitated and it is indicated by a white asterisk. The other bands that can be detected by silver staining in the same fraction of C12orf65 eluate (E) indicate that there are partners that C12orf65 interacts with. The controls for FLAG IPs have been

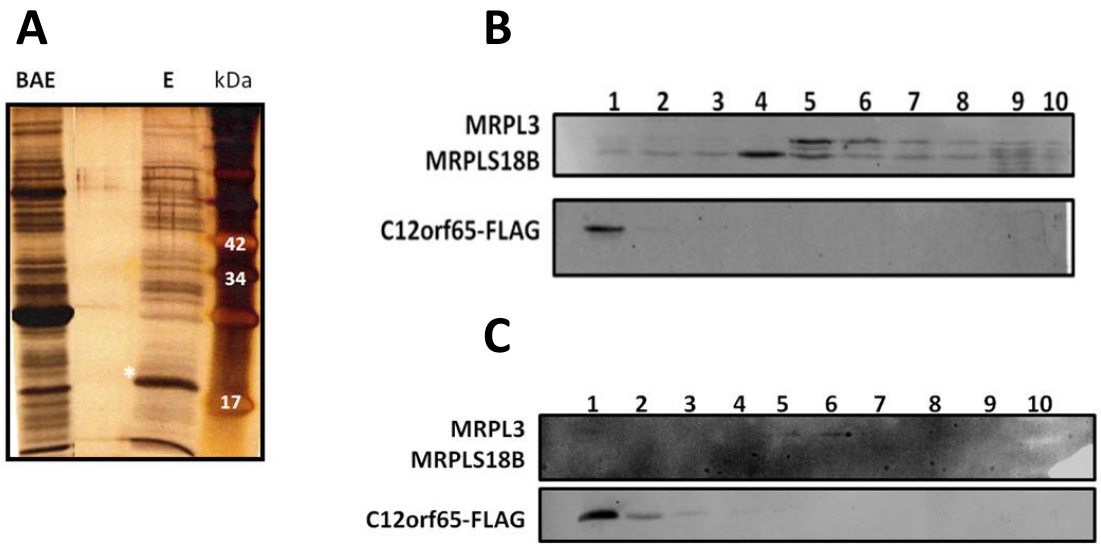

Figure 7. 11. Analysis of interactions between C12orf65 and other components of mitochondria.

(A) Co-immunoprecipitation of C12orf65-FLAG. HEK293T cells were induced with 1µg/ml tetracycline to express C12orf65-FLAG. Cells were harvested after 3 days and mitochondrial lysates (2mg) were used in anti-FLAG immunoprecipitations. Components of the IP (10% of elution fraction, E) and 5% of beads after elution (BAE) and examined by silver stain following separation on 14% SDS-PAGE. C12orf65-FLAG is indicated (*) and molecular weight marker sizes designated. **(B)** Western blot analysis was performed on the elution fraction following its separation by 10%-30% isokinetic sucrose gradient. Gradient fractions 1-10 were interrogated with antibodies to polypeptides of the 28S mt-SSU (MRPS18B) and the 39S mt-LSU (MRPL3). C12orf65-FLAG was detected with antibodies against the FLAG epitope. **(C)** In order to analyse the effect of C12orf65 overexpression on ribosome composition HEK293T cells were induced for 3 days with 1µg/ml tetracycline express C12orf65-FLAG. To determine if overexpression caused a change in MRP distribution lysates (700µg) were loaded on 10-30% isokinetic sucrose gradient and fractions analysed by western blot. Antibodies against the small (MRPS18B) with large mitochondrial subunits (MRPL3) were used in addition to anti-FLAG that revealed distribution and association of the over-expressed protein

done many times in the host lab with mitochondrially targeted luciferase and other proteins to show that neither the FLAG moiety nor high expression of proteins gives significant binding to anti-FLAG beads. Further, in order to identify C12orf65 binding partners, the content of the IP elution was loaded onto 10-30% density sucrose gradient and following the centrifugation, collected

fractions were subjected to western blot analysis. The resulting western blot was probed with FLAG antibodies to detect the position of C12orf65. As shown in Figure 7.11 B, its signal mostly locates to the top of the gradient (fractions 1-3). The same result was obtained from the sucrose gradient analysis of the total HEK293T cell lysate with the FLAG tagged version of protein overexpressed (Figure 7.11 C). These together imply if there is an interaction with mitoribosomes C12orf65 rather weakly associates with these binding partners. Blotting the western with antibodies against mitoribosomal subunits proteins, MRPL3 (mtLSU) and MRPS18B (mtSSU) gave only weak indication that C12orf65 may potentially interact with mtLSU or some of its component proteins. To further characterise all partners that interact with C12orf65 with the whole IP elution fraction was separated by SDS-PAGE, stained with SimplyBlueTM SafeStain (Invitrogen) and the gel lane was cut out. Together with a negative control, elution samples (IP of mtLuciferase-FLAG) were sent for LC MS/MS (Liquid chromatography - tandem mass spectrometry) analysis. In order to avoid unspecific binding and cytosolic contamination, mitochondria were rigorously purified prior to lysis and IP procedure. The results were compared with those of mtLUC negative control and any possible contaminants excluded. Amongst all the protein obtained of LC MS/MS there were 14 of 39S LSU proteins and 3 of 28S SSU protein detected (see Appendix 1.2). However emPAI value for all these detected proteins was very low. The earlier immunoprecipitation studies from other group members did not identify C12orf65 as being part of or intimately associated with the mitoribosome, suggesting C12orf65 to be a soluble matrix protein. The LC-MSMS data presented here confirms this, but may suggest that it has a transient association with some mitoribosomal proteins.

7.10. Can overexpression of ICT1-FLAG as a member of the mitochondrial RF family rescue the growth phenotype observed on C12orf65 depletion?

Thus far the loss of C12orf65 has been shown to cause a growth defect in both of the tested cell lines, increased levels of mt-mRNA and incomplete monosomes that potentially lack a full complement of MRPL12. It has been demonstrated that C12orf65 can pull down several ribosomal proteins confirming involvement in a protein synthesis mechanism. If C12orf65 really

functions on mitoribosomes during translation what is its exact mechanism of action?

There are some structural similarities between ICT1 and C12orf65, such as conserved GGQ motif, lack of codon recognition domains and their small size. ICT1 as a small protein when not associated with ribosome can easily enter the A-site of the ribosome and reach the PTC to hydrolyze any incomplete elongating polypeptide chain. This was shown in the *in vitro* RF assays and interestingly, it was shown that when ICT1-FLAG tagged is overexpressed in HEK293T cells, apart from a proportion of it being incorporated in newly assembled mitoribosomes, there is also a fair amount of ICT1 that is free, which also marginally affects the cells growth (Richter *et al*., 2010). However, if the function of C12orf65 depends on the functional GGQ motif, the free portion of ICT1 generated during overexpression may compensate for its loss.

To test the effect of ICT1 on C12orf65 depleted cells, three sets of HEK293T cells were prepared: a set overexpressing ICT-FLAG for 4 days, a set depleting C12orf65 for 4 days and a set overexpressing ICT1 and depleting C12orf65 at the same time for 4 days. As shown in Figure 7.12, the overexpression of ICT1-FLAG only resulted in a minor drop in number of cells compared with a control (Figure 7.12, Tet + and - ; NT+ and NT-), which was consistent with previous data.

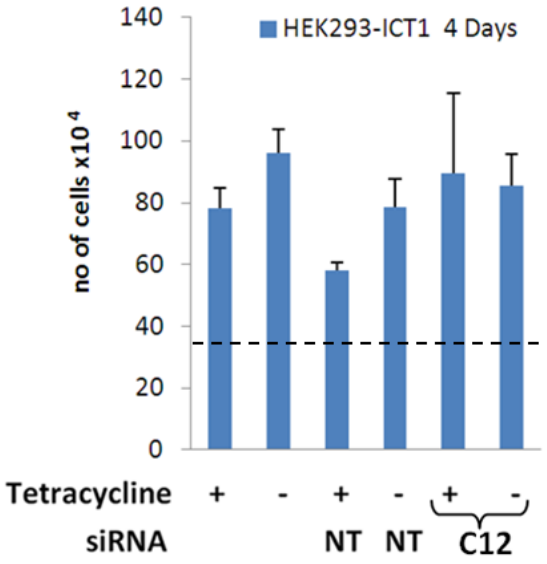

Figure 7. 12. Effect of ICT1 overexpression on cell growth upon C12orf65 depletion.

HEK293T cells were either treated with 1µg/mg tetracycline, siRNA (NT or against C12orf65) or both. After 4 days treatment cells were counted and data plotted based on the mean and standard deviation of three independent experiments. A dotted line indicates the initial number of cells seeded.

The depletion of C12orf65 did not show any growth defect relative to the uninduced ICT1 cell line (Tet -). The simultaneous overexpression of ICT1-FLAG in C12orf65 depleted cells also results in normal cell growth compared with uninduced control (Tet -). The apparently 'normal' growth of cells which were C12orf65 depleted but not induced, could be explained by, as seen before (chapter 6, Figure 6.5), leaky expression of ICT1. Thus, these data taken together may suggest that GGQ of C12orf65 may be required for its function as ICT1 could rescue the C12orf65 depletion caused grow defect.

7.11. Generation of stable inducible cell lines expressing versions of C12orf65 with wild type or mutated variants of the GGQ motif and silent mutations to render them immune to the siRNA targeting endogenous C12orf65 transcripts.

As a follow up from the experiment in the previous section in order to be unequivocally sure that the C12orf65's GGQ motif is fully functional and required for the function of the protein, it was necessary to generate cell lines that would inducibly overexpress C12orf65 with mutated versions of GGQ motif. Further aim would be to determine whether the presence of a mutated GGQ can have a dominant negative when expressed in cultured cells. It was also important to make sure that any effect was due to the mutant form of C12orf65 and not simply due to the presence of high levels of overexpressed protein, like seen in previous sections.

The presence of the evolutionarily conserved GGQ motif is a strong theoretical indicator that C12orf65 should have retained ribosome dependent PTH activity and mutations in the highly conserved GGQ motif, when present in release factor family members, result in the loss of peptidyl-tRNA hydrolysis activity (Frolova *et al.*, 1999). For this two mutations across this motif were designed, namely C12orf65-AGQ and C12orf65-GSQ and three stable cell lines (including the wild type variant, i.e C12orf65-GGQ) were generated. Moreover, these constructs were designed so that silent mutations (SM) would be incorporated in to the gene sequence to render these transcripts insensitive to the siRNA that is effective against endogenous C12orf65, which would allow depletion of the endogenous protein and expression of the mutants to the wild type levels. All the constructs have also a FLAG sequence attached to the C-terminus to allow detection on western blots.

After the Hek293-FlpIn TRex cells were transfected for a stable integration of the constructs, successful transfectants were selected over a 2 week period using Hygromycin^{B} (100ug/ml). Once a population of resistant cells was established a small culture was induced with tetracycline for 24 hours to analyse for expression. Cells were harvested, a cell lysate prepared and western blot analysis performed with anti-FLAG antibodies (Figure 7.13). Effective expression of C12orf65-WT-SM and both mutants was observed, the FLAG signal could be detected in only induced samples (Figure 7.13, lanes 2, 4, 6 and 8) and was not recognized in samples, which were not induced (lanes 1, 3, 5 and 7).

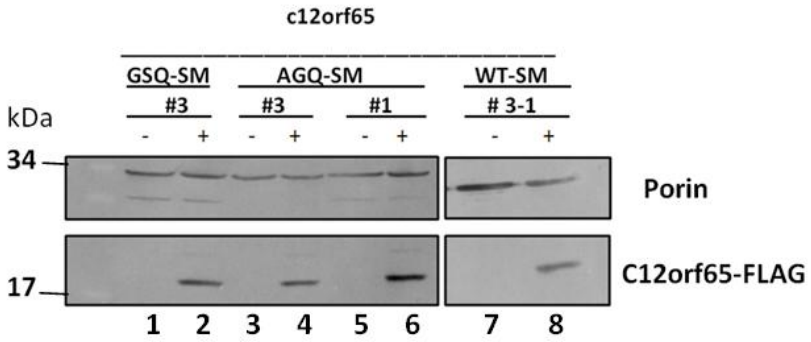

Figure 7. 13. Stable transfection of HEK293T cells with C12orf65-GGQ-SM-FLAG variants.

Clones (#) of HEK293T cells transfected with FLAG tagged variants of C12orf65 were tested, using anti-FLAG antibody, for levels of expression after 24h induction with 1µg/ml tetracycline. Wildtype GGQ (lanes 7-8), GSQ (lanes 1-2) and AGQ (lanes 3-6) variants were generated that carried FLAG tags

7.12. Import of C12orf65-GGQ-SM-FLAG mutants into mitochondria

Before the functional complementation in human cells could be carry out, it was necessary to assess whether the overexpressed FLAG tagged protein localised to the mitochondrion. Cells expressing each of the variants were treated with 1µg/ml of tetracycline for maximum induction for 3 days, then the organelles were isolated and following western blot analysis the expressed proteins could be detected via anti-FLAG antibodies. Clear expression and efficient translocation of each of the proteins to a mitochondrial compartment was shown (Figure 7.14). This was demonstrated as the FLAG-tagged proteins were protected from proteinase K treatment (1µg and 4µg; lanes 2 and 4 respectively in Figure 7.14). However, when the organelles were lysed with 1% Triton X-100

the proteins lacked protection and were efficiently digested in all cases with 4µg of proteinase K (Figure 7.14, lane 5).

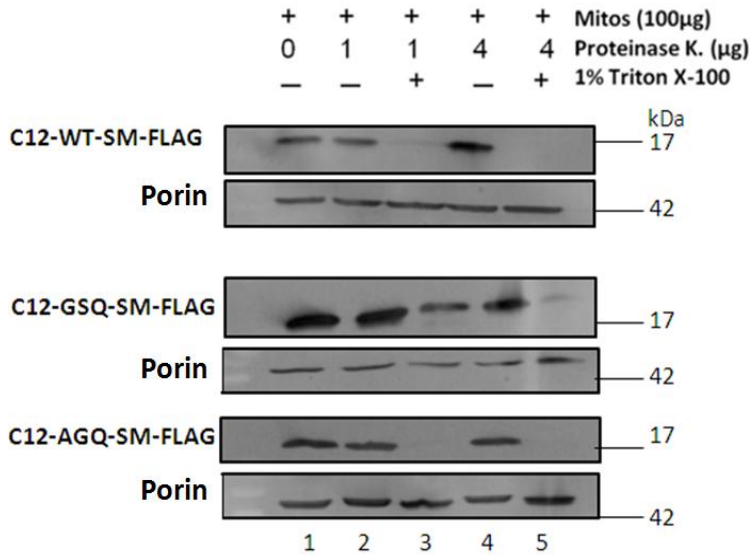

Figure 7. 14. All C12orf65-GGQ-SM-FLAG variants are successfully imported into mitochondria.

Western Blot analysis was performed on 10µg of isolated mitochondria from HEK293T cell lines expressing each of the three GGQ variants, C12orf65-wildtype-SM-FLAG, C12orf65-GSQ-SM-FLAG and C12orf65-AGQ-SM-FLAG. Isolated untreated control mitochondria are in lane 1. Similar aliquots were treated with proteinase K (1 or 4µg per 100µg mitochondria, lines 2-5) or with addition of 1% Triton X-100 (lanes 3 and 5) Anti-FLAG antibodies were used to confirm the presence of overexpressed protein

7.13. Discussion

This chapter describes the preliminary data obtained during the search for the specific function of C12orf65 and due to the time constraints, this project was taken over to be continued by another PhD student in my host lab, Maria Wesolowska. Based on the published data, C12orf65 a member of class I Release Factor family was shown to play an important role in mitochondrial protein synthesis. Previous analyses have shown that the lack of C12orf65 in HeLa cells causes ROS production, decreased membrane potential, mitochondrial mass and cytochrome *c* oxidase activity, all of which inhibits cell proliferation and leads to apoptotic cell death (Kogure *et al.,* 2012). These findings were in agreement with protein synthesis inhibition leading to decrease of OXPHOS complexes in fibroblasts from patients (Antonicka *et al*., 2010). This together with the solution structure of the GGQ- containing domain is not enough however to answer the questions about the exact function of C12orf65. Additionally, in this chapter it was confirmed that the depletion of C12orf65 in

both, HEK293T and HeLa cells resulted in significant growth defect with a drastic change in phenotype of cells and morphology of mitochondrial network, which is consistent with previous findings. Further, due to the lack of antibodies against ND polypeptides to test directly their steady state levels upon depletion, a nuclear encoded complex I protein, NDUFB8, an indicator for correct assembly and stability of the complex was employed. Its levels were not affected after 6 days of C12orf65 depletion, which was in contrast to what Antonicka *et al*., (2010), has shown. This could be due to the tissue specificity differences or to the fact that 6 day depletion was not long enough to cause such dramatic decreases as seen in patient's fibroblast where the mutation of C12orf65 was permanent. To confirm this however it would be ideal to analyze the cultured cell lines by BN-PAGE.

Functional and structural studies lead to a suggestion that like ICT1, C12orf65 may play a role in rescuing stalled ribosome, which may arise due to limiting amounts of charged tRNAs, stable secondary structures, premature stop codons, or truncated/degraded transcripts. Consequent analysis in this project revealed that upon C12orf65 depletion mitochondrial transcripts increase significantly, not being able to proceed for translation and accumulated, which was consisted with the hypothesis of C12orf65 may be participating in freeing the transcripts from blocked ribosomes. Surprisingly, the accumulation of those transcripts occurred not in the monosomes as predicted, but presumably at the mtSSU at the initiation phase. It would be interesting to pursue this investigation further by repeating the experiment from section 7.7 and after sucrose gradient centrifugation and fraction collection perform immunoprecipitation from fraction 5 where the transcripts accumulate. If accumulated transcripts associate with mtSSU, immunoprecipitating the SSU from the fraction would deplete the associated transcripts as well. If that is the case, it would confirm that those mRNAs accumulate on mtSSU, but what would be a rationale behind it?

C12orf65 being a matrix soluble protein has been suggested to play a role in processing peptidyl-tRNAs that have been prematurely released during elongation phase (Antonicka *et al*., 2010). The accumulation of such peptidyl-tRNAs would result in depletion of aminoacylated tRNAs blocking mitoribosomes, which in turn would result in protein synthesis inhibition, C12orf65 has no structural similarities with peptidyl-tRNA hydrolases (Pth) that

are responsible for such function in bacteria (Das *et al*., 2006). Pth is an esterase that cleaves the ester bond between the C-terminal end of the polypeptide and the tRNA, whereas C12orf65 contains a GGQ motif, which is known to promote peptidyl-tRNA hydrolysis (PTH) in the peptidyl-transferase centre located in the mtLSU. Moreover, the partial rescue of the phenotype in patients' fibroblasts (Antonicka *et al*., 2010), which was also confirmed in this investigation, supports the prediction that C12or65 would rather have a ribosomal dependent PTH activity. C12orf65's association with ribosomes as well as the functionality of its GGQ motif need to be confirmed.

Another possibility is that, due to the structural similarities, C12orf65 and ICT1 can perform the same function but on different substrates, or have overlapping functions in different species. C12orf65 may be responsible for releasing peptidyl-tRNA from mtLSU after it has been disassociated. It could be that such complex, mtLSU and tRNA in a P-site with long polypeptide chain firmly engaged in the exit tunnel so that it is not able to drop off spontaneously, has a changed conformation and ICT1 on the mtLSU is not able to reach the PTC to solve the problem. In the situation when C12orf65 is not functional those complexes accumulate depleting the pool of free mtLSU to initiate in the next rounds of translation. This in turn could result in accumulation of mtSSU with mRNA attached to it that is ready to initiate. This is consistent with observations of gradients presented here. Moreover, such a state of abnormal mtLSU may reflect a change in the ratio between free and ribosome associated MRPL12. As discussed earlier (in chapter 3), such a change of ratio towards the free form of MRPL12 may signal to the outside of the organelle the requirement of mitoribosome biogenesis to compensate for the impairment, similarly to the mechanism in bacteria (Ramagopal *et al*., 1976), where accumulation of non-ribosome associated L7 and L12 controls binding of RNA sequences inducing ribosome biogenesis. Such speculations need to be further investigated, and should take under consideration all the proteins of release factor family as they may all play in concert to rescue ribosome stalling and investigating one at a time *in vivo* may not shed much light on this process.

Chapter 8

Final Conclusions

8. Chapter 8. Final Conclusions

This work was focused on characterisation of two mitochondrial proteins, mitochondrial Release Factor 1 (mtRF1) and a factor without ascribed named called C12orf65. Both of those proteins were shown to be localised to the organelles (Antonicka *et al*., 2010, Soleimanpour-Lichaei et al., 2007) and suggested to participate in a quality control of mitochondrial protein synthesis (Huynen et al., 2012, Kogure et al., 2012). The concluding remarks will be made below regarding the progress presented by this project and its contribution to the published data together with the outline of potential future approaches for

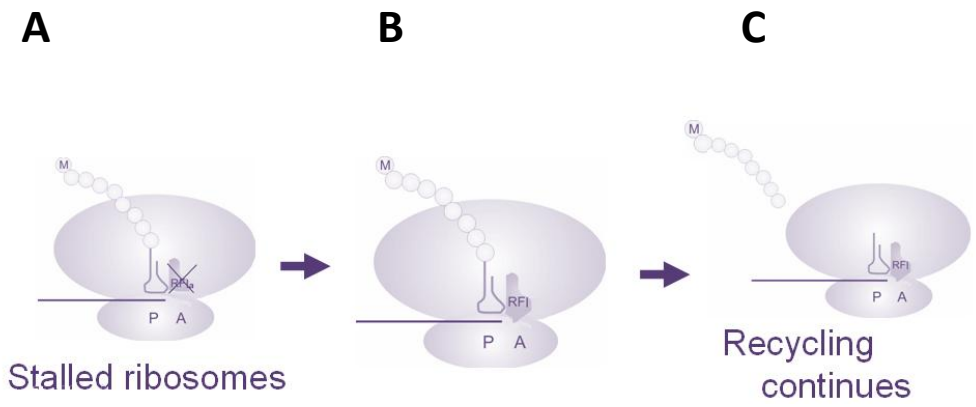

Figure 8. 1. The proposed function of mtRF1.

(A) Truncated mRNA may result in an incomplete ORF, peptidyl-tRNA in P-site and aberrant translation. Such a complex could not be recycled and used for further translation. **(B)** However, it was hypothesised that this could be recognise by mtRF1, which would bind to empty A-site promoting release of nascent peptide chain and allowing the translation termination to continue as in **(C).**

both investigated proteins.

The main part of this PhD thesis represents the investigation on mtRF1 in respect of its proposed function as a release factor that binds to stalled ribosomes, which lack a codon in A-site and which may be analogous to the other mRNA surveillance pathways, e.g. tmRNA in bacteria. The work presented in this project shows that mtRF1 is

- an essential protein that is required for maintaining viable cells and fully functional mitochondria with its loss resulting in an increased levels of free MRPL12
- a release factor family member protein, whose GGQ motif is essential for its function

- able to present a level of interaction with mitoribosomes *in vivo*, similar to that represented by mtRRF under the same conditions
- a protein that possibly functions in concert with other factors, which may have overlapping functions as mtRF1 substrate could not be characterised by different approaches.

Despite the extensive investigation presented here the function of mtRF1 is still not clear. However, none of the approaches undertaken could exclude the given hypothesis, thus further experiments are required in order to prove or disprove it. The further experimentation in this case is highly limited by the available techniques; mainly the lack of *in vitro* mitochondrial translation system prevents to test the direct mtRF1 function. If CLIP or any other experiments involving cross link agents could not show potential interaction with rRNA, the questions about mtRF1 functionality and specificity cannot be answered without suitable tools that would be able to investigate the direct interactions between mitoribosomes, mt-mRNAs and involved factors. Such a tool could be the ribosome profiling techniques. When optimized it would be an ideal strategy to monitor *in vivo* mitochondrial translation providing not only insights into the exact positions of mitoribosomes on mt-transcripts probably revealing naturally occurring stalling events, but also it can provide a great model to monitor mitoribosomal rescue strategies. Meanwhile without having access to such technique, and in order to test the hypothesis that mitochondrial release factor family members function in the rescue of aberrant transcripts or stalled mitoribosomes analogous to factors involved in ribosome rescue in bacteria candidates, another approach would have to be undertaken. The design of the experiments would be to test for complementation by expression of mitochondrial release factor family proteins in *E. coli* cells lacking both arfA and ssrA and looking for the suppression of the bacterial phenotype. In addition to this *in vivo* experimentation, an *in vitro* approach could be also used to test mitochondrial release factors on bacterial stalled ribosomes with the expectation that this would elucidate their functions in both systems. Those possibilities would definitely open a new chapter of our understanding about two highly understudied aspects of mitochondrial biology, the mechanisms regulating mitochondrial protein synthesis and the gene expression quality control.

The second part of this project focused on C12orf65, a mitochondrial protein that have been included into release factor family members based on the sequence similarities with other members. It has been shown to be essential protein for mitochondrial biology as mutations in its gene resulted in mitochondrial diseases (Antonicka et al., 2010; Shimazaki et al., 2012). This work presents a preliminary data in a search for the function of C12orf65 in mitochondrial protein synthesis quality control.

It was demonstrated here that C12orf65 is:

- important for a healthy cell growth
- found to transiently associate with some mitoribosomal proteins
- responsible for correct activities occurring on mt-mRNA, probably due to a positive effect on mitoribosome composition.

These conclusions however are only the first step in further investigations to characterise the real function of C12orf65 and needs to be expanded on. First, the functional characterisation of the GGQ motif in essential for the continuation of this project. Then, establishing whether the accumulation of the transcripts or failure in mitoribosomal maturation/fully assembly was a direct effect of the loss of this protein. Moreover, as suggested in section 7.13 looking for the complex on which the increased mt-mRNA accumulates would be informative and potentially could take the project forward. The ribosome profiling also has a great potential in this further work on this project and together with assigning mtPARN-N and mtRelE enzymes into the experimentations (similarly as described in sections 6.2-6.4).

Concluding, it is clear that mitochondria play a key role in maintaining a functionally healthy cell and in order to ensure that all mitochondrially encoded proteins are properly expressed and assembled into the individual respiratory chain complexes, the quality control mechanisms are crucial. It has been shown that truncated mRNA may occur in mitochondria as a result of incorrect transcription, misprocessing of polycistronic RNA precursors or/and due to exonucleases cleavage (Borowski *et al.* 2010). If the mt-mRNA transcript is truncated the subsequent addition of poly(A) tail fails to generate a termination signal at the true end of the open reading frame. Eventually this results in truncated ORF, stalled ribosome with a peptidyl-tRNA in the P-site and an

empty A-site. Therefore an obvious question arises: how can mitochondria cope with such a problem? Until recently the regulation of this coordinated biogenesis and the steps of translation, especially the process of termination has been neglected. Recent reports on functional and structural aspects of mitochondrial release family members together with the data presented here, as a potential for future full characterisation of their roles in mitochondrial gene expression, contribute to a better understanding of fundamental mitochondrial biology, which in turn impacts on the understanding of many mitochondrial dysfunctions that lead to, currently untreatable, mitochondrial diseases.

References

ADAMS, K. L. & PALMER, J. D. 2003. Evolution of mitochondrial gene content: gene loss and transfer to the nucleus. *Molecular Phylogenetics and Evolution,* 29, 380-395.
ALEKSANDROV, A. & SIMONSON, T. 2009. Molecular mechanics models for tetracycline analogs. *Journal of Computational Chemistry,* 30, 243-255.
ANDERSON, S., BANKIER, A. T. & BARRELL, B. G. 1981. Sequence and organization of the human mitochondrial genome. *Nature,* 290, 457-465.
ANDERSSON, S. G. E., ZOMORODIPOUR, A., ANDERSSON, J. O., SICHERITZ-PONTEN, T., ALSMARK, U. C. M., PODOWSKI, R. M., NASLUND, A. K., ERIKSSON, A.-S., WINKLER, H. H. & KURLAND, C. G. 1998. The genome sequence of Rickettsia prowazekii and the origin of mitochondria. *Nature,* 396, 133-140.
ANTONICKA, H., OSTERGAARD, E., SASARMAN, F., WERAARPACHAI, W., WIBRAND, F., PEDERSEN, A. M., RODENBURG, R. J., VAN DER KNAAP, M. S., SMEITINK, J. A. & CHRZANOWSKA-LIGHTOWLERS, Z. M. 2010. Mutations in C12orf65 in patients with encephalomyopathy and a mitochondrial translation defect. *Am J Hum Genet,* 87, 115-122.
ARAKI, Y., TAKAHASHI, S., KOBAYASHI, T., KAJIHO, H., HOSHINO, S.-I. & KATADA, T. 2001. Ski7p G protein interacts with the exosome and the Ski complex for 3[prime]-to-5[prime] mRNA decay in yeast. *EMBO J,* 20, 4684-4693.
ASHRAFI, G. & SCHWARZ, T. L. 2013. The pathways of mitophagy for quality control and clearance of mitochondria. *Cell Death Differ,* 20, 31-42.
ATKINSON, G., BALDAUF, S. & HAURYLIUK, V. 2008. Evolution of nonstop, no-go and nonsense-mediated mRNA decay and their termination factor-derived components. *BMC Evolutionary Biology,* 8, 290.
BALLARD, J. W. O. & WHITLOCK, M. C. 2004. The incomplete natural history of mitochondria. *Molecular Ecology,* 13, 729-744.
BARENDS, S., KARZAI, A. W., SAUER, R. T., WOWER, J. & KRAAL, B. 2001. Simultaneous and functional binding of SmpB and EF-Tu·GTP to the alanyl acceptor arm of tmRNA. *Journal of Molecular Biology,* 314, 9-21.
BARRIENTOS, A., KORR, D., BARWELL, K. J., SJULSEN, C., GAJEWSKI, C. D., MANFREDI, G., ACKERMAN, S. & TZAGOLOFF, A. 2003. MTG1 Codes for a Conserved Protein Required for Mitochondrial Translation. *Molecular Biology of the Cell,* 14, 2292-2302.
BAUERSCHMITT, H., MICK, D. U., DECKERS, M., VOLLMER, C., FUNES, S., KEHREIN, K., OTT, M., REHLING, P. & HERRMANN, J. M. 2010. Ribosome-binding Proteins Mdm38 and Mba1 Display Overlapping Functions for Regulation of Mitochondrial Translation. *Molecular Biology of the Cell,* 21, 1937-1944.
BECKER, T., ARMACHE, J.-P., JARASCH, A., ANGER, A. M., VILLA, E., SIEBER, H., MOTAAL, B. A., MIELKE, T., BERNINGHAUSEN, O. & BECKMANN, R. 2011. Structure of the no-go mRNA decay complex Dom34–Hbs1 bound to a stalled 80S ribosome. *Nat Struct Mol Biol,* 18, 715-720.
BENGTSON, M. H. & JOAZEIRO, C. A. P. 2010. Role of a ribosome-associated E3 ubiquitin ligase in protein quality control. *Nature,* 467, 470-473.
BHARGAVA, K. & SPREMULLI, L. L. 2005. Role of the N- and C-terminal extensions on the activity of mammalian mitochondrial translational initiation factor 3. *Nucleic Acids Research,* 33, 7011-7018.

BHARGAVA, K., TEMPLETON, P. & SPREMULLI, L. L. 2004. Expression and characterization of isoform 1 of human mitochondrial elongation factor G. *Protein Expression and Purification,* 37, 368-376.
BOGENHAGEN, D. F. 2012. Mitochondrial DNA nucleoid structure. *Biochimica et Biophysica Acta (BBA) - Gene Regulatory Mechanisms,* 1819, 914-920.
BOGENHAGEN, D. F., ROUSSEAU, D. & BURKE, S. 2008. The Layered Structure of Human Mitochondrial DNA Nucleoids. *Journal of Biological Chemistry,* 283, 3665-3675.
BONN, F., TATSUTA, T., PETRUNGARO, C., RIEMER, J. & LANGER, T. 2011. Presequence-dependent folding ensures MrpL32 processing by the m-AAA protease in mitochondria. *EMBO J,* 30, 2545-2556.
BOROWSKI, L. S., SZCZESNY, R. J., BRZEZNIAK, L. K. & STEPIEN, P. P. 2010. RNA turnover in human mitochondria: More questions than answers? *Biochimica et Biophysica Acta (BBA) - Bioenergetics,* 1797, 1066-1070.
BRASCHI, E., ZUNINO, R. & MCBRIDE, H. M. 2009. MAPL is a new mitochondrial SUMO E3 ligase that regulates mitochondrial fission. *EMBO Reports,* 10, 748-754.
BRODERSEN, D. E., CLEMONS, W. M., CARTER, A. P., MORGAN-WARREN, R. J., WIMBERLY, B. T. & RAMAKRISHNAN, V. 2000. The Structural Basis for the Action of the Antibiotics Tetracycline, Pactamycin, and Hygromycin B on the 30S Ribosomal Subunit. *Cell,* 103, 1143-1154.
CAI YC FAU - BULLARD, J. M., BULLARD JM FAU - THOMPSON, N. L., THOMPSON NL FAU - SPREMULLI, L. L. & SPREMULLI, L. L. 2000. Interaction of mammalian mitochondrial elongation factor EF-Tu with guanine nucleotides.
CAMARA, Y., ASIN-CAYUELA, J., PARK, C. B., METODIEV, M. D., SHI, Y., RUZZENENTE, B., KUKAT, C., HABERMANN, B., WIBOM, R., HULTENBY, K., FRANZ, T., ERDJUMENT-BROMAGE, H., TEMPST, P., HALLBERG, B. M., GUSTAFSSON, C. M. & LARSSON, N. G. 2011. MTERF4 regulates translation by targeting the methyltransferase NSUN4 to the mammalian mitochondrial ribosome. *Cell Metabolism,* 13, 527-539.
CANNONE, J., SUBRAMANIAN, S., SCHNARE, M., COLLETT, J., D'SOUZA, L., DU, Y., FENG, B., LIN, N., MADABUSI, L., MULLER, K., PANDE, N., SHANG, Z., YU, N. & GUTELL, R. 2002. The Comparative RNA Web (CRW) Site: an online database of comparative sequence and structure information for ribosomal, intron, and other RNAs. *BMC Bioinformatics,* 3, 2.
CHADANI, Y., ONO, K., KUTSUKAKE, K. & ABO, T. 2011. Escherichia coli YaeJ protein mediates a novel ribosome-rescue pathway distinct from SsrA- and ArfA-mediated pathways. *Molecular Microbiology,* 80, 772-785.
CHAN, N. C., SALAZAR, A. M., PHAM, A. H., SWEREDOSKI, M. J., KOLAWA, N. J., GRAHAM, R. L. J., HESS, S. & CHAN, D. C. 2011. Broad activation of the ubiquitin–proteasome system by Parkin is critical for mitophagy. *Human Molecular Genetics,* 20, 1726-1737.
CHEN, J., CHIANG, Y.-C. & DENIS, C. L. 2002. CCR4, a 3[prime]-5[prime] poly(A) RNA and ssDNA exonuclease, is the catalytic component of the cytoplasmic deadenylase. *EMBO J,* 21, 1414-1426.

CHRISTIAN, B. E. & SPREMULLI, L. L. 2009. Evidence for an Active Role of IF3mt in the Initiation of Translation in Mammalian Mitochondria†. *Biochemistry,* 48, 3269-3278.
CHRISTIAN, B. E. & SPREMULLI, L. L. 2010. Preferential Selection of the 5′-Terminal Start Codon on Leaderless mRNAs by Mammalian Mitochondrial Ribosomes. *Journal of Biological Chemistry,* 285, 28379-28386.
CHRISTIAN, B. E. & SPREMULLI, L. L. 2012. Mechanism of protein biosynthesis in mammalian mitochondria. *Biochimica et Biophysica Acta - Gene Regulatory Mechanisms*.
CHRZANOWSKA-LIGHTOWLERS, Z. M. A., PAJAK, A. & LIGHTOWLERS, R. N. 2011. Termination of Protein Synthesis in Mammalian Mitochondria. *Journal of Biological Chemistry,* 286, 34479-34485.
CHUJO, T., OHIRA, T., SAKAGUCHI, Y., GOSHIMA, N., NOMURA, N., NAGAO, A. & SUZUKI, T. 2012. LRPPRC/SLIRP suppresses PNPase-mediated mRNA decay and promotes polyadenylation in human mitochondria. *Nucleic Acids Research,* 40, 8033-8047.
CLEMENT, S. L. & LYKKE-ANDERSEN, J. 2006. No mercy for messages that mess with the ribosome. *Nature Structural and Molecular Biology,* 13, 299-301.
COENEN, M. J. H., ANTONICKA, H., UGALDE, C., SASARMAN, F., ROSSI, R., HEISTER, J. G. A. M. A., NEWBOLD, R. F., TRIJBELS, F. J. M. F., VAN DEN HEUVEL, L. P., SHOUBRIDGE, E. A. & SMEITINK, J. A. M. 2004. Mutant Mitochondrial Elongation Factor G1 and Combined Oxidative Phosphorylation Deficiency. *New England Journal of Medicine,* 351, 2080-2086.
CONNELL, S. R., TRACZ, D. M., NIERHAUS, K. H. & TAYLOR, D. E. 2003. Ribosomal protection proteins and their mechanism of tetracycline resistance. *Antimicrobial agents and chemotherapy,* 47(12), 3675-81.
CROSBY, A. H., PATEL, H., CHIOZA, B. A., PROUKAKIS, C., GURTZ, K., PATTON, M. A., SHARIFI, R., HARLALKA, G., SIMPSON, M. A., DICK, K., REED, J. A., AL-MEMAR, A., CHRZANOWSKA-LIGHTOWLERS, Z. M. A., CROSS, H. E. & LIGHTOWLERS, R. N. 2010. Defective Mitochondrial mRNA Maturation Is Associated with Spastic Ataxia. *American Journal of Human Genetics,* 87, 655-660.
DAIRAGHI, D. J., SHADEL, G. S. & CLAYTON, D. A. 1995. Addition of a 29 Residue Carboxyl-terminal Tail Converts a Simple HMG Box-containing Protein into a Transcriptional Activator. *Journal of Molecular Biology,* 249, 11-28.
DAS, A., GHOSH, J., BHATTACHARYA, A., SAMANTA, D., DAS, D. & DAS GUPTA, C. 2011. Involvement of Mitochondrial Ribosomal Proteins in Ribosomal RNA-mediated Protein Folding. *Journal of Biological Chemistry,* 286, 43771-43781.
DAS, G. & VARSHNEY, U. 2006. Peptidyl-tRNA hydrolase and its critical role in protein biosynthesis. *Microbiology,* 152, 2191-2195.
DAVIES, S. M. K., RACKHAM, O., SHEARWOOD, A.-M. J., HAMILTON, K. L., NARSAI, R., WHELAN, J. & FILIPOVSKA, A. 2009. Pentatricopeptide repeat domain protein 3 associates with the mitochondrial small ribosomal subunit and regulates translation. *FEBS Letters,* 583, 1853-1858.
DENNERLEIN, S., ROZANSKA, A., WYDRO, M., CHRZANOWSKA-LIGHTOWLERS, Z. M. A. & LIGHTOWLERS, R. N. 2010. Human ERAL1

is a mitochondrial RNA chaperone involved in the assembly of the 28S small mitochondrial ribosomal subunit. *Biochemical Journal,* 430, 551-558.
DOMA, M. K. & PARKER, R. 2006. Endonucleolytic cleavage of eukaryotic mRNAs with stalls in translation elongation. *Nature,* 440, 561-564.
DOMA, M. K. & PARKER, R. 2007. RNA Quality Control in Eukaryotes. *Cell,* 131, 660-668.
DZIEMBOWSKI, A., LORENTZEN, E., CONTI, E. & SERAPHIN, B. 2007. A single subunit, Dis3, is essentially responsible for yeast exosome core activity. *Nat Struct Mol Biol,* 14, 15-22.
FALKENBERG, M., GASPARI, M., RANTANEN, A., TRIFUNOVIC, A., LARSSON, N.-G. & GUSTAFSSON, C. M. 2002. Mitochondrial transcription factors B1 and B2 activate transcription of human mtDNA. *Nat Genet,* 31, 289-294.
FALKENBERG, M., LARSSON, N.-G. & GUSTAFSSON, C. M. 2007. DNA Replication and Transcription in Mammalian Mitochondria. *Annual Review of Biochemistry,* 76, 679-699.
FELDEN, B., HIMENO, H., MUTO, A., MCCUTCHEON, J. P., ATKINS, J. F. & GESTELAND, R. F. 1997. Probing the structure of the Escherichia coli 10Sa RNA (tmRNA). *RNA,* 3, 89-103.
FORNER, F., FOSTER, L. J., CAMPANARO, S., VALLE, G. & MANN, M. 2006. Quantitative Proteomic Comparison of Rat Mitochondria from Muscle, Heart, and Liver. *Molecular & Cellular Proteomics,* 5, 608-619.
FREY, T. G. & MANNELLA, C. A. 2000. The internal structure of mitochondria. *Trends in Biochemical Sciences,* 25, 319-324.
FRISCHMEYER, P. A., VAN HOOF, A., O'DONNELL, K., GUERRERIO, A. L., PARKER, R. & DIETZ, H. C. 2002. An mRNA surveillance mechanism that eliminates transcripts lacking termination codons. *Science,* 295(5563), 2258-61.
FROLOVA, L. Y., TSIVKOVSKII, R. Y., SIVOLOBOVA, G. F., OPARINA, N. Y., SERPINSKY, O. I., BLINOV, V. M., TATKOV, S. I. & KISSELEV, L. L. 1999. Mutations in the highly conserved GGQ motif of class 1 polypeptide release factors abolish ability of human eRF1 to trigger peptidyl-tRNA hydrolysis. *RNA,* 5, 1014-1020.
GAGLIARDI, D., STEPIEN, P. P., TEMPERLEY, R. J., LIGHTOWLERS, R. N. & CHRZANOWSKA-LIGHTOWLERS, Z. M. A. 2004. Messenger RNA stability in mitochondria: different means to an end. *Trends in Genetics,* 20, 260-267.
GAGNON, M. G., SEETHARAMAN, S. V., BULKLEY, D. & STEITZ, T. A. 2012. Structural basis for the rescue of stalled ribosomes: Structure of YaeJ bound to the ribosome. *Science,* 335, 1370-1372.
GAISNE, M. & BONNEFOY, N. 2006. The COX18 gene, involved in mitochondrial biogenesis, is functionally conserved and tightly regulated in humans and fission yeast. *FEMS Yeast Research,* 6, 869-882.
GALKIN, A., DRÖSE, S. & BRANDT, U. 2006. The proton pumping stoichiometry of purified mitochondrial complex I reconstituted into proteoliposomes. *Biochimica et Biophysica Acta (BBA) - Bioenergetics,* 1757, 1575-1581.
GARRICK, D., FIERING, S., MARTIN, D. I. K. & WHITELAW, E. 1998. Repeat-induced gene silencing in mammals. *Nat Genet,* 18, 56-59.

GATFIELD, D. & IZAURRALDE, E. 2004. Nonsense-mediated messenger RNA decay is initiated by endonucleolytic cleavage in Drosophila. *Nature,* 429, 575-578.
GHOSH, S., GANESAN, R., AMRANI, N. & JACOBSON, A. 2010. Translational competence of ribosomes released from a premature termination codon is modulated by NMD factors. *RNA,* 16, 1832-1847.
GLANCY, B. & BALABAN, R. S. 2012. Role of Mitochondrial Ca2+ in the Regulation of Cellular Energetics. *Biochemistry,* 51, 2959-2973.
GOTTESMAN, S., ROCHE, E., ZHOU, Y. & SAUER, R. T. 1998. The ClpXP and ClpAP proteases degrade proteins with carboxy-terminal peptide tails added by the SsrA-tagging system. *Genes & Development,* 12, 1338-1347.
GRAY, BURGER G FAU - LANG, B. F. & LANG, B. F. 1999. Mitochondrial evolution. *Science,* 283.
GRAY, M. W., LANG, B. F., CEDERGREN, R., GOLDING, G. B., LEMIEUX, C., SANKOFF, D., TURMEL, M., BROSSARD, N., DELAGE, E., LITTLEJOHN, T. G., PLANTE, I., RIOUX, P., SAINT-LOUIS, D., ZHU, Y. & BURGER, G. 1998. Genome structure and gene content in protist mitochondrial DNAs. *Nucleic Acids Research,* 26, 865-878.
GRUSCHKE, S., GRÖNE, K., HEUBLEIN, M., HÖLZ, S., ISRAEL, L., IMHOF, A., HERRMANN, J. M. & OTT, M. 2010. Proteins at the Polypeptide Tunnel Exit of the Yeast Mitochondrial Ribosome. *Journal of Biological Chemistry,* 285, 19022-19028.
GRUSCHKE, S., KEHREIN, K., RÖMPLER, K., GRÖNE, K., ISRAEL, L., IMHOF, A., HERRMANN, J. M. & OTT, M. 2011. Cbp3–Cbp6 interacts with the yeast mitochondrial ribosomal tunnel exit and promotes cytochrome b synthesis and assembly. *The Journal of Cell Biology,* 193, 1101-1114.
HAMMARSUND, M., WILSON, W., CORCORAN, M., MERUP, M., EINHORN, S., GRANDÉR, D. & SANGFELT, O. 2001. Identification and characterization of two novel human mitochondrial elongation factor genes, <SMALL>hEFG2</SMALL> and <SMALL>hEFG1,</SMALL> phylogenetically conserved through evolution. *Human Genetics,* 109, 542-550.
HANDA, Y., HIKAWA, Y., TOCHIO, N., KOGURE, H., INOUE, M., KOSHIBA, S., GÜNTERT, P., INOUE, Y., KIGAWA, T., YOKOYAMA, S. & NAMEKI, N. 2010. Solution Structure of the Catalytic Domain of the Mitochondrial Protein ICT1 That Is Essential for Cell Vitality. *Journal of Molecular Biology,* 404, 260-273.
HANDA, Y., INAHO, N. & NAMEKI, N. 2011. YaeJ is a novel ribosome-associated protein in Escherichia coli that can hydrolyze peptidyl–tRNA on stalled ribosomes. *Nucleic Acids Research,* 39, 1739-1748.
HAQUE, M. E., ELMORE, K. B., TRIPATHY, A., KOC, H., KOC, E. C. & SPREMULLI, L. L. 2010. Properties of the C-terminal Tail of Human Mitochondrial Inner Membrane Protein Oxa1L and Its Interactions with Mammalian Mitochondrial Ribosomes. *Journal of Biological Chemistry,* 285, 28353-28362.
HAQUE, M. E., KOC, H., CIMEN, H., KOC, E. C. & SPREMULLI, L. L. 2011. Contacts between mammalian mitochondrial translational initiation factor 3 and ribosomal proteins in the small subunit. *Biochimica et Biophysica Acta - Proteins and Proteomics,* 1814, 1779-1784.

HAQUE, M. E. & SPREMULLI, L. L. 2008. Roles of the N- and C-Terminal Domains of Mammalian Mitochondrial Initiation Factor 3 in Protein Biosynthesis. *Journal of Molecular Biology,* 384, 929-940.
HAYES, C. S. & KEILER, K. C. 2009. Beyond ribosome rescue: tmRNA and co-translational processes. *FEBS Lett,* 584, 413-419.
HAYES, C. S. & SAUER, R. T. 2003. Cleavage of the A Site mRNA Codon during Ribosome Pausing Provides a Mechanism for Translational Quality Control. *Molecular Cell,* 12, 903-911.
HE, F., BROWN, A. H. & JACOBSON, A. 1997. Upf1p, Nmd2p, and Upf3p are interacting components of the yeast nonsense-mediated mRNA decay pathway. *Molecular and Cellular Biology,* 17, 1580-94.
HE, H., CHEN, M., SCHEFFLER, N. K., GIBSON, B. W., SPREMULLI, L. L. & GOTTLIEB, R. A. 2001. Phosphorylation of Mitochondrial Elongation Factor Tu in Ischemic Myocardium. *Circulation Research,* 89, 461-467.
HE, J., COOPER, H. M., REYES, A., DI RE, M., KAZAK, L., WOOD, S. R., MAO, C. C., FEARNLEY, I. M., WALKER, J. E. & HOLT, I. J. 2012. Human C4orf14 interacts with the mitochondrial nucleoid and is involved in the biogenesis of the small mitochondrial ribosomal subunit. *Nucleic Acids Research,* 40, 6097-6108.
HE, J., MAO, C.-C., REYES, A., SEMBONGI, H., DI RE, M., GRANYCOME, C., CLIPPINGDALE, A. B., FEARNLEY, I. M., HARBOUR, M., ROBINSON, A. J., REICHELT, S., SPELBRINK, J. N., WALKER, J. E. & HOLT, I. J. 2007. The AAA+ protein ATAD3 has displacement loop binding properties and is involved in mitochondrial nucleoid organization. *The Journal of Cell Biology,* 176, 141-146.
HELL, K., NEUPERT, W. & STUART, R. A. 2001. Oxa1p acts as a general membrane insertion machinery for proteins encoded by mitochondrial DNA. *EMBO J,* 20, 1281-1288.
HERRMANN, J. M., WOELLHAF, M. W. & BONNEFOY, N. 2012. Control of protein synthesis in yeast mitochondria: The concept of translational activators. *Biochimica et Biophysica Acta (BBA) - Molecular Cell Research*.
HEURGUE-HAMARD, V., CHAMP, S., ENGSTROM, A., EHRENBERG, M. & BUCKINGHAM, R. H. 2002. The hemK gene in Escherichia coli encodes the N5-glutamine methyltransferase that modifies peptide release factors. *EMBO J,* 21, 769-778.
HEURGUÉ-HAMARD, V., CHAMP, S., MORA, L., MERKOULOVA-RAINON, T., KISSELEV, L. L. & BUCKINGHAM, R. H. 2005. The Glutamine Residue of the Conserved GGQ Motif in Saccharomyces cerevisiae Release Factor eRF1 Is Methylated by the Product of the YDR140w Gene. *Journal of Biological Chemistry,* 280, 2439-2445.
HOGG, J. R. & GOFF, S. P. 2010. Upf1 Senses 32UTR Length to Potentiate mRNA Decay. *Cell,* 143, 379-389.
HOPPER, R. K., CARROLL, S., APONTE, A. M., JOHNSON, D. T., FRENCH, S., SHEN, R.-F., WITZMANN, F. A., HARRIS, R. A. & BALABAN, R. S. 2006. Mitochondrial Matrix Phosphoproteome: Effect of Extra Mitochondrial Calcium†. *Biochemistry,* 45, 2524-2536.
HOPPINS, S. & NUNNARI, J. 2012. Mitochondrial Dynamics and Apoptosis—the ER Connection. *Science,* 337, 1052-1054.
HSU, C. L. & STEVENS, A. 1993. Yeast cells lacking 5'-->3' exoribonuclease 1 contain mRNA species that are poly(A) deficient and partially lack the 5' cap structure. *Molecular and Cellular Biology,* 13, 4826-4835.

HURLEY, J. M., CRUZ, J. W., OUYANG, M. & WOYCHIK, N. A. 2011. Bacterial toxin RelE mediates frequent codon-independent mRNA cleavage from the 5' end of coding regions in vivo. *Journal of Biological Chemistry,* 286, 14770-14778.

HUYNEN, M., DUARTE, I., CHRZANOWSKA-LIGHTOWLERS, Z. M. & NABUURS, S. 2012. Structure based hypothesis of a mitochondrial ribosome rescue mechanism. *Biology Direct,* 7, 14.

INAGAKI, Y. & FORD DOOLITTLE, W. 2000. Evolution of the Eukaryotic Translation Termination System: Origins of Release Factors. *Molecular Biology and Evolution,* 17, 882-889.

ISHIZAWA, T., NOZAKI, Y., UEDA, T. & TAKEUCHI, N. 2008. The human mitochondrial translation release factor HMRF1L is methylated in the GGQ motif by the methyltransferase HMPrmC. *Biochemical and Biophysical Research Communications,* 373, 99-103.

ISKEN, O. & MAQUAT, L. E. 2007. Quality control of eukaryotic mRNA: safeguarding cells from abnormal mRNA function. *Genes & Development,* 21, 1833-3856.

ITO-HARASHIMA, S., KUROHA, K., TATEMATSU, T. & INADA, T. 2007. Translation of the poly(A) tail plays crucial roles in nonstop mRNA surveillance via translation repression and protein destabilization by proteasome in yeast. *Genes & Development,* 21, 519-524.

IVANOVA, N., PAVLOV, M. Y., FELDEN, B. & EHRENBERG, M. 2004. Ribosome Rescue by tmRNA Requires Truncated mRNAs. *Journal of Molecular Biology,* 338, 33-41.

JEPPESEN, M. G., NAVRATIL, T., SPREMULLI, L. L. & NYBORG, J. 2005. Crystal Structure of the Bovine Mitochondrial Elongation Factor Tu·Ts Complex. *Journal of Biological Chemistry,* 280, 5071-5081.

JIA, L., DIENHART, M., SCHRAMP, M., MCCAULEY, M., HELL, K. & STUART, R. A. 2003. Yeast Oxa1 interacts with mitochondrial ribosomes: the importance of the C-terminal region of Oxa1. *EMBO J,* 22, 6438-6447.

JIA, L., KAUR, J. & STUART, R. A. 2009. Mapping of the Saccharomyces cerevisiae Oxa1-Mitochondrial Ribosome Interface and Identification of MrpL40, a Ribosomal Protein in Close Proximity to Oxa1 and Critical for Oxidative Phosphorylation Complex Assembly. *Eukaryotic Cell,* 8, 1792-1802.

JOHANSEN, J., ROSENBLAD, C., MOLLER, A., LUNDBERG, C., BJORLUND, A. & JOHANSEN, T. E. 2002. Evaluation of Tet-on system to avoid transgene down-regulation in ex vivo gene transfer to the CNS. *Gene Therapy* 19, 1291-301.

JOHNSON, D. T., HARRIS, R. A., FRENCH, S., BLAIR, P. V., YOU, J., BEMIS, K. G., WANG, M. & BALABAN, R. S. 2007. Tissue heterogeneity of the mammalian mitochondrial proteome. *American Journal of Physiology - Cell Physiology,* 292, C689-C697.

JONES, C. N., WILKINSON, K. A., HUNG, K. T., WEEKS, K. M. & SPREMULLI, L. L. 2008. Lack of secondary structure characterizes the 5′ ends of mammalian mitochondrial mRNAs. *RNA,* 14, 862-871.

KARRING, H., BJÖRNSSON, A., THIRUP, S., CLARK, B. F. C. & KNUDSEN, C. R. 2003. Functional effects of deleting the coiled-coil motif in Escherichia coli elongation factor Ts. *European Journal of Biochemistry,* 270, 4294-4305.

KEILER, K. C., WALLER, P. R. & SAUER, R. T. 1996. Role of a peptide tagging system in degradation of proteins synthesized from damaged messenger RNA. *Science* 271(5251), 990-3.
KOBAYASHI, K., KIKUNO, I., KUROHA, K., SAITO, K., ITO, K., ISHITANI, R., INADA, T. & NUREKI, O. 2010. Structural basis for mRNA surveillance by archaeal Pelota and GTP-bound EF1α complex. *Proceedings of the National Academy of Sciences,* 107, 17575-17579.
KOC, E. C., BURKHART, W., BLACKBURN, K., MOSELEY, A. & SPREMULLI, L. L. 2001a. The small subunit of the mammalian mitochondrial ribosome: Identification of the full complement of ribosomal proteins present. *Journal of Biological Chemistry,* 276, 19363-19374.
KOC, E. C., BURKHART, W., BLACKBURN, K., MOYER, M. B., SCHLATZER, D. M., MOSELEY, A. & SPREMULLI, L. L. 2001b. The large subunit of the mammalian mitochondrial ribosome: Analysis of the complement of ribosomal proteins present. *Journal of Biological Chemistry,* 276, 43958-43969.
KOC, E. C. & SPREMULLI, L. L. 2002. Identification of Mammalian Mitochondrial Translational Initiation Factor 3 and Examination of Its Role in Initiation Complex Formation with Natural mRNAs. *Journal of Biological Chemistry,* 277, 35541-35549.
KOGURE, H., HIKAWA, Y., HAGIHARA, M., TOCHIO, N., KOSHIBA, S., INOUE, Y., GÜNTERT, P., KIGAWA, T., YOKOYAMA, S. & NAMEKI, N. 2012. Solution structure and siRNA-mediated knockdown analysis of the mitochondrial disease-related protein C12orf65. *Proteins: Structure, Function, and Bioinformatics*, n/a-n/a.
KOLANCZYK, M., PECH, M., ZEMOJTEL, T., YAMAMOTO, H., MIKULA, I., CALVARUSO, M. A., VAN DEN BRAND, M., RICHTER, R., FISCHER, B., RITZ, A., KOSSLER, N., THURISCH, B., SPOERLE, R., SMEITINK, J., KORNAK, U., CHAN, D., VINGRON, M., MARTASEK, P., LIGHTOWLERS, R. N., NIJTMANS, L., SCHUELKE, M., NIERHAUS, K. H. & MUNDLOS, S. 2011. NOA1 is an essential GTPase required for mitochondrial protein synthesis. *Molecular Biology of the Cell,* 22, 1-11.
KOMINE, Y., KITABATAKE, M., YOKOGAWA, T., NISHIKAWA, K. & INOKUCHI, H. 1994. A tRNA-like structure is present in 10Sa RNA, a small stable RNA from Escherichia coli. *Proceedings of the National Academy of Sciences,* 91, 9223-9227.
KRUSE, B., NARASIMHAN, N. & ATTARDI, G. 1989. Termination of transcription in human mitochondria: Identification and purification of a DNA binding protein factor that promotes termination. *Cell,* 58, 391-397.
KUKAT, C., WURM, C. A., SPÅHR, H., FALKENBERG, M., LARSSON, N.-G. & JAKOBS, S. 2011. Super-resolution microscopy reveals that mammalian mitochondrial nucleoids have a uniform size and frequently contain a single copy of mtDNA. *Proceedings of the National Academy of Sciences,* 108, 13534-13539.
KYRIAKOULI, D. S., BOESCH, P., TAYLOR, R. W. & LIGHTOWLERS, R. N. 2008. Progress and prospects: gene therapy for mitochondrial DNA disease. *Gene Ther,* 15, 1017-1023.
LANGER, T., KÄSER, M., KLANNER, C. & LEONHARD, K. 2001. AAA proteases of mitochondria: quality control of membrane proteins and regulatory functions during mitochondrial biogenesis. *Biochemical Society Transactions* 29, 431-436. .

LAURBERG, M., ASAHARA, H., KOROSTELEV, A., ZHU, J., TRAKHANOV, S. & NOLLER, H. F. 2008. Structural basis for translation termination on the 70S ribosome. *Nature,* 454, 852-857.
LEE, H. H., KIM, Y.-S., KIM, K. H., HEO, I., KIM, S. K., KIM, O., KIM, H. K., YOON, J. Y., KIM, H. S., KIM, D. J., LEE, S. J., YOON, H. J., KIM, S. J., LEE, B. G., SONG, H. K., KIM, V. N., PARK, C.-M. & SUH, S. W. 2007. Structural and Functional Insights into Dom34, a Key Component of No-Go mRNA Decay. *Molecular Cell,* 27, 938-950.
LESNEFSKY, E. J. & HOPPEL, C. L. 2006. Oxidative phosphorylation and aging. *Ageing Research Reviews,* 5, 402-433.
LI, W., BENGTSON, M. H., ULBRICH, A., MATSUDA, A., REDDY, V. A., ORTH, A., CHANDA, S. K., BATALOV, S. & JOAZEIRO, C. A. P. 2008. Genome-Wide and Functional Annotation of Human E3 Ubiquitin Ligases Identifies MULAN, a Mitochondrial E3 that Regulates the Organelle's Dynamics and Signaling. *PLoS ONE,* 3, e1487.
LIGHTOWLERS, R. N. & CHRZANOWSKA-LIGHTOWLERS, Z. M. A. 2010. Terminating human mitochondrial protein synthesis a shift in our thinking. *RNA Biology,* 7.
LINDER, T., PARK, C., ASIN-CAYUELA, J., PELLEGRINI, M., LARSSON, N.-G., FALKENBERG, M., SAMUELSSON, T. & GUSTAFSSON, C. 2005. A family of putative transcription termination factors shared amongst metazoans and plants. *Current Genetics,* 48, 265-269.
LITONIN, D., SOLOGUB, M., SHI, Y., SAVKINA, M., ANIKIN, M., FALKENBERG, M., GUSTAFSSON, C. M. & TEMIAKOV, D. 2010. Human Mitochondrial Transcription Revisited: ONLY TFAM AND TFB2M ARE REQUIRED FOR TRANSCRIPTION OF THE MITOCHONDRIAL GENES IN VITRO. *Journal of Biological Chemistry,* 285, 18129-18133.
LIU, M. & SPREMULLI, L. 2000. Interaction of mammalian mitochondrial ribosomes with the inner membrane. *Journal of Biological Chemistry,* 275, 29400-29406.
LIVNAT-LEVANON, N. & GLICKMAN, M. H. 2011. Ubiquitin–Proteasome System and mitochondria — Reciprocity. *Biochimica et Biophysica Acta (BBA) - Gene Regulatory Mechanisms,* 1809, 80-87.
LU, J. & DEUTSCH, C. 2008. Electrostatics in the Ribosomal Tunnel Modulate Chain Elongation Rates. *Journal of Molecular Biology,* 384, 73-86.
LUPO, D., VOLLMER, C., DECKERS, M., MICK, D. U., TEWS, I., SINNING, I. & REHLING, P. 2011. Mdm38 is a 14-3-3-Like Receptor and Associates with the Protein Synthesis Machinery at the Inner Mitochondrial Membrane. *Traffic,* 12, 1457-1466.
MAQUAT, L. E., TARN, W.-Y. & ISKEN, O. 2010. The Pioneer Round of Translation: Features and Functions. *Cell,* 142, 368-374.
MARGINEANTU, D. H., EMERSON, C. B., DIAZ, D. & HOCKENBERY, D. M. 2007. Hsp90 Inhibition Decreases Mitochondrial Protein Turnover. *PLoS ONE,* 2, e1066.
MARTIN, S., T., HUANG, K. S., STROBEL, S. A. & STEITZ, T. A. 2005. An induced-fit mechanism to promote peptide bond formation and exclude hydrolysis of peptidyl-tRNA. *Nature,* 438, 520-524.
MCBRIDE, H. M., NEUSPIEL, M. & WASIAK, S. 2006. Mitochondria: More Than Just a Powerhouse. *Current Biology,* 16, R551-R560.
MCCULLOCH, V. & SHADEL, G. S. 2003. Human Mitochondrial Transcription Factor B1 Interacts with the C-Terminal Activation Region of h-mtTFA

and Stimulates Transcription Independently of Its RNA Methyltransferase Activity. *Molecular and Cellular Biology,* 23, 5816-5824.
METODIEV, M. D., LESKO, N., PARK, C. B., CÁMARA, Y., SHI, Y., WIBOM, R., HULTENBY, K., GUSTAFSSON, C. M. & LARSSON, N.-G. 2009. Methylation of 12S rRNA Is Necessary for In Vivo Stability of the Small Subunit of the Mammalian Mitochondrial Ribosome. *Cell Metabolism,* 9, 386-397.
MEYER-FICCA, M. L., MEYER, R. G., KAISER, H., BRACK, A. R., KANDOLF, R. & KÜPPER, J.-H. 2004. Comparative analysis of inducible expression systems in transient transfection studies. *Analytical Biochemistry,* 334, 9-19.
MILLER, J. L., CIMEN, H., KOC, H. & KOC, E. C. 2009. Phosphorylated proteins of the mammalian mitochondrial ribosome: Implications in protein synthesis. *Journal of Proteome Research,* 8, 4789-4798.
MITRA, K., WUNDER, C., ROYSAM, B., LIN, G. & LIPPINCOTT-SCHWARTZ, J. 2009. A hyperfused mitochondrial state achieved at G1–S regulates cyclin E buildup and entry into S phase. *Proceedings of the National Academy of Sciences,* 106, 11960-11965.
MONTOYA, J., OJALA, D. & ATTARDI, G. 1981. Distinctive features of the 5'-terminal sequences of the human mitochondrial mRNAs. *Nature,* 290(5806), 465-70.
MOORE, S. D. & SAUER, R. T. 2007. The tmRNA System for Translational Surveillance and Ribosome Rescue. *Annual Review of Biochemistry,* 76, 101-124.
MORA, L., HEURGUÉ-HAMARD, V., CHAMP, S., EHRENBERG, M., KISSELEV, L. L. & BUCKINGHAM, R. H. 2003. The essential role of the invariant GGQ motif in the function and stability in vivo of bacterial release factors RF1 and RF2. *Molecular Microbiology,* 47, 267-275.
NAGAIKE, T., SUZUKI, T., KATOH, T. & UEDA, T. 2005. Human Mitochondrial mRNAs Are Stabilized with Polyadenylation Regulated by Mitochondria-specific Poly(A) Polymerase and Polynucleotide Phosphorylase. *Journal of Biological Chemistry,* 280, 19721-19727.
NARENDRA, D., TANAKA, A., SUEN, D.-F. & YOULE, R. J. 2008. Parkin is recruited selectively to impaired mitochondria and promotes their autophagy. *The Journal of Cell Biology,* 183, 795-803.
NEUBAUER, C., GILLET, R., KELLEY, A. C. & RAMAKRISHNAN, V. 2012. Decoding in the absence of a codon by tmRNA and SmpB in the ribosome. *Science,* 335, 1366-1369.
NICHOLSON, P., JONCOURT, R. & MÜHLEMANN, O. 2001. Analysis of Nonsense-Mediated mRNA Decay in Mammalian Cells. *Current Protocols in Cell Biology.* John Wiley & Sons, Inc.
NOSEK, J., TOMÁŠKA, L. U. R., FUKUHARA, H., SUYAMA, Y. & KOVÁČ, L. 1998. Linear mitochondrial genomes: 30 years down the line. *Trends in Genetics,* 14, 184-188.
NOZAKI, Y., MATSUNAGA, N., ISHIZAWA, T., UEDA, T. & TAKEUCHI, N. 2008. HMRF1L is a human mitochondrial translation release factor involved in the decoding of the termination codons UAA and UAG. *Genes to Cells,* 13, 429-438.
O'BRIEN, T. W. 2003. Properties of Human Mitochondrial Ribosomes. *IUBMB Life,* 55, 505-513.

O'BRIEN, T. W., KALF, G. F. & WITH THE TECHNICAL ASSISTANCE OF KATHLEEN, D. 1967. Ribosomes from Rat Liver Mitochondria. *Journal of Biological Chemistry,* 242, 2180-2185.
O'BRIEN, T. W., WITH THE TECHNICAL ASSISTANCE OF DEMETERIA, L. & ANN, H. 1971. The General Occurrence of 55 S Ribosomes in Mammalian Liver Mitochondria. *Journal of Biological Chemistry,* 246, 3409-3417.
OJALA, D., MONTOYA, J. & ATTARDI, G. 1981. tRNA punctuation model of RNA processing in human mitochondria. *Nature,* 9; 290(5806), 470-4.
PARISI, M. A. & CLAYTON, D. A. 1991. Similarity of human mitochondrial transcription factor 1 to high mobility group proteins. *Science,* 252 (5008), 965-969.
PARK, J., LEE, S. B., LEE, S., KIM, Y., SONG, S., KIM, S., BAE, E., KIM, J., SHONG, M., KIM, J.-M. & CHUNG, J. 2006. Mitochondrial dysfunction in Drosophila PINK1 mutants is complemented by parkin. *Nature,* 441, 1157-1161.
PARK, M. K., ASHBY, M. C., ERDEMLI, G., PETERSEN, O. H. & TEPIKIN, A. V. 2001. Perinuclear, perigranular and sub-plasmalemmal mitochondria have distinct functions in the regulation of cellular calcium transport. *EMBO J,* 20, 1863-1874.
PARSONS, M. J. & GREEN, D. R. 2010. Mitochondria in cell death. *Essays in Biochemistry* 47, 99-114.
PASSOS, D. O., DOMA, M. K., SHOEMAKER, C. J., MUHLRAD, D., GREEN, R., WEISSMAN, J., HOLLIEN, J. & PARKER, R. 2009. Analysis of Dom34 and Its Function in No-Go Decay. *Molecular Biology of the Cell,* 20, 3025-3032.
PAUL, M.-F., ALUSHIN, G. M., BARROS, M. H., RAK, M. & TZAGOLOFF, A. 2012. The Putative GTPase Encoded by MTG3 Functions in a Novel Pathway for Regulating Assembly of the Small Subunit of Yeast Mitochondrial Ribosomes. *Journal of Biological Chemistry,* 287, 24346-24355.
PECH, M. & NIERHAUS, K. H. 2012. Three mechanisms in Escherichia coli rescue ribosomes stalled on non-stop mRNAs: one of them requires release factor 2. *Molecular Microbiology,* 86, 6-9.
PEDERSEN, K., ZAVIALOV, A. V., PAVLOV, M. Y., ELF, J., GERDES, K. & EHRENBERG, M. 2003. The Bacterial Toxin RelE Displays Codon-Specific Cleavage of mRNAs in the Ribosomal A Site. *Cell,* 112, 131-140.
PELLEGRINI, M., ASIN-CAYUELA, J., ERDJUMENT-BROMAGE, H., TEMPST, P., LARSSON, N.-G. & GUSTAFSSON, C. M. 2009. MTERF2 is a nucleoid component in mammalian mitochondria. *Biochimica et Biophysica Acta (BBA) - Bioenergetics,* 1787, 296-302.
PERALTA, S., WANG, X. & MORAES, C. T. 2012. Mitochondrial transcription: Lessons from mouse models. *Biochimica et Biophysica Acta (BBA) - Gene Regulatory Mechanisms,* 1819, 961-969.
PETRY, S., BRODERSEN, D. E., MURPHY, F. V., DUNHAM, C. M., SELMER, M., TARRY, M. J., KELLEY, A. C. & RAMAKRISHNAN, V. 2005. Crystal Structures of the Ribosome in Complex with Release Factors RF1 and RF2 Bound to a Cognate Stop Codon. *Cell,* 123, 1255-1266.
PHANEUF, S. & LEEUWENBURGH, C. 2002. Cytochrome c release from mitochondria in the aging heart: a possible mechanism for apoptosis with

age. *American Journal of Physiology - Regulatory, Integrative and Comparative Physiology,* 282, R423-R430.
PIAO, L., LI, Y., KIM, S. J., BYUN, H. S., HUANG, S. M., HWANG, S.-K., YANG, K.-J., PARK, K. A., WON, M., HONG, J., HUR, G. M., SEOK, J. H., SHONG, M., CHO, M.-H., BRAZIL, D. P., HEMMINGS, B. A. & PARK, J. 2009. Association of LETM1 and MRPL36 Contributes to the Regulation of Mitochondrial ATP Production and Necrotic Cell Death. *Cancer Research,* 69, 3397-3404.
PIOLETTI, M., SCHLUNZEN, F., HARMS, J., ZARIVACH, R., GLUHMANN, M., AVILA, H., BASHAN, A., BARTELS, H., AUERBACH, T., JACOBI, C., HARTSCH, T., YONATH, A. & FRANCESCHI, F. 2001. Crystal structures of complexes of the small ribosomal subunit with tetracycline, edeine and IF3. *EMBO J,* 20, 1829-1839.
PISAREVA, V. P., SKABKIN, M. A., HELLEN, C. U. T., PESTOVA, T. V. & PISAREV, A. V. 2011. Dissociation by Pelota, Hbs1 and ABCE1 of mammalian vacant 80S ribosomes and stalled elongation complexes. *EMBO J,* 30, 1804-1817.
RAMAGOPAL, S. 1976. Accumulation of Free Ribosomal PrÖteins S1, L7, and L12 in Escherichia coli. *European Journal of Biochemistry,* 69, 289-297.
RAMRATH, D. J. F., YAMAMOTO, H., ROTHER, K., WITTEK, D., PECH, M., MIELKE, T., LOERKE, J., SCHEERER, P., IVANOV, P., TERAOKA, Y., SHPANCHENKO, O., NIERHAUS, K. H. & SPAHN, C. M. T. 2012. The complex of tmRNA-SmpB and EF-G on translocating ribosomes. *Nature,* 485, 526-529.
RASMUSSEN, B. A., GLUZMAN, Y. & TALLY, F. P. 1994. Inhibition of protein synthesis occurring on tetracycline-resistant, TetM-protected ribosomes by a novel class of tetracyclines, the glycylcyclines. *Antimicrobial Agents and Chemotherapy,* 38, 1658-1660.
REYES, A., HE, J., MAO, C. C., BAILEY, L. J., DI RE, M., SEMBONGI, H., KAZAK, L., DZIONEK, K., HOLMES, J. B., CLUETT, T. J., HARBOUR, M. E., FEARNLEY, I. M., CROUCH, R. J., CONTI, M. A., ADELSTEIN, R. S., WALKER, J. E. & HOLT, I. J. 2011. Actin and myosin contribute to mammalian mitochondrial DNA maintenance. *Nucleic Acids Research,* 39, 5098-5108.
RICHTER, R., RORBACH, J., PAJAK, A., SMITH, P. M., WESSELS, H. J., HUYNEN, M. A., SMEITINK, J. A., LIGHTOWLERS, R. N. & CHRZANOWSKA-LIGHTOWLERS, Z. M. 2010. A functional peptidyl-tRNA hydrolase, ICT1, has been recruited into the human mitochondrial ribosome. *EMBO J,* 29, 1116-1125.
RIZZUTO, R. 2003. Calcium mobilization from mitochondria in synaptic transmitter release. *The Journal of Cell Biology,* 163, 441-443.
RIZZUTO, R., PINTON, P., FERRARI, D., CHAMI, M., SZABADKAI, G., MAGALHAES, P. J., VIRGILIO, F. D. & POZZAN, T. 2003. Calcium and apoptosis: facts and hypotheses. *Oncogene,* 22, 8619-8627.
RORBACH, J. & MINCZUK, M. 2012. The post-transcriptional life of mammalian mitochondrial RNA. *The Biochemical Journal* 444(3):357-73.
RORBACH, J., NICHOLLS, T. J. J. & MINCZUK, M. 2011. PDE12 removes mitochondrial RNA poly(A) tails and controls translation in human mitochondria. *Nucleic Acids Research,* 39, 7750-7763.
RORBACH, J., RICHTER, R., WESSELS, H. J., WYDRO, M., PEKALSKI, M., FARHOUD, M., KÃ¼HL, I., GAISNE, M., BONNEFOY, N., SMEITINK, J. A., LIGHTOWLERS, R. N. & CHRZANOWSKA-LIGHTOWLERS, Z. M. A.

2008. The human mitochondrial ribosome recycling factor is essential for cell viability. *Nucleic Acids Research,* 36, 5787-5799.
ROSENTHAL, L. P. & BODLEY, J. W. 1987. Purification and characterization of Saccharomyces cerevisiae mitochondrial elongation factor Tu. *Journal of Biological Chemistry,* 262, 10955-10959.
ROSS, J. I., EADY, E. A., COVE, J. H. & CUNLIFFE, W. J. 1998. 16S rRNA Mutation Associated with Tetracycline Resistance in a Gram-Positive Bacterium. *Antimicrobial Agents and Chemotherapy,* 42, 1702-1705.
ROSSMANITH, W. 2011. Localization of Human RNase Z Isoforms: Dual Nuclear/Mitochondrial Targeting of the <italic>ELAC2</italic> Gene Product by Alternative Translation Initiation. *PLoS ONE,* 6, e19152.
ROSSMANITH, W., TULLO, A., POTUSCHAK, T., KARWAN, R. & SBIS, E. 1995. Human Mitochondrial tRNA Processing. *Journal of Biological Chemistry,* 270, 12885-12891.
RUTTER, J., WINGE, D. R. & SCHIFFMAN, J. D. 2010. Succinate dehydrogenase – Assembly, regulation and role in human disease. *Mitochondrion,* 10, 393-401.
RUZZENENTE, B., METODIEV, M. D., WREDENBERG, A., BRATIC, A., PARK, C. B., CAMARA, Y., MILENKOVIC, D., ZICKERMANN, V., WIBOM, R., HULTENBY, K., ERDJUMENT-BROMAGE, H., TEMPST, P., BRANDT, U., STEWART, J. B., GUSTAFSSON, C. M. & LARSSON, N.-G. 2012. LRPPRC is necessary for polyadenylation and coordination of translation of mitochondrial mRNAs. *EMBO J,* 31, 443-456.
SARASTE, M. Oxidative phosphorylation at the fin de siecle.
SASARMAN, F., BRUNEL-GUITTON, C., ANTONICKA, H., WAI, T., SHOUBRIDGE, E. A. & CONSORTIUM, L. 2010. LRPPRC and SLIRP Interact in a Ribonucleoprotein Complex that Regulates Posttranscriptional Gene Expression in Mitochondria. *Molecular Biology of the Cell*.
SEIT-NEBI, A., FROLOVA, L., JUSTESEN, J. & KISSELEV, L. 2001. Class-1 translation termination factors: invariant GGQ minidomain is essential for release activity and ribosome binding but not for stop codon recognition. *Nucleic Acids Research,* 29, 3982-3987.
SHARMA, M. R., BOOTH, T. M., SIMPSON, L., MASLOV, D. A. & AGRAWAL, R. K. 2009. Structure of a mitochondrial ribosome with minimal RNA. *Proceedings of the National Academy of Sciences of the United States of America,* 106, 9637-9642.
SHARMA, M. R., KOC, E. C., DATTA, P. P., BOOTH, T. M., SPREMULLI, L. L. & AGRAWAL, R. K. 2003. Structure of the mammalian mitochondrial ribosome reveals an expanded functional role for its component proteins. *Cell,* 115, 97-108.
SHAW, J. J. & GREEN, R. 2007. Two Distinct Components of Release Factor Function Uncovered by Nucleophile Partitioning Analysis. *Molecular Cell,* 28, 458-467.
SHIMIZU, Y. 2012. ArfA Recruits RF2 into Stalled Ribosomes. *Journal of Molecular Biology*.
SHOJI, S., WALKER, S. E. & FREDRICK, K. 2009. Ribosomal Translocation: One Step Closer to the Molecular Mechanism. *ACS Chemical Biology,* 4, 93-107.
SHUTT, T. E. & SHADEL, G. S. 2010. A compendium of human mitochondrial gene expression machinery with links to disease. *Environmental and Molecular Mutagenesis,* 51, 360-379.

SLOMOVIC, S. & SCHUSTER, G. 2008. Stable PNPase RNAi silencing: Its effect on the processing and adenylation of human mitochondrial RNA. *RNA,* 14, 310-323.
SMIRNOV, A., COMTE, C., MAGER-HECKEL, A.-M., ADDIS, V., KRASHENINNIKOV, I. A., MARTIN, R. P., ENTELIS, N. & TARASSOV, I. 2010. Mitochondrial Enzyme Rhodanese Is Essential for 5 S Ribosomal RNA Import into Human Mitochondria. *Journal of Biological Chemistry,* 285, 30792-30803.
SMIRNOV, A., ENTELIS, N., MARTIN, R. P. & TARASSOV, I. 2011. Biological significance of 5S rRNA import into human mitochondria: role of ribosomal protein MRP-L18. *Genes & Development,* 25, 1289-1305.
SOLEIMANPOUR-LICHAEI, H. R., KÃ¼HL, I., GAISNE, M., PASSOS, J. F., WYDRO, M., RORBACH, J., TEMPERLEY, R., BONNEFOY, N., TATE, W., LIGHTOWLERS, R. & CHRZANOWSKA-LIGHTOWLERS, Z. 2007. mtRF1a Is a Human Mitochondrial Translation Release Factor Decoding the Major Termination Codons UAA and UAG. *Molecular Cell,* 27, 745-757.
SOLOGUB, M., LITONIN, D., ANIKIN, M., MUSTAEV, A. & TEMIAKOV, D. 2009. TFB2 Is a Transient Component of the Catalytic Site of the Human Mitochondrial RNA Polymerase. *Cell,* 139, 934-944.
SOUBANNIER, V., MCLELLAND, G.-L., ZUNINO, R., BRASCHI, E., RIPPSTEIN, P., FON, EDWARD A. & MCBRIDE, HEIDI M. 2012. A Vesicular Transport Pathway Shuttles Cargo from Mitochondria to Lysosomes. *Current biology : CB,* 22, 135-141.
SPEAKMAN, J. R., TALBOT, D. A., SELMAN, C., SNART, S., MCLAREN, J. S., REDMAN, P., KROL, E., JACKSON, D. M., JOHNSON, M. S. & BRAND, M. D. 2004. Uncoupled and surviving: individual mice with high metabolism have greater mitochondrial uncoupling and live longer. *Aging Cell,* 3, 87-95.
SPENCER, A. C. & SPREMULLI, L. L. 2004. Interaction of mitochondrial initiation factor 2 with mitochondrial fMet-tRNA. *Nucleic Acids Research,* 32, 5464-5470.
SPENCER, A. C. & SPREMULLI, L. L. 2005. The interaction of mitochondrial translational initiation factor 2 with the small ribosomal subunit. *Biochimica et Biophysica Acta (BBA) - Proteins & Proteomics,* 1750, 69-81.
STEMMLER, T. L., LESUISSE, E., PAIN, D. & DANCIS, A. 2010. Frataxin and Mitochondrial FeS Cluster Biogenesis. *Journal of Biological Chemistry,* 285, 26737-26743.
STIBUREK, L., FORNUSKOVA, D., WENCHICH, L., PEJZNOCHOVA, M., HANSIKOVA, H. & ZEMAN, J. 2007. Knockdown of Human Oxa1l Impairs the Biogenesis of F1Fo-ATP Synthase and NADH:Ubiquinone Oxidoreductase. *Journal of Molecular Biology,* 374, 506-516.
SUNOHARA, T., JOJIMA, K., TAGAMI, H., INADA, T. & AIBA, H. 2004a. Ribosome stalling during translation elongation induces cleavage of mRNA being translated in Escherichia coli. *J. Biol. Chem.,* 279, 15368-15375.
SUNOHARA, T., JOJIMA, K., YAMAMOTO, Y., INADA, T. & AIBA, H. 2004b. Nascent-peptide-mediated ribosome stalling at a stop codon induces mRNA cleavage resulting in nonstop mRNA that is recognized by tmRNA. *RNA,* 10, 378-386.

SUROVTSEVA, Y. V., SHUTT, T. E., COTNEY, J., CIMEN, H., CHEN, S. Y., KOC, E. C. & SHADEL, G. S. 2011. Mitochondrial Ribosomal Protein L12 selectively associates with human mitochondrial RNA polymerase to activate transcription. *Proceedings of the National Academy of Sciences,* 108, 17921-17926.

SUZUKI, H., UEDA, T., TAGUCHI, H. & TAKEUCHI, N. 2007. Chaperone Properties of Mammalian Mitochondrial Translation Elongation Factor Tu. *Journal of Biological Chemistry,* 282, 4076-4084.

SUZUKI, T., TERASAKI, M., TAKEMOTO-HORI, C., HANADA, T., UEDA, T., WADA, A. & WATANABE, K. 2001a. Proteomic analysis of the mammalian mitochondrial ribosome: Identification of protein components in the 28 S small subunit. *Journal of Biological Chemistry,* 276, 33181-33195.

SUZUKI, T., TERASAKI, M., TAKEMOTO-HORI, C., HANADA, T., UEDA, T., WADA, A. & WATANABE, K. 2001b. Structural compensation for the deficit of rRNA with proteins in the mammalian mitochondrial ribosome. Systematic analysis of protein components of the large ribosomal subunit from mammalian mitochondria. *Journal of Biological Chemistry,* 276, 21724-21736.

TANAKA, A., CLELAND, M. M., XU, S., NARENDRA, D. P., SUEN, D.-F., KARBOWSKI, M. & YOULE, R. J. 2010. Proteasome and p97 mediate mitophagy and degradation of mitofusins induced by Parkin. *The Journal of Cell Biology,* 191, 1367-1380.

TEMPERLEY, R., RICHTER, R., DENNERLEIN, S., LIGHTOWLERS, R. N. & CHRZANOWSKA-LIGHTOWLERS, Z. M. 2010a. Hungry codons promote frameshifting in human mitochondrial ribosomes. *Science,* 327, 301.

TEMPERLEY, R. J., SENECA, S. H., TONSKA, K., BARTNIK, E., BINDOFF, L. A., LIGHTOWLERS, R. N. & CHRZANOWSKA-LIGHTOWLERS, Z. M. A. 2003. Investigation of a pathogenic mtDNA microdeletion reveals a translation-dependent deadenylation decay pathway in human mitochondria. *Human Molecular Genetics,* 12, 2341-2348.

TEMPERLEY, R. J., WYDRO, M., LIGHTOWLERS, R. N. & CHRZANOWSKA-LIGHTOWLERS, Z. M. 2010b. Human mitochondrial mRNAs-like members of all families, similar but different. *Biochim Biophys Acta,* 1797, 1081-1085.

TOMECKI, R., DMOCHOWSKA, A., GEWARTOWSKI, K., DZIEMBOWSKI, A. & STEPIEN, P. P. 2004. Identification of a novel human nuclear-encoded mitochondrial poly(A) polymerase. *Nucleic Acids Research,* 32, 6001-6014.

TSUBOI, M., MORITA, H., NOZAKI, Y., AKAMA, K., UEDA, T., ITO, K., NIERHAUS, K. H. & TAKEUCHI, N. 2009. EF-G2mt Is an Exclusive Recycling Factor in Mammalian Mitochondrial Protein Synthesis. *Molecular Cell,* 35, 502-510.

TWIG, G., HYDE, B. & SHIRIHAI, O. S. 2008. Mitochondrial fusion, fission and autophagy as a quality control axis: The bioenergetic view. *Biochimica et Biophysica Acta (BBA) - Bioenergetics,* 1777, 1092-1097.

ULE, J., JENSEN, K., MELE, A. & DARNELL, R. B. 2005. CLIP: A method for identifying protein–RNA interaction sites in living cells. *Methods,* 37, 376-386.

UNSELD, M., MARIENFELD, J. R., BRANDT, P. & BRENNICKE, A. 1997. The mitochondrial genome of Arabidopsis thaliana contains 57 genes in 366,924 nucleotides. *Nat Genet,* 15, 57-61.
VALLE, M., GILLET, R., KAUR, S., HENNE, A., RAMAKRISHNAN, V. & FRANK, J. 2003. Visualizing tmRNA Entry into a Stalled Ribosome. *Science,* 300, 127-130.
VAN ACKEN, U. 1975. Proteinchemical studies on ribosomal proteins S4 and S12 from ram (ribosomal ambiguity) mutants of Escherichia coli. *Molecular and General Genetics,* 140, 61-68.
VAN HOOF, A., FRISCHMEYER, P. A., DIETZ, H. C. & PARKER, R. 2002. Exosome-Mediated Recognition and Degradation of mRNAs Lacking a Termination Codon. *Science,* 295, 2262-2264.
VEATCH, J. R., MCMURRAY, M. A., NELSON, Z. W. & GOTTSCHLING, D. E. 2009. Mitochondrial Dysfunction Leads to Nuclear Genome Instability via an Iron-Sulfur Cluster Defect. *Cell,* 137, 1247-1258.
VIVANCO-DOMÍNGUEZ, S., BUENO-MARTÍNEZ, J., LEÓN-AVILA, G., IWAKURA, N., KAJI, A., KAJI, H. & GUARNEROS, G. 2012. Protein Synthesis Factors (RF1, RF2, RF3, RRF, and tmRNA) and Peptidyl-tRNA Hydrolase Rescue Stalled Ribosomes at Sense Codons. *Journal of Molecular Biology,* 417, 425-439.
VOGEL, A., SCHILLING, O., SPATH, B. & MARCHFELDER, A. 2005. The tRNase Z family of proteins: physiological functions, substrate specificity and structural properties. *Biological Chemistry* 386(12), 1253-64.
VOGEL, R. O., SMEITINK, J. A. M. & NIJTMANS, L. G. J. 2007. Human mitochondrial complex I assembly: A dynamic and versatile process. *Biochimica et Biophysica Acta (BBA) - Bioenergetics,* 1767, 1215-1227.
WANG, Z., COTNEY, J. & SHADEL, G. S. 2007. Human mitochondrial ribosomal protein MRPL12 interacts directly with mitochondrial RNA polymerase to modulate mitochondrial gene expression. *Journal of Biological Chemistry,* 282, 12610-12618.
WANSCHERS, SZKLARCZYK R, PAJAK A, VAN DEN BRAND MA, GLOERICH J, RODENBURG RJ, LIGHTOWLERS RN, NIJTMANS LG & MA., H. 2012. C7orf30 specifically associates with the large subunit of the mitochondrial ribosome and is involved in translation. *Nucleic Acids Res*, 1-12.
WENG, Y., CZAPLINSKI, K. & PELTZ, S. W. 1996. Genetic and biochemical characterization of mutations in the ATPase and helicase regions of the Upf1 protein. *Molecular and Cellular Biology,* 16, 5477-90.
WENZ, T., LUCA, C., TORRACO, A. & MORAES, C. T. 2009. mTERF2 Regulates Oxidative Phosphorylation by Modulating mtDNA Transcription. *Cell Metabolism,* 9, 499-511.
WERAARPACHAI, W., ANTONICKA, H., SASARMAN, F., SEEGER, J., SCHRANK, B., KOLESAR, J. E., LOCHMULLER, H., CHEVRETTE, M., KAUFMAN, B. A., HORVATH, R. & SHOUBRIDGE, E. A. 2009. Mutation in TACO1, encoding a translational activator of COX I, results in cytochrome c oxidase deficiency and late-onset Leigh syndrome. *Nat Genet,* 41, 833-837.
WILLIAMS, K. P., MARTINDALE, K. A. & BARTEL, D. P. 1999. Resuming translation on tmRNA: a unique mode of determining a reading frame. *EMBO J,* 18, 5423-5433.
WORIAX, V. L., BULLARD, J. M., MA, L., YOKOGAWA, T. & SPREMULLI, L. L. 1997. Mechanistic studies of the translational elongation cycle in

mammalian mitochondria. *Biochimica et Biophysica Acta (BBA) - Gene Structure and Expression,* 1352, 91-101.
WYDRO, M., BOBROWICZ, A., TEMPERLEY, R. J., LIGHTOWLERS, R. N. & CHRZANOWSKA-LIGHTOWLERS, Z. M. 2010. Targeting of the cytosolic poly(A) binding protein PABPC1 to mitochondria causes mitochondrial translation inhibition. *Nucleic Acids Research,* 38, 3732-3742.
YAKUBOVSKAYA, E., MEJIA, E., BYRNES, J., HAMBARDJIEVA, E. & GARCIA-DIAZ, M. 2010. Helix Unwinding and Base Flipping Enable Human MTERF1 to Terminate Mitochondrial Transcription. *Cell,* 141, 982-993.
YOSHIDA, M., MUNEYUKI, E. & HISABORI, T. 2001. ATP synthase — a marvellous rotary engine of the cell. *Nat Rev Mol Cell Biol,* 2, 669-677.
YOULE, R. J. & KARBOWSKI, M. 2005. Mitochondrial fission in apoptosis. *Nat Rev Mol Cell Biol,* 6, 657-663.
YOULE, R. J. & VAN DER BLIEK, A. M. 2012. Mitochondrial Fission, Fusion, and Stress. *Science,* 337, 1062-1065.
YOUNG, D. J., EDGAR, C. D., MURPHY, J., FREDEBOHM, J., POOLE, E. S. & TATE, W. P. 2010. Bioinformatic, structural, and functional analyses support release factor-like MTRF1 as a protein able to decode nonstandard stop codons beginning with adenine in vertebrate mitochondria. *RNA,* 16, 1146-1155.
YOUNGMAN, E. M., MCDONALD, M. E. & GREEN, R. 2008. Peptide Release on the Ribosome: Mechanism and Implications for Translational Control. *Annual Review of Microbiology,* 62, 353-373.
ZHANG, Y. & SPREMULLI, L. L. 1998. Identification and cloning of human mitochondrial translational release factor 1 and the ribosome recycling factor. *Biochim Biophys Acta,* 1443, 245-250.

Publications arising

Publications arising during my thesis studies:

Wanschers BF, Szklarczyk R, Pajak A, van den Brand MA, Gloerich J, Rodenburg RJ, Lightowlers RN, Nijtmans LG, Huynen MA.

C7orf30 specifically associates with the large subunit of the mitochondrial ribosome and is involved in translation.

Nucleic Acids Res. 2012 May;40(9):4040-51.

Chrzanowska-Lightowlers ZM, Pajak A, Lightowlers RN.

Termination of protein synthesis in mammalian mitochondria.

J Biol Chem. 2011 Oct 7;286(40):34479-85.

Richter R, Pajak A, Dennerlein S, Rozanska A, Lightowlers RN, Chrzanowska-Lightowlers ZM.

Translation termination in human mitochondrial ribosomes.

Biochem Soc Trans. 2010 Dec;38(6):1523-6.

Richter R, Rorbach J, Pajak A, Smith PM, Wessels HJ, Huynen MA, Smeitink JA, Lightowlers RN, Chrzanowska-Lightowlers ZM.

A functional peptidyl-tRNA hydrolase, ICT1, has been recruited into the human mitochondrial ribosome.

EMBO J. 2010 Mar 17;29(6):1116-25.

Appendices

Appendix 1.1.

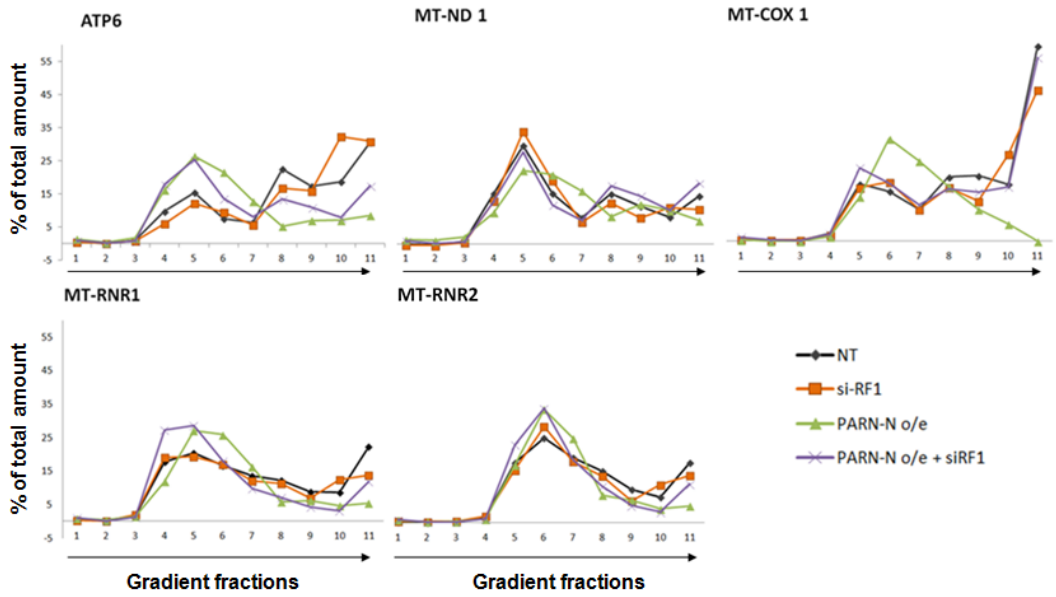

Figure S 1. The signals presented in chapter 3 (Figure 3.7) and chapter 6 (Figures 6.2 and 6.3) were quantified and presented as the graph of mean from three independent experiment repeats (merged version). For description of experiments see chapters 3 (section 3.7) and 6 (section 6.2 and 6.2).

Appendix 1.2. LC MS/MS analysis of C12orf65-FLAG IP

The LC MS/MS was performed and analysed by H. Wessels (UNMC, Nijmegen). All identified proteins are listed in the table below. Contaminants such as keratin, and cytosolic ribosomal proteins were excluded. Mitoribosomal protein are highlighted in yellow.

Protein ID	Protein Name	EMPAI Values	
		C12orf65	Control
NP_619520.1	putative ATP-dependent RNA helicase DHX30 isoform 1	0.188502227	0
NP_001164015.1	serine/threonine-protein phosphatase PGAM5, mitochondrial isoform 2	0.668100537	0
NP_001129125.1	polyadenylate-binding protein 4 isoform 1	0.285555732	0
NP_002559.2	polyadenylate-binding protein 1	0.274274986	0
NP_057134.1	39S ribosomal protein L11, mitochondrial isoform a	1.053525026	0
NP_004514.2	kinesin-like protein KIF11	0.111402987	0
NP_005372.2	nucleolin	0.324192792	0
NP_001034708.1	protein arginine N-methyltransferase 5 isoform b	0.206792641	0
NP_000916.2	pyruvate dehydrogenase E1 component subunit beta, mitochondrial isoform 1 precursor	0.232846739	0
NP_009204.1	prohibitin-2 isoform 2	0.232846739	0
NP_075066.1	39S ribosomal protein L44, mitochondrial precursor	0.279802214	0
NP_001922.2	dihydrolipoyllysine-residue acetyltransferase component of pyruvate dehydrogenase complex, mitochondrial precursor	0.139209961	0
NP_112570.2	28S ribosomal protein S15, mitochondrial precursor	0.36887451	0
NP_057575.2	39S ribosomal protein L37, mitochondrial precursor	0.165914401	0
NP_001924.2	dihydrolipoyllysine-residue succinyltransferase component of 2-oxoglutarate dehydrogenase complex, mitochondrial	0.249609141	0
NP_065142.2	39S ribosomal protein L47, mitochondrial isoform a	0.318256739	0
NP_003290.1	endoplasmin precursor	0.102182525	0
NP_056255.2	monofunctional C1-tetrahydrofolate synthase, mitochondrial precursor	0.060025849	0
NP_115867.2	39S ribosomal protein L38, mitochondrial precursor	0.154781985	0
NP_054894.1	39S ribosomal protein L15, mitochondrial precursor	0.172102298	0
NP_055578.2	39S ribosomal protein L19, mitochondrial precursor	0.154781985	0
NP_387506.1	28S ribosomal protein S29, mitochondrial isoform 1	0.115883993	0
NP_000265.1	ornithine aminotransferase, mitochondrial isoform 1 precursor	0.140624924	0
NP_036216.2	glutamate dehydrogenase 2, mitochondrial precursor	0.089022962	0
NP_064576.1	28S ribosomal protein S22, mitochondrial	0.128837892	0
NP_004918.1	39S ribosomal protein L49, mitochondrial	0.258925412	0
NP_054880.2	39S ribosomal protein L18, mitochondrial precursor	0.359356391	0
NP_115866.1	39S ribosomal protein L41, mitochondrial	0.519911083	0
NP_002071.2	aspartate aminotransferase, mitochondrial precursor	0.113042193	0
NP_054899.2	39S ribosomal protein L22, mitochondrial isoform a	0.258925412	0
NP_054737.1	28S ribosomal protein S28, mitochondrial	0.291549665	0
NP_060441.2	39S ribosomal protein L20, mitochondrial precursor	0.359356391	0

NP_066270.1	creatine kinase U-type, mitochondrial precursor	0.149756995	0
NP_001035971.1	polyadenylate-binding protein 1-like 2	0.258925412	0
NP_009139.1	39S ribosomal protein L3, mitochondrial	0.178768635	0
NP_001159831.1	serine hydroxymethyltransferase, mitochondrial isoform 3	0.100694171	0
NP_066957.3	39S ribosomal protein L23, mitochondrial	0.42510267	0
NP_859047.1	peroxiredoxin-1	0.245197085	0
NP_002148.1	10 kDa heat shock protein, mitochondrial	0.519911083	0
NP_005338.1	78 kDa glucose-regulated protein precursor	0.084145869	0
NP_005909.2	malate dehydrogenase, mitochondrial precursor	0.136463666	0
NP_689482.1	probable peptide chain release factor C12orf65, mitochondrial	0.389495494	0
NP_976317.1	ribonuclease inhibitor	0.102943312	0
NP_036205.1	T-complex protein 1 subunit epsilon	0.090776692	0